Faculty of Science and Engineering
Department of Chemistry

Aluminous Goethite in the Bayer Process and Its Impact on Alumina Recovery and Settling

Fei Wu

This thesis is presented for the Degree of
Doctor of Philosophy
of
Curtin University

January 2012

To the best of my knowledge and belief this thesis contains no material previously published by any other person except where due acknowledgment has been made.

This thesis contains no material which has been accepted for the award of any other degree or diploma in any university.

Signature:

Date:

Acknowledgements

This thesis would have been an unrealistic dream without those who offered their guidance, patience, help, encouragement and support along the journey.

First of all, I would like to express my sincere gratitude to all my supervisors, principal supervisor Dr. Franca Jones at Department of Chemistry, Curtin University, supervisor Dr. Peter Smith at CSIRO Minerals, Waterford and associate supervisor Prof. Kate Wright at Curtin University, for their guidance and patience. Thanks for having faith in me!

A special thank-you goes to Dr. Peter Smith who has dedicated himself with tremendous passion to this project throughout my PhD study. As an international authority in the Bayer Process, he offered invaluable help in tackling the numerous challenges that I faced along the way.

I deeply appreciate the enormous effort that Dr. Franca Jones has made to organize various resources for my research, which ensured a smooth completion of the project and the thesis. Her insightful thoughts, critiques, and encouragement provided much of the impetus for this thesis.

Prof./Dr. Kate Wright's constructive advice on my academic writing and her knowledge on mineralogy have been inspirational.

I also extend my appreciation to my former supervisors. Dr. William Richmond, who kindly helped with my PhD application, was of great assistance until his departure from the University. Dr. Mitch Loan provided an industrial perspective to this research and has been enthusiastically involved in the support of the project.

My grateful thanks go to the Department of Chemistry and the Department of Imaging and Applied Physics, Curtin University and CSIRO Minerals, Waterford for the facilities provided and to the CSIRO Light Metal Flagship, ALCOA Australia and Curtin University for providing the research funding and the scholarship which were crucial to the research project.

I would also like to take the opportunity to acknowledge the co-operation from members of the research team. The *'Red Side'* of the Alumina Group at CSIRO, Waterford under the leadership of Dr. Peter Smith has provided the crucial experimental

and analytical facilities. Importantly, I have benefited from the unconditional help of the team members. Dr. Bingan Xu's expertise in mineral processing and experience on analytical technology helped to resolve difficulties on many occasions. I am grateful for the assistance from Takuo Harato, Christine Wingate, Lynette De Silva and Michael Davies. Furthermore, Dr. Philip Fawell and Andrew Owen helped me with the settling tests in their laboratory.

The analytical teams from both CSIRO Minerals and Curtin University have been extremely invaluable to my project with their assistance in mineral characterizations.

I cherish the friendships developed with fellow PhD students, Alex Senaputra, Xiaodong Wang and Lawrence Dyer during my study and appreciate the help and encouragement from them.

Over the past three and half years of study, there were times that I was jubilant when having obtained the satisfied experimental data, but there were also times that I was frustrated by the pains of failure. I have enjoyed the pleasure that the project progress has brought to me, but I sometimes feel confused over my career future. I am so blessed to have love and support from my family, especially my husband who stands by me and encourages me to chase my lifetime dream. The distance of seven thousand kilometers between Shanghai and Perth has never stopped my mother from missing me, for which I feel both grateful and sorry.

I dedicate this thesis to my father who had great expectations of me!

Abstract

Aluminium substituted goethite present in the Bayer process is closely related to settling problem and reduction of alumina recovery. The finer particle size and larger specific surface area of Al-substituted goethite compared with those of hematite contribute to the negative effects to the Bayer circuit.

The project aims to improve the settling performance and recover alumina from aluminous goethite by hydrothermal transformation of Al-goethite to hematite/Al-hematite in the Bayer digestion process.

A hypothesis of the solubility limit in goethite-diaspore solid solution (Al-goethite) has been developed through the characteristic study on synthetic Al-goethite. The mechanism of Al for Fe substitution has presumably been considered to be a partial Al substitution in the core of goethite structure with the remainder forming a surface diaspore coating.

The thermal transformation of goethite to hematite does not change the goethite structure until temperature 600 ℃ since the phase change happens in the temperature range of 300 to 400 ℃. On the other hand, the study of hydrothermal transformation of goethite suggests that 230 ℃ is the sensitive reaction temperature. Hematite seeding is beneficial to the transformation while alumina content is an inhibitor.

Natural aluminous goethite in the Bayer digestion performs differently due to the effects of impurities in the bauxite on the process. The presence of anatase adversely affects the transformation through the reaction with caustic to form into sodium titanate, which forms a film-like coating on the surface of goethite to prevent further transformation. However, adding $CaCO_3$ directly to the digestion zone at 250 ℃ can largely improve the transformation of Al-goethite to hematite by consuming anatase with $CaCO_3$ to prevent the formation of sodium titanate. It is noted that the adding point of $CaCO_3$ is crucial to the enhancement.

A near completion of hydrothermal transformation of aluminous goethite to hematite has been achieved through the addition of $CaCO_3$ directly to the digestion zone at 250 ℃ within 30 minutes. The extent of Al substitution in the original goethite from 25 mol% reduces to 5~6 mol% in hematite. More importantly, alumina recovery increased by 20% and the settling rate greatly improves as a result of the transformation of Al-goethite to hematite.

Abbreviations

BET	Brunauer, Emmett and Teller
DRIFT	Diffuse Reflectance Infra-red Fourier Transform
DSC	Differential Scanning Calorimetry
DTA	Differential Thermal Analysis
EDS	Energy Dispersive X-ray Spectroscopy
GCE	Goethite Conversion Extent
GFR	Gas Fired Reactor
ICP	Inductively Coupled Plasma
IR	Infra-red Spectrum
hcp	hexagonal close packed
LOI	Loss on Ignition
PEG	Polyethylene Glycol
PSD	Particle Size Distribution
ss	solid solution
SSA	Specific Surface Area
TCA	Tri-calcium Aluminate Hexahydrate
TEM	Transmission Electron Microscopy
TG	Thermogravimetry
WHH	Width of Half-Height
XRD	X-Ray Diffraction
XRF	X-Ray Fluorescence

Symbols

Symbol	Unit	Description
a, b, c		crystal dimensions
d(h, k, l)	Å, nm	d spacing at peak position (h, k, l)
W_0	*g*	weight of empty crucible
W_1	g	crucible with initial goethite samples
W_2	g	crucible with thermal-treated goethite samples
D_f	g/t d	dose of per ml flocculant
C_f	wt.%	concentration of flocculant
V	L	volume
C_s	g/L	concentration of solids
Vs	m/s	settling rate
D	m	distance for settling
t	sec	time for settling
λ	Å	wavelength
I		intensity of crystal peak in XRD
C	g/L	caustic concentration as Na_2CO_3
E_a	kJ/mol	activation energy
T	K, ℃	temperature
A		frequency factor
R		universal gas constant
k		reaction rate coefficient

n		time component
y		reaction extent
RE		relative error
γ		stretching bond in IR
δ		plantar bending bond in IR
v		vibration in bond IR
ΔH_{mix}	J/g, kJ/mol	enthalpy of mixing
M	g	mass of molecule

Table of Contents

List of Tables

List of Figures

Chapter 1
Introduction

1.1 Background

The Bayer process has become the principal method for the alumina production worldwide since it was first invented by Karl Josef Bayer in 1887. The process involves four major steps, which are digestion, clarification, precipitation and calcination, with variations in different refineries greatly depending on compositions of the ores processed. Bauxite is the most important aluminium ore and is made up of the minerals gibbsite ($Al(OH)_3$), boehmite (γ-AlOOH) and diaspore (α-AlOOH), in a mixture with iron and titanium oxides along with silicates.

The iron oxides in bauxite commonly comprise goethite and hematite. In terms of goethite-rich bauxite, Al for Fe substitution in the goethite structure is more likely to occur in nature. Al-substituted goethite, also referred to as aluminous goethite and Al-goethite in literature, has long been recognised as an undesirable iron oxide in the Bayer process. The negative effects of Al-goethite upon the Bayer process that the alumina industry has faced are basically settling problems caused by the properties of aluminous goethite and loss of alumina caused by the stranded alumina in the goethite structure. Al-goethite has relatively small particle size and large specific surface area mostly due to the smaller Al^{3+} iso-structural substitution for Fe^{3+}. As a result the settling rate for the red mud of Al-goethite containing bauxite in the clarification step is considerably slow compared to red mud with hematite as the major iron oxide. Various techniques have been taken into account to minimise the settling problem in the alumina industry. For example, acid washings to lower the pH, flocculation to increase the mud settling rate, dewatering by centrifugation and electro-kinetic techniques. However, the methods were either inefficient or not cost effective (Li, 2001). This disappointing settling performance of Al-goethite-containing red mud economically and environmentally impacts on the alumina industry. In addition to this, alumina stranded in the goethite structure causes the loss of alumina.

The attempt to minimize the adverse influence of Al-goethite in the Bayer circuit recently has been concentrated on the possible transformation of goethite to hematite in the Bayer digestion process. In such cases, digestion conditions for boehmite-bauxite at

relatively high temperature tend to easily accommodate the transformation process. This alumina industry has potential to benefit from the revolution in improving the settling performance by the transformation of Al-goethite to more desirable hematite. More importantly, alumina incorporated in the goethite structure is more likely to be released from Al-goethite as a result of the transformation since the ability of hematite for accommodation of Al substitution is much weaker than that of goethite. This promising process has been widely investigated. However, substantial industrial application is still limited due to the uncertainty of a number of impurities in the bauxite operated in individual refineries as well as the relatively strict digestion conditions required.

A number of studies relating to the hydrothermal transformation of Al-goethite to hematite in the Bayer digestion process are yet to be implemented to establish a good understanding with the process. In this project, the study was started with the synthesis and the characteristics of Al-substituted goethite. The fundamental understanding with the minerals and aspects related to the further study, such as the thermal behaviours, would likely to be developed. Subsequently, transformation behaviours of synthetic Al-goethite/goethite were investigated both thermally and hydrothermally. The mechanism study for both processes was intensively conducted. Aluminous goethite in natural bauxite was then investigated in the Bayer digestion process. The interactions between goethite, Bayer liquor and impurities in the bauxite and the corresponding kinetics and mechanisms would be the interests in this part. Finally and most importantly, the improvement of alumina reversion from aluminous goethite and the settling rate by the transformation of Al-goethite to hematite were determined.

A number of advanced analytical technologies and experimental equipment have been employed in the project. Gas Fired Reactor (GFR) and the Autoclave reaction system are the major reaction systems used in this study to carry out the digestion process. In terms of analytical technologies, titration, X-ray Diffraction (XRD), Transmission Electron Microscopy (TEM), Differential Scanning Calorimetry (DSC), Infra-red Spectrum (IR) and much more have been used to evaluate experimental results. Furthermore, analytical and design software were used to assist the data processing.

1.2 Objectives

This project aims to 1) study the miscibility gap of aluminium substitution during the synthesis of goethite in alkaline environment; 2) investigate the transformation

behaviour of Al-goethite both thermally and hydrothermally and reveal the mechanism of the transformation; 3) discover the chemistry and the process of aluminous goethite in the Bayer digestion; 4) determine experimental conditions relevant to the Bayer process; 5) identify the optimised conditions for the hydrothermal transformation of Al-goethite to hematite; 6) evaluate the improvement of alumina reversion and settling behaviour as a result of the hydrothermal transformation of aluminous goethite to hematite.

1.3 Significance

Bauxite rich in aluminous goethite has severe negative effects on the Bayer process. This is also one of the problems that alumina industry has faced. This research project aims to minimize the negative influence through exploring the kinetics and improving reaction conditions. Alumina industry could benefit from the attempt not only in improving quality of alumina, increasing productivity, but also in saving energy or recovering alumina to lower production cost. Most importantly, the possibility of success of this project would help avoid environmental hazards from the residue produced in the Bayer process.

1.4 Outline

The outline of the PhD thesis is listed as follows.

Chapter 1: Introduction
Chapter 2: Literature Review
Chapter 3: Methodology and Materials
Chapter 4: Characterisations of Synthetic Al-substituted Goethite
Chapter 5: Transformation of Synthetic Goethite
Chapter 6: Al-substituted Goethite in the Bayer Digestion Process
Chapter 7: Improvement on Alumina Reversion and Settling Performance
Chapter 8: Conclusions and Future Work

Chapter 2
Literature Review

2.1 Introduction

2.1.1 Scope

This Chapter will primarily review existing processes in relation to the Bayer digestion of goethite-bauxite. Forms of goethite in bauxite are normally referred to goethite or aluminium substituted goethite with Al substitution up to 33 mol %. Prior to the critical review, the Bayer process and properties of goethite that influence the process will be briefly demonstrated to give a fundamental knowledge of the project.

2.1.2 Bauxite

Bauxite is the most important aluminium ore and is made up of the minerals gibbsite ($Al(OH)_3$), boehmite (γ-AlOOH) and diaspore (α-AlOOH), in a mixture with iron and titanium oxides along with silicates. **Table 2.1** presents a typical mineralogical distribution. The conditions of extraction of alumina from bauxite depend to great extent on the type of aluminium hydroxide present.

Table 2.1 Mineralogical composition of bauxite

Constituent	Mineralogical composition
Al_2O_3	Gibbsite, boehmite, diaspore
Fe_2O_3	Hematite, goethite, maghemite
SiO_2	Kaolinite, quartz
TiO_2	Anatase, rutile, ilmenite

Classified by the weathering conditions of their formation, bauxites are with two major types being lateritic bauxites and karst bauxites (Smith, 2009). Lateritic bauxites (silicate bauxites) were formed by laterization of alumino-silicate rocks and are found mostly in tropical countries. The intense weathering conditions in a location with good drainage enable the dissolution of kaolinite and the precipitation of gibbsite. The aluminous minerals in the lateritic bauxite deposits are predominately gibbsite (Bardossy and Aleva, 1990).

Karst bauxites can be distinguished from lateritic bauxites. They were formed by weathering and residual accumulation of intercalated clays or by the dissolution of carbonate residues. Karst bauxites were found mostly in Europe and Jamaica on carbonate rocks, however, more recently they have been also found in Eastern Europe and Northern Asia (Bardossy, 1982; Smith, 2009). Aluminous minerals in the karst bauxites are mostly boehmite and diaspore with kaolinite also as the dominant silicate mineral.

The difference between the two major bauxites, especially the aluminous minerals, determines how they are processed. Generally, lateritic bauxites are easier to digest than karst bauxites and are processed by the Bayer process with milder conditions of caustic soda concentration, digestion temperature and holding times.

2.1.3 Overview of the Bayer process

The Bayer process was first developed in 1887 by Karl Josef Bayer and has become the principal method for the extraction of alumina from bauxite worldwide with variations depending on differences in the source and quality of the ore (Hind *et al.*, 1999; Atasoy, 2005; Smith, 2009). The extraction of alumina is achieved by combining ground bauxite with caustic soda under elevated temperature and pressure. Aluminium (oxy)hydroxides are dissolved, while the remaining solid (bauxite residue) is separated from the process. The principle of the process is that aluminium hydroxide is soluble in alkaline solution upon heating but the other minerals cannot be dissolved at the same conditions due to the fact that they are relatively inert in the alkaline solution.

The Bayer process is operated as a continuous cycle that involves four main stages, digestion, clarification, precipitation and calcination (Hind *et al.*, 1999). A schematic diagram of a typical Bayer process is shown in **Figure 2.1**. In many modern industrial operations, there is a pre-desilication stage to encourage the re-precipitation of the solubilised silica to desilication products, known as DSP (Smith, 2009). Initially the bauxite is reduced to the appropriate size by crushing and grinding. The crushed bauxite is then mixed with spent liquor to form a slurry, which is held at a temperature of 95-100 ℃ in agitated storage tanks for several hours to sufficiently transform the reactive silica to DSP (Whittington *et al.*, 1998; Smith, 2009). This minimises soluble silica in the Bayer liquor and avoids downstream issues such as silica in the final product and silicate scaling during heat transfer.

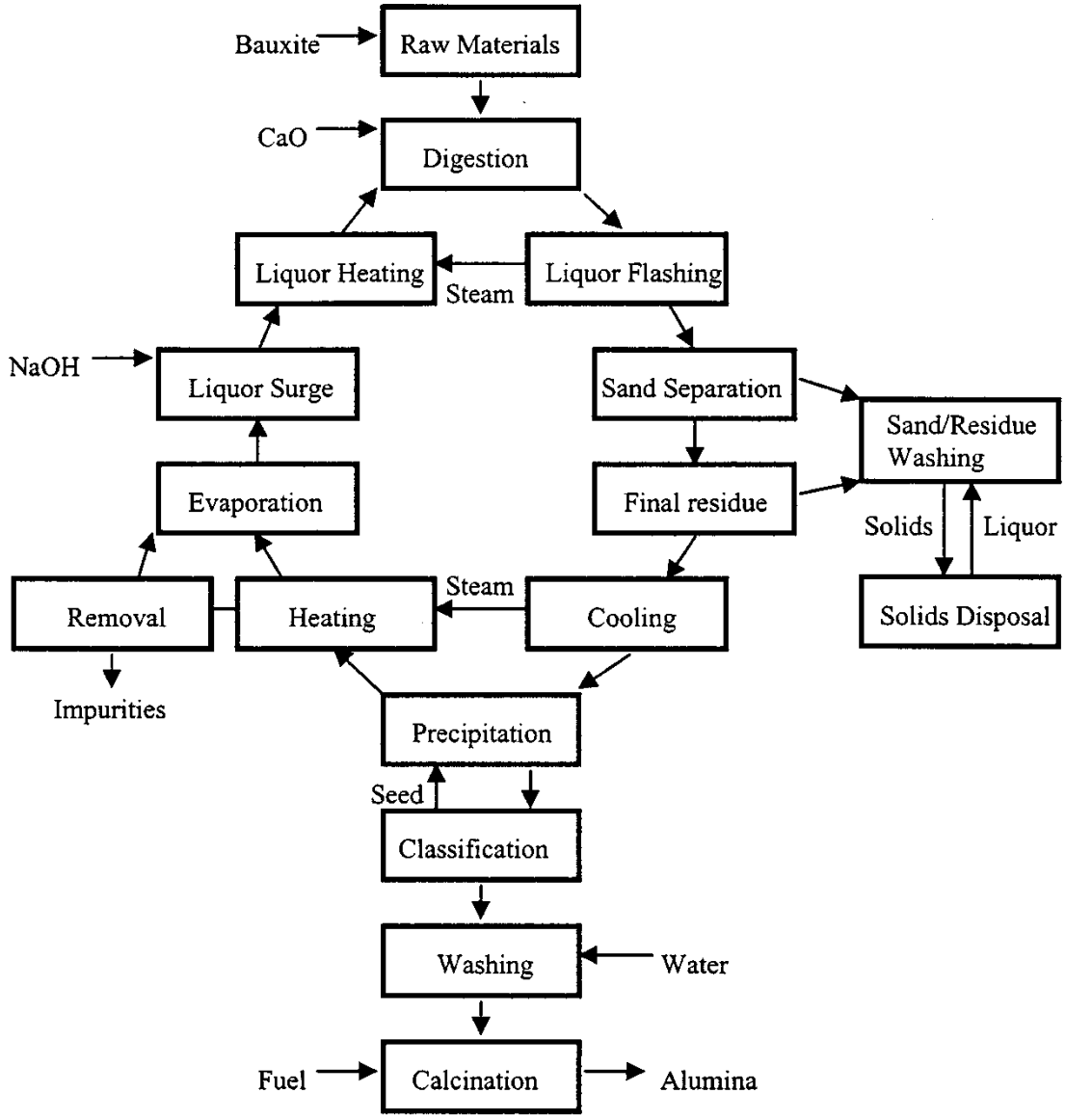

Figure 2.1 Schematic diagram of the basic Bayer process (Hind *et al.*, 1999)

2.1.3.1 Digestion

Digestion stage is used to extract alumina from the ground bauxite slurry. Initially, ground bauxite is mixed with caustic soda solution at an elevated temperature to dissolve the soluble aluminium species. The solubility of gibbsite $Al(OH)_3$ is higher than that of boehmite/ diaspore (AlOOH); hence the conditions of digestion for boehmite-bauxite are more severe than that of gibbsite. The low temperature digestion is conducted typically at 145 ℃ for gibbsite compared to higher operation temperature for boehmite ranging from 220 ℃ to 270 ℃ (Hudson, 1987; Whittington, 1996; Smith, 2009).

The reaction in digestion is either gibbsite dissolution:

$$Al(OH)_3 + NaOH \rightarrow NaAl(OH)_4 \quad \textbf{(2.1)}$$

Gibbsite

Or boehmite dissolution as

$$AlO(OH) + NaOH + H_2O \rightarrow NaAl(OH)_4 \quad \textbf{(2.2)}$$

Boehmite

Side reactions along with the extraction of alumina, including the conversion of the remaining silica from pre-desilication stage, could occur at such digestion conditions. Silicon-containing minerals, which are usually present as kaolinite, react with caustic soda to form into DSP (desilication product). It is believed to proceed by following two steps (Hudson, 1987; Whittington *et al.*, 1998; Smith, 2009).

Kaolin dissolution:

$$3Al_2Si_2O_5(OH)_4 + 18NaOH \rightarrow 6Na_2SiO_3 + 6NaAl(OH)_4 + 3H_2O \quad \textbf{(2.3)}$$

Kaolin

Further precipitation of DSP:

$$6Na_2SiO_3 + 6NaAl(OH)_4 + Na_2X \rightarrow Na_6[Al_6Si_6O_{24}].Na_2X + 12NaOH + 6H_2O$$

DSP

where Na_2X represents "included" salts, e.g. $2NaCl$, Na_2SO_4, Na_2CO_3, $2NaAl(OH)_4$.

As shown in Equation **2.3** and **2.4**, the reaction leads to a loss of both alumina and caustic and so is a cost to the Bayer process.

2.1.3.2 Clarification

The sodium aluminate solution from digestion, commonly called as pregnant or green liquor, is then separated from the insoluble solid residues by settling and filtration. The resulting residue, also called red mud in alumina industry, primarily composes iron oxides, silicates, titanium oxide and other metal oxide impurities (Hind *et al.*, 1999). The green liquor is sent to the precipitation step and red mud is sent to a counter-current washing system to remove soluble caustic soda to the Bayer circuit (Smith, 2009). However, at present caustic soda consumed by forming DSP is not recoverable.

It is worth noting that settling behaviour of the red mud is of great economic concern since it impacts on purity of alumina products. Additionally, it has an environmental concern since it affects the final liquid content of the red mud (Li and Rutherford, 1996; Li, 2001). The settling behaviour of red mud is heavily influenced by the presence of iron minerals in the bauxites. Generally speaking, iron minerals with larger surface area and finer particle size, such as goethite or aluminous goethite, have relatively slow settling rate compared to iron oxides with smaller surface area and larger particle size, such as hematite.

2.1.3.3 Precipitation

After solid separation, the green liquor from clarification is cooled and seeded with gibbsite and agitated for a period to precipitate alumina. The reverse reaction of digestion takes place (Atasoy, 2005).

$$NaAl(OH)_4 \rightarrow Al(OH)_3 + NaOH \quad \textbf{(2.5)}$$

Spent caustic liquor essentially free from solid is then returned through an evaporation operation where it is re-concentrated, heated and recycled to dissolve more alumina in the digesters. Fresh caustic soda is added to the stream to make up for process losses (Mylona *et al.*, 2008).

2.1.3.4 Calcination

$Al(OH)_3$ is washed prior to calcination and then heated to form smelting grade alumina.

$$2Al(OH)_3 \rightarrow Al_2O_3 + 3H_2O \quad \textbf{(2.6)}$$

2.2 Goethite and aluminous goethite in the Bayer process

2.2.1 Properties and morphology of goethite/ Al-substituted goethite

Goethite, α-FeO(OH)[1], is a common iron oxy-hydroxide mineral found in soil and other low-temperature environments. The formation of goethite is generally through the weathering of other iron minerals. However, it may also be formed as a primary iron mineral in hydrothermal deposits. Goethite has an orthorhombic unit cell with a = 0.9956 nm, b = 0.30215 nm, c = 0.4608 nm (Szytuta *et al.*, 1968; Cornell and

[1] Information for the other major iron oxides can be found in Appendix I.

Schwertmann, 2003). The goethite structure (**Figure 2.2**) is based on a hexagonal close packing (*hcp*) of anions (O^{2-} and OH^-) with Fe^{3+} ions occupying half of the octahedral sites (Gualtieri and Venturelli, 1999; Cornell and Schwertmann, 2003).

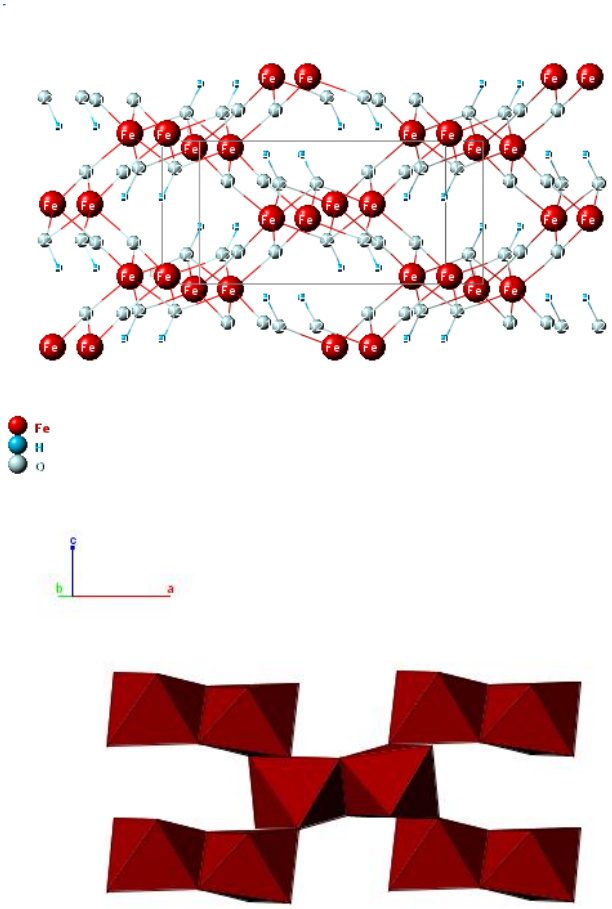

Figure 2.2 Structure of goethite. Top: Atom-bond model with unit cell outlined; bottom: Octahedral model.

The basic morphology of goethite is acicular crystal although it appears in a range of shapes and size (Pomiès *et al.*, 1999; Cornell and Schwertmann, 2003). Acicular goethite crystals range in size from tens of nm to several microns. The forms and the crystal shape are respectively shown as **Figure 2.3** and **Figure 2.4**. A well-crystallized goethite would particularly present the forms shown in Figure 2.3. Goethite morphology is strongly influenced by factors such as pH and the ambient environment during the formation.

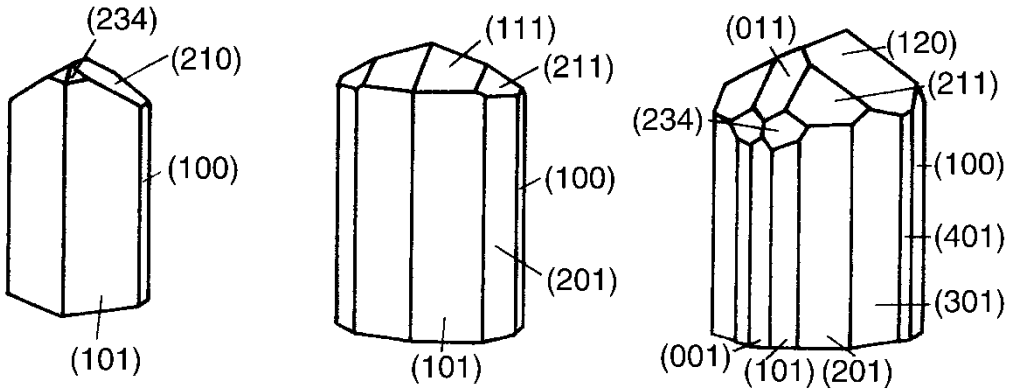

Figure 2.3 Crystal forms of goethite (Cornell and Schwertmann, 2003)

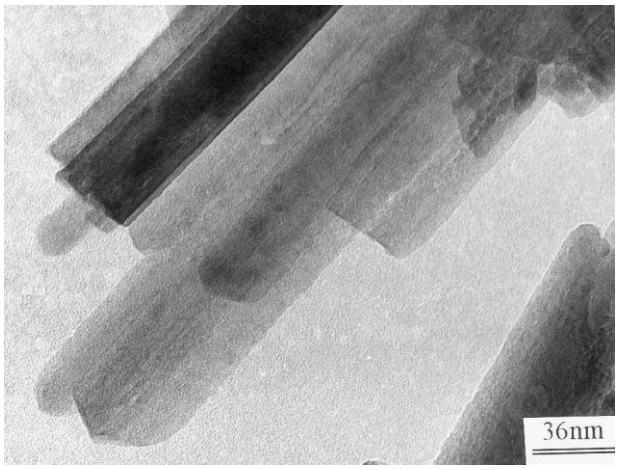

Figure 2.4 TEM pattern of synthetic acicular goethite. (Pomiès *et al.*, 1999)

An XRD pattern of well-crystallised goethite is shown in **Figure 2.5**. The parameters provided by XRD, such as line position, width and intensity, are derived from the nature of the goethite crystal, from which the quantity of the oxides, its unit cell parameters and its crystal size can be deduced (Cornell and Schwertmann, 2000). More importantly, the extent of Fe substitution by Al in Al-goethite may be calculated by deviations from the unit cell parameters obtained from an XRD of a pure goethite, which has been one of the most important methods to estimate the amount of Al substitution in Al-goethite (Schulze, 1984; Li *et al.*, 2006a). Apparently, the deviation is attributed to the difference of the ionic radius of Fe^{3+} and the foreign cation Al^{3+}.

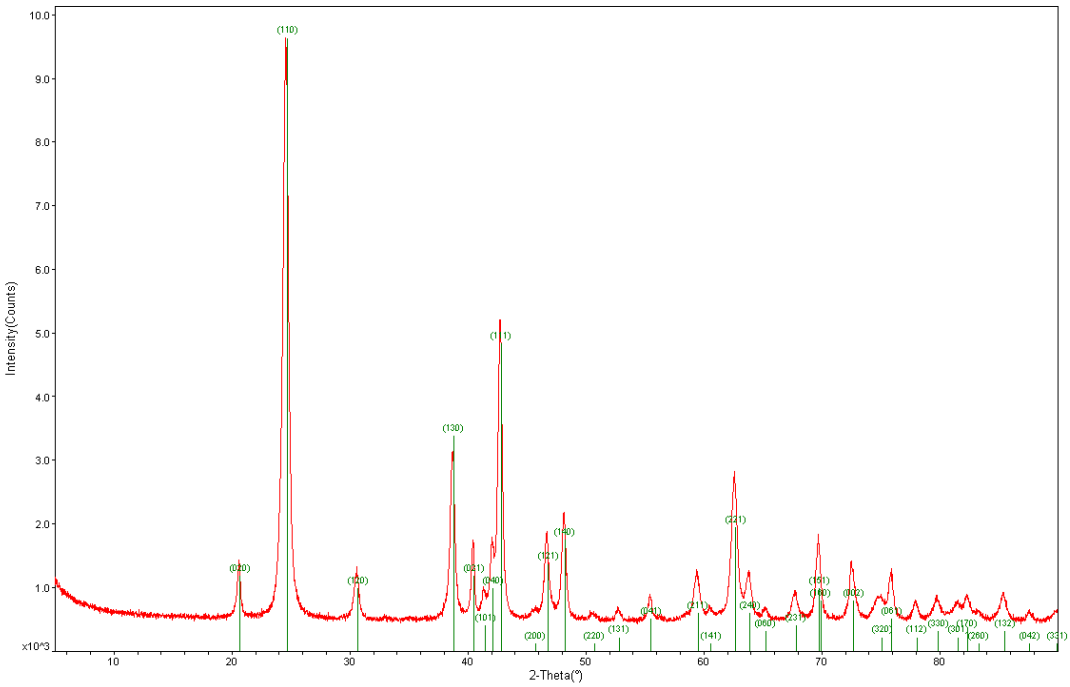

Figure 2.5 XRD pattern of well-crystallised goethite

Isomorphously substituted aluminium for iron in goethite has been well studied (Li *et al.*, 2006a). It is worth noting that the aluminium substituted goethite in literature has been expressed in various ways, among which Al-substituted goethite, Al-goethite and aluminous goethite are most commonly used. In this thesis, Al-goethite will be strictly limited between these three expressions unless otherwise mentioned. Al^{3+} can replace part of Fe^{3+} in synthetic and natural goethite due to the similarity of orthorhombic lattice structures of diaspore (α-AlOOH) and goethite (α-FeOOH). The Al^{3+} substitution reduces lattice constants because the size of Al^{3+}, 0.053nm, is slightly smaller than that of the Fe^{3+}, 0.065 nm (Schulze, 1984; Schulze and Schwertmann, 1984; Sudakar *et al.*, 2004b; Li *et al.*, 2006a). Schulze (1984) and Sudakar et al. (2004b) concluded that the substitution does not change the goethite structure itself but the size of unit cell, as evidence from X-ray diffraction (XRD) shows. With increasing Al^{3+} substitution, the goethite crystallites become smaller observed from transmission electron microscopy (TEM) (Sudakar *et al.*, 2004b). TEM micrographs of different Al substitution ratio are shown in **Figure 2.6**.

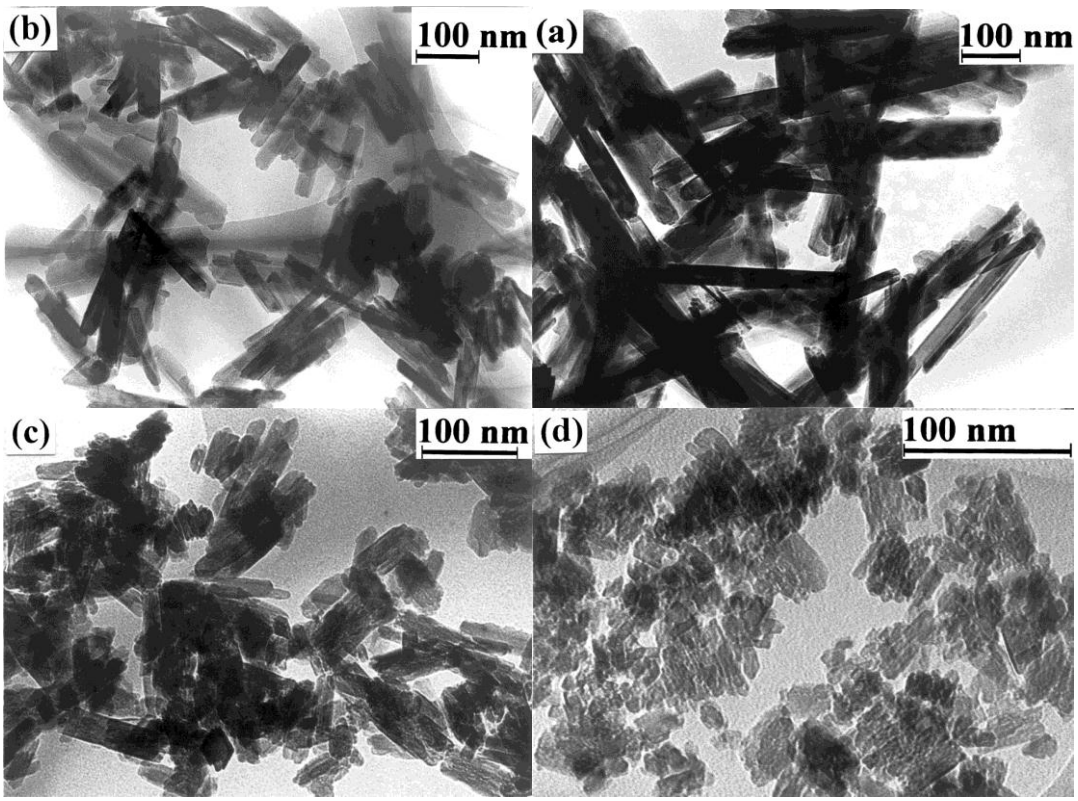

Figure 2.6 Electron micrograph of Al-substituted goethite for different %mol of Al^{3+}. (a) 0% Al; (b) 0.4% Al; (c) 2% Al; (d) 9%. (Sudakar *et al.*, 2004b)

Figure 2.7 shows the X-ray diffraction patterns of goethite with different amount of Al substitution (Sudakar *et al.*, 2004b). Sample HG is the crystalline XRD pattern corresponding to that of phase-pure goethite (α-FeOOH), which has the space group *Pbma*. It should bear in mind that the space group *Pbma* for goethite replaced the previous *Pbnm* decade ago (Hahn, 1996). Thus, the *c* axis, which has been used to estimate the degree of Al substitution in this study, is now the *b* axis (Schwertmann *et al.*, 2000). However *c* axis is still used in this thesis to keep consistent with a number of the researches on this issue which had carried out before this replacement. Full width at half maximum (FWHM) of the (110) peak increases as a result of decrease in particle size which occurs with increasing Al^{3+} substitution. In addition, slight shifts in the peak position are observed in Al-substituted goethite, which indicate the changes in lattice parameters. Concern also has been raised on the obvious disappearance of some peaks as Al increases. However, the paper where the figure was extracted does not provide the explanation of the disappearance of those peaks.

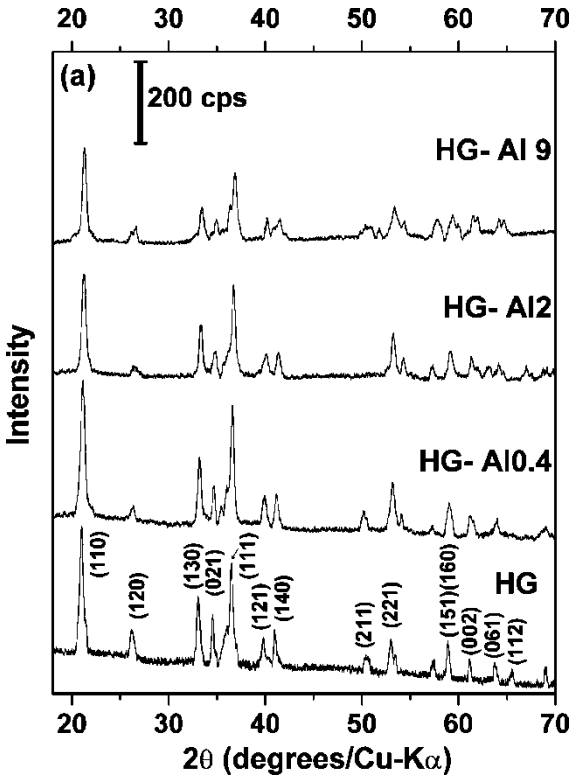

Figure 2.7 XRD patterns of Al-substituted goethite samples (HG Al_x; x = 0, 0.4, 2 and 9 mol % Al). (Sudakar *et al.*, 2004b)

2.2.2 Impacts of iron oxides to the Bayer process

The most common iron minerals in bauxite are goethite ($\alpha - FeOOH$)/Al-goethite ($Al_xFe_{1-x}OOH$) and hematite (Fe_2O_3) (Hind *et al.*, 1999). These iron minerals are also the major solid components in red mud tailings resulting from the Bayer process. The type of iron minerals and the relative ratio between them in the original bauxite are the key factors that influence the settling behaviour of red mud (Li and Rutherford, 1996; Li, 2001). **Table 2.2** shows the mineralogy of some typical bauxite. Goethite or aluminous goethite is the predominant iron oxide in some of the bauxites.

Table 2.2 Mineralogy of some typical bauxites

Element (%)	Minerals	Weipa [a]	Guinea Boke [b]	Darling Range [c]	Jamaica [d]
Al_2O_3	Gibbsite $Al(OH)_3$	46.2	73.1	50	65.2
	Boehmite $AlOOH$	19.0	2.5	0.5	2.0
Fe_2O_3	Goethite/Al-goethite $FeOOH / (Al_xFe_{1-x})OOH$	1.8	8.3	17	19.7
	Hematite Fe_2O_3	10.7	7.8	12	5.0
SiO_2	Kaolin, $Al_2O_3 \cdot 2SiO_2 \cdot 2H_2O$	16.0	2.3*	0.6	3.0
	Quatz, SiO_2	Trace*	0*	11	NR
TiO_2	Anatase TiO_2	2.0*	1.8	1.6	2.7
	Rutile TiO_2	0.7*	1.5	0	0.9

a. McArthur (2006) b. Suss et al. (2010) c. Anand et al. (1991) d. Kirwan et al. (2009) *. Whittington (1996). NR=not reported

In alumina industry, bauxite rich in goethite cause adverse effect on the Bayer process, while the presence of hematite in bauxite, on the other hand, is favourable to the process. The presence of Al-goethite in bauxite, in particular, can retard the settling rate of red mud derived from bauxite with Al-goethite, inhibit the recovery of alumina, cause extra caustic soda and alumina losses, and reduce the quality of alumina production.

2.2.2.1 Retardation of settling rate

The results of many studies have indicated that iron oxides in bauxite have significant effects on the settling behaviour of red mud, and that the presence of goethite or Al-goethite is the main problem for red mud that retards the settling rate (Davis, 1973; Orban *et al.*, 1973; Parekh and Goldberger, 1976; Grubbs *et al.*, 1980; Ostap, 1984; Li and Rutherford, 1996). Grubbs et al. (1980) stated that slow settling of red mud is related to bauxite in which the main iron oxide is Al-goethite rather than hematite. Davis (1973) further indicated that higher hematite to goethite ratio causes quicker settling. Orban et al. (1973) concluded that red mud containing hematite has a higher settling rate than that containing goethite or Al-goethite. In agreement with the above

conclusion, Solymar et al. (1992) suggested that increasing the temperature of digestion can lead to a faster settling rate for the bauxite with Al-goethite due to the transformation of Al-goethite to hematite.

Mineralogical, chemical and physical properties of the source bauxite, especially specific surface area and specific gravity, significantly influence settling behaviours of red mud.

Generally, larger specific surface areas of iron minerals in bauxite result in lower settling rates of red mud. Orban et al. (1973) suggested that the settling rate of red mud is related to the surface area of particles in that mud. The greater the surface area of iron minerals, the lower the settling rate of red mud. For example, the surface area (m^2/g) of iron minerals decreases in the order: Al-goethite > goethite > hematite. However, their settling rates are exactly in reverse order.

Settling of bauxite residues is also influenced by the specific gravity of its components. For example, settling rate in bauxites containing hematite is faster than those containing goethite or Al-goethite as major iron minerals, due to its larger specific gravity (about 4.9- 5.26) compared to goethite (about 3.3-4.3) and to Al-goethite (about 3.2). Li and Rutherford (1996) showed that the settling behaviours of Brazil bauxites was significantly related to their source minerals, that is, mineralogical and chemical composition. They further concluded that the specific gravity plays a dominant role in settling behaviour.

Parekh and Goldberger (1976) systemically studied the settling behaviour of red mud using various techniques to identify the influencing factors. Their research is largely in agreement with goethite present in the bauxite retarding the settling rate due to its larger surface area and smaller specific gravity compared to hematite containing bauxite. Moreover, they revealed that chemical factors such as pH and the presence of metal salts such as ferric (Fe^{3+}), and magnesium (Mg^{2+}) appear to have little effect on the settling rate.

In summary, the presence of very fine iron minerals, especially Al-goethite, is the major cause of slow red mud settling rate due to its low specific gravity and high surface area.

2.2.2.2 Difficulty of alumina recovery

It is widely accepted that aluminous goethite is actually a diaspore-goethite solid solution (Wolska and Schwertmann, 1993; Blanch *et al.*, 2008). However, alumina present in aluminous goethite is not recoverable under the low temperature Bayer digestion (~150ºC) and thus reduces total alumina recovery. Research on alumina recovery from Al-goethite in the Bayer process suggested that alumina content cannot be extracted unless the goethite is transformed into hematite or magnetite under high temperature (~250ºC) Bayer digestion (Crombie *et al.*, 1973; Garing *et al.*, 1980; Murray *et al.*, 2009). However, research carried out by Suss and Maltz (1992) indicated that part of alumina can be digested out from aluminous goethite structure at a temperature 105 ~ 120ºC if Al substitution is higher than 18 ~ 20 mol %. No further detailed evidence was reported for the finding. Nevertheless, aluminous goethite present in bauxite causes difficulty of alumina recovery so that higher digestion temperature or enhancement additive is needed to improve the conversion of alumina. It is usually considered a ~250ºC digestion temperature or lime addition to the system for the goethitic bauxite digestion to have goethite/Al-goethite transformed to hematite to release the alumina trapped in Al-goethite and also get a better settling result.

2.2.2.3 Extra losses of caustic soda and alumina

In a clarification circuit, goethite-containing red mud causes high swelling and low thickening ability, which causes extra caustic and alumina losses in the circuit (Suss *et al.*, 2010).

2.2.2.4 Reduction of the quality of alumina production

The fine aluminous goethite is floated by the air bubbles and can be carried into the thickeners overflow, which reduces the quality of the product alumina (Suss *et al.*, 2010).

2.2.3 Strategies to eliminate the negative effects: transformation

The disposal and management of red mud has been one of the most challenging problems in the alumina industry. So far, several techniques have been taken into consideration, of which acid washing to lower the pH, flocculation to increase the mud settling velocity, dewatering by centrifugation and electro-kinetic techniques are common treatments (Li, 2001). However, these methods were either ineffective or not

cost effective. One of the most effective ways of combating the problem is to transform goethite or Al-goethite to hematite during the digestion.

It is desirable to convert the goethite or Al-goethite into hematite to counter the negative effects that Al-goethite brings to the Bayer process and encourage better performance obtained with hematite. By transforming Al-goethite to hematite, it is possible to not only extract its alumina content, but also to produce a red mud which has acceptable properties of settling (Crombie *et al.*, 1973). It therefore reduces the losses of alumina and caustic soda.

The two principal methods of transformation of goethite or Al-substituted goethite to hematite are thermal transformation and hydrothermal transformation (Murray *et al.*, 2009).

2.3 Thermal transformation

2.3.1 Principles

Phase transformations normally occur during heating or mechanical grinding of solid goethite/ Al-goethite (Diamandescu *et al.*, 1993; Wolska *et al.*, 1994; González *et al.*, 2000; Ruan *et al.*, 2001). Increasing temperature induced by either heating or chemical treatment causes the dehydration of goethite/ Al-goethite. The dehydration transformation is topotactic that the habit plan remains unchanged (González *et al.*, 2000). The dehydration of goethite or Al-goethite to hematite is described in the following equations (Cornell and Schwertmann, 2000; Walter *et al.*, 2001; Sudakar *et al.*, 2004b; Atasoy, 2005):

Goethite dehydration:

$$2\alpha - FeOOH \rightarrow \alpha - Fe_2O_3 + H_2O \qquad \textbf{(2.7)}$$

Goethite

Al-goethite dehydration:

$$2Fe_{1-x}Al_xOOH \rightarrow Fe_{2(1-x)}Al_{2x}O_3 + H_2O \qquad \textbf{(2.8)}$$

Al-goethite

2.3.2 Transformation temperature

Thermal transformation of goethite/Al-goethite has been widely investigated. In terms of source of materials, research on both natural (Mendelovici and Yariv, 1981; Frost *et al.*, 2003; Prasad *et al.*, 2006) and synthetic goethite (Fey and Dixon, 1981; Walter *et al.*, 2001; Ruan *et al.*, 2002b; Sudakar *et al.*, 2004b) were carried out, while thermal transformations through either heating (Walter *et al.*, 2001; Ruan *et al.*, 2002b; Sudakar *et al.*, 2004b) or mechanical treatment (Mendelovici and Yariv, 1981; González *et al.*, 2000) were also investigated. A number of analytical techniques were employed to study the solid state transformation, such as DSC, TGA, TEM, XRD, Synchrotron (XRD), IR (FTIR) and Mossbauer spectra.

There is a general agreement on the fact that the temperature of thermal transformation rises with the increase of Al substitution in Al-goethite. However, the temperature range for **complete** transformation reported by various authors is apparently different as a consequence of different proposed mechanisms.

The suggestion of temperature range for complete transformation to hematite usually splits into two groups, low temperature range at 200-400 ºC and high temperature ranging from 800 ºC to 1050 ºC. Both groups supported that the initial transformation of pure goethite to hematite happens at a temperature range 200-350 ºC and shifts to higher temperature range near 400 ºC as Al substitution increases in Al-substituted goethite (**Figure 2.8**). Slight difference on this temperature range between authors was reported. Wolska et al. (1992b) studied this transformation by XRD and DTA using synthetic Al-goethite. They reported the transformation of pure goethite similarly started from 520K (247 ºC) and concluded at about 593K (320 ºC). With Al substitution for Fe up to 14 mol %, the temperature range shifted to 280-360 ºC, which was slightly lower than that obtained by Schulze and Schwertmann (1984) in **Figure 2.8**. However, the most conflicting conclusion between the two groups is the temperature range for complete transformation of goethite/Al-goethite to hematite. Researchers who supported the low temperature range for complete transformation believed that transformation at a temperature of ~400 ºC reached a full goethite to hematite conversion (González *et al.*, 2000; Walter *et al.*, 2001; Frost *et al.*, 2003; Prasad *et al.*, 2006), while the other authors suggested that a full hematite conversion requires a much higher temperature at 800-1050ºC. Wolska et al. (Wolska, 1988; Wolska *et al.*, 1992b) studied the transformation using thermal analysis techniques combined with XRD and IR and reported the

formation of an intermediate during the dehydration of goethite in the temperature range of 180-250 ºC. This phase eventually transformed into hematite in the temperature range of 800-1050 ºC. Gualtieri and Venturelli (1999) investigated the transformation of goethite using real-time XRD and also reported that the dehydration of goethite stated from 200 ºC and concluded at ~270 ºC. The phase, an intermediate called proto-hematite, obtained during this dehydration finally converted to hematite at ~800 ºC.

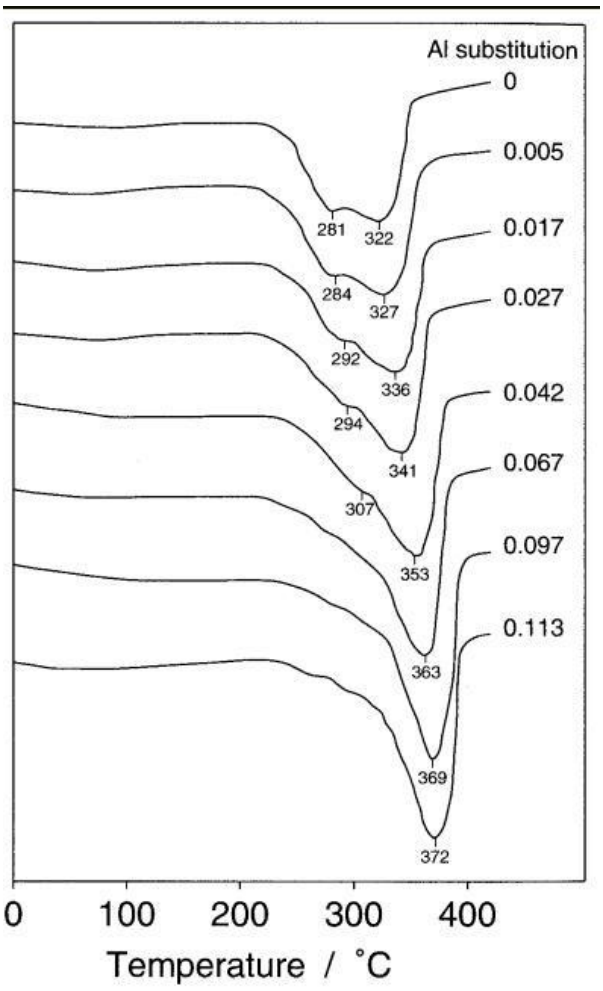

Figure 2.8 DTA curves of goethites with increasing Al substitution Al/(Al+Fe). (Schulze and Schwertmann, 1984)

The difference for the complete transformation of goethite to hematite gives rise to two different proposed mechanisms of thermal transformation of goethite to hematite, direct transformation and transformation via intermediate.

2.3.3 Mechanism

The mechanism of thermal transformation from goethite to hematite has been widely investigated. It has been suggested that the thermal transformation can be either (a) a transformation via an intermediate superstructure phase referred to as 'hydro-hematite' or 'proto-hematite' before the final conversion to hematite (Mendelovici and Yariv, 1981; Wolska, 1988; Wolska *et al.*, 1992a; Wolska *et al.*, 1994; Gualtieri and Venturelli, 1999; Ruan *et al.*, 2002b), or (b) a direct transformation from goethite to hematite (Gonzâlez *et al.*, 2000; Walter *et al.*, 2001; Frost *et al.*, 2003; Prasad *et al.*, 2006). (a) is described by equation 2.9, while (b) is written as 2.10. In (a), it is generally assumed that the OH^- occupies the O^{2-} -position in the intermediate hematite structure forming associates along with vacancies in the Fe^{3+} sub-lattice (Wolska, 1988).

Transformation via intermediate:

$$2\alpha - FeOOH \rightarrow \text{superstructure} \rightarrow \alpha - Fe_2O_3 + H_2O \qquad \textbf{(2.9)}$$

Direct transformation:

$$2\alpha - FeOOH \rightarrow \alpha - Fe_2O_3 + H_2O \qquad \textbf{(2.10)}$$

2.3.3.1 Transformation via intermediate

Transformation of goethite via intermediate has been recognised for authors who concluded that goethite fully converts to hematite at temperature range of 800 - 1000 ºC. However, the identification of intermediate reported for this proposed mechanism is in fact very vague in literature. The intermediates are normally referred to as hydro-hematite or proto-hematite, which some used quite randomly while the others defined them by stages of formation of intermediate species.

The intermediate is believed to be a non-stoichiometric species that is hardly detected by XRD. Ruan et al. (Ruan *et al.*, 2001; Ruan *et al.*, 2002b; Ruan *et al.*, 2002a) investigated the de-hydroxylation behaviour of synthetic goethite samples using a combination of Fourier transform infrared (FTIR) spectroscopy and X-ray diffraction (XRD) during thermal transformation of goethite to hematite in the temperature range of 180-270 ℃. The vibrations of non-stoichiometric hydroxyl units were detected in FTIR

spectroscopy, which indicates that the formation of "hydro-hematite" is likely to take place during the thermal transformation of goethite to hematite. Mendelovici and Yariv (1981) investigated the thermal dehydration of natural Al-goethite by IR spectroscopy and suggested the formation of proto-hematite takes place at temperature above 600 ℃. For the above research, the existence of the intermediate was acknowledged but the definition of hydro- or proto-hematite is quite confusing.

However, Wolska (1988) provided a relatively clearer definition for the intermediate. Formation of a "hydrated" hematite was reported during the thermal dehydration of goethite at temperatures ranging from 180-250 ℃ and the "hydrated" species finally transforms into hematite during further dehydration in the temperature of 900-1100 ℃. The general formula for this phase is $Fe_{2-x/3}O_{3-x}(OH)_x (1 \geq x \geq 0)$, in which value x provides the basis for the distinction between different species obtained during the dehydration, i.e. proto-hematite ($1 \geq x > 0.5$), hydro-hematite ($0.5 \geq x > 0$) and hematite ($x=0$). The mechanism of thermal transformation of goethite to hematite via intermediate provided by Wolska (1988) was described as a continuous dehydroxylation process: $goethite \rightarrow protohematite \rightarrow hydrohematite \rightarrow hematite$. The changes of structure accompanied by the gradual removal of water and rearrangement of cations can be detected by FTIR and XRD. The changes bring an apparent gradual decrease of peaks broadening and an increase of intensity of cation-depending reflections on XRD patterns (**Figure 2.9**), but to FTIR, it shows a replacement of Fe-O vibration bands and disappearance of OH-vibration bands (**Figure 2.10**). The dehydration species at different steps during the thermal transformation can be distinguished by the value of x in the general formula, $Fe_{2-x/3}O_{3-x}(OH)_x$.

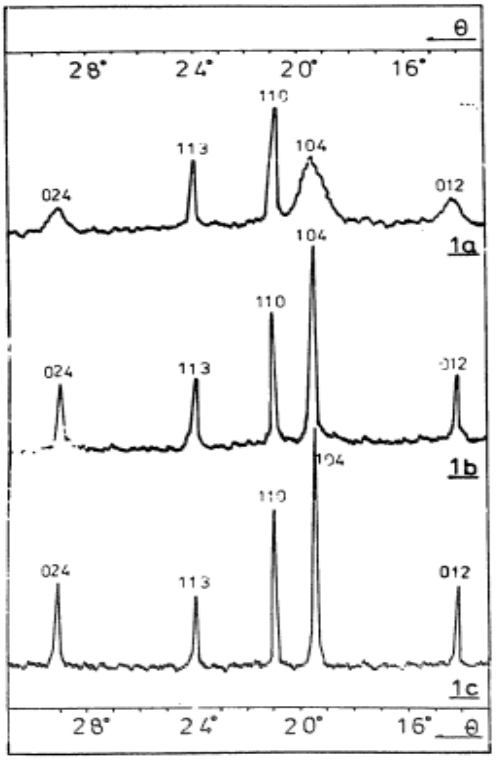

Figure 2.9 XRD patterns of samples with hematite structure obtained by dehydration of well-crystallized goethite at a) 200 ℃, b) 500 ℃ and c) 900 ℃. (Wolska, 1988)

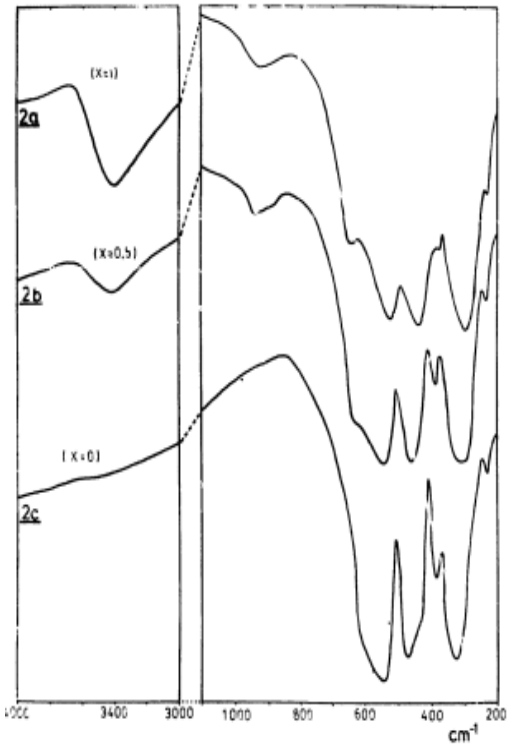

Figure 2.10 Infrared spectra of samples with hematite structure obtained by dehydration of well-crystallized goethite at a) 200 ℃, b) 500 ℃ and c) 900 ℃. (Wolska, 1988)

2.3.3.2 Direct Transformation

The transformation of goethite to hematite may directly proceed to hematite rather than form such intermediates (Cornell and Schwertmann, 2000; Gonzâlez *et al.*, 2000; Walter *et al.*, 2001; Frost *et al.*, 2003; Prasad *et al.*, 2006). Walter et al. (2001) investigated goethite samples with various sizes using the characteristics of XRD, TEM, DTA, IR, DSC and TG. **Figure 2.11** shows the DTA plots of the samples. An endothermic double peak was observed at around 272 ℃ and 315 ℃ for samples with large particle size, while only single endothermic peak was found in small particle size goethite. They questioned the existence of a stable intermediate by the observed result although a double peak emerged in the plots, because a double-peak should be expected as well during the dehydration of the sample with small particle size (goethite-4).

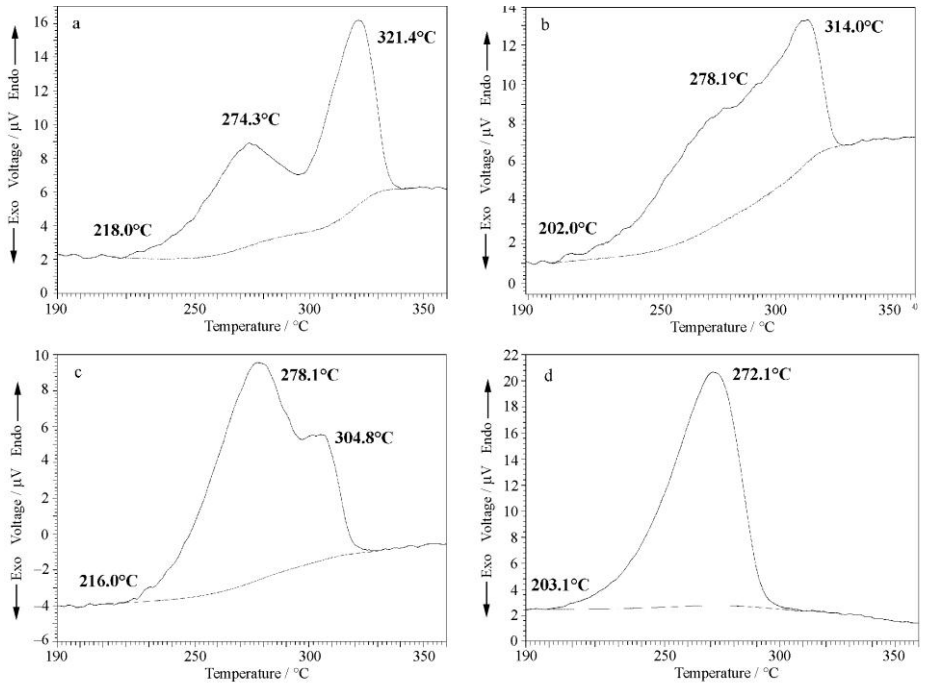

Figure 2.11 DTA-plots of a: goethite-1 (a = 10 m^2g^{-1}; g = 1.2×0.25×0.25 10^{-18}m3); b: goethite-2 (a = 14.5 m^2g^{-1}; g = 1.0×0.15×0.15 $10^{-18}m^3$); c: goethite-3 (a = 67 m^2g^{-1}; g = 0.3×0.03×0.03 $10^{-18}m^3$); d: goethite-4 (a = 149 m^2g^{-1}; g = 0.1×0.01×0.01 $10^{-18}m^3$). (a: specific surface area; g: particle geometry; heating rate: 5 °C min^{-1}) (Walter *et al.*, 2001).

Walter et al. (2001) proposed the following model (**Figure 2.12**) for the mechanism of the dehydration process according to the thermal analysis combined with TEM results. During the dehydration process, the structure of goethite leads to the initial dehydration producing channels along c axis along which water diffuses and escapes (the formation of first peak in **Figure 2.11**). The regions in between the channels become hematite-like. If the dehydration process is not finished before the hematite regions grow together, blocking the channels, the water is trapped and must find another pathway, and this gives rise to the second peak (samples with large particle size). However, in case of very small particle size (goethite-4) the complete dehydration can be achieved before the thickness of hematite forms, thus no further barrier needs to be conquered (single peak).

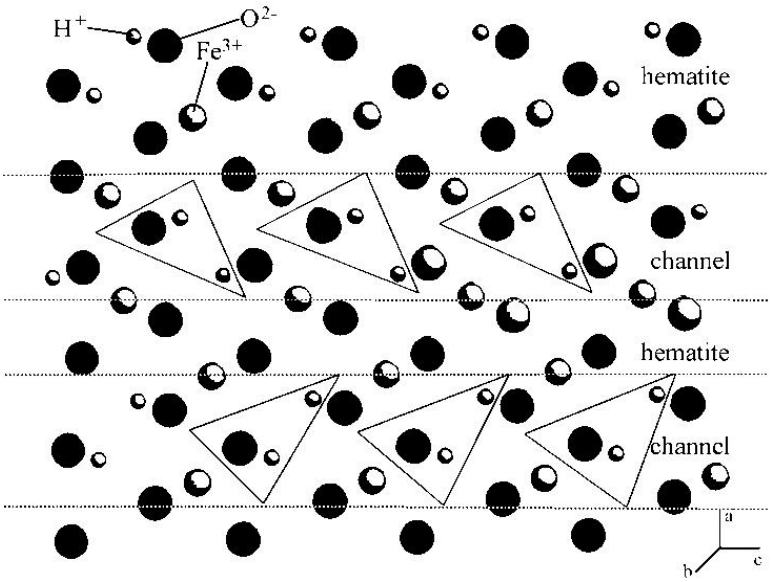

Figure 2.12 Excerpt of the goethite crystal structure. The water molecules formed by dehydration are marked by triangles. (Walter *et al.*, 2001)

Direct transformation mechanism suggests that thermal conversion of goethite is a topotactic[2] reaction, that is, the original goethite shape remains intact in hematite under 800 ºC (Gialanella *et al.*, 2010). Water removal from acicular goethite crystal only creates pores. Recrystallization occurs only at temperatures in excess of 800 ºC. Overall, the direct transformation of goethite is a particle size-dependent mechanism which also applicable to Al-goethite dehydration. Al-goethite thermal transformation can be also found in **Figure 2.8**. There are double-peak endothermic peaks in goethite with relatively low Al-substitution (Al ≤ 4.2 mol %), while only single endothermic peaks occur in higher Al substitution goethite.

2.3.4 Barriers

The thermal transformation cannot substantially modify the morphology of the hematite generated from heat-treated goethite until the temperature exceeds 800 ºC. Thus, it is unlikely that the settling problems in the Bayer process caused by goethite morphology can be easily solved through thermal transformation. In addition, thermal transformation means an independent operation system from the Bayer process in which additional energy and equipment are required. The high operation temperature ranging from 350 to

[2] Topotactic transformation: is characterized by internal atomic displacements, which may include loss or gain of material, so that the initial and final lattices are in coherence.

nearly 800 ºC for the transformation is also considered as an energy consuming process. Therefore, thermal transformation of goethite to hematite would not be the ultimate solution for the problems in relation to goethite in the Bayer process, but it could provide possibilities for the pre-treatment of bauxite and red mud to remove iron from the Bayer liquor (Murray *et al.*, 2009). For example, Yamada et al. (1974) reported that an efficient way to remove Fe compounds from the Bayer liquor is to calcine red mud by transforming goethite to hematite under optimised calcination temperature of 400 ℃. However, such a thermal pre-treatment would render the alumina phases more difficult to extract and therefore be uneconomic.

2.4 Hydrothermal transformation

2.4.1 Principles

Hydrothermal transformation of goethite to hematite in caustic soda or sodium aluminate solution is generally believed to be one of the most effective ways to eliminate the adverse effect of goethite to the Bayer process. More importantly, this thermal transformation can be implemented simultaneously in the Bayer digestion step due to the similar requirement for the reaction environment. In such cases, the transformation would possibly take advantage of the Bayer environment to get goethite/Al-goethite converted to more favourable hematite without requiring plenty of additional energy consumption and equipment. The hydrothermal transformation of Al-goethite to hematite is described as follows.

$$\underset{\text{Al-goethite}}{2(Fe_{1-x}Al_x)OOH} + 2xNaOH + (1-x)H_2O \rightarrow \underset{\text{Hematite}}{(1-x)Fe_2O_3} + 2xNaAl(OH)_4 \qquad \textbf{(2.11)}$$

As shown in Equation 2.11, Al-goethite reacts with caustic solution to form hematite during the digestion so that aluminium trapped in the goethite structure can be released into the Bayer liquor and also desirable iron oxides, hematite, can be obtained. As a result, both clarification problem and aluminium recovery would be achieved by the transformation of goethite to hematite.

In the following section **2.4,** kinetics and mechanism of hydrothermal transformation of goethite/Al-goethite to hematite in the Bayer digestion step will be reviewed through

the existing literature. The optimisation of the transformation under the Bayer environment will be also mentioned.

2.4.2 Kinetics of hydrothermal transformation

Kinetics of hydrothermal transformation of goethite to hematite has been widely studied (Crombie *et al.*, 1973; Brown and Tremblay, 1974; Garing *et al.*, 1980; Basu, 1983; Suss and Maltz, 1992; Li, 2001; Murray *et al.*, 2009; Suss *et al.*, 2010). Results from these studies suggested that digestion temperature, caustic soda (or free caustic) concentration, the presence of hematite and anatase to different extent all affect the hydrothermal transformation of goethite to hematite.

2.4.2.1 Effect of digestion temperature

Experimental evidence has shown that temperature plays a significant role on the hydrothermal transformation of goethite to hematite. High temperature favours hydrothermal transformation of goethite to hematite. The digestion temperature for the Bayer process varies from 145 ºC to 250 ºC depending on the types of alumina in bauxite. As mentioned, gibbsite normally requires a relatively lower digestion temperature (~150 °C), while digestion of boehmite bauxite prefers a much higher temperature (~250 °C). During this temperature range, it is unlikely that transformation of goethite to hematite occur in a low temperature below 190 °C. Li (1998) studied hydrothermal transformation in the Bayer process and concluded that neither hematite, nor goethite, nor aluminous goethite is attacked during digestion at a low-temperature (135 – 143 ℃). Basu (1983) also indicated that hematite starts to form in Bayer liquor once the digestion temperature is over 175 ℃ and, similarly, Suss and Maltz (1992) believed the formation of hematite starts from 190 ℃. Therefore, the hydrothermal transformation of goethite to hematite only happens beyond some 200 ºC in caustic solution. In Li's study (Li, 1998), a temperature ranging from 220 to 250 ºC was reported to achieve the dissolution of goethite to hematite in caustic soda. Although slightly difference of the temperature range for the hydrothermal transformation were suggested, the majority of the studies supported that the digestion temperature range of 225 to 275 ℃ is the ideal temperature zone to achieve a fully or nearly fully transformation to hematite, of which temperature at 230 – 250 ℃ is practically employed (Crombie *et al.*, 1973; Brown and Tremblay, 1974; Garing *et al.*, 1980; Li, 2001; Murray *et al.*, 2009). It is worth noting that Al-goethite to hematite conversion in

caustic solution leads to a higher digestion temperature which is possibly even up to 320 ºC (Suss and Maltz, 1992).

2.4.2.2 Effect of caustic concentration

Caustic soda concentration is a strong driving force for goethite transformation and hematite crystallization which is clearly shown in **Equation 2.11**. Higher caustic concentration gives rise to a faster transformation rate (Murray *et al.*, 2009). Basu (1983) investigated the influence of free caustic concentration to the transformation of goethite to hematite in both pure caustic and sodium aluminate solution (**Figure 2.13**). She found that the transformation rate increases with increasing free caustic concentration. In Murray et al.'s research (2009), rate constant k increased rapidly from $5.9x10^{-4}$ s^{-1} to $1.63x10^{-3}$ s^{-1} when increasing caustic soda concentration from 2.83 M to 4.53 M NaOH.

2.4.2.3 Effect of alumina content in the Bayer liquor

The presence of alumina in caustic solution also has impact on hydrothermal transformation of goethite to hematite in the Bayer digestion. **Figure 2.13** (Basu, 1983) shows the reaction rate of hydrothermal transformation of goethite in pure caustic and sodium aluminate solution (Bayer liquor). The rate for the transformation in Bayer liquor is far smaller than that in pure caustic. The retardation by alumina content on the transformation is attributed to the greater solubility of goethite in sodium aluminate solution than that in pure caustic solution at a given concentration of free caustic. However, the study on the influence of alumina to the transformation is not widely conducted and therefore is not completely understood.

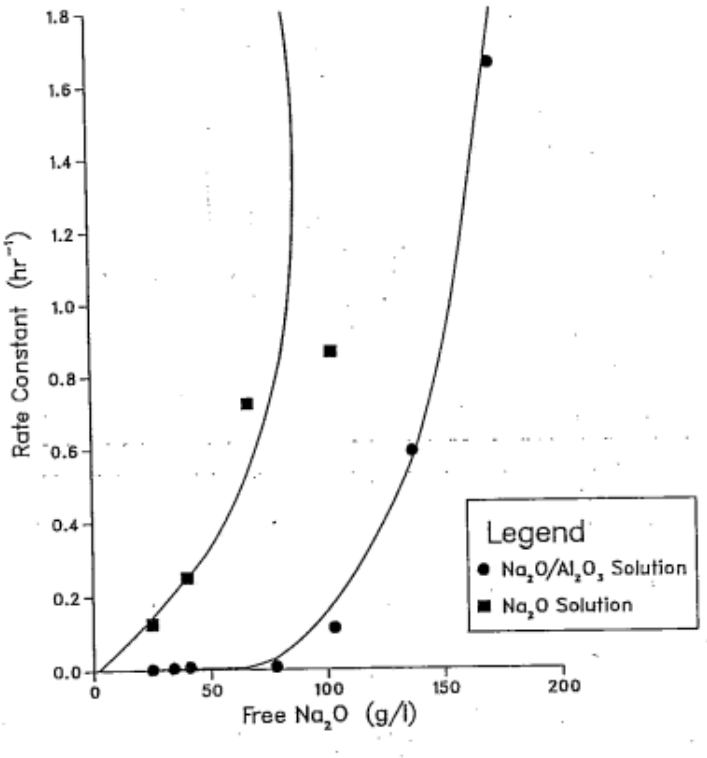

Figure 2.13 Rates of goethite transformation against free caustic soda concentration (Basu, 1983).

2.4.2.4 Effect of the presence of hematite seeding

Hematite seeding is another crucial factor to affect the conversion of goethite to hematite (Crombie *et al.*, 1973; Brown and Tremblay, 1974; Murray *et al.*, 2009). **Figure 2.14** shows the influence of goethite to hematite ratio to the extent of conversion (Murray *et al.*, 2009). The G/H ratio of 1.44 appears a better transformation performance than the other two higher ratios, which suggests increasing hematite seeds is beneficial to the transformation. Brown (1974) achieved a similar conclusion with addition of hematite (2% - 5%) to the goethite. The presence of hematite as a seed enhances the rate of transformation due to the increase of available surface area, which provides the growth sites for dissolved iron (Brown and Tremblay, 1974) and further enhance its precipitation (Crombie *et al.*, 1973).

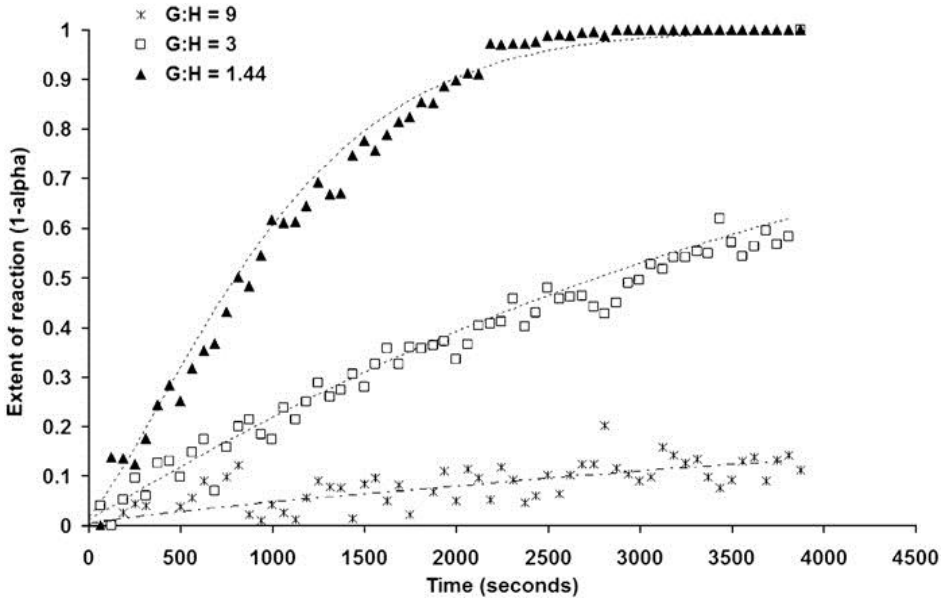

Figure 2.14 Influence of hematite seeding to the hydrothermal transformation of goethite to hematite. Digestion temperature = 250 ℃, pressure = 42 bar with NaOH = 3.77 M, $Al(OH)_3$ = 2.65 M and Na_2CO_3 = 0.24 M. (Murray *et al.*, 2009)

2.4.2.5 Effect of the presence of anatase

The anatase (TiO_2) present in bauxite is treated as an inhibitor to the transformation. No transformation of goethite to hematite had been detected in the presence of anatase at 250 ℃ even with hematite seeding (Murray *et al.*, 2009). This adverse effect of anatase is believed to only take place at temperatures greater than 180 ℃ (Croker *et al.*, 2006; Croker *et al.*, 2009). Brown and Tremblay (1974) reported that anatase significantly reduces the transformation of goethite to hematite in sodium aluminate solution at 260 ℃. It is likely that the addition of anatase interferes with the dissolution of goethite and, as a result, prevents the transformation to hematite (Murray *et al.*, 2009). It has been believed that this inhibition caused by anatase is attributed to the formation of amorphous or poor crystalline sodium titanate in Bayer digestion (Malts, 1991; Croker *et al.*, 2006; Xu *et al.*, 2010). Various forms of sodium titanates, $NaHTiO_3$, $Na_2Ti_6O_{13}$, $Na_2Ti_3O_7$ $2H_2O$, Na_2TiO_3 etc., have been reported as the consequence of different digestion conditions (Malts, 1991; Croker *et al.*, 2006). The sodium titanate, with a broad XRD reflection at ~0.83 nm, forms a protective coating or adsorbs on the surface of minerals such as goethite or boehmite, which leads to low alumina extraction from Al-bearing minerals or a further transformation of goethite to hematite.

2.4.2.6 Kinetics

The kinetics data obtained from published results revealed that temperature has significant effect on the hydrothermal transformation of goethite to hematite. It is widely recognised that the increase of temperature, free caustic concentration and hematite seeding positively raises the rate of transformation (King, 1971; Basu, 1983; Malts *et al.*, 1985; Authier-Martin *et al.*, 2001; Murray *et al.*, 2009). However, the presence of anatase and alumina heavily inhibit the transformation.

A study on kinetics of hydrothermal transformation of goethite to hematite was conducted by Murray et al. (2009). They used Sharp-Hancock method on the collected kinetic data and adopted a kinetic model, the Avrami-Erofe'v Equation 2.12, to establish a linear relationship between the extent of the transformation and time.

$$\alpha = 1 - \exp\left\{-\left(k\left(t - t_0\right)\right)^n\right\} \qquad \textbf{(2.12)}$$

where α is the extent of the reaction, t is the time and t_0 the induction time for the reaction, k is the relative rate constant and n the Avrami exponent.

The kinetics information, such as k and n, can be accordingly obtained from the slope and axis intercept by the conversion of the Equation 2.12 as follows.

$$\ln\left[-\ln\left(1-\alpha\right)\right] = n\ln t = n\ln k \qquad \textbf{(2.13)}$$

Through the kinetics analysis on the basis of the above theory, they calculated the reaction order n~1. This indicates that the reaction determining step is the reaction at the phase boundary between the product and the reagent. A surface controlled mechanism was therefore developed. Combined the kinetics results and Arrhenius equation (Equation 2.14), the activation energy for the transformation was obtained at 137.8 kJ^{-1}. This further gives the evidence that the transformation is more likely to be a surface controlled reaction, because general aqueous diffusion reaction has much lower activation energy (normally less than 21 kJ^{-1}).

$$k = A \cdot \exp\left(-\frac{Ea}{RT}\right) \qquad \textbf{(2.14)}$$

where A is pre-exponential constant, R the gas constant, and E_a the activation energy.

2.4.3 Mechanism

The mechanism of hydrothermal transformation of goethite to hematite under Bayer conditions is proposed to be a dissolution/re-precipitation process(Basu, 1983). This is driven by thermodynamics due to hematite being less soluble than goethite (Li, 1998; Cornell and Schwertmann, 2003). Basu (1983) revealed a classic mechanism from the outcomes of a series of experiments on the hydrothermal transformation of goethite to hematite. With increasing digestion temperature, the dissolution of metastable goethite occurs and the rate increases dramatically, which leads to the formation of an intermediate solute species, named as sodium ferrate ($NaFeO_2$). At high temperatures, the sodium ferrate is further precipitated as hematite (α-Fe_2O_3) shown in Equation 2.15:

$$\alpha - FeOOH \Leftrightarrow [NaFeO_2] \Leftrightarrow \alpha - Fe_2O_3 \qquad (2.15)$$

Sodium ferrate

A mechanism of dissolution of goethite and precipitation of hematite was accordingly established. Murray et al. (2009) suggested that the transformation of goethite to hematite is a surface controlled mechanism via dissolution/re-precipitation process. A schematic diagram of the proposed "dissolution/re-precipitation" mechanism for hydrothermal transformation according to the literature is given in **Figure 2.15**. However, the suggestion of hydrothermal transformation of goethite to haematite via the proposed intermediate, sodium ferrate, is not possible in the Bayer digestion conditions. In fact, the formation of sodium ferrate requires strongly oxidising conditions (Jeannot *et al.*, 2002) but these conditions are not able to be met in the Bayer process. It is, however, believed that the possible intermediate is still a species bearing Al and Fe in its structure(Cornell and Schwertmann, 2003).

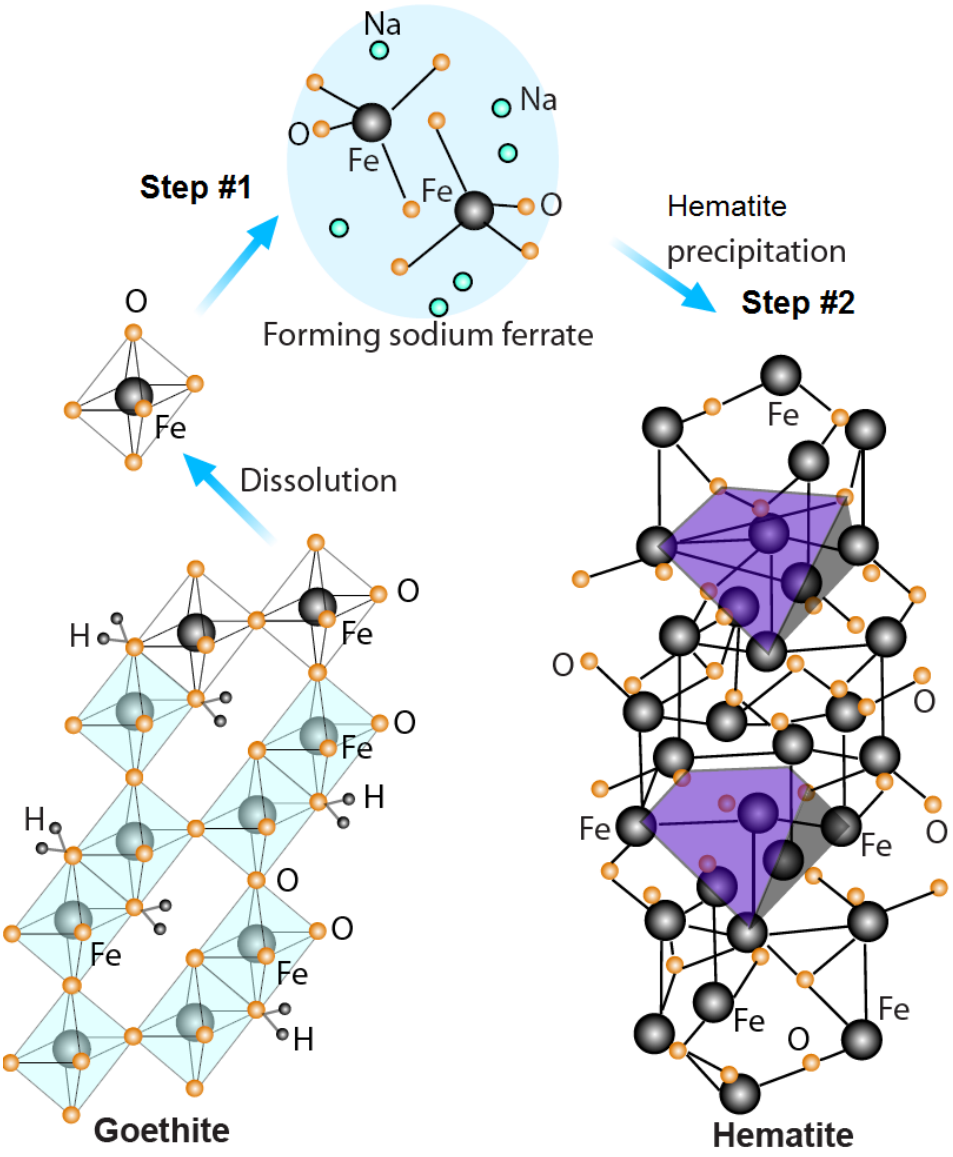

Figure 2.15 Schematic diagram of proposed mechanism for hydrothermal transformation of goethite to hematite (drawn after Basu (1983) and Murray et al. (2009)).

The adverse effect of alumina content to the transformation (see 2.4.2.3) may be also explained by the development of the mechanism of hydrothermal transformation (Basu, 1983). It should be noted that dissolution of goethite in sodium aluminate solution is considered as a reaction of goethite in the quaternary system Na_2O-Al_2O_3-Fe_2O_3-H_2O rather than a ternary system Na_2O-Fe_2O_3-H_2O in the pure caustic solution. Therefore, a solute species bearing Al and Fe is formed in the quaternary system, which is different with $NaFeO_2$ resulted from ternary system. The structure of the species could be similar with that of aluminous goethite given the fact that diaspore-goethite solid solution has been widely reported both in the laboratory and in nature.

2.4.4 Optimization of the hydrothermal transformation: Lime addition

As mentioned in kinetics of the transformation, the presence of anatase usually inhibits the transformation of goethite to hematite in the Bayer environment. In such cases, lime is widely used to improve the transformation. There is no doubt that the wide use of lime or calcium-containing additives is beneficial to the Bayer process. The main useful functions of lime have been well-studied and published (Crombie *et al.*, 1973; Garing *et al.*, 1980; Malts, 1991; Whittington, 1996; Croker *et al.*, 2009; Suss *et al.*, 2010; Xu *et al.*, 2010). The most emphasized benefits of lime are the enhancement of the extraction of alumina, the control of liquor impurities, the assistance of the removal of impurities from the pregnant liquor and the reduction of soda losses in the red mud (Whittington, 1996) .

The addition of lime or calcium-containing additives, such as $Ca(OH)_2$ and $CaCO_3$, can improve the hydrothermal transformation of goethite to hematite in the Bayer digestion from two aspects, improvement of the transformation and elimination of the negative effect of sodium titanate.

2.4.4.1 Enhancement of aluminous goethite to hematite transformation

The addition of lime simply enhances the hydrothermal transformation of goethite/Al-goethite to hematite in the Bayer digestion. Whittington (1996) indicated that, even at low temperature digestion (140 ℃), the partial conversion of goethite to hematite occurs to a Jamaican bauxite with adding lime (2% CaO). As temperature increases, the conversion significantly improves in the presence of lime. An increase from 25% without lime to 70% with adding lime has been achieved at 240 ℃. Suss et al. (2010) discovered that the alumina recovery from Al-goethite of Debele bauxite grows by ~50% at 260 ℃ with dosage of calcium containing additive 3% of bauxite weight.

It is generally believed that this enhancement is attributed to the catalytic impact of $Ca(OH)_2$ to the conversion of goethite in the Bayer liquor (Whittington, 1996; Whittington and Cardile, 1996; Suss *et al.*, 2010). The following mechanism of lime reaction in the bauxite slurry heating / digestion zone has been established (Malts, 1991).

Firstly, the calcium oxide reacts with caustic aluminate solution to form into calcium hydro-aluminate, $3CaO \cdot Al_2O_3 \cdot 6H_2O$, also known as tri-calcium aluminate

hexahydrate (TCA). With temperature further increases up to 200-240 ℃, TCA intensively decomposes with formation of $Ca(OH)_2$. (Whittington and Cardile, 1996).

Subsequently, the catalytic effect of $Ca(OH)_2$ on the goethite to hematite conversion is then suggested due to the formation of an intermediate with the formula $3CaO \cdot Fe_2O_3 \cdot 2H_2O$ (Malts *et al.*, 1985; Whittington, 1996). The mechanism of transformation with $Ca(OH)_2$ is considered in the following ways:

Transformation from goethite (Malts et al., 1985; Whittington, 1996):

$$2Ca(OH)_2 + 2FeOOH \rightarrow 2[CaO \cdot Fe(OH)_3] \xrightarrow{Ca(OH)_2} 3[CaO \cdot Fe_2O_3 \cdot 2H_2O] + 2H_2O$$

Unstable intermediate **(2.16)**

$$3CaO \cdot Fe_2O_3 \cdot 2H_2O \xrightarrow{H_2O} 3Ca(OH)_2 + Fe_2O_3 \quad \textbf{(2.17)}$$

where $CaO \cdot Fe_2O_3 \cdot 2H_2O$ is an unstable intermediate formed during the transformation.

The hydrothermal transformation of Al-goethite to hematite has a very similar pathway with pure goethite conversion in the Bayer digestion. The following equations show that the unstable intermediate, $CaO \cdot Fe_2O_3 \cdot 2H_2O$, also presents in the process.

Transformation from Al-goethite (Suss et al., 2010):

$$(Al_xFe_{1-x})OOH + CaO + H_2O \xrightarrow{Na+} Al(OH)_6^{-3} + Fe_2(OH)_6 * 4aq + Ca(OH)_2 \quad \textbf{(2.18)}$$

$$Fe_2(OH)_6 * 4aq + 3Ca(OH)_2 \xrightarrow{Na+} 3CaO \cdot Fe_2O_3 \cdot 2H_2O \quad \textbf{(2.19)}$$

$$3CaO \cdot Fe_2O_3 \cdot 2H_2O \xrightarrow{Na+} 3Ca(OH)_2 + Fe_2O_3 \quad \textbf{(2.20)}$$

As described from the above processes, lime is likely to improve the transformation of goethite to hematite by the formation of calcium hydroxide, $Ca(OH)_2$, in the Bayer liquor. The catalytic effect of $Ca(OH)_2$ to the transformation has been suggested.

2.4.4.2 Elimination of inhibiting effect of sodium titanate

The addition of lime has also been considered to be an effective way to eliminate the inhibiting effects of sodium titanates by forming calcium titanates instead (see 2.4.2.5). Various forms of calcium titanates have been reported in different Bayer digestion

conditions, among which perovskite, $CaTiO_3$, is the most common compound. It is therefore worth determining the factors in favour of $CaTiO_3$ formation. Firstly, high temperature is critical to the formation of perovskite. Schultze-Rhonof and Winkhaus (1972) and Schultze-Rhonof (1973) reported the formation of $CaTiO_3$ in sodium aluminate solution (C~150-200 g/L, A≥ 80 g/L) at temperatures over 175 ℃. Increasing temperatures were found to favour $CaTiO_3$ stability. Garing et al. (1980) patented that the digestion zone should be maintained at a temperature between 230 ℃ and 250 ℃.

Crocker et al. (2009) proposed the following potential reaction routes for the reaction of anatase, TiO_2, and a calcium phase (i.e. CaO, $Ca(OH)_2$ or $CaCO_3$) to form calcium titanate, in particular $CaTiO_3$, in alkaline media.

The reaction of Ca-containing additives and TiO_2:

$$Ca^{2+} + TiO_2 + 2OH^- \rightarrow CaTiO_3 + H_2O \quad \textbf{(2.21)}$$

Catalytic effect of $Ca(OH)_2$ in the formation of perovskite:

$$Ca(OH)_2 + TiO_2 \rightarrow CaTiO_3 + H_2O \quad \textbf{(2.22)}$$

$$CaCO_3 + 2OH^- \leftrightarrow Ca(OH)_2 + CO_3^{2-} \quad \textbf{(2.23)}$$

The interaction between $CaCO_3$ and TiO_2:

$$CaCO_3 + TiO_2 + 2OH^- \leftrightarrow CaTiO_3 + H_2O + CO_3^{2-} \quad \textbf{(2.24)}$$

where $CaTiO_3$ is perovskite, which is a desired compound to the hydrothermal transformation of goethite to hematite.

The adding point of lime or calcium phases is another determining factor to the formation of $CaTiO_3$. The addition of CaO to bauxite at low temperature may form hydrogarnet or TCA, which reduces available CaO for reaction with anatase (Suss and Maltz, 1992). It therefore allows the formation of sodium titanate by the reduction of available CaO and consequently reduces the alumina extraction and goethite to hematite conversion. Suss (2010) reported a significant increase (from 7.5% to 27.5%) of alumina recovery from aluminous goethite when lime added in the digestion zone compared to lime added in to the initial slurry prior to digestion. An explanation based on XRD analysis was established. With head feeding under the temperature 200 – 220

℃, part of the CaO reacts with carbonate ions in the liquor with formation of a stable component, calcite. With lime feeding directly in the digestion zone, part of CaO reacts with TiO_2 generating perovskite ($CaTiO_3$), which considerably improves the recovery of alumina as well as the performance of goethite to hematite conversion. Garing (1980) patented a similar operation that lime is added directly to the digestion zone where the bauxite slurry is being heated to a desired digestion temperature of at least 225 ℃. The extraction of alumina from both goethite and boehmite in the bauxite was thus improved.

2.4.5 Barriers

The hydrothermal transformation of goethite/Al-goethite to hematite in the Bayer process has been greatly recognised to eliminate the detrimental effects caused by goethite/Al-goethite to the Bayer process. However, some problems relating to the transformation are still yet to be tackled. The hydrothermal transformations of goethite to hematite in the literature were mostly investigated with synthetic goethite rather than natural goethite/Al-goethite in bauxites. The abundant impurities, other than alumina and iron minerals, in the bauxites would possibly impact the process of goethite to hematite conversion more or less. Although it would be solved by adding similar minerals in the synthetic system, examination on natural bauxites is still considered as a promising strategy due to the compositions of natural bauxite vary from bauxite to bauxite. Apart from that, the mechanisms of some influential factors to the transformation, such as the presence of alumina, remain unclear. In terms of the addition of calcium-containing additives to enhance the transformation, the report on the formation of Ca compound in different stages, for example, preheating or digestion step is very limited.

The study on hydrothermal transformation in this thesis has targeted the aspects mentioned above and corresponding discussion has been developed.

2.5 Summary

Iron oxides (or hydroxides, oxy-hydroxides), primarily goethite/Al-goethite and hematite, in bauxite are the main components in red mud produced from the Bayer process. Goethite rich bauxite is normally associated with settling difficulties of red

mud compared to hematite-bauxite. The properties of goethite, such as relatively larger surface area, smaller specific gravity etc., heavily contribute to the negative settling behaviour. In addition, partial Fe, up to 33%, substituted by Al in goethite structure frequently occurs in natural bauxite due to the isomorphous structures between diaspore (AlOOH) and goethite (FeOOH). This part of Al trapped in the goethite is extremely difficult to extract under the regular Bayer digestion operation, usually with the digestion temperature at ~150 ºC for gibbsite-containing bauxite. Transformation of goethite to hematite is believed to be the most effective way to eliminate the adverse effects caused by goethite in the Bayer digestion. Two principal methods of transformation are thermal transformation or hydrothermal transformation. Thermal transformation is practically considered to be a possibility for pre-treatment of bauxite and red mud because it is a topotactic process through which the crystallographic shape of hematite retains unchanged with parent goethite, unless heating temperatures in excess of 600 ºC are used(Gialanella *et al.*, 2010). However, hydrothermal transformation via a dissolution/re-precipitation mechanism in alkaline environment is widely accepted in the alumina industry. The advantages of the method are (1) the transformation of goethite to hematite can be simultaneously achieved with the Bayer digestion step in a high digestion temperature range (~250 ºC); (2) Al incorporated in the goethite can be partly or fully recovered during the process which would improve the productivity of alumina; (3) The settling rate of red mud has been evidently improved.

Through the critical review of literature, gaps between the studies to date have been indicated and thus will be the emphasis of the project. The thesis will accordingly focus on these aspects which have been demonstrated as “Objects” in Chapter 1.

References

Anand, R. R., Gilkes, R. J. & Roach, G. I. D. (1991) Geochemical and mineralogical characteristics of bauxites, Darling Range, Western Australia. *Applied Geochemistry,* 6**,** 233-248.

Atasoy, A. (2005) An investigation on characterization and thermal analysis of the Aughinish red mud. *Journal of Thermal Analysis and Calorimetry,* 81**,** 375-361.

Authier-Martin, M., Forte, G., Ostap, S. & See, J. (2001) The mineralogy of bauxite for producing smelter-grade alumina. *Journal of Mineralogy,* 53**,** 36-40.

Bardossy, G. (1982) Karst Bauxites. Bauxite deposits on carbonate rocks. *Elsevier* 14**,** 441.

Bardossy, G. & Aleva, G. J. J. (1990) Lateritic Bauxites. *Developments in Economic Geology,* 27**,** 624.

Basu, P. (1983) Reaction of iron minerals in sodium aluminate solutions. IN ADKINS, E. M. (Ed.) *Light Metals.* New York, The Metallurgical Society of AIME.

Blanch, A. J., Quinton, J. S., Lenehan, C. E. & Pring, A. (2008) The crystal chemistry of Al-bearing goethites: an infrared spectroscopic study. *Mineralogical Magazine,* 72**,** 1043-1056.

Brown, N. & Tremblay, R. J. (1974) Some studies of the mineral transformations during high temperature digestion of Jamaican bauxite. *Light Metals,* 3**,** 825 - 844.

Cornell, R. M. & Schwertmann, U. (2000) *The Iron Oxides: Structure, Properties, Reactions, Occurrences and Uses,* Weinheim, Wiley-VCH.

Cornell, R. M. & Schwertmann, U. (2003) *The Iron Oxides: Structure, Properties, Reactions, Occurrences and Uses,* Weinheim:Wiley-VCH.

Croker, D., Loan, M. & Hodnett, B. K. (2009) Kinetics and mechanisms of the hydrothermal crystallization of calcium titanate species *Crystal Growth and Design,* 9**,** 2207-2213.

Croker, D., Loan, M. & Hodnett, K. (2006) Sodium titanate formation in high temperature Bayer digestion. *TRAVAUX,* 33**,** 154-165.

Crombie, T., Davis, M. & Laurie, J. E. (1973) Method of digesting bauxite via the Bayer process with the addition of reducing agents. United States, Revere Copper and Brass Incorporated, New York.

Davis, C. E. (1973) The mineralogy of Jamaican bauxites. . *The Journal of Geological Society of Jamaican Proceedings of Bauxite Symposium II.*

Diamandescu, L., Mihăil à-T àr ăb ăsanu, D. & Feder, M. (1993) On the solid phase transformation goethite --> hematite. *Materials Letters,* 17**,** 309-311.

Fey, M. V. & Dixon, J. B. (1981) Synthesis and properties of poorly crystalline hydrated aluminous goethite. *Clays and Clay Minerals,* 29**,** 91-100.

Frost, R. L., Ding, Z. & Ruan, H. D. (2003) Thermal analysis of goethite. *Journal of Thermal Analysis and Calorimetry,* 71**,** 783-797.

Garing, M. L., Wright, J. R., Featherston, R. H. & Fischer, J. P. (1980) Lime Feeding for Bayer Process. C01F 7/06 ed. United States of America.

Gialanella, S., Girardi, F., Ischia, G., Lonardelli, I., Mattarelli, M. & Montagna, M. (2010) On the goethite to hematite phase transformation. *Journal of Thermal Analysis Calorimetry,* 102**,** 867-873.

González, G., Sagarzazu, A. & Villalba, R. (2000) Study of the mechano-chemical transformation of goethite to hematite by TEM and XRD. *Materials Research Bulletin,* 35**,** 2295-2308.

Grubbs, D. K., Libby, S. C., Rodenburg, J. K. & Wefers, K. A. (1980) The geology, mineralogy and clarification properties of red and yellow Jamaican bauxites. *Journal of the Geological Society of Jamaican Proceeding of Bauxite Symposium IV***.,** 176-186.

Gualtieri, A. F. & Venturelli, P. (1999) In situ study of the goethite-hematite phase transformation by real time, synchrotron powder diffraction, Sample at T = 25 C *American Mineralogist,* 84**,** 895-904.

Hahn, T. (ed.) 1996. *International Tables for Crystallography, Vol. A: Space-group Symmetry,* Dordrecht, The Netherlands: Kluwer Academic Publisher.

Hind, A. R., Bhargava, S. K. & Grocott, S. C. (1999) The surface chemistry of Bayer process solids: a review. *Colloids and Surfaces A: Physicochemical and Engineering Aspects,* 146**,** 359-374.

Hudson, L. K. (1987) Alumina Production. IN BURKIN, A. R. (Ed.) *Production of Aluminium and Alumina.* Chichester, John Wiley and Sons.

King, W. R. (1971) The iron minerals in Jamaican bauxites. IN EDGEWORTH, T. C. (Ed.) *The Metallurgical Society of AIME.* New York, Light metals.

Kirwan, L. J., Deeney, F. A., Croke, G. M. & Hodnett, K. (2009) Characterisation of various Jamaican bauxite ores by quantitative Rietveld X-ray powder diffraction and 57Fe Mössbauer spectroscopy. *International Journal of Mineral Processing,* 91**,** 14-18.

Li, D., O'connor, B. H., Low, I. M. & Riessen, A. (2006) Mineralogy of Al-substituted goethites. *Powder Diffraction,* 21**,** 289-299.

Li, L. Y. (1998) Properties of red mud tailings produced under varying Bayer process conditions. *Journal of Environmental Engineering,* 124**,** 254-264.

Li, L. Y. (2001) A study of iron mineral transformation to reduce red mud tailings. *Waste Management,* 21**,** 525-534.

Li, L. Y. & Rutherford, G. K. (1996) Effect of bauxite properties on the settling of red mud. *International journal of mineral processing,* 48**,** 169-182.

Malts, N. S. (1991) Efficiency of lime use in Bayer alumina production. *Light Metals***,** 257-262.

Malts, N. S., Poddymov, V. P., Rudashevski, L. S. & Kiselev, V. E. (1985) The intensifying action of lime upon the kinetics of bauxite leaching. *Non-ferrous Metals***,** 38-40.

Mcarthur, L. & Greensill, C. (2006) Mineralogical analysis of Weipa bauxite using NIR spectroscopy. *Australian Institute of Physics 17th National Congress 2006.* Brisban.

Mendelovici, E. & Yariv, S. (1981) Interactions between the iron and the aluminum minerals during the heating of Venezuelan lateritic bauxites. I. Infrared spectroscopy investigation. *Thermochimica Acta,* 45**,** 327-337.

Murray, J., Kirwan, L., Loan, M. & Hodnett, B. K. (2009) In-situ synchrotron diffraction study of the hydrothermal transformation of goethite to hematite in sodium aluminate solutions. *Hydrometallurgy,* 95**,** 239-246.

Mylona, E., Kalamboki, T. & Xenidis, A. (2008) Processing of bauxite ores. IN MEGGYES, T., ROEHL, K.-E. & DIXON-HARDY, D. (Eds.) *Tailings Management Facilities.* EPP Publications.

Orban, F., Pinter, T., Sigmond, G., Siklosi, P., Solymar, K., Toth, P. & Zambo, J. (1973) Processing of bauxites containing goethite. *Hung Teljes,* 6**,** 758.

Ostap, S. (1984) Effect of bauxite mineralogy on its processing characteristics. IN JR., L. J. (Ed.). Los Angeles.

Parekh, B. K. & Goldberger, W. M. (1976) An assessment of technology for possible of Bayer process muds. *Environmental Protection Technology Series*.

Pomiès, M. P., Menu, M. & Vignaud, C. (1999) TEM observations of goethite dehydration: application to archaeological samples. *Journal of the European Ceramic Society,* 19**,** 1605-1614.

Prasad, P. S. R., Shiva Prasad, K., Krishna Chaitanya, V., Babu, E. V. S. S. K., Sreedhar, B. & Ramana Murthy, S. (2006) In situ FTIR study on the dehydration of natural goethite. *Journal of Asian Earth Sciences,* 27**,** 503-511.

Ruan, H. D., Frost, R. L. & Kloprogge, J. T. (2001) The behavior of hydroxyl units of synthetic goethite and its dehydroxylated product hematite. *Spectrochimica Acta Part A: Molecular and Biomolecular Spectroscopy,* 57**,** 2575-2586.

Ruan, H. D., Frost, R. L., Kloprogge, J. T. & Duong, L. (2002) Infrared spectroscopy of goethite dehydroxylation. II. Effect of aluminium substitution on the behaviour of hydroxyl units. *Spectrochimica Acta Part A: Molecular and Biomolecular Spectroscopy,* 58**,** 479-491.

Ruan, H. D., Frost, R. L., Kloprogge, J. T. & Duong, L. (2002) Infrared spectroscopy of goethite dehydroxylation: III. FT-IR microscopy of in situ study of the thermal transformation of goethite to hematite. *Spectrochimica Acta Part A: Molecular and Biomolecular Spectroscopy,* 58**,** 967-981.

Schultze-Rhonof, E. (1973) On the chemistry of bauxite extraction II. Studies in the system Na_2O-CaO-Al_2O_3-TiO_2-H_2O between 100°C and 275°C. *Z. Anorg. Allg. Chem.,* 396**,** 303-307.

Schultze-Rhonof, E. & Winkhaus, G. (1972) On the chemistry of bauxite extraction I. Studies in the system Na_2O-CaO-Al_2O_3-TiO_2-H_2O at 100°C and atmospheric pressure. *Z. Anorg. Allg. Chem.,* 390**,** 97-103.

Schulze, D. G. (1984) The influence of aluminum on iron oxides. VIII. Unit cell dimensions of Al-substituted goethites and estimation of Al from them. *Clays and Clay Minerals,* 32**,** 36-44.

Schulze, D. G. & Schwertmann, U. (1984) The influence of aluminium on iron oxides. X. Properties of Al-substituted goethites. *Clay Minerals,* 19**,** 521-539.

Schwertmann, U., Friedl, J., Stanjek, H. & Schulze, D. G. (2000) The effect of clay minerals on the formation of goethite and hematite from ferrihydrite after 16 years' ageing at 25 °C and pH 4-7. *Clay Minerals,* 35**,** 613-623.

Smith, P. (2009) The processing of high silica bauxites -- Review of existing and potential processes. *Hydrometallurgy,* 98**,** 162-176.

Solymar, K., Sajo, I., Steiner, J. & Zoldi, J. (1992) Characteristics and separability of red mud. *Light Metals***,** 209-223.

Sudakar, C., Subbanna, G. N. & Kutty, T. R. N. (2004) Effect of cationic substituents on particle morphology of goethite and the magnetic properties of maghemite derived from substituted goethite. *Journal of Materials Science,* 39**,** 4271-4286.

Suss, A., Fedyaev, A., Kuznetzova, N., Damaskin, A., Kuvyrkina, A., Panov, A., Paromova, I. & Lukyanov, I. (2010) Technology solutions to increase alumina recovery from aluminogoethitic bauxites. *Light Metals*.

Suss, A. G. & Maltz, N. S. (1992) Aluminium and chromium containing goethite: composition, properties, behaviour in soda aluminate liquors in presence of silicon, titanium and calcium conpounds. *Light Metals***,** 1343-1347.

Szytuta, A., Burewicz, A., Dimitrijevic, Z., Krasnicki, S., Rzany, H., Todorovic, J., Wanic, A. & Wolski, W. (1968) Neutron diffraction studies of α-FeOOH. *Physica Status Solidi,* 26**,** 429-434.

Walter, D., Buxhaum, G. & Laqua, W. (2001) The mechanism of the transformation from goethite to hematite. *Journal of Thermal Analysis and Calorimetry,* 63**,** 733-748.

Whittington, B. I. (1996) The chemistry of CaO and Ca(OH)2 relating to the Bayer process. *Hydrometallurgy,* 43**,** 13-35.

Whittington, B. I. & Cardile, C. M. (1996) The chemistry of tricalcium aluminate hexahydrate relating to the Bayer industry. *International Journal of Mineral Processing,* 48**,** 21-38.

Whittington, B. I., Fletcher, B. L. & Talbot, C. (1998) The effect of reaction conditions on the composition of desilication product (DSP) formed under simulated Bayer conditions. *Hydrometallurgy,* 49**,** 1-22.

Wolska, E. (1988) Relations between the existence of hydroxyl ions in the anionic sublattice of hematite and its infrared and X-ray characteristics. *Solid State Ionics,* 28-30**,** 1349-1351.

Wolska, E. & Schwertmann, U. (1993) The mechanism of solid solution formation between goethite and diaspore. 213-223.

Wolska, E., Szajda, W. & Piszora, P. (1992) Determination of solid solution limits based on the thermal behaviour of aluminium substituted iron hydroxides and oxides. *Journal of Thermal Analysis,* 38**,** 2115-2122.

Wolska, E., Szajda, W. & Piszora, P. (1992) Synthetic solid solutions formed between goethite and diaspore. *Z. Pflanzenernahr. Bodenk.* , 155**,** 479-482.

Wolska, E., Szajda, W. & Piszora, P. (1994) Mechanism of Al- for Fe-substitution during the α-(Fe, Al) OOH to γ-(Fe, Al)$_2O_3$ transformation. *Solid State Ionics,* 70/71**,** 537-541.

Xu, B., Smith, P., Wingate, C. & Silva, L. D. (2010) The effect of anatase and lime on the transformation of sodalite to cancrite in Bayer digestion at 250C. *Light Metals***,** 81-86.

Yamada, K., Harato, T. & Furumi, Y. (1974) Removal of iron compounds from the Bayer liquor. *The Mettallurgical Society of AIME*, New York. 713-723.

Chapter 3
Research Methodology and Experimental Materials

3.1 Overview

This chapter is designed to summarise the methodology and all the experimental materials that are involved in the project. To achieve the aims of the PhD project, a large range of methods, such as the GFR (gas fired reactor) digestion and LOI (loss on ignition), has been carefully considered. Multiple analytical techniques including XRD (X-ray diffraction), TEM (transmission electron microscopy), XRF (X-ray fluorescence), IR (Infrared spectroscopy) etc. have also been used throughout the thesis. A comprehensive description, therefore, of the methodology, analytical techniques, equipment and experimental materials related to the project will be provided in this chapter.

Figure 3.1 shows the layout of the chapter, which is divided into three subsections, methodology, characterisation and materials respectively. Methodology will be demonstrated on the basis of different processes which are, respectively, the synthesis of Al-goethite, transformation of goethite to hematite under both thermal and hydrothermal environments and hydrothermal transformation of natural goethite/Al-goethite in the Bayer process. The research methods used in the above processes will be detailed and discussed. In the first part, the synthesis of Al-goethite, the fundamental synthetic methods for Al-goethite will be investigated. The properties of Al-goethite that have potential impact on the Bayer process will then be examined. In the second part, both thermal transformation through heating goethite to hematite and hydrothermal transformation of goethite to hematite under the Bayer environment have been carried out to investigate the reaction conditions, kinetic data and mechanism of the transformation. In the final stage, the hydrothermal behaviours of natural goethite/Al-goethite in bauxite under the Bayer conditions will be studied to examine the applicability of the results obtained from the first two steps. In addition, the improvement that hydrothermal transformation of goethite brings to the Bayer process will be identified. However, the characterisation and materials used throughout the thesis will be discussed separately.

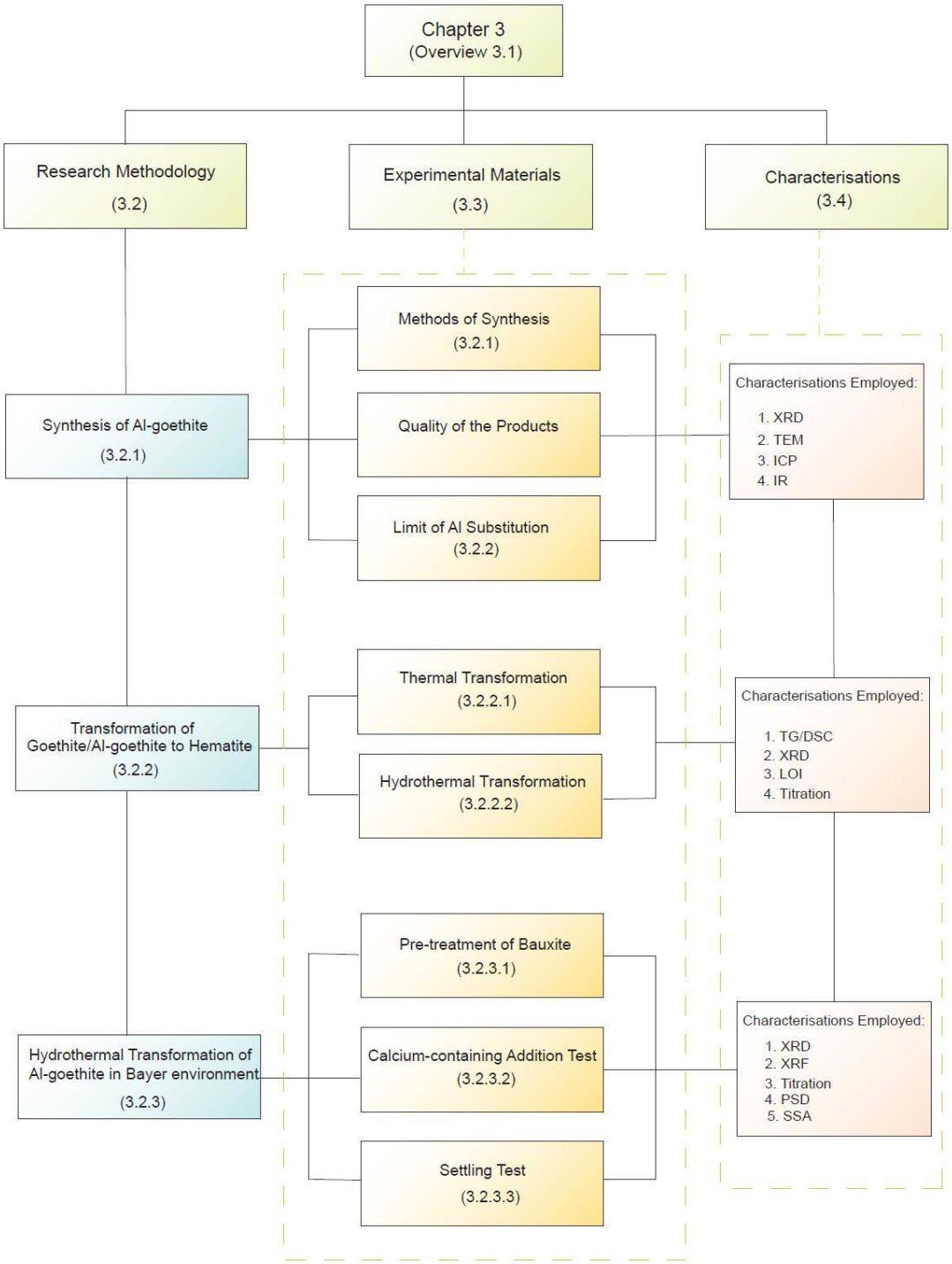

Figure 3.1 The layout of Chapter 3

3.2 Research methodology

3.2.1 Synthesis of Al-substituted goethite

It is widely reported that synthesis of Al-substituted goethite can be achieved by various methods including ageing Fe(III) in alkaline solution (Schwertmann *et al.*, 1979; Stanjek and Schwertmann, 1992; Wolska and Schwertmann, 1993; Strauss *et al.*, 1997; Schwertmann and Cornell, 2000; Blanch *et al.*, 2008; Kaur *et al.*, 2009) and oxidative hydrolysis of an Fe(II) salt (Schwertmann *et al.*, 1979; Piszora and Wolska, 1998; Schwertmann and Cornell, 2000; Majzlan and Navrotsky, 2003). The methods used in this study were originally adopted from Schwertmann and Cornell (Schwertmann and Cornell, 2000), but have been developed in a number of alternative ways by the researchers mentioned above.

3.2.1.1 Transformation from ferrihydrite in alkaline media

The aluminium substituted goethite samples were prepared by the method described by Schwertmann and Cornell (Schwertmann and Cornell, 2000). A series of samples were prepared by mixing aluminate solution, 5M KOH solution and 1 M $Fe(NO_3)_3$ solution in a 1 L polyethylene bottle. The aluminate solution was prepared by the slow addition of 0.5 M $Al(NO_3)_3$ - solution into 5 M KOH with constant stirring until a clear solution is obtained. Predetermined amounts of aluminate solution (**Table 3.1**) were then put into a 1L polyethylene bottle and 5 M KOH and 1M $Fe(NO_3)_3$ were quickly added into each bottle and shaken thoroughly. Additional deionised water was added to the bottle to make up to 1L solution and effectively mixed. The solution storage in polyethylene bottles was necessary to avoid contamination by Si from glass beakers. The mixtures were placed into an oven at 70 ℃ for 14 days and were swirled thoroughly once per day. At the end of the period, the solids were removed by vacuum filtration, washed twice by 0.1 M KOH and deionised water, and then dried at room temperature for two days. In order to avoid adherence of Al on the samples, acid treatment for the products was carried out. Finally, the solids were collected and finely ground to meet the requirement for characterisation. The detailed volume of solution used in the synthesis is shown in **Table 3.1**.

Table 3.1 Chemicals used in Al-goethite synthesis

Sample ID	Initial Al/(Al+Fe)	Aluminate / 0.3125M	KOH / 5M	$Fe(NO_3)_3$ / 1M	H_2O	Total
	mol %	mL	mL	mL	mL	mL
ALGOE-1	0	0	90.0	50	860.0	1000
ALGOE-2	13.5	25	87.0	50	838.0	1000
ALGOE-3	10.6	19	87.5	50	843.5	1000
ALGOE-4	14.9	28	86.2	50	835.8	1000
ALGOE-5	19.2	38	85.1	50	826.9	1000
ALGOE-6	20.4	41	84.9	50	824.1	1000
ALGOE-7	26.9	59	82.4	50	808.6	1000
ALGOE-8	30.4	70	81.0	50	799.0	1000
ALGOE-9	39.6	105	76.5	50	768.5	1000
ALGOE-10	50	160	69.5	50	720.5	1000

3.2.1.2 Oxidative Hydrolysis of Fe^{II} Salt

The preparation of higher aluminium substituted samples was carried out with the oxidation of Fe^{II} salt method also introduced by Schwertmann and Cornell (2000). A mixture of 50 mL freshly prepared 1 M $FeCl_2$ and 25 mL 1 M $AlCl_3$ was diluted to 1 L with deionised water into a polypropylene bottle. After adjusting the pH to 11.7 with 1 M KOH the solution was mixed thoroughly. To make sure complete oxidation was achieved, the suspension was opened and swirled daily. Oxidation was completed after approximately 2-3 months when yellow dense solids were formed. Separation of the liquid-solid system was with the use of a centrifuge. The solids were washed twice with 0.01 M KOH to remove the excess Al. The solids were then washed thoroughly with deionised water and dried at room temperature for two days. The samples were collected and finely ground for further characterisation. The change of colour of the solids can be found during the preparation. The initial solution gradually changes colour from dark red to a yellow-brown suspension at about 30 days and finally turns into yellow condensed slurry of product.

3.2.1.3 Estimation of Al substitution

The accurate determination of the aluminium substitution in both synthetic and natural goethite is a challenging task. The extent of Al substituted in goethite is normally

determined by two different methods, chemical analysis by such techniques as ICP (inductively coupled plasma) and XRF and calculation from unit cell parameters in XRD patterns. However, both methods are potentially affected by a variety of factors. Chemical analysis, commonly used in synthetic samples, is greatly influenced by preparation skills and impurities in the products, while it is not recommended in natural samples due to the interference of co-existing aluminium-containing minerals. Calculation from the unit cell parameters in XRD patterns, on the other hand, is in fact a method of estimation with fitting equations. Thus, the choice of appropriate fitting equations can overlap the peaks of other minerals present and so the accuracy of parameters derived from *Rietveld* refinement methods are critical to the calculation. In this thesis, calculation Al-substitution using XRD data has been adopted as the primary method given that chemical analysis is not appropriate for natural samples. The principle of the method and the calculation equations used in the study are demonstrated below.

As previously mentioned, up to 33% iron in goethite can be replaced by aluminium both in nature and under synthetic condition (Cornell and Schwertmann, 2003). The structure of goethite (α-FeOOH) and the isostructural diaspore (α-AlOOH) are based on the hexagonal close packed array, in which Al^{3+} can substitute part of the Fe^{3+} ions in goethite. However, Al^{3+} can replace 33 mole % of the Fe^{3+} in synthetic goethite, compared to about 36% in natural goethite (Thiel, 1963; Schwertmann and Carlson, 1994; Schwertmann and Cornell, 2000). Scheinost et al. (1999) speculates that the reason for Al substitution being restricted to 33 mole % may be attributed to the increasing strain in the crystal structure due to the size mismatch and limited contractibility of octahedral Fe^{3+} in goethite (α-FeOOH).

Even a tiny change in the lattice parameters induced by Al substitution can be observed as a slight shift in the peak position in X-ray diffraction (Sudakar *et al.*, 2004a). Thus, the shift of X-ray diffraction lines has been commonly used to estimate Al substitution in unknown goethites. Early in 1960's, Thiel (1963) studied the process of Al-substituted goethite synthesized under hydrothermal conditions at high pH and found that the *d*-spacing of the (111) peak (*d*(111)) and the unit cell dimensions decreased linearly with Al substitution, which are usually regarded as "standard" curves. However, Schulze (1984) investigated a series of Al-substituted goethites ranging from 0 to 31 mole % and pointed out that the relationship between d(111) and Al substitution

deviates from that predicted by Thiel (1963). Schulze (1984) further concluded that the *c* dimension shows the greatest linear dependency on Al substitution and the least deviation from Vegard's law[3] among all the samples than the *b* dimension. Compared to the *c* dimension, the *b* dimension deviates to some extent for substitutions > 20 mole % Al, while the *a* dimension shows irregular trends. Structural considerations can, to some extent, help understand the reason why the *a* dimension is more sensitive to structural defects, which is probably the cause of the large amount of scatter in the *a* value, compared to the *b* or *c* lattice dimensions. As the metal atoms are arranged in double lines, what is formed can be described as double octahedral chains which extend in the direction of the *c* axis (Ewing, 1935). Given the linear relationship between the *c* lattice parameter and most part of the *b* lattice parameter and Al substitution, this suggests Al substitution is apparently in the direction of the *b* and *c* axes, i.e., in the *b*-*c* plane, that the integrity of the double chains is retained. This is because all bonds within the double chains are covalent and a relatively stable configuration is adopted in which each octahedron shares four of its edges with adjacent octahedra. However, these double chains are only linked to each other by shared apical oxygens and hydrogen bonds, which is less stable than shared octahedral edges. Such relatively weak bonding will lead to easy disruption of the stacking of the double chains along the *a* axis during crystal growth.

Estimating Al substitution from the *c* cell dimension in detail is also given by Schulze (1984). The linear regression relationship between the *c* lattice parameter value and Al mole % substitution is shown as (Eq. 3.1):

$$mole\%Al = 1730 - 572.0c \qquad \textbf{(3.1)}$$

The *c* lattice parameter can be calculated from the positions of the 110 and 111 diffraction lines, which are the two strongest goethite lines and can be measured even when considerably small amounts of goethite exists, using the following formula:

$$c = [(1/d(111)^2 - (1/d(110)^2]^{-1/2} \qquad \textbf{(3.2)}$$

[3] Vegard's law: is an approximate empirical rule which holds that a linear relation exists, at constant temperature, between the crystal lattice constant of an alloy and the concentrations of the constituent elements.(Denton and Ashcroft, 1991)

where *c* is the unit cell parameter, *d(111)* and *d(110)* are the d spacing at peak position 111 and 110.

A three-step procedure to estimate mole % Al substitution in an unknown goethite is as follows (Schulze, 1984). Firstly, measure the position and width at half-height (WHH) for the goethite 110 and 111 lines. Secondly, correct the observed WHH errors induced by instruments. Finally, calculate d(110) and d(111) for each line using the corrected positions and calculate the *c* dimension with formula (3.2), then estimate mole % Al substitution with formula (3.1). It is worth noting that changes to the above calculation equations are available when gibbsite and/or anatase are also present in the samples, which is more likely to happen in natural bauxite. In such cases, alternative estimation methods will be discussed in the relevant chapters.

3.2.2 Transformation of goethite/Al-goethite to hematite

3.2.2.1 Thermal transformation

Thermal transformation of goethite to hematite was carried out using a furnace manufactured by Ceramic Engineering equipped with a EUROTHERM 818 thermal controller (**Figure 3.2**). The heat-up rate for the furnace is 40 ºC/min. Small and dry ceramic crucibles were weighed accurately to four decimal places (W_0) and were half-filled with goethite samples. The crucibles were re-weighed (W_1) and placed into the high temperature oven. The temperature was pre-set to the desired temperature (200, 300, 400, 600, 800 and 1000ºC for thermal test) and left to reach the target temperature. Once at temperature, the samples were left for 1 hour and then were removed and cooled in a desiccator. The samples were then re-weighed (W_2).

Figure 3.2 Furnace equipped with thermal controller for the thermal treatment of goethite

The extent of transformation of goethite to hematite was examined by the following three methods, 1) Loss on ignition (LOI) – weight loss of the samples; 2) X-ray diffraction (XRD) – phase change; 3) Transmission Electron Microscopy (TEM) – morphology change. The description of the operation of XRD and TEM will be discussed later in Section 3.4. For the weight loss during the thermal treatment, the calculation is subject to the following equation.

$$\text{Weight loss (LOI, \%)} = \frac{W_2 - W_1}{W_1 - W_0} \times 100\% \qquad \textbf{(3.3)}$$

where W_0, W_1, W_2 are the weight of empty crucible, crucible with initial goethite samples and crucible with thermal-treated goethite samples respectively. It should be mentioned here that the thermal transformation of goethite at 1000ºC for at least 2 hours is needed to establish a baseline for the weight loss evaluation.

The theoretical weight loss of goethite to hematite according to the following formula can be obtained.

$$FeOOH \xrightarrow{Heating} 0.5Fe_2O_3 + 0.5H_2O \qquad \textbf{(3.4)}$$

$$\text{Theoretical weight loss (\%)} = \frac{0.5M_{H_2O}}{M_{FeOOH}} \times 100\% = \frac{0.5 \times 18}{89} \times 100\% = 10.1\% \qquad \textbf{(3.5)}$$

where M_{H2O} is the weight loss measured and M_{FeOOH} the initial mass of goethite. The percentage of goethite and hematite then can be calculated using the following equations.

$$\text{wt\% Goethite} = \left(\frac{LOI}{10.1\%}\right) \times 100\% \quad \textbf{(3.6)}$$

$$wt\% \text{ Hematite} = \left(1 - \frac{LOI}{10.1\%}\right) \times 100\% \quad \textbf{(3.7)}$$

where wt% Goethite and wt% Hematite are the proportion (%) of goethite and hematite accounting for the thermally treated residue. LOI is the weight loss of the residue obtained from the Equations 3.3.

To investigate the process of the thermal transformation of goethite/Al-goethite, thermal to hematite, analytical techniques were also conducted using a NETZSCH QMS 403C Mass Spectrometer. The description of TG (Thermogravimetry)/DSC (Differential scanning calorimetry) will be discussed later in Section **3.4**. The software used to analyse the TG/DSC data is NETZSCH Proteus Thermal Analysis software.

3.2.2.2 Hydrothermal Transformation

Hydrothermal transformation of goethite to hematite was conducted to examine the effects of various reaction conditions on the transformation by simulating the Bayer digestion environment. A bomb digestion vessel, heated up in the gas-fired reactor (GFR) was employed to carry out the tests. To analyse the amount of the component in the residues, Loss on Ignition (LOI) was used to determine the weight loss of the residue within a certain temperature range and therefore calculate the ratio of goethite to hematite.

All the digestion tests in this study were conducted using the system with the gas-fired reactor system with the same operation procedure unless otherwise indicated. **Figure 3.3** shows the GFR where the bomb digestion vessel is heated up to the desired temperature. The bomb digestion was conducted using a bomb digestion vessel (250mL capacity) with a rapid heat-up rate (~40 ℃/min) and cool-down rate (~70 ℃/min). ~ 2g goethite were mixed in 150 mL pure caustic soda or Bayer liquor, which is equivalent to 160 g/L charge of bauxite with a 10% goethite content, for a desired period of time at a given temperature. Any other additives, such as hematite seeding, were added before the

vessel was sealed. The bomb digester was rotated horizontally at a rate of 72 RPM to ensure sufficient mixing of the reactants (Xu *et al.*, 2010). Reaction time in this study started once the pre-set temperature of digestion was reached.

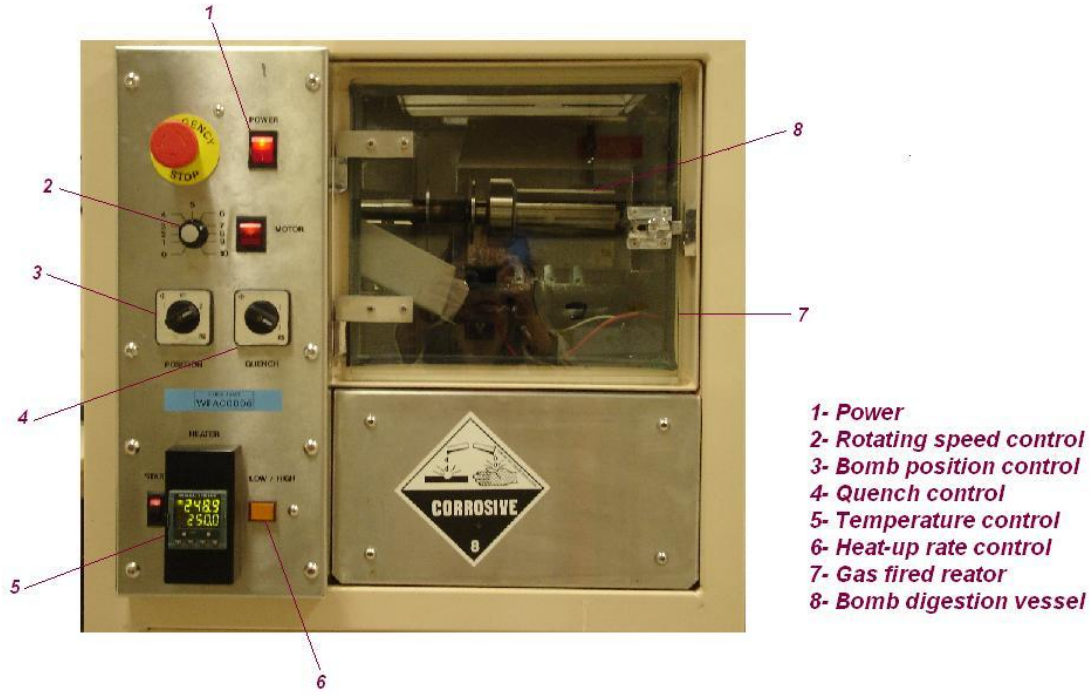

Figure 3.3 Gas fired reactor (GFR) – digestion/ hydrothermal transformation operating system

At the completion of digestion, the cooled slurry was pressure filtered through a 0.45 μm membrane filter (**Figure 3.4**). The residue was washed with deionised water several times and then dried at 100 ℃ overnight. The samples were characterised by XRD to determine the phase and LOI to investigate the content of goethite and hematite in the residues. The exit filtrate was analysed by the titration method for A/C ratio using the gluconate method (Xu *et al.*, 2010). The characterization details will be given later in this chapter.

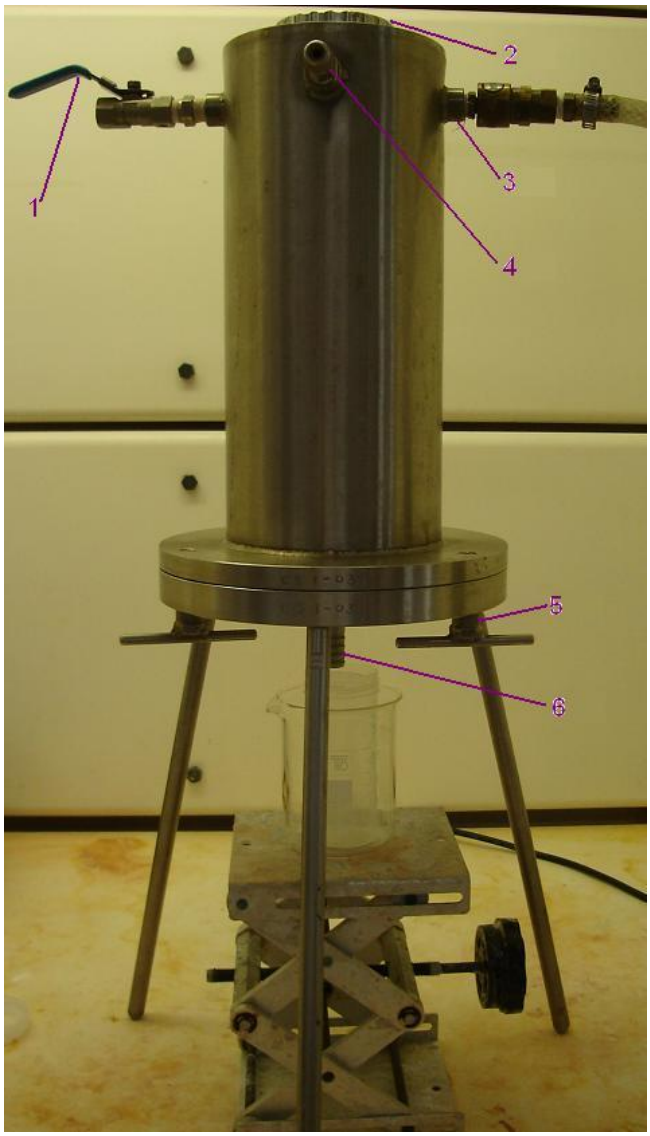

Pressure filtration vessel:

1. Pressure release ball valve
2. Screw lid
3. Nitrogen/air inlet
4. Spare outlet
5. Base screw
6. Liquor exit

Figure 3.4 A complete set-up of a 2L pressure filtration vessel

3.2.3 Hydrothermal transformation of Al-goethite in natural bauxite in Bayer conditions

The same digestion system, namely the GFR system combined with bomb digestion, as that for hydrothermal transformation of synthetic goethite to hematite was adopted for digestion of Al-goethite in natural bauxite. However, dose and treatment of the raw material differed.

3.2.3.1 Pre-treatment of Jamaican Bauxite

Twelve Jamaican bauxites provided by Alcoa World Alumina were investigated in this study. The detailed information for the bauxites, including XRD patterns, XRF and inductively coupled plasma (ICP) chemical analyses, can be found in Appendix B.

However, the complication caused by the effects of a high concentration of gibbsite will be further discussed in Chapter 5. For now, it is worth mentioning that the peaks of gibbsite overlap with those of goethite and hematite which makes it difficult to calculate the aluminium substitution in both goethite and hematite from XRD patterns alone. As a result, pre-treatment of Jamaican bauxites were conducted to eliminate the influence of gibbsite.

The bauxite samples were slurried in 80 g/L NaOH for 2 hours at 90 ℃. It should be noted that the charge of bauxite for the pre-treatment is equivalent to 1g of solid in 20mL solution to assure a complete dissolution of the available gibbsite. The solid residues were then filtered, washed with deionised water and dried for further transformation (digestion) tests. By doing this, the majority of gibbsite was removed from the bauxites. The residue was characterised by X-ray diffraction (XRD) to monitor the removal of gibbsite, the proportion of goethite to hematite G/(G+H), and the extent of aluminium substitution in goethite and hematite. The corresponding results for the above analyses will be comprehensively explored in Chapter 6. The extra benefit of the pre-treatment process is that measurement of the available alumina in the Jamaican bauxites was also achieved by analysis of the solution by ICP and titration. The corresponding results for pre-treated Jamaican bauxites can be found in Appendix C.

3.2.3.2 Digestion of Jamaican bauxites (pre-treated and/or raw)

The same gas-fired reactor system, as that for hydrothermal transformation of goethite to hematite, was employed for the digestion of Jamaican bauxites or pre-treated bauxites. However, the charge of the samples depended on the content of goethite in the bauxite and will be discussed separately in the relevant chapter.

3.2.3.3 Injection point test

It has long been believed that the addition of calcium-containing materials, such as lime, calcium hydroxide and calcium carbonate, can enhance the hydrothermal transformation of goethite/Al-goethite to hematite. However, the injection point, also referred to as the addition point, is critical to the process due to the possible interactions between minerals. Therefore, the injection (adding point) test was carried out at different digestion stages: i) head feeding with the addition of calcium compounds in the raw material and ii) digestion zone feeding, to investigate the impact of the addition point of calcium-containing additives to the transformation of goethite to hematite.

The injection point tests were conducted by an autoclave reaction system, PARR 4843, manufactured by PARR Instrument Company which allows a separate feeding system for calcium-containing additives to the main digestion reactor once the desired digestion temperature is reached. **Figure 3.5** shows the autoclave reaction system employed in the study. A floor stand reactor is mounted on a sturdy stand which accommodates a stirrer drive motor. Due to the capacity of the autoclave reactor, 600 mL Bayer liquor and 60 grams raw bauxite material are initially added to the reactor. Care should be taken to assemble all the parts for the instrument appropriately and check all the pressure valves with great caution. Control of the PARR instrument was with a remote control: for heating rate, stirring rate, temperature control and pressure feeding during the digestion. The heating rate is set to 4˚°C/min and the stirring rate at middle rate control which is modified on the charge of solids. During heating up, dilute feeding lime (~2 wt. % of bauxite) or calcium compounds (equivalent to 2 wt. % lime charge of bauxite) with deionised water are poured into the pressure burette. The beaker was washed with deionised water to ensure all solids were obtained and the burette was assembled to the main instrument. The pressure was checked before feeding the slurry into the vessel. Once the digestion temperature reaches the set value at 250 °C, the dissolved lime or calcium compounds were pressure fed into the main reactor. The slurry was collected after the completion of digestion and the vessel was washed with deionised water until no solids remained. The slurry was transferred to the pressure filter. The solids were subsequently dried overnight in a 100 °C oven and analysed with XRD and XRF for the determination of mineral phases present and the chemical composition. The collected spent liquor was titrated for A/C ratio and analysed with ICP for Al and Fe contents.

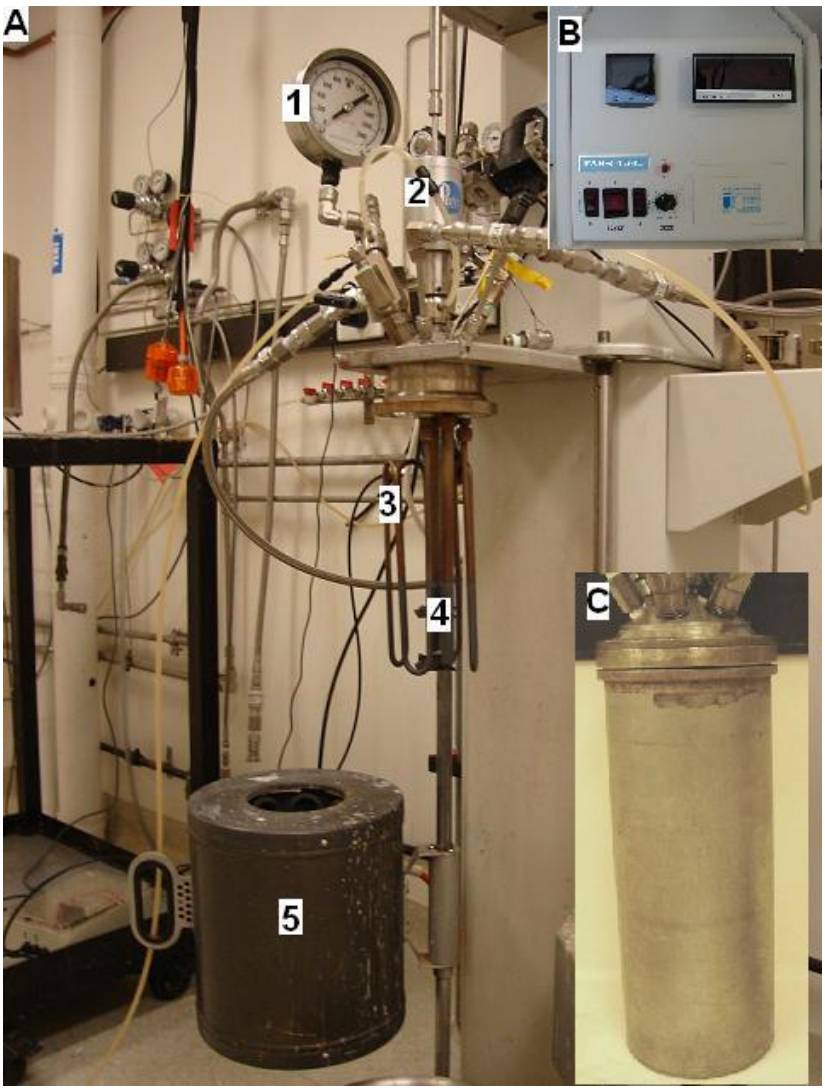

Figure 3.5 Floor Stand Autoclave Reactor (PARR 4843) used in the injection test

A: The major set-up for autoclave; **B:** Remote control; **C:** 2000mL reaction vessel.
The parts in the major set-up: 1. Pressure control gauge; 2. electrical gear;
3. heating coil; 4. spiral stirrer; 5. heat protector.

3.2.3.4 Settling Test

The settling test was undertaken to investigate settling performance for the digested bauxites and to monitor any improvement of different digestion conditions to the transformation of goethite to hematite. The settling tests were carried out with the in-house-designed equipment by Alumina Group at CSIRO Minerals, Waterford shown in **Figure 3.6**.

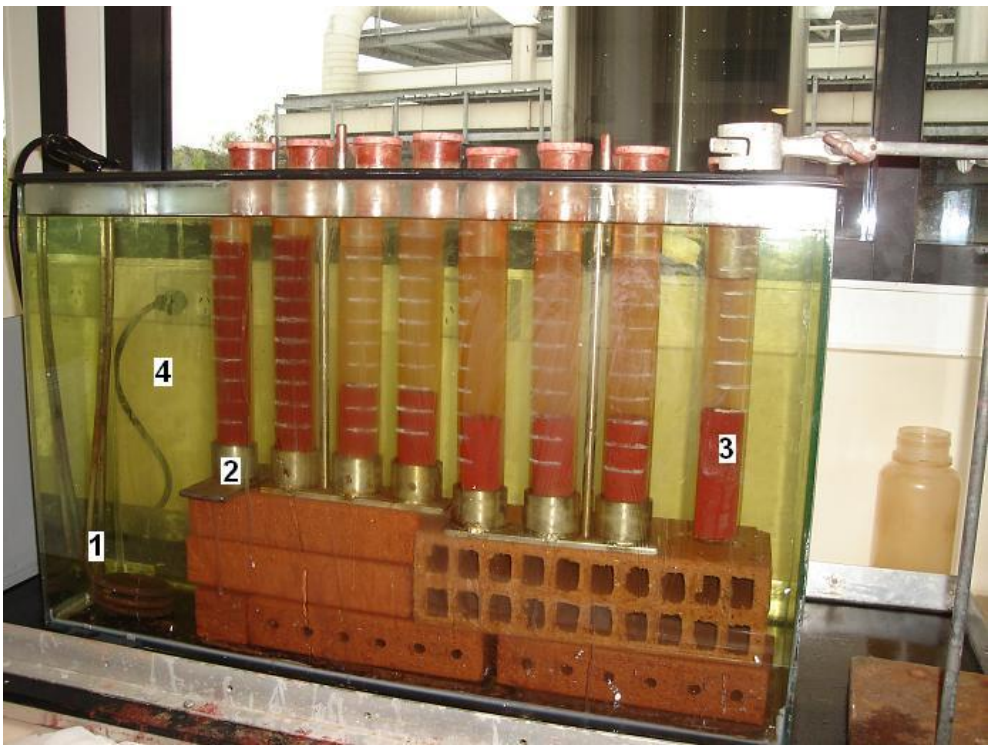

Figure 3.6 Settling Test Equipment

1 – Heating unit; **2** – Testing volumetric cylinder holder;
3 – Testing volumetric cylinder; **4** – Polyethylene Glycol (PEG) media

The slurry from digestion was initially cooled down to just less than 100ºC and then transfer to the testing volumetric cylinder. The cylinder was filled with the pre-heated Bayer liquor to 250 ml. If flocculant was required in the settling test, it was added into the suspension at this stage. The dose of per ml flocculant added can be calculated by the Equation 3.8.

$$D_f = C_f \times \frac{1000 \times 1000}{V \cdot C_s}$$

where D_f (g/t) is the dose of per ml flocculant added to the suspension, C_f (wt. %) is the concentration of flocculant; V (L) is the volume of the suspension and C_s is the concentration (g/L) of solids. For example, if the solids concentration and the volume of the suspension in the settling test are 35 g/L and 250 ml respectively and the concentration of flocculant is 0.02 wt. %, the dosage of per ml flocculant (D_f) should be:

$$D_f = 0.02\% \text{ x } \frac{1000 \times 1000}{0.25 \times 35} = 22.86 \text{ g/t} \qquad \textbf{(3.8)}$$

The temperature for the settling tests in this work ranged from 90 – 95 ºC. Once a stable temperature is reached, the suspension is carefully mixed using a plunger several times to ensure an even dispersion of the solids in the solution. The settling rate is measured by recording the mud-line versus time and determining a linear settling rate from this data.

$$V_s = \frac{D}{t} \quad \textbf{(3.9)}$$

where *Vs* is the settling rate (m/s), *D* (meter) is the distance for settling and *t* (second) is the time for settling.

3.3 Materials used in the project

Materials used in the project mainly comprise two sources: commercial products and laboratory-synthesized materials. In this part, both materials will be listed and further details in preparing the synthetic materials will be also demonstrated.

3.3.1 Experimental Materials

Table 3.2 lists all the materials used in this study.

Table 3.2 Chemicals used in the project (in alphabetic order)

Compound	Chemical Formula	Molecular Mass	Grade	Manufacture/ Supplier	Experiment involved
Aluminium chloride	$AlCl_3 \cdot 6H_2O$	241.43	Analytical Reagent	APS Finechem	Synthesis of Al-goethite
Aluminium hydroxide	$Al(OH)_3$	78.90	Analytical Reagent	Sigma-Aldrich	Bayer digestion
Aluminium nitrate	$Al(NO_3)_3 \cdot 9H_2O$	375.19	Laboratory Reagent	AJAX Chemicals	Synthesis of Al-goethite
Calcium carbonate	$CaCO_3$	100.09	Analytical Reagent	Rowe Scientific	Bayer digestion
Calcium hydroxide	$Ca(OH)_2$	74.09	Laboratory Reagent	Rowe Scientific	Bayer digestion
Calcium oxide	CaO	56.08	Laboratory Reagent	AJAX Finechem	Bayer digestion
Ferric nitrate	$Fe(NO_3)_3 \cdot 9H_2O$	404.06	Analytical Reagent	CHEM-SUPPLY	Synthesis of Al-goethite
Ferrous chloride	$FeCl_2 \cdot 4H2O$	198.81	Laboratory Reagent	AJAX Chemicals	Synthesis of Al-goethite
Goethite	α-FeOOH	88.87	Commercial product	Diggers	Bayer digestion, thermal transformation
Hematite	α-Fe_2O_3	159.69	Commercial product	Diggers	Bayer digestion
Hydrochloric acid	HCl	36.46	Analytical Reagent	Rowe Scientific	Synthesis of Al-goethite
Jamaican Bauxites				ALCOA	Bayer digestion
Potassium hydroxide	KOH	56.11	Laboratory Reagent	CHEM-SUPPLY	Synthesis of Al-goethite
Sodium hydroxide	NaOH	40.00	Analytical Reagent	Rowe Scientific	Bayer digestion
Synthetic flocculant			Freshly prepared	CSIRO Waterford	Settling test

3.3.2 Preparation of Caustic and Sodium Aluminate Solutions

To prepare sodium aluminate solution, the amount of caustic soda and alumina, as well as lime if applicable, was calculated in advance for a desired A/C ratio.

Firstly, a hotplate is heated to approximately 300 ℃. In the meantime, a stainless steel pot with a stirrer bar is weighed before adding in the required amounts of alumina followed by caustic. A little more than a quarter of the total volume of deionised water needed for the final liquor, is then added to dissolve the alumina and caustic. The liquor is mixed in a fume hood with a Teflon rod and the pot is placed on preheated hotplate at 200 ℃. The pot is left with slow stirring for about half an hour or until the liquor is almost clear (slightly cloudy).

For aluminate solution with lime added, a separate hotplate is used to dissolve carbonate. When heating up to ~ 300 °C, lime is added to the pot slowly to ensure it does not cause the liquor to crash out. Stirring is continued for about 15 minutes to ensure a homogenous solution. The liquor is then cooled for 15 minutes and then filtered using 0.45 μm filter membrane in a vacuum tower. After the liquor is filtered, the pot is washed to remove solids and the solids are washed with hot deionised water three times. Once cooled to room temperature, the liquor is made up to volume in a volumetric flask. The aluminate solution is titrated to ensure the appropriate A/C level has been obtained. **Table 3.3** shows the composition of solutions used in the experiments.

Table 3.3 Composition of solutions in the experiments

	Al_2O_3 (g/L)	NaOH as Na_2CO_3 (g/L)	A/C ratio	Free caustic (g/L)
Pure caustic solutions	0	100	0	100.00
	0	115	0	115.00
	0	140	0	140.00
	0	150	0	150.00
	0	165	0	165.00
	0	240	0	240.00
Sodium aluminate solutions	168	240	0.70	65.41
	156	240	0.65	77.88
	144	240	0.60	90.35
	132	240	0.55	102.82
	96	240	0.40	140.24
	72	240	0.30	165.18
	48	240	0.20	190.12

3.4 Characterisation methods

3.4.1 Titration

Titration was employed to examine the alumina, caustic and total alkalinity concentration of the Bayer liquors. The method involves an acid-base titration that uses the Gran method of endpoint detection. The titrator consists of a Metrohm hardware (**Figure 3.7**) and a Tiamo software. To accurately measure the level of alumina and caustic concentration in the Bayer liquor, daily pH electrode calibration and pH measurement of gluconate were carried out before any measurement of the Bayer liquor. After choosing the appropriate method for the measurement, 2.5 mL liquor was injected into the beaker and the weight of the sample inputted to the computer. Additional ~ 98 mL deionised water was added into the beaker, before placing it into the corresponding position on the sample changer. The result was e for further analysis.

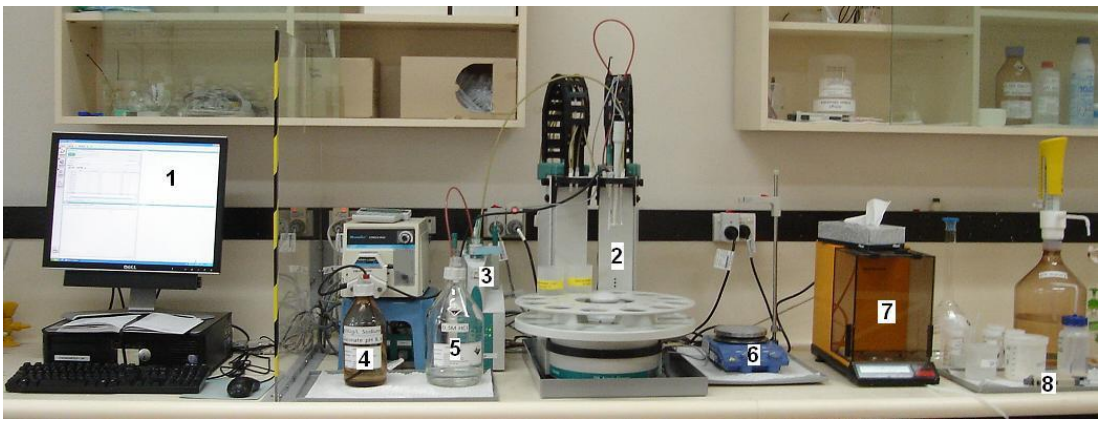

Figure 3.7 An entire set up for Titrator and the computer control end

1. Tiamo software; 2. 730 sample changer and tower; 3. Titrando 808;
4. Gluconate; 5. HCl; 6. Magnetic stirrer; 7. Sartorius balance.

3.4.2 Loss on Ignition (LOI)

Loss on ignition (LOI) was performed with a furnace equipped with a EUROTHERM 818 Controller to determine the change in mass percentage of water resulting from the transformation of goethite to hematite both in the solid state (demonstrated previously) and in the Bayer environment. The fundamental operation in both circumstances remains the same. Thus the detailed description of LOI can be obtained in Section 3.2.2.1. The phase change can be monitored by XRD analysis.

3.4.3 Inductively Coupled Plasma (ICP)

ICP-OES (optical emission spectrometer) tests for element analysis were performed by the Analytical Team at CSIRO Waterford. ICP analysis has been widely used in this study for elemental determination and quantitative analysis. Solid materials analysed by ICP comprises synthetic Al-goethites, natural bauxite samples and the digested residues; Solutions include spent liquor from the digestion process and also solution from solubility test for iron oxides in the Bayer liquor.

3.4.4 X-ray Fluorescence (XRF)

XRF was employed in this study for the component analysis of the samples, in particular, the components found in Jamaican bauxites before and after digestion. With XRF analysis results, not only is the content of various mineral components in the bauxites obtained but also the distribution of those components can be collected. More

importantly, Al substitution in goethite in the digested bauxites in which goethite is the only iron oxides can be accurately obtained due to gibbsite and boehmite being completely removed by high temperature (230-250ºC) digestion. Thus the accuracy of estimation of Al substitution in digested residue using the empirical equation developed by (Schulze, 1984) can be verified by comparing the results from XRF and XRD.

XRF analysis for this project was conducted by Ultra Trace Pty. Ltd.

3.4.5 Differential Scanning Calorimetry (DSC) and Thermogravimetry (TG)

To investigate the thermal decomposition behaviour of Al-goethite and the change of enthalpy during the process, DSC/TG analysis was carried out with NETZSCH 403C Aeolos Quadrupole Mass Spectrometer equipped with a heated capillary inlet system for thermal analysis. Initially, the goethite or Al-goethite sample was placed to obtain a ~3/4 full crucible with the reference crucible placed in the other pan in the furnace. Both the sample and reference were maintained at the same temperature throughout the experiment. The furnace temperature started from 30 ℃ controlled by a water bath and heated up to 1200 ℃ at a 10 ℃/min heating rate under the pre-programmed temperature/time profile. The TG/DSC curves were recorded for further analysis. The gas flow was set at 30mL/min for air and 20mL/min for nitrogen. The heating process control and the consequent analysis were carried out by the Proteus Analysis software.

3.4.6 Particle Size Distribution (PSD)

A Malvern Mastersizer was used to analyse particle size distribution of synthetic goethite and Al-goethite, raw and digested bauxite samples and other samples when mentioned. The measurement range was from 20nm to 2000 μm with a precision better than 0.5%. Particles were dispersed in water with 10 mL sodium hexa-metaphosphate additive. The size distribution was determined from the laser light scattering profiles.

3.4.7 Specific Surface Area (SSA)

A TriStar 3000 was used to analyse the BET (Brunauer, Emmett and Teller) surface area of goethite samples and raw and digested bauxite samples. The analysis employed nitrogen as the adsorptive at the bath temperature at -196 ℃. The degas temperature was at 150 ℃ over 180 minutes.

3.4.8 X-ray Powder Diffraction (XRD)

X-ray powder diffraction (XRD) was used to identify the phase present, determine the weight fractions of the phases and obtain the lattice parameters. XRD patterns in the thesis were obtained on a Philips XPERT diffract-meter with $CoK\alpha_1$ radiation (λ = 1.78897 Å). Powder diffraction patterns were collected over the 2θ range from 5 ºto 90 º with a step size of 0.02 ºand 1 s per step scanning speed. The *Rietveld* refinement was used to refine unit cell parameters.

3.4.9 Transmission Electron Microscopy (TEM)

Transmission electron microscopy (TEM) is a useful characterisation method for the morphology of small sized samples such as goethite or aluminium-substituted goethite. The JEOL JEM2010 transmission electron microscope at Department of Physics, Curtin University was employed to analyse the morphology of the samples. The filament available on the instrument is an LaB_6. The camera used to acquire digital images is a Model 780 DualView™ Digital Micrograph manufactured by Gatan. The machine is operated with a 200 kV accelerating voltage.

Sample preparation for TEM: The sample preparation is critical for high quality observations in the TEM analysis. A tiny amount of sample (~ 1 mg) is added to a 1 mL sample bottle and deionised water or ethanol as solvent is then added to the bottle. In this study, deionised water was used unless otherwise indicated. The suspension is thoroughly mixed together with the assistance of ultra sound to make an evenly dispersed suspension. A micro-syringe was used to take some of the suspension and one drop was placed onto the carbon-filmed copper grid which is used as sample holder for the TEM instrument. The suspension was allowed to dry on the grid overnight.

3.4.10 pH measurement

It is critical to control and monitor pH of the solution during the synthesis of Al-substituted goethite under both acidic and caustic environments. The pH meter used in this study is AQUA CP Handheld Conductivity-TDS-pH-Temperature Meter along with the TPS pH electrode both manufactured by TPS Pty Ltd. Careful calibration for temperature and pH was carried out prior to pH measurement. Proper buffers, pH 7.00 and 10.00, were used in this study. It should be noted that constant stirring and a stabilising time for the pH reading are applied to the pH measurement.

3.4.11 Infrared spectroscopy (IR)

IR spectra were collected for samples on Bruker IFS 66 Fourier Transform Infrared spectrometer (FTIR). The spectra were recorded with a frequency spacing of 2 cm^{-1} over the region 600-4000 cm^{-1}. A reference spectrum was also taken for pure KBr disc (produced in the same manner as that of the sample disc described in the sample preparation) and was used to reduce the background interference. The spectrometer sample chamber is purged by dry nitrogen to eliminate the absorption from ambient water vapour. The software for processing the data is OPUS version 5.5 under Windows XP.

Sample preparation for KBr discs (Transmission FTIR): Approximately 20-30 mg of each sample was ground in an agate mortar and pestle for 2 minutes, while ~ 1 g of potassium bromide (KBr) was also ground separately to guarantee particles as fine as possible. 1 mg of ground sample and ~0.5 g ground KBr were mixed together thoroughly with a mortar and pestle. The mixture was then transferred to a hydraulic vacuum press and left for ~ 2 minutes under 10 tons per square meter of pressure to obtain a thin and near transparent disc.

DRIFT (Diffuse Reflectance Infra-red Fourier Transform) samples preparation, **(Reflective FTIR):** Each sample was ground in an agate mortar and pestle for 2 minutes. Excessive amount of ground sample was placed into a sample cup and the excess was scraped off to level the surface with cup rim.

References

Blanch, A. J., Quinton, J. S., Lenehan, C. E. & Pring, A. (2008) The crystal chemistry of Al-bearing goethites: an infrared spectroscopic study. Mineralogical Magazine, 72, 1043-1056.

Cornell, R. M. & Schwertmann, U. (2003) The Iron Oxides: Structure, Properties, Reactions, Occurrences and Uses., Weinheim:Wiley-VCH.

Ewing, F. J. (1935) The crystal structure of diaspore. Journal of Chemical Physics, 3, 203-207.

Kaur, N., Grafe, M., Singh, B. & Kennedy, B. (2009) Simultaneous Incorporation of Cr, Zn, Cd, and Pb in the Goethite Structure. Clays and Clay Minerals, 57, 234-350.

Majzlan, J. & Navrotsky, A. (2003) Thermodynamics of the goethite-diaspore solid solution. Eur. J. Mineral, 15.

Piszora, P. & Wolska, E. (1998) X-Ray Powder Diffraction Study on the Solubility Limits in the Goethite-diaspore Solid Solutions. Materials Science Forum, 278, 584-588.

Scheinost, A. C., Schulze, D. G. & Schwertmann, U. (1999) Diffuse reflectance spectra of Al substituted goethite; a ligand field approach. Clays and Clay Minerals, 47, 156-164.

Schulze, D. G. (1984) The influence of aluminum on iron oxides. VIII. Unit cell dimensions of Al-substituted goethites and estimation of Al from them. Clays and Clay Minerals, 32, 36-44.

Schwertmann, U. & Carlson, L. (1994) Aluminum influence on iron oxides: XVII. Unit-cell parameters and aluminum substitution of natural goethites. Soil Science Society of American Journal, 58, 256-261.

Schwertmann, U. & Cornell, R. M. (2000) Iron Oxides in the Laboratory: Preparation and Characterization, Weinheim, Wiley-VCH.

Schwertmann, U., Fitzpatrick, R. W., Taylor, R. M. & Lewis, D. G. (1979) The influence of aluminum on iron oxides: Part II. Preparation and properties of Al-substituted hematites. Clays and Clay Minerals, 27, 105-112.

Stanjek, H. & Schwertmann, U. (1992) The influence of aluminum on iron oxides. Part XVI: hydroxyl and aluminum substitution in synthetic hematite. Clays and Clay Minerals, 40, 347-354.

Strauss, R., Brummer, G. W. & Barrow, N. J. (1997) Effects of crystallinity of goethite: I. Preparation and properties of goethites of differing crystallinity. European Journal of Soil Science, 48, 87-99.

Sudakar, C., Subbanna, G. N. & Kutty, T. R. N. (2004) Effect of cationic substituetes on particle morphology of goethite and the magnetic properties of maghemite derived from substituted goethite. Journal of Materials Science, 39, 4271-4286.

Thiel, R. (1963) Zum system FeOOH-AlOOH. Z.Anorg. Allg. Chem, 326.

Wolska, E. & Schwertmann, U. (1993) The mechanism of solid solution formation between goethite and diaspore. 213-223.

Xu, B., Smith, P., Wingate, C. & Silva, L. D. (2010) The effect of anatase and lime on the transformation of sodalite to cancrite in Bayer digestion at 250C. Light Metals, 81-86.

Chapter 4
Characterisation of Synthetic Al-substituted Goethite

4.1 Introduction

Aluminium substituted goethite ($Fe_{1-x}Al_xOOH$) has been widely reported in the literature (Fey and Dixon, 1981; Schulze and Schwertmann, 1984; Cornell and Schwertmann, 2003). It is an important mineral to the Bayer refinery since it affects the extraction of alumina due to the unrecoverable Al content in the structure and also retards the settling rate of red mud due to the fine particle size (Crombie *et al.*, 1973; Li and Rutherford, 1996; Suss *et al.*, 2010).

The substitution of Al for Fe is reported to be up to 33 mol % in synthetic samples (Schulze, 1984; Cornell and Schwertmann, 2003) and up to ~50 mol % in natural goethite (Cornell and Schwertmann, 2000). Al substituted goethite is normally thought of as a random solid solution between the isostructrual diaspore (α-AlOOH) and goethite (α-FeOOH) (Majzlan and Navrotsky, 2003). The solubility limits for the system suggests a miscibility gap in the solid solution, which means that only part of the Al introduced into the system incorporates into the goethite structure (Wolska and Schwertmann, 1993; Majzlan and Navrotsky, 2003; Blanch *et al.*, 2008). It was found that the substitution causes the structural strain due to the difference in size between the smaller Al^{3+} and the larger Fe^{3+}. X-ray diffraction studies reveal that the unit parameters do not always obey Vegard's law, whereby lattice parameters of a solid solution series change linearly with composition between those of the pure end members of the series, to form a linear relationship between the unit cell dimensions and Al substitution (Fey and Dixon, 1981). In addition, Sculze (1984) and Wolska et al. (1992a) reveal that the method of synthesis is also critical to the Al content.

The study in this chapter is 1) to investigate methods of preparing aluminous goethite; 2) to determine the relationship between the Al substitution and unit cell parameters; 3) to identify the deviation from Vergard's law in the goethite-diaspore solid solution; 4) to establish the mechanism for the solubility limits of the solid solution based on XRD, TEM and thermal analysis.

4.2 Synthesis of Al-substituted goethite

The detailed description of the synthetic methods can be found in Section 3.1.2. **Table 4.1** shows the comparison of reaction conditions and the characteristics of the products of the two synthetic methods used in the study. Except for the lower Al substitution levels, synthesis from Fe^{3+} in alkaline environment is preferred over oxidation from Fe^{2+} to prepare Al-substituted goethite due to its relatively shorter preparation time and very well crystallised product. However, synthesis from Fe^{3+} is not suitable for preparation of goethite with Al substitution higher than 12 mol % (Schwertmann and Cornell, 2000). It should be noted that the method of oxidation of Fe^{2+} is a time-consuming process with three months or more to complete the preparation. Since the selectivity of the reaction depends to a great extent on the ambient environment, the conditions need to be carefully monitored and controlled during the process. The following discussion on synthesis methods mainly focuses on the synthesis from Fe^{3+} in alkaline environment, which is the main synthetic method of Al-goethite used in the study. The Fe^{2+} oxidation method will be briefly demonstrated.

Table 4.1 A comparison of synthetic methods of Al-substituted goethite

Items \ Methods		Synthesis from Fe^{3+} in alkaline media	Oxidative hydrolysis of Fe^{2+}
Reaction Conditions	Temperature (℃)	70	25
	Duration (days)	14	60-90
	pH	>14	11.7
Production	Crystallinity	Good	Poor
	Al substitution (mol %)	<12	Up to 30
	Surface Area (m2/g)	10-30	~35
	Potential Impurities	Hematite	Magnetite

4.2.1 Synthesis from Fe^{2+} oxidation system

It is believed that synthesis of Al-substituted goethite from oxidation of Fe^{2+} is a time consuming process with wide time frame ranging from months even to years (Cornell and Schwertmann, 2003). The synthesis from Fe^{2+} system used in this study is adopted from Schwertmann and Cornell (2000) with 2-3 months of preparation. This method, however, has been considered only as a comparison synthetic method to the synthesis

from Fe^{3+} system in this study due to not only the long preparation time involved but also the poorly crystallised products, which do not favour further investigation.

4.2.2 Synthesis from Fe^{3+} in Alkaline Media

Preparation of Al substituted goethite from Fe^{3+} under alkaline environment has been recognised as a promising method for synthesis of Al-goethite (Wolska *et al.*, 1994; Schwertmann and Cornell, 2000) due to the production of pure and well crystallised Al-goethite within a reasonable preparation time frame. Furthermore, the synthesis conditions are relatively mild and, more importantly, easily controlled. However, the limitation of the method is that less than 12 mol % Al substitution can be practically achieved even with increased initial concentration of Al^{3+} (up to 33 mol %) in the solution. To understand the limitation of the method, the synthesis of Al-goethite from Fe^{3+} system was closely monitored and the factors that possibly affect the process were investigated.

4.2.2.1 Effect of Initial Al/(Al+Fe)

In this study, the Al-Fe-O-H system varies its crystalline profiles between the goethite structure and hematite structure depending on the relative amount of aluminium versus iron. The XRD pattern of aluminium free goethite is used as the baseline to demonstrate the structural change of crystals caused by introducing various amount of aluminium into the system. **Figure 4.1** shows XRD patterns for some of the synthetic samples prepared with different initial Al/(Al+Fe) in 5M KOH solution at 70 ºC for 14 days. When the initial Al/(Al+Fe) is less than 30 mol% , the Al ions act as 'impurities' to substitute a small portion of the Fe ions in the process of crystallization, which still largely conforms to the goethite structure. The spatial displacement due to Al-Fe substitution does not cause sufficient disruption to the initial goethite structure to warrant a radical phase transformation. Therefore a series of well-crystallized Al-goethites was synthesized in which the aluminium level is relatively low. However, as the Al/(Al+Fe) ratio in the solution approaches 30 mol%, the amount of hematite formed becomes increasingly significant and this phase displaces goethite as the main species observed at Al/(Al+Fe) ratio of 50%. The increased Al level in the Al-Fe-O-H

system favours the phase transformation from the initial goethite structure to the end hematite structure.

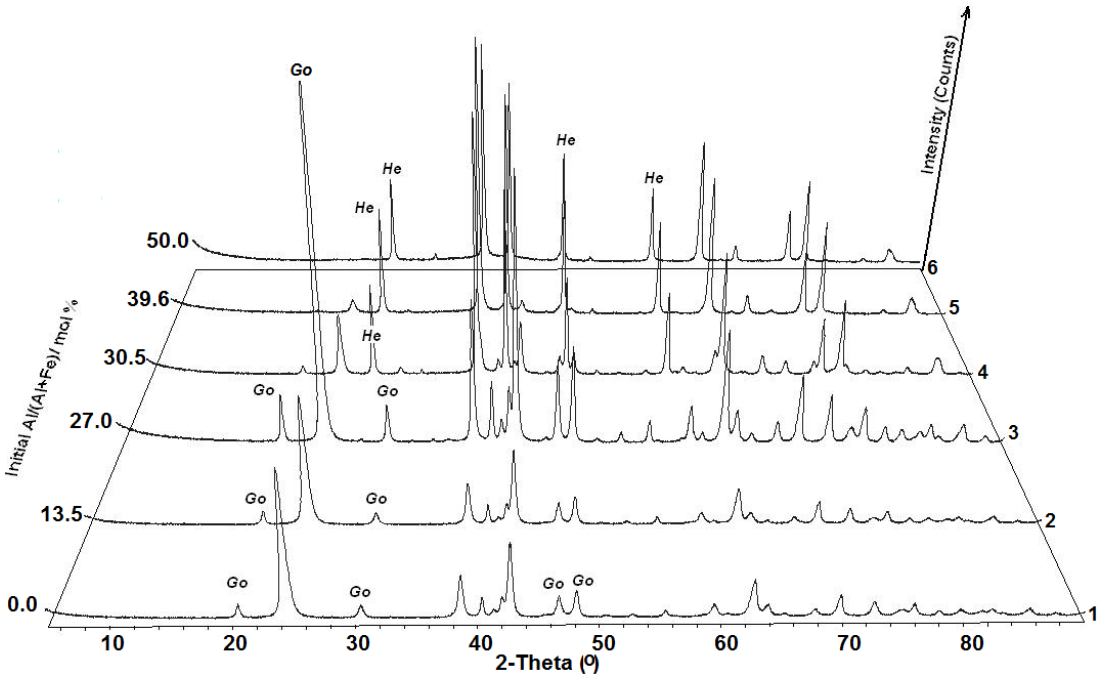

Figure 4.1 XRD overlays in 3D for synthetic Al-substituted goethite (Go-goethite; He-hematite) with respect to initial Al/(Al+Fe). All the syntheses were conducted at 70 ℃ in 5M KOH within 14 days.

Table 4.2 presents the phases and the extent of Al substitution in synthetic Al-goethite samples with different initial Al^{3+} concentration. It is found that the Al substitution in the synthetic samples is apparently much lower than the initial Al introduced into the solution. A maximum to ~11 mol % Al can be incorporated into the goethite structure even though as high as 27.0 mol % initial Al^{3+} is added to the solution. Further increasing the amount of Al ions to the system (> 30 mol %) tends to lead to increased formation of hematite rather than an increase in Al substitution. As seen in samples ALGOE-8, 9 and 10, hematite is formed more and more (77.6 wt. %) and finally dominates the samples (99.1 wt.%) as the initial Al/(Al+Fe) increases from 30.5 to 50.0 mol %.

In some cases such as Al-goethite in bauxite, using a chemical method to determine the extent of aluminium substitution is difficult due to interferences from other components in the minerals. Therefore, an estimation of aluminium substitution in goethite using XRD data is additionally adopted to solve the problem. There is a relationship between

Al substitution and unit cell dimensions. A regression equation proposed by Schulze (1984) is used to calculate aluminium substitution in the goethite structure:

$$\text{mol \% Al} = -562.5\,c + 1701.1 \qquad \textbf{(4.1)}$$

To verify the reliability of this method, the results derived from this regression equation are compared with the ICP results in **Table 4.2**. The unit cell axis parameter *c* is refined by the *Rietveld* method. The detailed description of the method and its reliability will be further discussed later in this chapter.

Table 4.2 Summary of synthesis of Al-goethite from Fe^{3+} salt in alkaline solution

Sample ID	Initial	Results		
		XRD		ICP
	Al/(Al+Fe) (mol %)	Minerals[a]	Al/(Al+Fe)[b] (mol %)	Al/(Al+Fe) (mol %)
ALGOE-1	0.0	Go	0.89	0.00
ALGOE-2	13.5	Go	3.48	3.34
ALGOE-3	10.6	Go	3.81	3.83
ALGOE-4	15.1	Go	5.95	5.75
ALGOE-5	19.3	Go	7.07	7.30
ALGOE-6	20.5	Go	6.10	8.01
ALGOE-7	27.0	Go	9.35	10.17
ALGOE-8	30.5	Go, He	Go: 22.4 wt. %; He: 77.6wt. %	
ALGOE-9	39.6	Go, He	Go: 5.6 wt. %; He: 94.4 wt. %	
ALGOE-10	50.0	Go, He	Go: 0.9 wt. %; He: 99.1 wt. %	

Note:

a. Go-goethite; He-hematite;

b. Calculated by regression equation proposed by Schulze (1984):
Al mol %= -562.5*c* +1701.0; *c* is refined unit cell in XRD pattern of the samples.

Figure 4.2(A) shows that the amount of aluminium incorporated into the goethite structure increases monotonically with the initial addition of aluminium content. In other words, the more aluminium is added during synthesis the higher is the aluminium content in the Al-goethite product. Such a correlation holds when Al/(Al+Fe) is within the range of 0 - 30 mol % in the raw material. It appears to be increasingly harder to incorporate more aluminium into the synthetic Al-goethite structure despite the

continuous increase in the aluminium content in the starting solution. **Figure 4.2(B)** shows that the proportion of aluminium that unable to get in the goethite structure via Al-Fe substitution is constant at ≥ 10 mol % Al/(Al+Fe). This 'unutilized aluminium' level fluctuates around 67 ±5 % compared to the total aluminium added to the system.

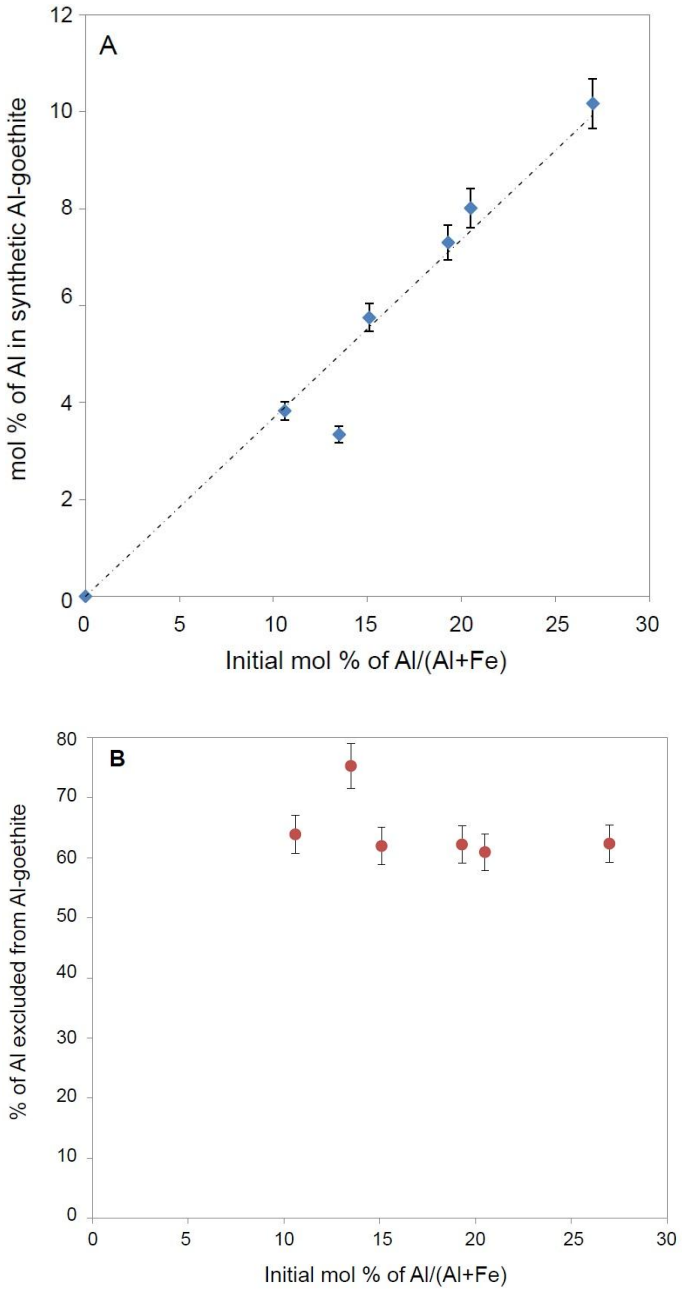

Figure 4.2 (**A**) monotonic relationship between initial aluminium content and aluminium incorporation in synthetic Al-goethite. (**B**) proportion of aluminium excluded from synthetic Al-goethite structure with increased aluminium content. **Note:** The straight dash line in (**A**) is a linear fit using Least Square Method.

Less than 30 mol % initial Al added to the solution positively influences the Al substitution in the goethite product although a large gap between the initial and final Al/(Al+Fe) occurs. It is very likely that no more than 11 mol % Al is incorporated into the goethite structure by using this method. The Al substitution rises as initial Al concentration increases, however, further increasing the initial Al concentration in excess of 30 mol % gives rise to the formation of hematite. Thus, this method is very likely to be suitable for synthesis of goethite with low Al substitution only. Although the amount of aluminium used in the synthesis process appears to be linearly proportional to the Al-Fe substitution in the goethite structure, not all aluminium ions in the Al-Fe-O-H system are incorporated into the goethite structure. This monotonic relationship between aluminium content in the system and Al-Fe substitution is only valid for Al/(Al+Fe) ratio $\leq$ 30 mol%. Beyond this point, high level of aluminium stabilised ferrihydrite against dissolution so that the hematite pathway becomes more competitive.

4.2.2.2 Effect of Temperature of Synthesis

To investigate the impact of temperature on synthesis and extent of Al substitution, a series of experiments at different temperatures were carried out. **Table 4.3** shows the information of Al-goethite samples synthesized at different temperatures and different holding times and **Figure 4.3** visually demonstrates the data extracted from **Table 4.3**.

Table 4.3 Al substitution and unit cell data for Al-goethite synthesized at different temperatures in 5M KOH solution with different holding times

Reaction Conditions			Results			
Temp.	Initial Al/(Al+Fe)	Duration	Al substitution	Unit Cell Parameters		
(℃)	(mol %)	(days)	(mol %)	a	b	c
25	14.5	6	4.67	4.63520	9.92510	3.01569
		10	5.71	4.62553	9.92334	3.01385
		12	5.99	4.62852	9.92711	3.01335
		14	6.56	4.62676	9.91797	3.01233
50	14.5	6	1.77	4.63332	9.94190	3.02085
		10	2.58	4.62594	9.94314	3.01941
		12	3.14	4.62710	9.93843	3.01841
		14	3.89	4.62355	9.93447	3.01709
70	14.5	6	1.49	4.64252	9.98520	3.02135
		10	2.62	4.61572	9.93993	3.01934
		12	3.12	4.62722	9.93813	3.01846
		14	3.41	4.62226	9.93969	3.01793
90	14.5	6	2.12	4.62157	9.94558	3.02024
		10	2.95	4.62214	9.93719	3.01875
		12	3.01	4.62236	9.93767	3.01865
		14	3.24	4.62212	9.94004	3.01824

Note: Al substitution was calculated by regression equation proposed by Schulze (1984): Al mol %= -562.5 *c* +1701.0; *a*, *b* and *c* are the unit cells refined by the *Rietveld* method.

The extent of Al substitution is significantly affected by increasing the synthesis temperature. Al substitution generally reduces with increasing temperature from 6.56 mol % at 25ºC down to 3.89 mol % at 50 ºC in a 14-day synthesis. The downward trend of Al substitution tends to slow down as the temperature increases further, c/f 3.41 mol % at 70 ºC and 3.24 mol % at 90 ºC. This trend is also applicable to Al-goethite synthesized for different holding times.

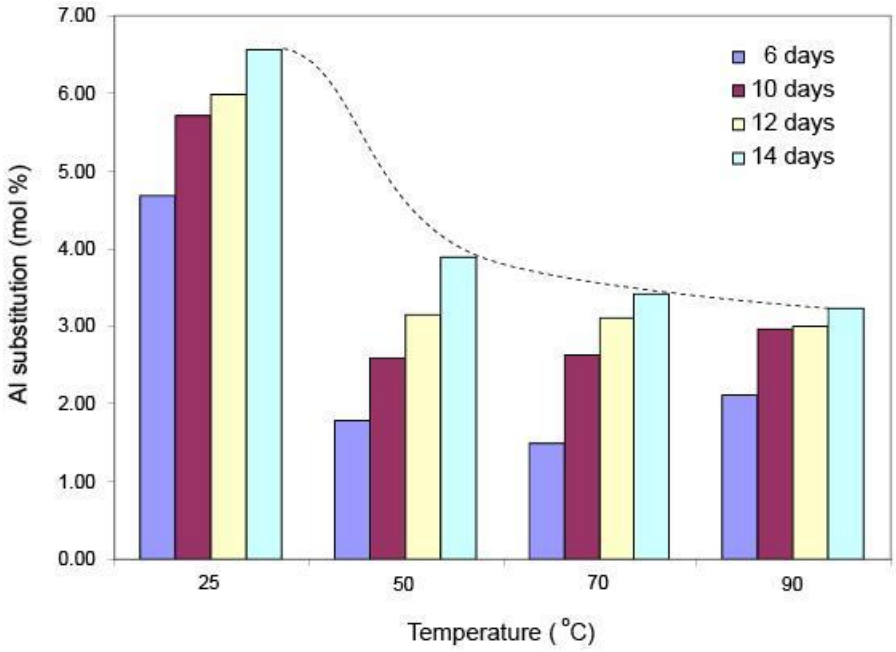

Figure 4.3 Extent of Al substitutions with different synthesis duration against temperature. The dash line is the trend line.

The crystallinity of synthetic Al-goethite, however, is negatively influenced by the increase of temperature. XRD patterns of pure and Al substituted goethite synthesized in 5M KOH at temperature of 25 and 70 ℃ are given in **Figure 4.4**. It is found that the Al-goethite samples synthesized at 25ºC are poorly-crystallized which is indicated by a set of broad peaks on its XRD pattern. This is attributed to the more sluggish crystallization process at lower temperatures (Schwertmann and Cornell, 2000). On the contrary, both pure and Al substituted goethites synthesized at 70 ℃ are well crystallized with sharp peaks in XRD patterns.

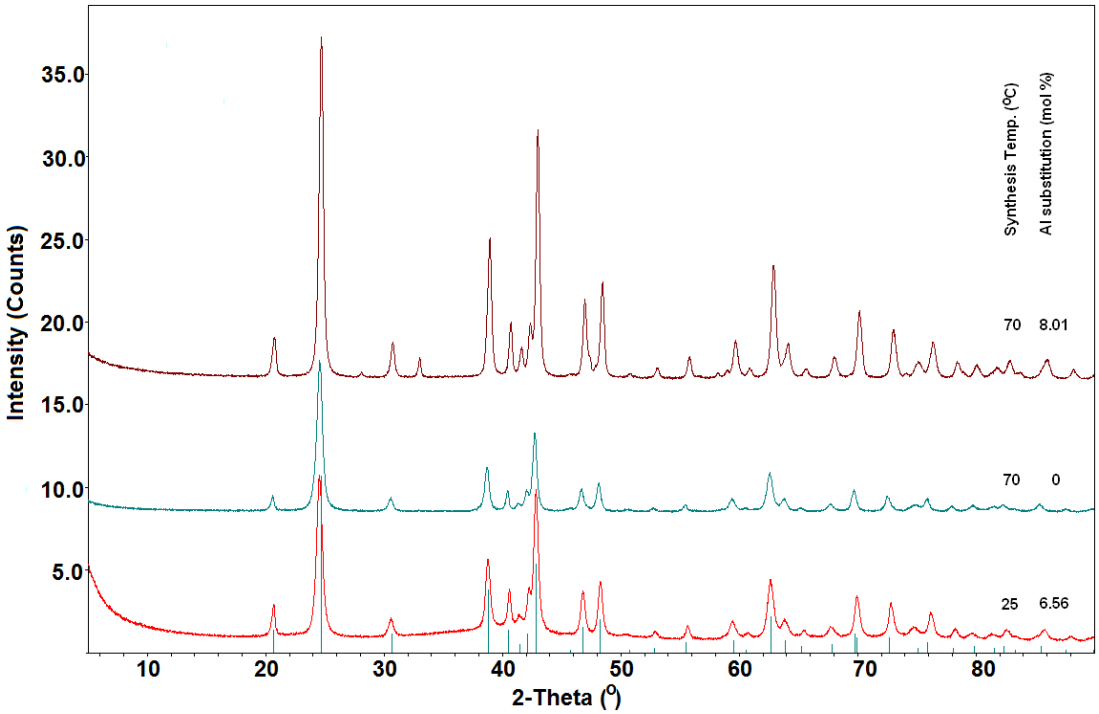

Figure 4.4 XRD patterns of pure and Al substituted goethites prepared in 5M KOH at 70 or 25 ℃.

Thus, synthesis temperature has significant effect on the quality of Al-goethite product. The aluminium substitution in goethite products decreases with increasing synthesis temperature. However, low temperature compromises the crystallinity of the products. Therefore, a temperature of 70 ºC is employed to synthesize Al-goethite samples that will be used in the investigations described in the next few chapters. This ensures only high quality Al-goethite samples with good crystallinity and a reasonable degree of Al substitution are used in the current study.

4.2.2.3 Effect of Reaction Time

As shown in **Figure 4.3**, the Al substitution increases with the extension of reaction time regardless of temperature. However, further increasing the holding time beyond 10 days shows little influence on Al substitution. Since time is crucial to the extent of Al substitution only in the early stage of the synthesis, further extending the synthesis time over 14 days is not suggested.

4.2.2.4 Kinetics of the Al Substitution in Synthesis of Al-goethite

Our kinetic analysis adopts the classic *Arrhenius* method (Equation 4.2) and the Al substitution in goethite was followed up by XRD analysis. The reaction rate constant *k*

in the temperature range 25-90 ℃ is uniformly small and in the order of 10^{-13} ($\ln k \approx -13$ shown in **Table 4.4**). This explains the sluggish formation rate of Al-goethite under the current hydrothermal conditions. Under these conditions, the activation energy E_a of the Al-goethite formation is difficult to determine due to the complex reaction mechanisms involved.

$$k = A\exp[-\frac{E_a}{RT}] \quad \textbf{(4.2)}$$

where A is the frequency factor for the reaction, R is the universal gas constant, T is the temperature (in kelvins), and k is the reaction rate coefficient.

However, the kinetics study on the time component still can be established using the classic *Avrami* equation:

$$y = 1 - \exp[-(kt)^n] \quad \textbf{(4.3)}$$

where k is a reaction rate constant, t is the reaction time, y is the reaction extent and n is a time exponent that depends on the reaction mechanism (Burke, 1965).

Another form of *Avrami* equation can be written as follows.

$$\ln\ln(1/(1-y)) = n\ln k + n\ln t \quad \textbf{(4.4)}$$

If a reaction conforms to the *Avarmi* equation, a plot of $\ln\ln(1/(1-y))$ vs. $\ln k$ should appear linear. The slope of the plot is the time component, n.

Before processing the kinetic data, it should be mentioned how the reaction end point has been chosen and how it is incorporated into the kinetic calculation. A crucial point in the kinetic data analysis of solid/solution reactions is the choice of a reaction end point. This end point is the time when the reaction reaches its plateau phase. Beyond this point the reaction progresses little with further extension of reaction time. The choice of reaction end point within a reasonable time frame is especially important for reactions involved in industrial processes, as it is impractical to allow a reaction to continue indefinitely with little gain in products. In the current kinetic study, the end point of reaction is chosen as 14 days because a further prolonging of the reaction time renders very little increase in the end product. However, we cannot assume the reaction

extent is 100% at 14 days even though the reaction appears to slow to a halt. According to the *Arrhenius* equation, solid/solution reactions become exponentially slow with prolonged reaction time. It will take an unacceptably long time for the remaining unreacted compound to convert to its end product. Due to the lack of thermodynamic data, the exact reaction extent at 14 days is unknown. In this study a fixed final product reaction extent independent of temperature has been adopted (Wang *et al.*, 2005) and then the molar fraction by mass balance was calculated. The estimated reaction extent at 14 days is arbitrarily defined as within a 10% error margin for 100% completion of reaction. Therefore the extent of reaction (*y)* is used to represent the estimated reaction extent with $y \sim 0.9$ for all end points. Although this estimated end point reaction extent may not be the true reaction extent, the calculated kinetic results are comparable since the same '10% error margin' policy is applied to all data and the kinetic trend obtained from the calculation is still of value to guide industrial processes. This method was also used by Yund and Hall (1970), Yund and McCallister (1970) and Vaughan and Craig (1978) where the extent of the end point reaction was calculated at an arbitrary time (to approximate $t = \infty$).

Table 4.4 shows that the time component, *n*, varies from as low as 0.91 to up 1.83 with the reaction temperature. This means the formation of Al-goethite shifts from an apparent 'first degree' reaction to a 'second degree' reaction in the temperature range 25-90^{o}C. Therefore, the true activation energy E_a should be more appropriately investigated by narrowing the temperature range in a 'real time' and high resolution setup such as in an in-situ study using Synchrotron (XRD) radiations. Cornell and Schwertmann (2003) reviewed kinetics study of transformation of ferrihydrite to goethite carried out by Schwertmann and Fischer (1966) and Schwertmann et al. (2000). The transformation was indicated following first order kinetics which varies from the synthesis of Al-goethite in this study. When compared these two pathways of preparation of goethite/Al-goethite, it is found that the reaction conditions greatly affect the kinetics of transformation. For example, increasing temperature and pH accelerates the transformation of ferrihydrite and reduces the activation energy. This findings would be valuable for future study using real time XRD on activation energy E_a. However, it should borne in mind that increasing temperature higher than 100 ℃ is not practical given that possible transformation of goethite could occur.

Table 4.4 Kinetic data of Al-goethite synthesized at different temperatures.

T (K)	t (s)	y	lnln(1/1-y)	lnt	lnk	n
298	518400	0.644138	0.03267246	13.1585	-13.156	0.91
	864000	0.787586	0.43775096	13.6693		
	1036800	0.826207	0.55955278	13.8516		
	1209600	0.904828	0.85529373	14.0058		
323	518400	0.413648	-0.62766834	13.1585	-13.603	1.63
	864000	0.602945	-0.07939013	13.6693		
	1036800	0.733816	0.28033161	13.8516		
	1209600	0.909091	0.87459138	14.0058		
343	518400	0.397227	-0.6807932	13.1585	-13.541	1.83
	864000	0.69848	0.18142138	13.6693		
	1036800	0.831778	0.57800110	13.8516		
	1209600	0.909091	0.87459138	14.0058		
363	518400	0.594837	-0.1015162	13.1585	-13.229	1.12
	864000	0.827722	0.56454297	13.6693		
	1036800	0.844557	0.62136870	13.8516		
	1209600	0.909091	0.87459138	14.0058		

Note:

- The units of temperature and reaction time in this table are Kelvin and second rather than Celsius and days used in the rest of the thesis for the convenience for kinetic calculations. ***y*** is the estimated reaction extent; ***k*** is the rate constant; ***n*** is a time exponent that depends on the reaction mechanism (Burke, 1965; Hu *et al.*, 1999).

- The unit value '1' was not used as the reaction extent *y* at the end point, 14 days, as '1' will render lnln(1/1-*y*) calculation invalid. Therefore a 10% error was applied throughout all end data sets.

Figure 4.5 (A-D) show the *Arrhenius* plots of lnln[1/(1-*y*)] vs lnt for Al-goethite formation in the temperature range 25-90 °C, with the best linearity observed at 70°C. This evidence supports the decision of choosing 70 °C as the preferred Al-goethite synthesis temperature in the previous discussion, since at this temperature the reaction conforms to classic solid/solution kinetics. This means a better predictability of Al-goethite production when other parameters are given. The lnln[1/(1-*y*)] vs lnt curves calculated for the 25 °C, 50 °C and 90 °C data, however, appear to deviate from the

kinetic predications of *Arrhenius* equation. According to Vyazovkin (Vyazovkin, 2000) this non-linearity may coincide with the change of reaction mechanism and variation in activation energy (E_a) over the course of mineral formation.

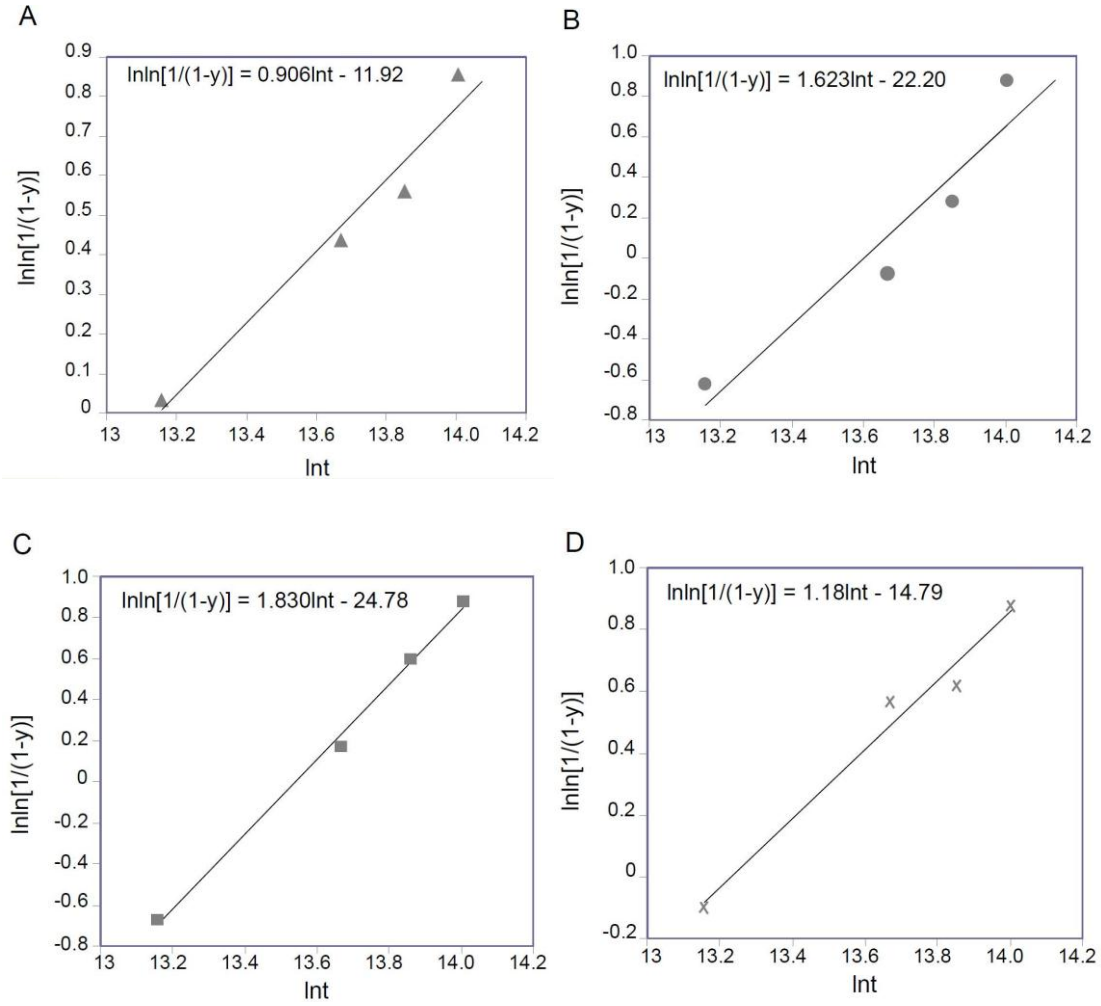

Figure 4.5 Arrhenius plots of lnln[1/(1-y)] vs lnt for Al-goethite formation at (**A**) 25 °C, (**B**) 50 °C, (**C**) 70 °C, and (**D**) 90 °C.

4.3 Unit cell parameters and estimation of Al substitution

Although an aluminium atom (0.143 nm) is larger than an iron atom (0.124 nm), their ionic particles bear a reverse relationship with Fe^{3+} (0.064 nm) being slightly bigger than Al^{3+} (0.060 nm). The substitution of Fe^{3+} with Al^{3+} in the goethite structure, therefore, produces a slight contraction of its crystal lattice, which is most evident along the c axis. A higher Al-Fe substitution correlates to a larger dimensional contraction in

the goethite unit cell. Therefore, unit cell parameter changes can be used to estimate the degree of aluminium substitution in Al-goethite. **Figure 4.6** shows the X-ray diffraction patterns of synthetic goethite samples (ALGOE-1, 2, 6 and 7) with aluminium substitution 0%, 3.34%, 8.01% and 10.17% respectively. The pure, well-crystallised goethite phase can be observed from the XRD patterns. This suggests that the isovalent substitution of Al to Fe does not change the crystal structure of goethite α-FeOOH. The small peak of KCl seen only in sample ALGOE-6 could be attributed to insufficient washing. Slight shifts in the peak position indicate changes in the lattice parameters with aluminium substitution.

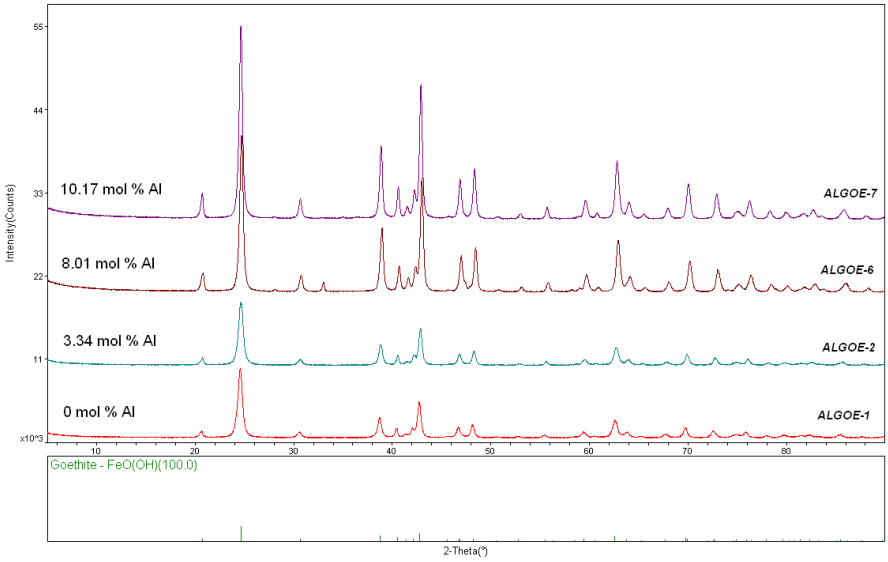

Figure 4.6 XRD patterns of aluminium substituted goethite samples synthesized in 5 M KOH at 70 ºC.

Table 4.5 summarises the unit cell parameters of synthetic Al-goethite collected from XRD analysis. The corresponding plots of unit cells against Al substitution is shown in **Figure 4.7**.

Table 4.5 Unit cell parameters of synthetic Al-goethite

Sample ID	ICP	XRD Unit Cell Parameters			
	Al/(Al+Fe) (mol %)	*a* (Å)	*b* (Å)	*c* (Å)	*V* (Å3)
ALGOE-1	0.00	4.6151	9.9621	3.0226	138.97
ALGOE-2	3.34	4.6135	9.9369	3.0180	138.36
ALGOE-3	3.83	4.6129	9.9360	3.0174	138.30
ALGOE-4	5.75	4.6112	9.9355	3.0136	138.07
ALGOE-5	7.30	4.6095	9.9327	3.0116	137.89
ALGOE-6	8.01	4.6074	9.9316	3.0133	137.88
ALGOE-7	10.17	4.6034	9.9047	3.0076	137.13

Note: Cell parameters *a*, *b* and *c* of Al-goethite were solved by Rietveld refinement. *V* is the volume of unit cells.

The straight dash lines indicate linear relationship between cell parameters and aluminium substitution derived from the Vegard's law (Schulze, 1984; Blanch *et al.*, 2008). Vegard's law states that the lattice parameters of a solid solution series change linearly with composition between those of the pure end members of the series (Klug and Alexander, 1974; Fey and Dixon, 1981). Unit parameters, in particular *b* and *c*, decrease with increasing Al substitution. It seems that there is a significant deviation along a dimension against Vergard's law, while *b* and *c* are more likely to obey the law. The difference varies from 4.6151 to 4.6034 for *a*, 9.9621 to 9.9047 for *b* and 3.0226 to 3.0076 for *c* (**Table 4.5**) compared to the standard unit parameters of *α*–FeOOH *a*=4.6188, *b*=9.9528 and *c*=3.0236 respectively. This finding to great extent matches the results widely reported in literature (Fey and Dixon, 1981; Schulze, 1984; Wolska *et al.*, 1992a; Sudakar *et al.*, 2004b). However, a significant deviation for *c* unit parameter was also observed by Piszora and Wolska (1998) if Al substitution is higher than 14%, although it was not applicable in this study since less than 11% Al substitution in all samples.

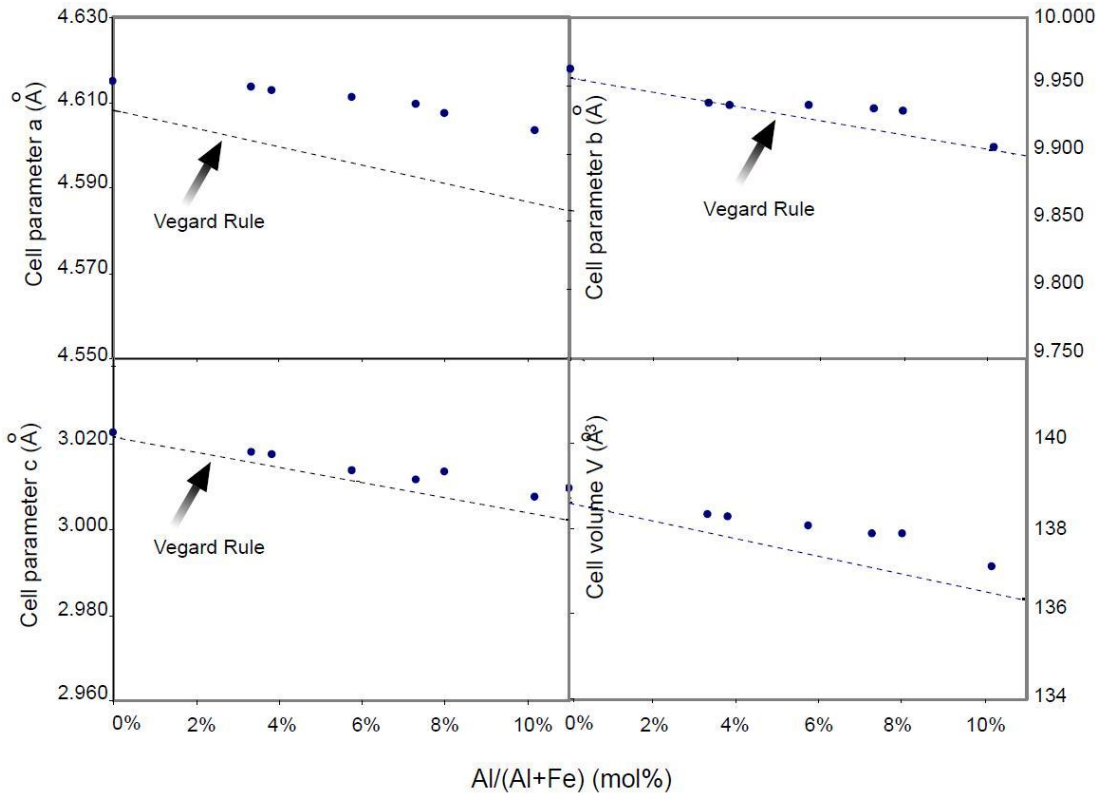

Figure 4.7 Plots of cell parameters *a, b, c* and cell volume *V* against Al substitution for synthetic Al-goethite. The dots demonstrate the experimental data from the synthesis and the dash lines indicate the Vergard's law.

Estimation of Al in the samples can be calculated due to a better fit of the linear relationship between unit cell *c* and Al substitution. Schulze (1984) described the relationship between Al substitution (mol %) in aluminous goethite and the unit-cell dimensions from the shifts in X-ray diffraction (XRD) line positions and accordingly deduced a regression equation. Other researches (Piszora and Wolska, 1998; Li *et al.*, 2006b; Blanch *et al.*, 2008) also revealed that c parameter was more preferred rather than a and b to determine Al substitution due to its excellent linear regression with mol% Al. In this study, **Equation 4.1** is used to evaluate aluminium substitution in the synthetic Al-substituted goethite.

The value of unit cell *c* in **Equation 4.1** is obtained by XRD refinement using the Rietveld refinement method (Schulze, 1984). To test the accuracy of Al substitution estimation, **Figure 4.8** shows a comparison between the estimated result by the equation 4.1 and determined Al substitution obtained from ICP (data based on **Table 4.2**). The calculated values of Al substitution mostly match the results obtained from ICP

analysis. The "Relative errors (*RE*)" for the calculated Al substitutions to the measured values are also marked in the figure. The following equation is used to calculate the RE for Al substitution in each sample.

$$RE = \frac{\left| Al_{XRD,i} - Al_{ICP,i} \right|}{(Al_{XRD,i} + Al_{ICP,i})/2} \times 100\% \qquad \textbf{(4.5)}$$

where *RE* means "relative error", $Al_{XRD,i}$ is the value for Al substitution calculated from XRD data, $Al_{ICP,i}$ is the Al substitution measured by ICP technique, and *i* (*i* = 1, 2, ⋯ ⋯, 7) is the sample number for the synthetic Al-goethite,. The *RE*s for samples, except ALGOE-6, are all within acceptable range. Therefore, the method provides a practical application, which has been widely employed by the mineral industry (Zwingmann *et al.*, 2008), to estimate extent of Al substitution via collecting data from XRD technique.

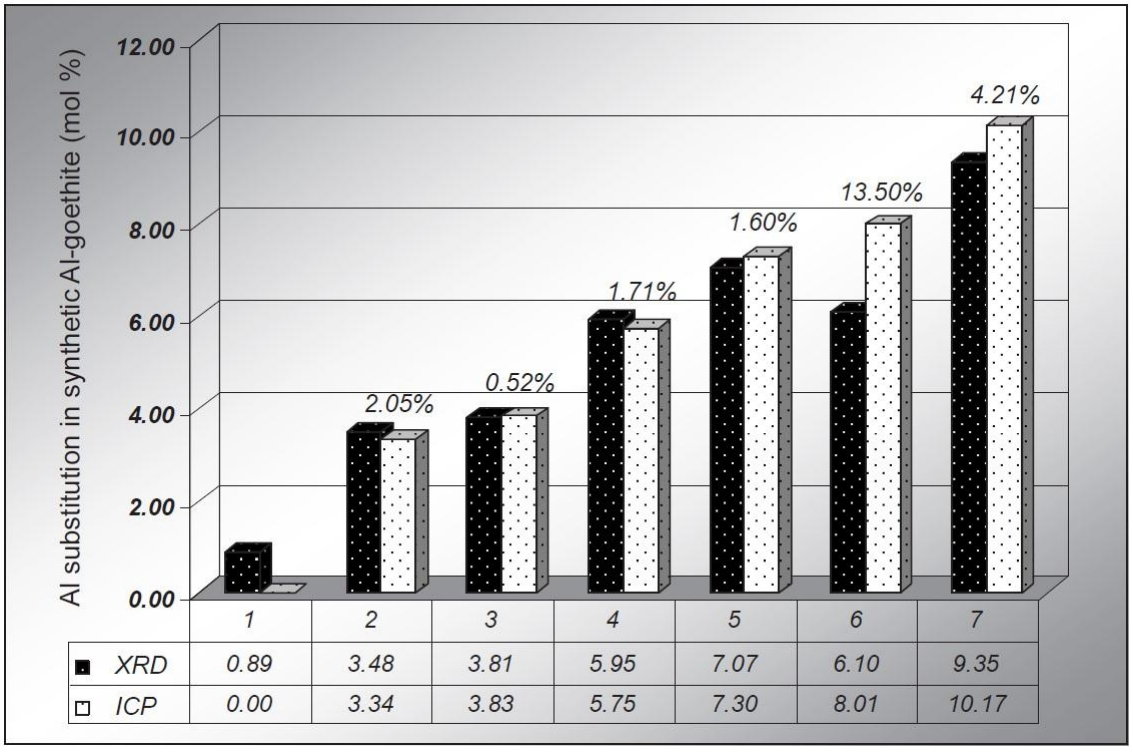

Figure 4.8 A comparison of the extent of Al substitution in synthetic samples (ALGOE-1, 2, 3, 4, 5, 6 and, 7) between calculated results from XRD data and measured data from ICP. The percentage on the top of each pair of columns is "relative error (*RE*)" for calculated Al substitution to the chemical measured value.

4.4 Morphology of Al-substituted goethite

TEM study was conducted to investigate the effect of aluminium substitution on the particle morphology. Comparisons of crystalline of Al substitution are shown in **Figure 4.9**. Both pure goethite and Al-substituted goethite are well crystallized. Elongated shaped goethite crystals can be clearly seen for pure goethite in (*a*) which tends to become stubby with increasing Al substitution in (*b*), in agreement with the description in literature (Cornell and Schwertmann, 2000; Sudakar *et al.*, 2004b).

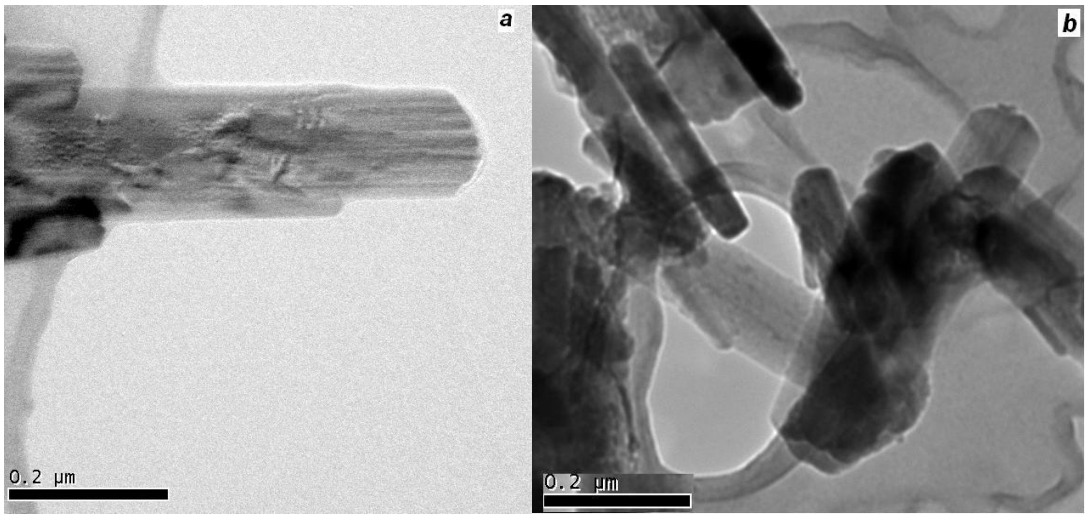

Figure 4.9 TEM (Transmission electron microscope) of synthetic Al-goethite with *a*) 0 mol % Al; *b*) 10.17 mol % in caustic solution at 70 ºC.

To further demonstrate the impact of Al substitution on Al-goethite, the TEM micrographs of Al-goethite with different extent of Al substitution are shown in **Figure 4.10**. It is apparent that the particle size of Al-substituted goethite becomes smaller as the Al substitution increases. The particle length gradually reduces from 1500nm for pure goethite to 300nm for 10.17 mol % Al. This indicates that the substitution of smaller Al^{3+} for Fe^{3+} results in a smaller particle size of Al-goethite. The domain of crystals tends to be parallel and the number of domains reduces with increasing Al substitution. Schulze and Schwertmann (1984) thoroughly investigated the unit cell parameters and the estimation of Al substitution from these data. The classic equation of estimation Al substitution in goethite derived from their research has been employed in this study and the detailed information can be found in section 3.2.1.3.

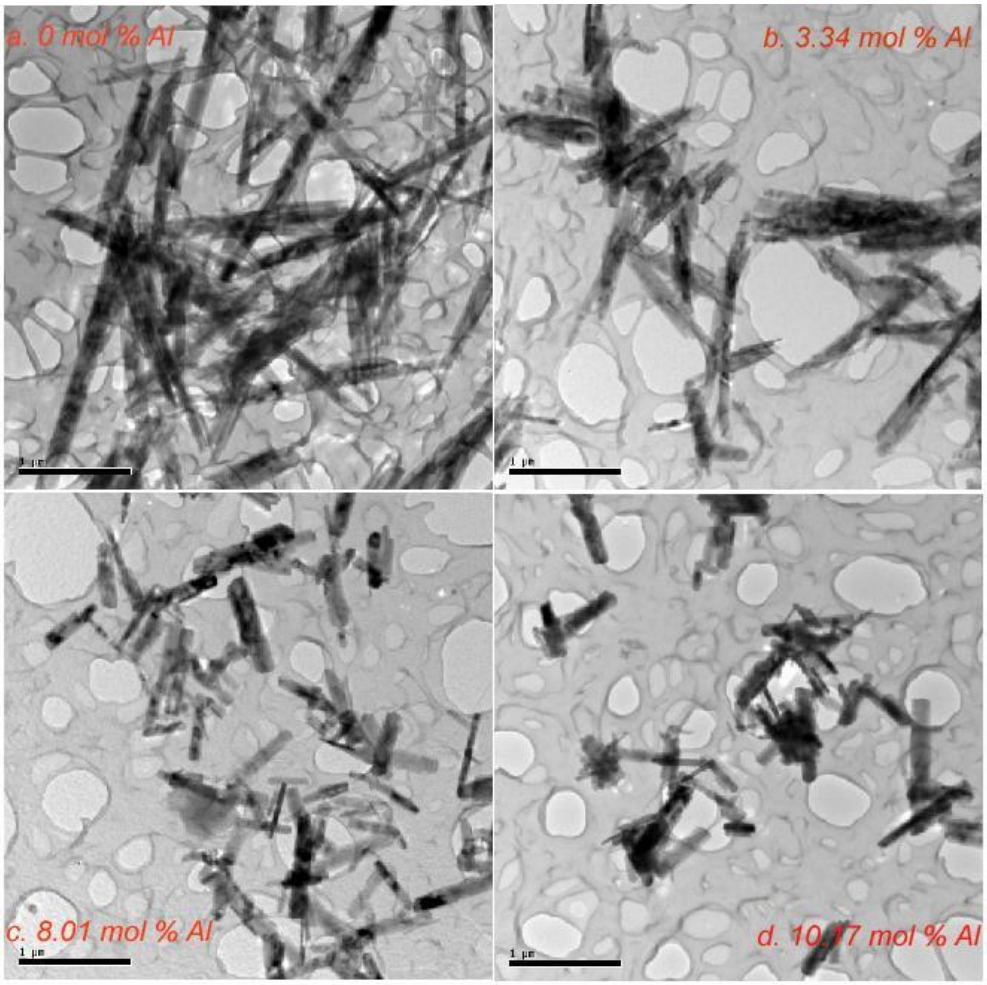

Figure 4.10 Transmission electron micrograph of Al substituted goethite for different mole % Al. *a*) 0%; *b*) 3.34%; *c*) 8.01%; *d*) 10.17%. The scale bar presents 1 micrometer.

In terms of crystal growth, two kinds of domains were observed in this study as shown in **Figure 4.11**. Star-shape twinned crystals were found in commercial goethite which has been used in thermal transformation of goethite to hematite tests and acicular goethite crystals were observed in the synthetic Al-goethite samples. Atkinson et al. (1968) established the mechanism of formation of twinned goethite crystals while Cornell and Schwertmann (2003) discussed the conditions under which they form. Nucleation of twinned goethite is associate with the ferrihydrite aggregated and only occurs at the early stages of precipitation reaction (**Figure 4.11** *left*); while rapid preferential growth along the needle axis, such as formation at high [OH], is more likely to form acicular crystals (**Figure 4.11** *right*) due to inhibition of twinning (Cornell and Schwertmann, 2003). It provides the evidence that preparation condition of high [OH] contributes to the formation of acicular crystals in our study.

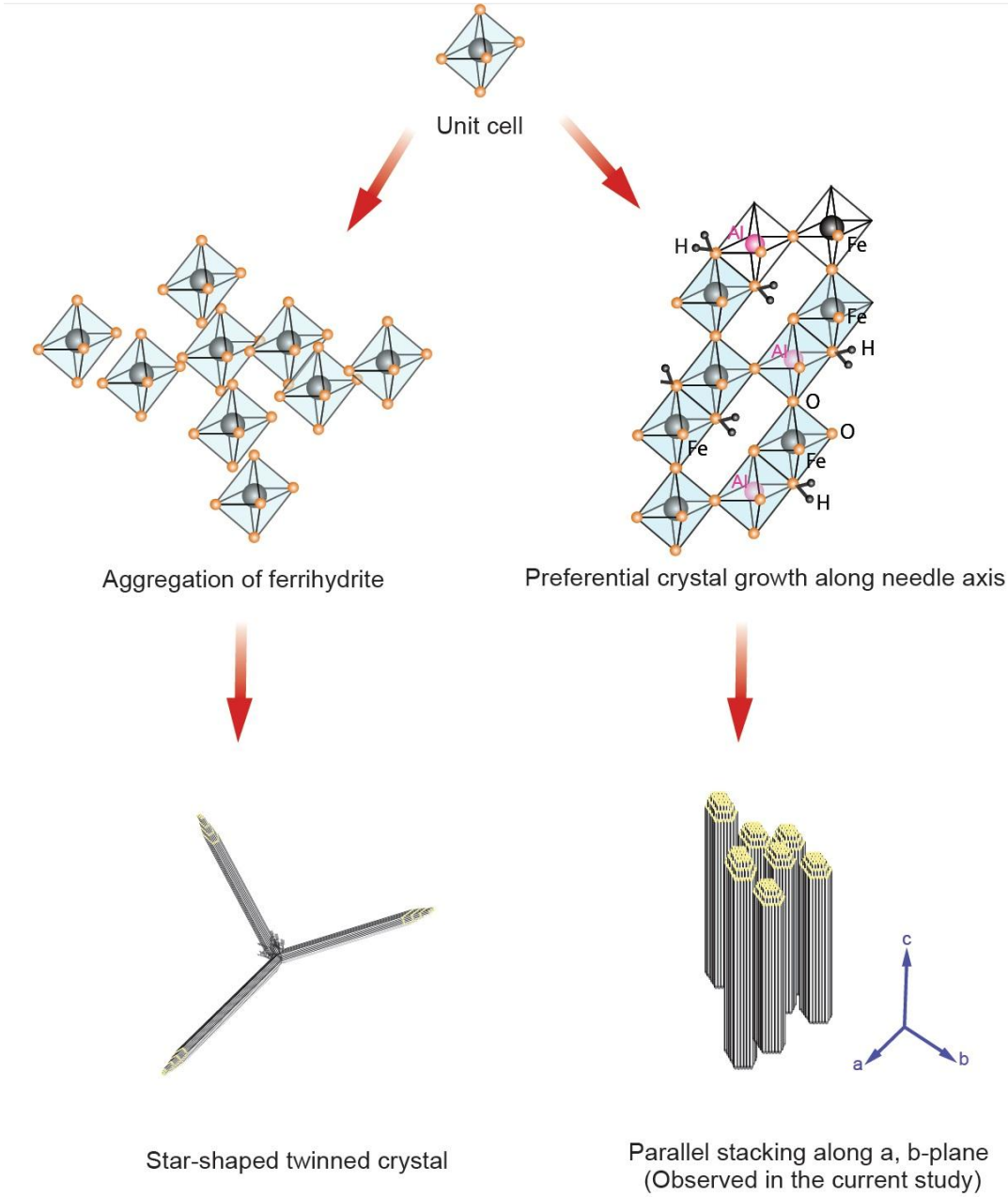

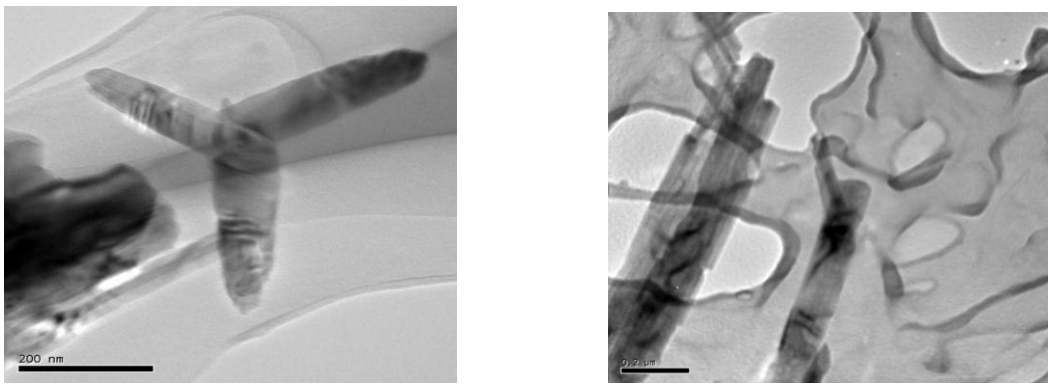

TEM for star-shaped twinned crystal
(Commercial product)

TEM for acicular crystal
(Synthetic Al-goethite)

Figure 4.11 A schematic diagram and TEM illustration of Al-goethite crystal domain stacking.

4.5 Solubility limit of diaspore-goethite solid solution in alkaline environment

It is obvious that the iso-structural replacement of Fe by Al in aluminium substituted goethite is very limited in Fe^{3+} synthesis system according to the data of synthesis (**Table 4.2** and **Table 4.3**). Lower than 11 mol % Al was incorporated into the goethite structure although up to 27 mol % Al was initially introduced into the system. Further increased the intake of Al^{3+} to the synthesis system tends to favour the formation hematite and other iron impurities rather than the increase of the Al substitution in goethite structure. With alternative synthetic path for Al-goethite from Fe^{2+} slow oxidation, higher Al substitution is more likely to be achieved although the process is hardly controlled due to more impurities present in the product. However, the gap between the intake of Al^{3+} and the incorporated Al^{3+} to the goethite structure still remains.

Al-substituted goethite is widely accepted as a diaspore-goethite solid solution considering the iso-structural substitution of diaspore to goethite. A number of studies have been focused on the solubility limits of goethite-diaspore solid solution. A group of researchers (Wolska *et al.*, 1992a; Wolska and Schwertmann, 1993; Wolska *et al.*, 1994; Piszora and Wolska, 1998) reported very similar data that the maximum of Al substitution seems to stay at 10-11 mol % with various synthetic methods, pH ranging from 3.5 to 13 and temperature between 25 ℃ and 155 ℃. They state that the level of aluminium that is incorporated in the goethite structure is below the possible maximum of 33 mol% because high levels of aluminium in the system promote hematite formation and also form separate $Al(OH)_3$ phase, particularly when Al-goethite is prepared at high pH. Under the same conditions as we did in this study, Blanch et al. (2008) obtained the same level of Al substitution as well. Higher Al substitution up to 33 mol % has been reported in other synthetic methods (i.e. Fe^{2+} synthetic system in our study), however, the gap between the original Al/(Al+Fe) and Al in the goethite structure is still around 5 to 20 mol % (Fey and Dixon, 1981). In addition, it is suggested in a number of reports (Cornell and Schwertmann, 2003) that up to 33 mol % Al substitution, rather than unlimited substitution, occurs in both natural and synthetic goethite. It is therefore worth studying the causes of the widely existing limit of Al substitution in both synthetic and natural Al-goethite.

In terms of synthesis of Al-substituted goethite from Fe^{3+} in alkaline environment in this study, the substitution gap between the initial Al^{3+} in the system and the incorporated Al/(Al+Fe) in the goethite structure is shown in **Figure 4.12**. There is an apparent difference between the experimental data and theoretical Al substitution; despite a linear relationship between initial Al and incorporated Al in the goethite structure is also observed as suggested by Cornell and Schwertmann (2003).

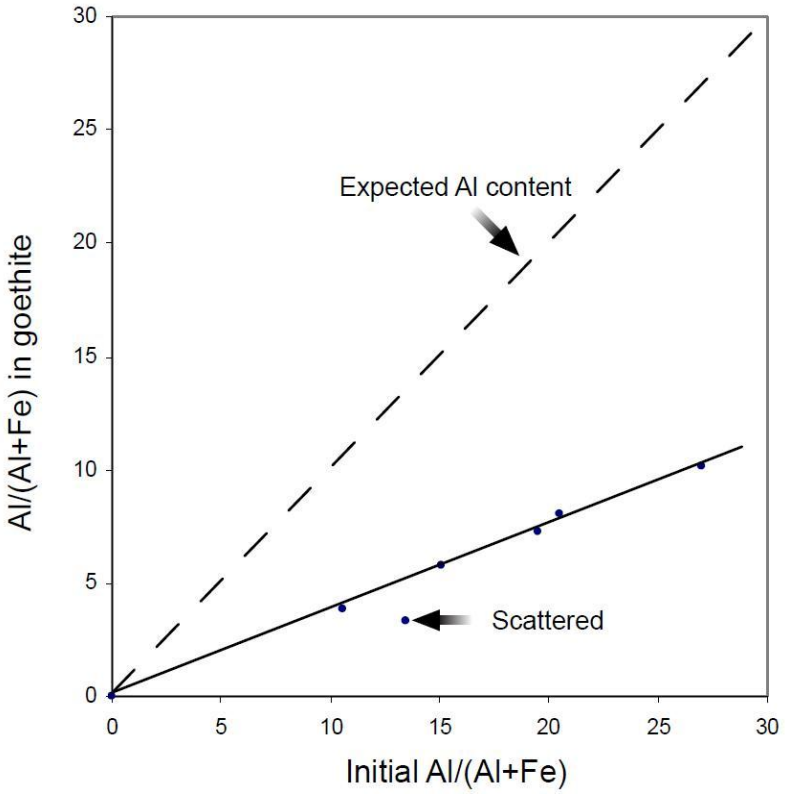

Figure 4.12 Extent of Al substitutions in goethite structure. The dots present the experimental data and the dash line shows the expected Al content in Al-goethite. The linear relationship between the initial and incorporated Al/(Al+Fe) (mol %) is presented by the straight line.

In order to investigate the reasons that cause the Al substitution gap between the initial Al intake and the incorporated Al in the goethite structure, multiple analytical techniques, such as infrared spectroscopy (IR), differential scanning calorimetry (DSC) and transmission electron microscopy (TEM), were employed to examine the limit of Al substitution in the goethite structure.

4.5.1 IR study: Structure strain

A mineral's Infrared (IR) spectrum is often altered by its structural changes. The structural strain induced by Al inclusion in goethite manifests as shifts of six absorption peaks. A series of Al-substituted goethite over the frequency interval 600 to 4000cm^{-1} are shown in **Figure 4.13**. Three samples with lower Al substitution at 0, ~3 and ~10 mol % were synthesized in the laboratory and, for comparison, the other sample with much higher Al substituted level (~25 mol %) was extracted from natural sample. The purpose of comparison is to test if there are differences in micro-structures between the synthetic and naturally occurring specimens. It sheds light on the causes for the difficulties in achieving high Al substitution for Fe in the goethite structure. The dominant phase is goethite in all samples, which is verified by the characteristic IR spectrum of α-FeOOH. However, subtle structural changes are manifested as shifts and widening of the typical IR absorption peaks due to the alterations in rotational and vibrational movements of goethite's function groups.

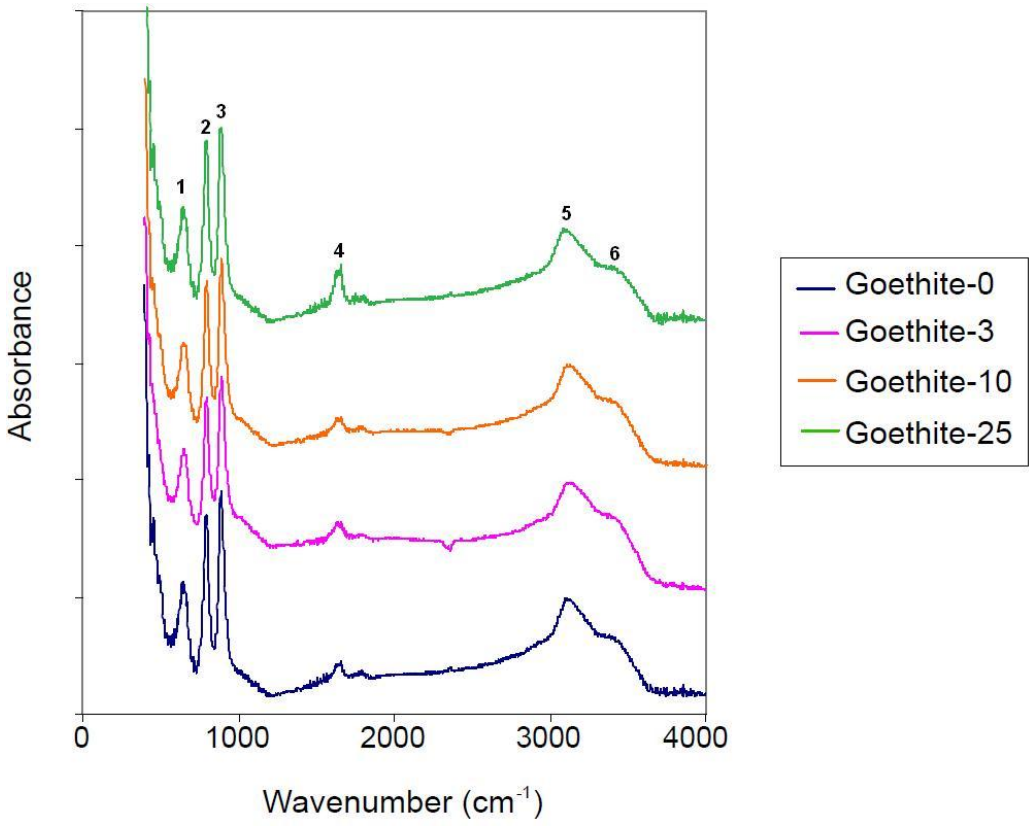

Figure 4.13 IR-transmission spectra of Al-goethites. Al-goethites with Al = 0, 3, 10 mol% are synthetic samples; Al 25 mol % is natural Al-goethite sample.

The function groups of interest in the current IR study are -Fe-O, -Fe-OH, -H_2O, and –OH. Their momentum components 'stretching', 'plantar bending' and 'vibration' are typically defined as 'γ', 'δ', and 'ν' respectively (e.g. $\gamma_{Fe\text{-}O}$ represents stretching of Fe-O group). They are often referred to as 'peak assignments' in many literatures. The structural strain caused by Al incorporation within goethite lattice is typically reflected by the slight changes in movement frequencies of these momentum components. The peak assignments for the Al-goethites in the IR spectra are listed in **Table 4.6**. The main absorption peaks for goethite in IR pattern occur at ~635, 795, 890, 1652, 3139 and 3400 cm^{-1} and their corresponding function groups are also given in the table (Sudakar *et al.*, 2004b). With increasing Al substitution, the positions for the absorption peaks relating to Fe-O bonds tend to shift to higher frequencies. Blanch et al. (2008) demonstrated that the shape of IR spectra of goethite and diaspore is very similar if not identical, only differs in presenting frequencies. In other words, if moving an entire goethite IR spectrum towards the higher frequencies it will almost coincide with a diaspore spectrum. This frequency shift between the two minerals is ranging from 75 and 190 cm^{-1} across the spectrum. The shift of the characteristic absorption peaks of the synthetic goethite samples to higher frequencies is a result of the increase in Al substitution for Fe. It can be seen as a mixing process on a micro-structural level between the two end members in a solid solution, namely diaspore and goethite.

Table 4.6 Positions of IR peaks for Al-goethites

Peak no.	Peak assignment As per Sudakar et al. (2004b)		Al-substituted samples			
			Al-0	Al-3	Al-10	Al-25
1	Fe-O stretch in FeOOH (γ_{Fe-O})	635	642.0	648.0	650.4	650.2
2	O-H out-of-plane bend (δ_{Fe-OH})	795	792.6	794.5	796.4	796.5
3	O-H in-plane bend (δ_{Fe-OH})	890	890.9	892.9	895.1	895.3
4	H-O-H bending from H_2O (δ_{H_2O})	1652	1655	1657	1660	1660
5	O-H stretch (ν_{O-H})	3139	3132	3135	3138	3139
6	H-O-H stretch	3400	3404	3404	3405	3405

Note: Wavenumbers in the table are given in cm^{-1}.

In addition to this, it is found that the shift to higher frequency tends to slow down with increasing Al substitution. This trend is especially obvious when Al level is greater than 10 mol %. Comparing peak positions and the shape of peak for 10 mol % and 25 mol % Al-goethite, it seems that there is no significant shift or limited shift to higher frequencies with the increase of Al substitution (see **Figure 4.14**). An increased in Al level in goethite beyond 10 mol% is causing a broadening peaks of O-H stretch and H-O-H stretch rather than shifting these peaks. This finding in the current study is in close agreement with Blanch et al. (2008)'s experimental data. It appears that 10 mol % Al substitution marks the onset of transition from IR frequency shift to peak shape changes. In a lower Al substitution level ([Al] < 10 mol%), right shift of goethite spectrum dominates, whereas in a higher Al substitution level ([Al] > 10 mol%), the widening of absorption peaks prevails. The shift of absorption peak is caused by changes in function groups' momentum movement and the widening of peak is likely due to decreased homogeneity of mineral phases (Murad and Bowen, 1987). The decreased crystal homogeneity in high Al goethite is demonstrated by TEM in the next section as an encapsulation of goethite with diasporic-like material along the brim of Al-goethite core (a schematic diagram shown in **Figure 4.14**).

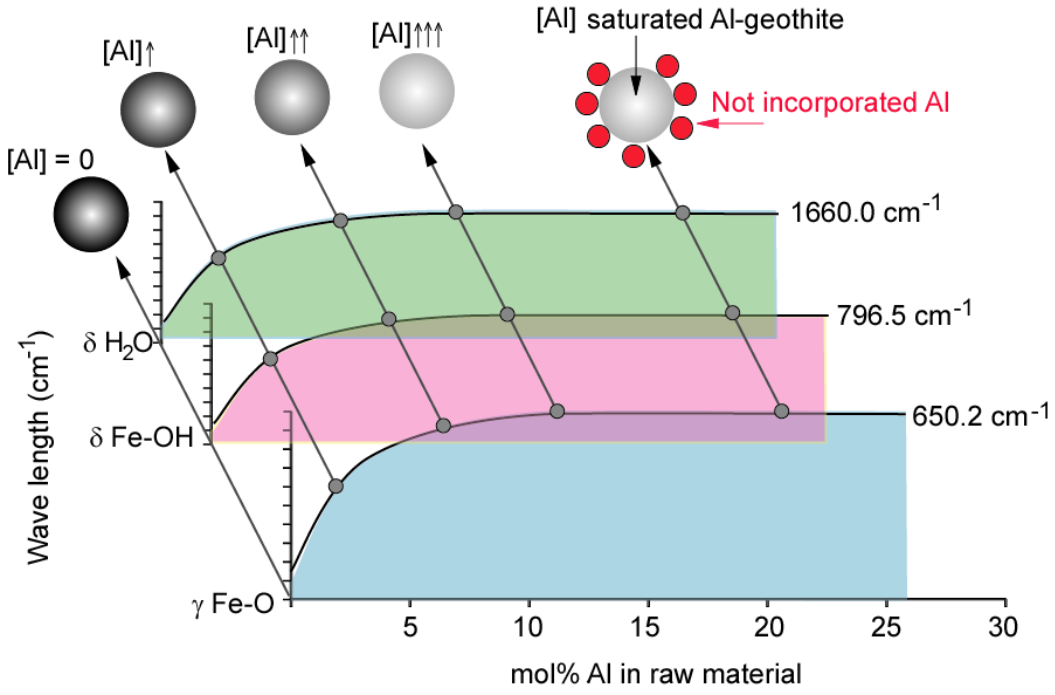

Figure 4.14 The relationship between IR absorption peak shift and mol% Al used in producing Al-goethite.

This hypothesis is further identified by DRIFT-IR spectra of synthetic Al-goethite (shown in **Figure 4.15**). The shift and the broadening of absorption peaks as the increase of the Al substitution appear more notable. Given that DRIFT-IR is a more surface-sensitive spectrum than IR-transmission, this tendency of shift and broadening with increasing of Al substitution could be attributed to the surface "accumulation" of diaspore.

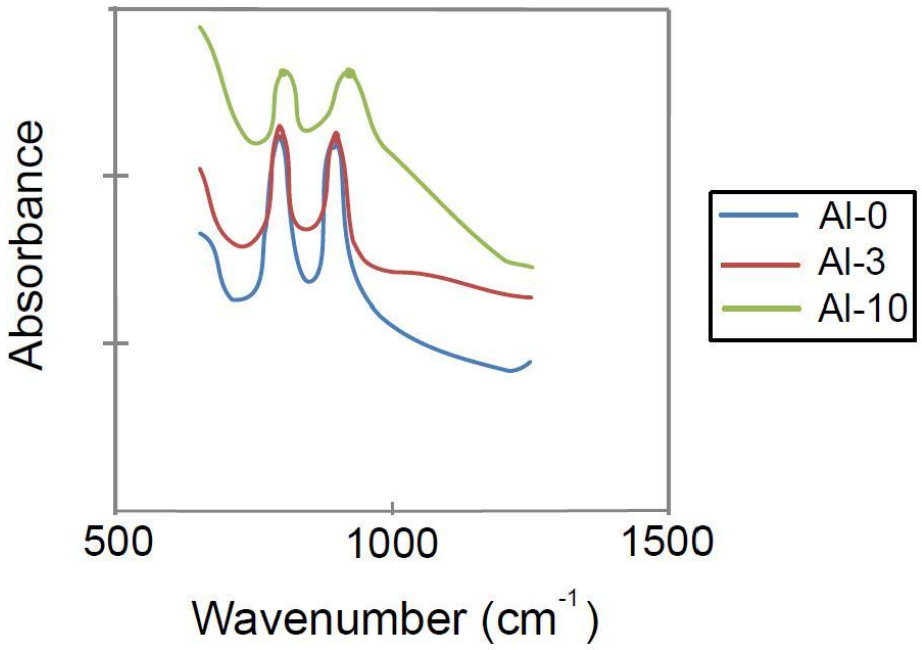

Figure 4.15 DRIFT-IR spectra of synthetic Al-goethites.

4.5.2 Thermal analysis: Enthalpy of mixing

Thermal analysis for synthetic Al-goethites has been conducted to investigate their thermal behaviour in the following Chapter 5. Thermal analysis was adopted for the quantitative study of the thermal transformation of goethite to hematite. Enthalpy of mixing determines the level of difficulty in producing a solid solution. An ideal solid solution is characterised by zero mixing enthalpy, which is rarely achieved in common experimental conditions (Hu *et al.*, 1999). The more positive is the enthalpy, the more difficult it is in forming solid solution at a given temperature. A higher enthalpy of mixing often leads to a meta-stable mineral phase that hosts abundant crystal structural defects (Ibach and Lüth, 2010). The mol% Al in goethite structure is inversely related to the structural stability of Al-goethite. Therefore, the Al concentration at which a meta-stable Al-goethite develops is a primary concerning factor in the thermodynamic study.

In the current experimental setting, the enthalpy of mixing for Al-goethite, was obtained from differential scanning calorimetry (DSC) provides the information regarding Al substitution limit in Al-goethite, which can be viewed as a goethite-diaspore solid solution. **Table 4.7** lists the enthalpy of mixing for synthetic Al-goethite with different extent of Al substitution. The thermal data could be measured by calculating the thermochemical cycle for Al-goethite (Majzlan and Navrotsky, 2003), however, in this study the thermal data were obtained through evaluation of the DSC spectra using the Proteaus Analysis software. In addition, the enthalpy of mixing for Al-goethite has been also converted to unit $kJ \cdot mol^{-1}$ for further analysis and discussion.

Table 4.7 The enthalpy of mixing for goethite-diaspore solid solution

Synthetic sample ID	Al substitution (mol %)	Molecular weight of $(Al_xFe_{1-x})OOH$ ($M_{Al\text{-}goethite}$)	Enthalpy of mixing (ΔH_{mix})	
			[1]detected from DSC ($J\ g^{-1}$)	[2]converted to $kJ\ mol^{-1}$
ALGOE-1	0	89.00	206.7	18.40
ALGOE-3	3.83	87.89	226.8	19.93
ALGOE-4	5.75	87.33	232.1	20.27
ALGOE-7	10.17	86.05	242.9	20.90
[3]Calculated	28.50	80.74	309.6	25.00
[3]Calculated	33.33	79.33	325.4	25.82

Note:

1. The enthalpy of mixing [ΔH_{mix} ($J\ g^{-1}$)] is obtained from the differential scanning calorimetry (DSC) spectra using the Proteaus Analysis software;
2. $\Delta H_{mix}(kJ \cdot mol^{-1}) = \frac{\Delta H_{mix}(J \cdot g^{-1})}{1000} \times M_{AlxFe(1-x)OOH}$
3. The data in the last two rows are calculated by the provided data from synthetic Al-goethite using the Least Square method (refer to **Figure 4.17**).

As seen in **Figure 4.16**, it appears that there is a linear relationship between Al substitution (mol %) and the enthalpy of mixing for Al-goethite (ΔH_{mix}). With the increase of Al substitution in Al-substituted goethite the enthalpy of mixing increases linearly. Using the Least Square method, a trend line and the corresponding formula for the linear relationship has been achieved as shown in the figure.

$$\Delta H_{mix}\ (J \cdot g^{-1}) = 3.5007 * Al\ mol\ \% + 209.84 \qquad \textbf{(4.6)}$$

where ΔH_{mix} ($J \cdot g^{-1}$) is the enthalpy of mixing in the format of $J \cdot g^{-1}$ for goethite-diaspore solid solution and *Al mol %* is the extent of Al substitution in Al-goethite.

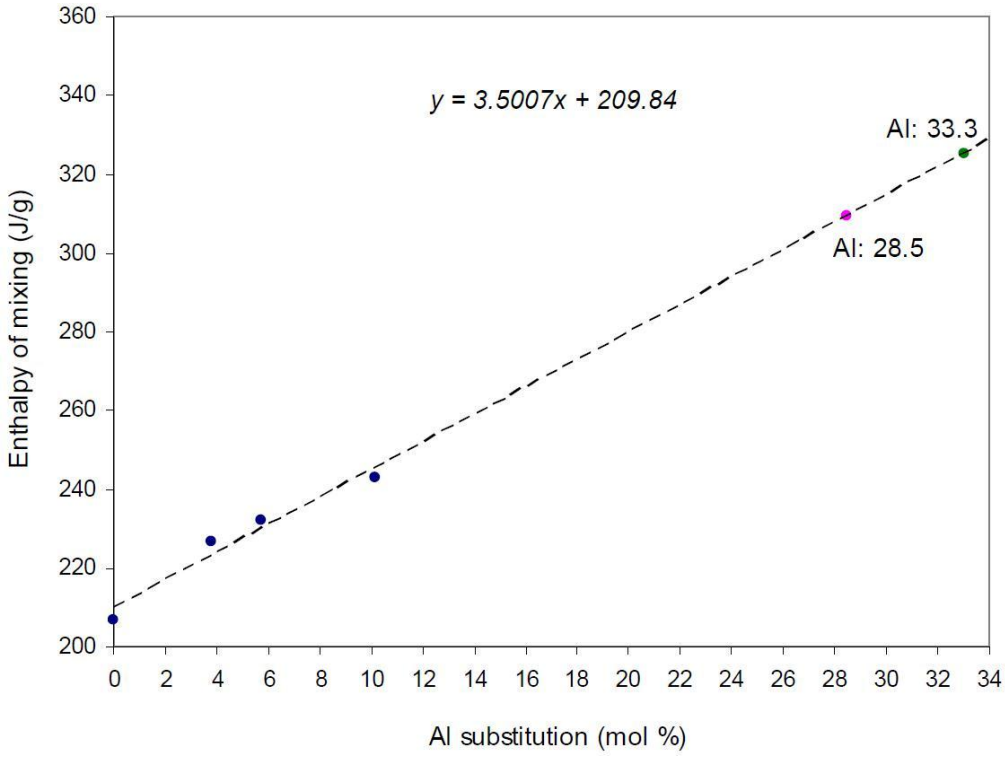

Figure 4.16 The enthalpy of mixing for synthetic Al-goethite [$\Delta H_{mix}(J \cdot g^{-1})$] against the extent of Al substitution (Al mol%). The values for enthalpy of mixing $\Delta H_{mix}(J \cdot g^{-1})$ are obtained from the DSC data for synthetic Al-goethite using the Proteaus Analysis software. The blue dots are those measured synthetic Al-goethite data; the dash line is the trend line derived from the provided data (blue dots) using Least Square method. The pink and the green dots are the potential influential data which are calculated as per the trend (dash) line.

The increase of enthalpy of mixing (ΔH_{mix}) is more likely due to the mismatch of the molar volumes between these two end members, goethite and diaspore, in the goethite-diaspore solid solution. As the increased amount of diaspore mixed with goethite, the enthalpy of mixing eventually reaches to its limit value, which is referred to the metastable phases of the solid solution. In other words, the solid solution tends to be a meta-stable phase over this limit which can persist only for short time or cannot be formed at all (Majzlan and Navrotsky, 2003). It should be noted that enthalpy at 20-25 $kJ \cdot mol^{-1}$ has been suggested as the maximum enthalpy for metastable diaspore-goethite solid solution. With the establishment of this internal connection between the enthalpy of mixing and the limit of the maximum Al substitution, it is not difficult to find out as to why the synthesis of Al-goethite with higher than 11 mol % Al substitution cannot be achieved with Fe^{3+} system. In **Table 4.7**, the enthalpy of mixing for Al-goethites with

more than 5.75 mol % Al substitution has already reached the low end of the metastable zone. This may explain the difficulty for the synthesis of Al-goethite with Al substitution > ~10-12 mol %. A further calculation according to the **Equation 4.6** verifies that enthalpy of mixing could be an ideal parameter to determine the maximum limit for the Al substitution in goethite. It is assumed here that natural goethite has a similar path during the formation process with that in this study. Since there is a possible linear relationship existing between the enthalpy of mixing and Al substitution, two key points, the widely recognised maximum Al substitution for natural Al-goethite at 33 mol % and the matching Al substitution for maximum enthalpy of metastable phases, have been calculated according to the Equation 4.3. Coincidently it is found that the enthalpy of mixing for 33.3 mol % Al-goethite is 25.82 $kJ \cdot mol^{-1}$, which is just over the maximum of enthalpy of mixing for metastable phases. This suggests that goethite with more than 33.3 mol % Al substitution cannot be achieved at all due to the extremely high enthalpy of mixing required. Meanwhile it has raised a question as to what is the corresponding Al substitution value for the maximum enthalpy of mixing (25 $kJ \cdot mol^{-1}$). As also seen in **Table 4.7**, 28.5 mol % Al substitution may hold the maximum enthalpy mixing which is also coincidently in agreement with the reality that it is hardly to obtain a natural Al-substituted goethite with more than ~28 mol % Al substitution.

The thermodynamics of Fe^{3+}/Al^{3+} mixing has been studied in several other solid solutions (ss) (Newton and Smith, 1967; Perchuk and Aranovich, 1979; Davies and Navrotsky, 1983; Majzlan and Navrotsky, 2003). The miscibility gap was also found in clinozoisite-pistacite $(Ca_2Al_3[Si_3O_{12}(OH)]\text{-}Ca_2Al_2Fe[Si_3O_{12}(OH)])_{ss}$ (Perchuk and Aranovich, 1979) with positive ΔH_{mix} which is regarded as non-ideal mixing for the solid solutions. However, study from Stoffregen et al. (2000) on synthetic and natural jarosite-alunite $(KFe_3[(SO_4)_2(OH)_6]\text{-}KAl_3[(SO_4)_2(OH)_6])_{ss}$ indicated that miscibility gap in this solid solution is unlikely and the Fe/(Fe+Al) = 0.5 of jarosite-alunite, which is ideal mixing for solid solutions, can be synthesized in the laboratory. The structure strain induced by Fe^{3+}/Al^{3+} substitution seems to be able to be accommodated more easily with more complex structures with larger molar volumes than the structures of hematite or goethite (Majzlan and Navrotsky, 2003). Greater mismatch "can be tolerated by a structure in which the ions being mixed are embedded in a matrix which can itself change geometry slightly to absorb the strain" (Davies and Navrotsky, 1983).

4.5.3 Proposed model for Al-goethite

The study is accentuated in understanding the discrepancy between the Al replacement for Fe in goethite achieved in laboratory settings and that typically presents in the nature. Depending on the laboratory technique of synthesizing Al-goethite, the extent of Al incorporation may vary between 10 and 33 mol % which is invariably lower than the ideal mixing state (Ruan et al., 2002; Blanch et al., 2008). There is always a gap between the amount of Al used in synthesizing Al-goethite than the amount of Al that is actually incorporated in the Al-goethite structure regardless of the type of synthesis techniques used. Experiments in the current study were designed to explore plausible mechanisms that explain the very existence of this "miscibility gap" rather than investigating how much the gap is in different types of methods of Al-goethite production. The miscibility between two minerals is associated with mixing enthalpy (ΔH_{mix}), which is affected by numerous factors e.g. temperature, pressure, and pH. The interplay among these factors is complex and subsequently leads to difference in the grade of Al-goethite products using different synthesize methods. A complete spectrum of ΔH_{mix} variation with the mentioned parameters is beyond the scope of current study. One of the main impact factors on ΔH_{mix}, temperature, is illustrated in Appendix D.

As mentioned and discussed in the previous XRD and TEM results, the substitution of Al for Fe modifies the crystal size due to the smaller size of Al^{3+} despite the similarity in structure of goethite with diaspore. The structure strain increases with more Al substituted into the goethite structure. The goethite structure consists of a hexagonal close packed (*hcp*) arrangement of anions (O^{2-} and OH^-) stacked along the a- direction. Thus, octahedral interstices are formed within layers. Fe^{3+} ions occupy half of the interstices (Cornell and Schwertmann 2000). The substitution of Al for Fe is limited due to rigidity of anions as well as the strain caused by the size mismatches between Al^{3+} and Fe^{3+} (Sudakar et al. 2004-16). The enthalpy study in the previous section shows the evidence that little structural changes occur once the Al exceeds 10 mol% in Al-goethite, despite the apparent Al level may be still rising. The following proposed model provides an explanation (**Figure 4.17**).

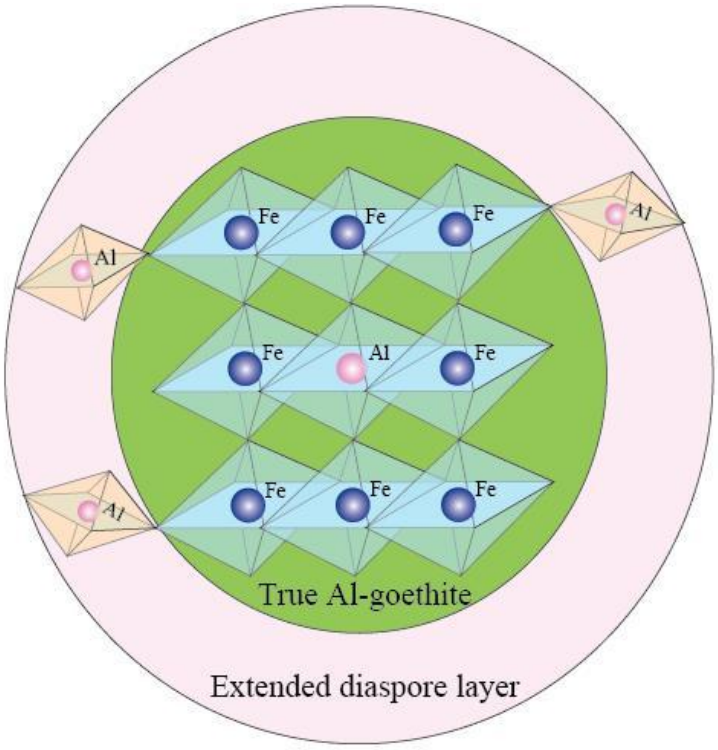

Figure 4.17 A proposed mechanism for solubility limit of alumina-diaspore solid solution

The true diaspore-goethite solid solution occurs when the added Al is within the range of 0 to 10 mol%. This hypothesis is supported by monotonic increasing relationship between [Al] and IR peak shifts in **Figure 4.14**. We believe the apparent increase in [Al] without any obvious structural changes in Al-goethite is due to the formation of rim of Al rich diasporic-like material that coats the true Al-goethite core. Even though this core composition of Al is more or less around 10 mol%, the apparent Al content is much higher (up to 33 mol%) simply due to the diasporic material coating. This coating is observed in a series of TEM micrographs shown in **Figure 4.18**. The reason natural occurring Al-goethite can reach as high as Al mol% of 33% is likely attributed to the slow and continuous Al migration from the outer-rim of diasporic coating towards the central core of true Al-goethite over thousands or even millions of years. However, it should bear in mind that this "Al-rich outer layer" goethite structure need to be further identified with the aid of Electron Energy Loss Spectroscopy (EELS) and High Resolution Transmission Electron Microscopy (HRTEM) on the synthetic Al-goethite samples, which has been suggested in the future work.

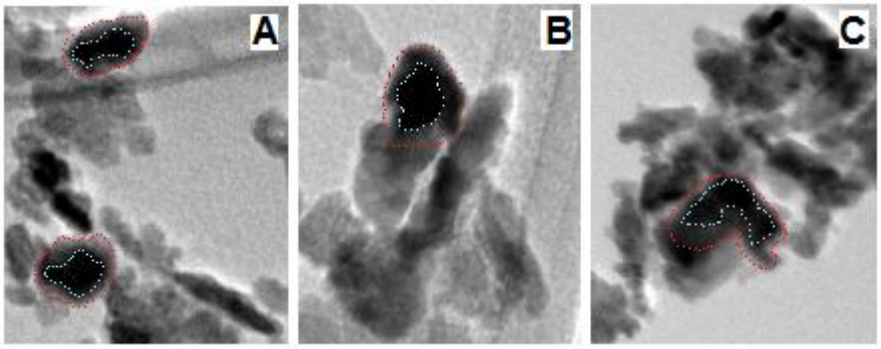

Figure 4.18 TEM of Al-goethite with compositions of (A) 15 mol% Al substitution, (B) and (C) are 25 mol% Al substitution. The inner core of Al-goethite is highlighted with blue dashed lines. The outer rim is believed to be diasporic-like coating outlined with red dashed lines.

However, this hypothetical model is oversimplified, as the structure strain formed by the substitution of Al for Fe may not be the only contributing factor towards the solubility limits in the solid solution. As mentioned with XRD results, the unit cell parameters *a*, *b* and *c* show different tendency with the increase of Al substitution. This indicates that the solubility limits are affected by multiple factors. Wolska et al. (1992; 1993), Cornell and Schwertmann (2000) provided possible explanation for the assumption. The general formula of Al-substituted goethite is described as α-$(Fe_{1-x}Al_x)_{1-y/3}O_{1-y}(OH)_{1+y}$. This means not only cation substitution (Al replacing Fe) occurs during the Al-goethite formation but also a lesser degree of anion substitution (OH replacing O) may also occur. At this stage, how these factors affect the unit cell parameters and how much contribution they make respectively have yet to be established. A more comprehensive investigation of the impact factors on Al-goethite structural changes is suggested to be carried out in the future work.

References

Atkinson, R. J., Posner, A. M. & Quirk, J. P. (1968) Crystal nucleation in Fe(III) solutions and hydroxide gels. *Journal of Inorganic and Nuclear Chemistry,* 30**,** 2371-2381.

Blanch, A. J., Quinton, J. S., Lenehan, C. E. & Pring, A. (2008) The crystal chemistry of Al-bearing goethites: an infrared spectroscopic study. *Mineralogical Magazine,* 72**,** 1043-1056.

Burke, J. (1965) *The kinetics of phase transformations in metals,* Oxford, Pergamon Press.

Cornell, R. M. & Schwertmann, U. (2000) *The Iron Oxides: Structure, Properties, Reactions, Occurrences and Uses,* Weinheim, Wiley-VCH.

Cornell, R. M. & Schwertmann, U. (2003) *The Iron Oxides: Structure, Properties, Reactions, Occurrences and Uses,* Weinheim:Wiley-VCH.

Crombie, T., Davis, M. & Laurie, J. E. (1973) Method of digesting bauxite via the Bayer process with the addition of reducing agents. United States Patent 4059672.

Davies, P. K. & Navrotsky, A. (1983) Quantitative correlations of deviations from ideality in binary and pseudobinary solid solutions. *Journal of Solid State Chemistry,* 46**,** 1-22.

Fey, M. V. & Dixon, J. B. (1981) Synthesis and properties of poorly crystalline hydrated aluminous goethite. *Clays and Clay Minerals,* 29**,** 91-100.

Hu, Y., Lv, R., Liu, G. & Ye, R. (1999) *Physical Chemistry (Chinese),* Beijing, Higher Education Press.

Ibach, H. & Lüth, H. (2010) *Solid-State Physics: An Introduction to Principles of Materials Science,* London, Springer.

Klug, H. P. & Alexander, L. E. (1974) *X-ray Diffraction Precedures for Polycrystalline and Amorphous Materials,* New York, Wiley.

Li, D., O'connor, B. H., Low, I. M. & Riessen, A. (2006) Mineralogy of Al-substituted goethites. *Powder Diffraction,* 21**,** 289-299.

Li, L. Y. & Rutherford, G. K. (1996) Effect of bauxite properties on the settling of red mud. *International journal of mineral processing,* 48**,** 169-182.

Majzlan, J. & Navrotsky, A. (2003) Thermodynamics of the goethite-diaspore solid solution. *Eur. J. Mineral,* 15.

Murad, E. & Bowen, L. H. (1987) Magnetic ordering in Al-rich goethites: Influence of crystallinity. *American Mineralogy,* 72**,** 194-200.

Newton, R. C. & Smith, J. V. (1967) Investigations concerning the breakdown of albite at depth in the Earth. *Journal of Geology,* 75**,** 268-286.

Perchuk, L. L. & Aranovich, L. Y. (1979) Thermodynamics of minerals of variable composition: Andradite-grossularite and pistacite-clinozoisite solid solutions. *Physical Chemistry of Minerals,* 5**,** 1-14.

Piszora, P. & Wolska, E. (1998) X-Ray Powder Diffraction Study on the Solubility Limits in the Goethite-diaspore Solid Solutions. *Materials Science Forum,* 278**,** 584-588.

Schulze, D. G. (1984) The influence of aluminum on iron oxides. VIII. Unit cell dimensions of Al-substituted goethites and estimation of Al from them. *Clays and Clay Minerals,* 32**,** 36-44.

Schulze, D. G. & Schwertmann, U. (1984) The influence of aluminium on iron oxides. X. Properties of Al-substituted goethites. *Clay Minerals,* 19**,** 521-539.

Schwertmann, U. & Cornell, R. M. (2000) *Iron Oxides in the Laboratory: Preparation and Characterization,* Weinheim, Wiley-VCH.

Schwertmann, U. & Fischer, W. R. (1966) Zur Bildung von a-FeOOH und c~-Fe2O3 aus amorphem Eisen(III)-hydroxid.III. *Z. Anorg. Allg. Chem.*, 346, 137-142.

Schwertmann, U., Friedl, J., Stanjek, H. & Schulze, D. G. (2000) The effect of clay minerals on the formation of goethite and hematite from ferrihydrite after 16 years' ageing at 25 ^{o}C and pH 4-7. *Clay Minerals,* 35**,** 613-623.

Stoffregen, R. E., Alpers, C. N. & Jambor, J. L. (2000) Alunite-jarosite crystallography, thermodynamics, and geochronology. IN ALPERS, C. N., JAMBOR, J. L. & NORDSTROM, D. K. (Eds.) *Review of Mineral Geochemistry.* Mineralogical Society of America.

Sudakar, C., Subbanna, G. N. & Kutty, T. R. N. (2004) Effect of cationic substituents on particle morphology of goethite and the magnetic properties of maghemite derived from substituted goethite. *Journal of Materials Science,* 39**,** 4271-4286.

Suss, A., Fedyaev, A., Kuznetzova, N., Damaskin, A., Kuvyrkina, A., Panov, A., Paromova, I. & Lukyanov, I. (2010) Technology solutions to increase alumina recovery from aluminogoethitic bauxites. *Light Metals*.

Vaughan, D. J. & Craig, J. R. (1978) *Mineral Chemistry of Metal Sulfides,* Cambridge, Cambridge University Press.

Vyazovkin, S. (2000) Computational aspects of kinetic analysis.: Part C. The ICTAC Kinetics Project — the light at the end of the tunnel? *Thermochimica Acta,* 355**,** 155-163.

Wang, H., Pring, A., Ngothai, Y. & O'Neill, B. (2005) A low-temperature kinetic study of the exsolution of pentlandite from the monosulfide solid solution using a refined Avrami method. *Geochimica et Cosmochimica Acta,* 69**,** 415-425.

Wolska, E. & Schwertmann, U. (1993) The mechanism of solid solution formation between goethite and diaspore. 213-223.

Wolska, E., Szajda, W. & Piszora, P. (1992) Synthetic solid solutions formed between goethite and diaspore. *Z. Pflanzenernahr. Bodenk.* , 155**,** 479-482.

Wolska, E., Szajda, W. & Piszora, P. (1994) Mechanism of Al- for Fe-substitution during the α-(Fe, Al) OOH to γ-(Fe, $Al)_2O_3$ transformation. *Solid State Ionics,* 70/71**,** 537-541.

Yund, R. A. & Hall, H. T. (1970) Kinetics and mechanism of pyrite exsolution from pyrrhotite. *Journal of Petrol,* 11**,** 381-404.

Yund, R. A. & McCallister, R. H. (1970) Kinetics and mechanism of exsolution. *Chemical Geology,* 6**,** 5-30.

Zwingmann, N., Gilkes, R. J. & Swash, P. M. (2008) Iron oxyhydroxide characterisation and modification in bauxite: tools for predicting and improving Bayer performance. Perth, Minerals and Energy Research Institute of Western Australia.

Chapter 5
Transformation of Synthetic Goethite/Al-goethite

5.1 Introduction

Goethite (α-FeOOH) present in Bayer residue negatively affects the settling rate of red mud in the refinery and causes reversion of gibbsite in settlers and washers due to its similar surface structure. High goethite content in bauxite can lead to the formation of fluffy colloidal residue, seriously inhibiting the solid-liquid separation process (Basu *et al.*, 1986; Authier-Martin *et al.*, 2001) and so increased goethite to hematite transformation in caustic liquors generally improves post digestion settling properties. The better settling properties of hematite are largely due to its reduced specific surface area and larger particles compared to goethite (Li, 2001).

Goethite can transform to hematite by thermal or hydrothermal transformation pathways. Thermal transformation is relevant for either the pre-treatment of bauxite or the reprocessing of red mud (290 °C to 550 °C) (Basu, 1983; Walter *et al.*, 2001; Cornell and Schwertmann, 2003; Frost *et al.*, 2003). The mechanism of thermal transformation has not been unequivocally determined. Some researchers believe that goethite transforms via an intermediate structure, referred to as "proto-hematite" and/or "hydro-hematite" (Mendelovici and Yariv, 1981; Wolska *et al.*, 1994), while others insist that the process is a direct transformation from goethite to hematite without forming any intermediate (González *et al.*, 2000; Walter *et al.*, 2001; Frost *et al.*, 2003; Prasad *et al.*, 2006). Understanding the mechanism of thermal transformation is key to optimising any bauxite pre-treatment process (Gialanella *et al.*, 2010).

Hydrothermal transformation under Bayer conditions has also been widely studied (King, 1971; Basu, 1983; Schwertmann and Cornell, 2000; Murray *et al.*, 2009). The mechanism of hydrothermal transformation proposed is a dissolution-precipitation process (King, 1971; Basu, 1983) and the driving force is the solubility difference between goethite and hematite in caustic liquor. Hematite is expected to be less soluble than goethite under all Bayer digestion conditions (Cornell and Schwertmann, 2003). Several authors (King, 1971; Basu, 1983; Murray *et al.*, 2009) have suggested a two-step process: the dissolution of goethite and the precipitation of hematite.

In this chapter, both thermal and hydrothermal transformation from goethite/Al-goethite to hematite will be discussed. The factors that affect the transformation of goethite to hematite and the mechanism were outlined. In addition, the practical application of the methods to alleviate the problems caused by goethite in the Bayer process is accordingly examined. More importantly, the results from this chapter will establish a fundamental understanding for further study in the following chapter in this thesis.

5.2 Thermal transformation

To investigate the behaviours of thermal transformation of goethite/Al-goethite, several experimental methods were employed for the transformation temperature range and the characterisation thereof during the change. This method was designed with two parts: *in situ* thermal analysis and *ex situ* thermal treatment and characterisation. The thermal transformation from goethite and Al-goethite to hematite was initially conducted with thermal analysis techniques, differential scanning calorimetry (DSC), differential thermal analysis (DTA) and thermogravimetry (TG), with which the transformation behaviour of goethite would be generally understood. Bearing the brief results in mind, the annealing treatment of goethite under certain temperatures was subsequently performed to monitor the morphological change during the heating process, by which the mechanism of the thermal transformation is likely to be established.

5.2.1 Thermal Analysis: DSC and TG

Thermal analysis has been widely used in the study of impact of Al substitution on Al-goethite's thermodynamic properties (Ruan *et al.*, 2001; Frost *et al.*, 2003; Majzlan and Navrotsky, 2003). The thermal analysis data are not only able to explain the thermal behaviour of Al-goethite but also provide the evidence for the formation of the diaspore-goethite solid solution via thermal enthalpy analysis.

The synthetic Al-goethite samples through the precipitation of Fe^{3+} and Al^{3+} in the alkaline solution were analysed by differential scanning calorimetry (DSC) and thermogravimetry (TG). **Figure 5.1** demonstrates the simultaneous TG/DSC curves of synthetic Al-substituted goethite. The main features on DSC/TG observed from **Figure 5.1** are summarised as follows: (1) Endothermic peaks are observed in two temperature ranges, ~75 ℃ and 290–320 ℃ respectively; (2) A shoulder appears on the low temperature side of the second endothermic peaks which eventually merges with the original peak as a result of increasing Al substitution; (3) The second endothermic peak

(290-320 ℃) shifts to higher temperatures as Al substitution increased, while the other peak (~75 ℃) remains in a relative steady temperature zone; (4) Weight loss obtained from TG analysis is apparently greater than the theoretical weight loss for conversion of Al-goethite to hematite (see **Table 5.1**).

The first peaks in all Al-goethite samples appear at about 75 ℃. They are accompanied by minor mass loss, which could be attributed to the surface water loss absorbed in the goethite structure. It should be noticed that the presence of structurally retained water molecules is inevitable (Sudakar *et al.*, 2004b). It is widely accepted that water physically absorbed within the goethite, termed hydro-goethite, is responsible for an endothermic peak at the early stage of thermal treatment (Fey and Dixon, 1981; Prasad *et al.*, 2006). Frost et al. (2003) further identified the result with similar observation for the first peaks at around 75 ℃. However, the observations of no mass loss for the first peaks in their research was explained with a structural rearrangement at the molecular level.

The endothermic peaks at high temperature ranges (>200 ℃) are more complicated by a major endothermic peak at temperatures ranging from 290 ℃ to 320 ℃. In this study, the peaks shift from 290.2 ℃ for pure goethite to 318.4 ℃ for goethite with 8.01 mol % Al substitution. The onset of the peaks also shifts to higher temperature as Al substitution increases, 221 ℃ for pure goethite, 256 ℃ for 3.83 mol %, 268 ℃ for 5.01 mol % and 284 ℃ for 10.17 mol % Al-goethite respectively. Combined with the result from TG shown in **Table 5.1**, this is apparently associated with the de-hydroxylation of Al-goethite to hematite. It is worth noting that a shoulder on the low temperature side (~250 ℃) of the main endothermic peak occurs in pure and low Al substituted goethite (<4 mol %) and finally merges into the main peak. Particle size effects (induced by Al substitution) contribute to the merging peak as does Al substitution to the temperature shift of the main peak. Similar results were also reported (Fey and Dixon, 1981; Walter *et al.*, 2001; Frost *et al.*, 2003; Sudakar *et al.*, 2004b). However, the observed temperature range for the main endothermic peaks varies from 290 ℃ to 320 ℃ although the contribution of the de-hydroxylation is widely acknowledged. The difference is due to the amount of Al substitution, quality of crystalline Al-goethite and particle sizes caused by the Al substitution.

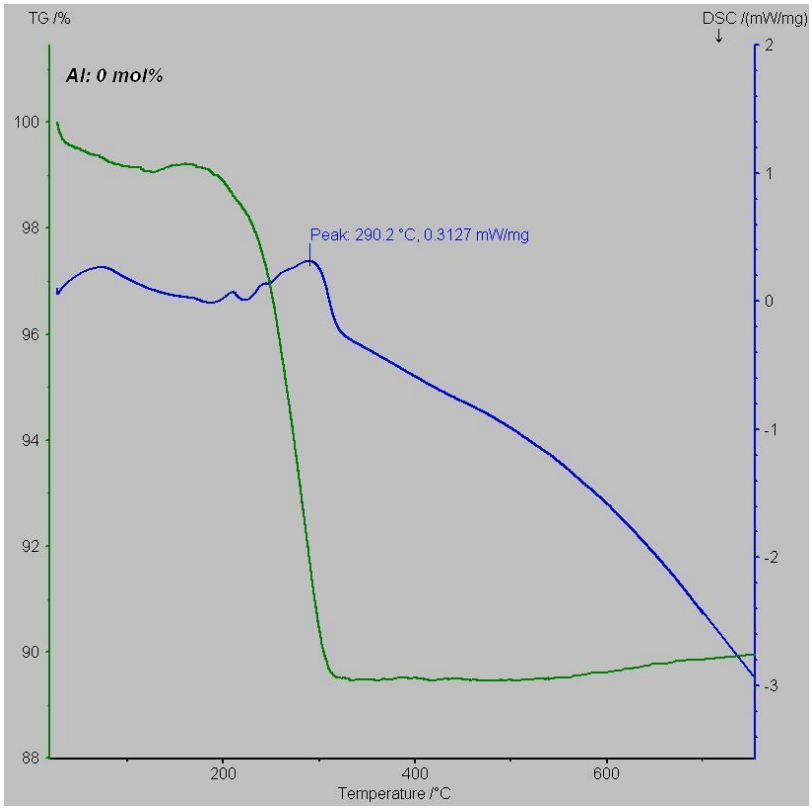

(A) TG/DTA curves for pure synthetic goethite

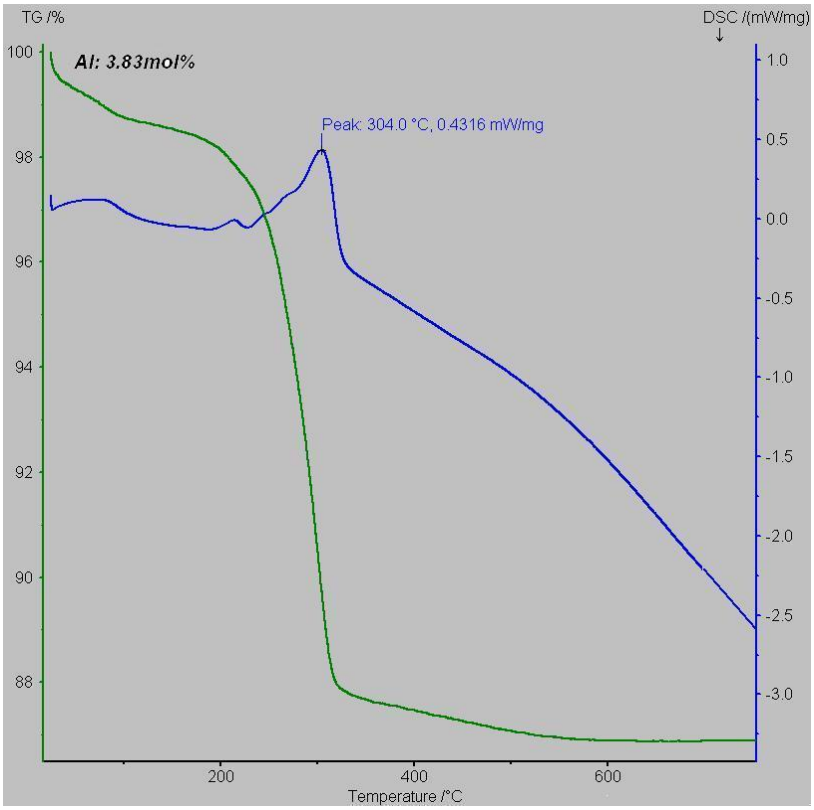

(B) TG/DTA curves for Al-goethite with 3.83 mol% Al substitution

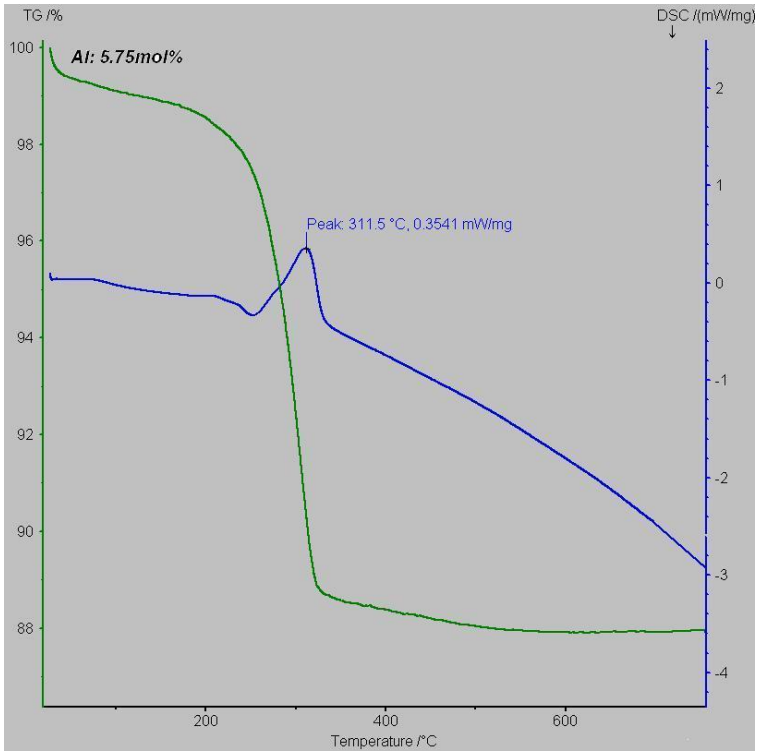

(C) TG/DTA curves for Al-goethite with 5.75 mol% Al substitution

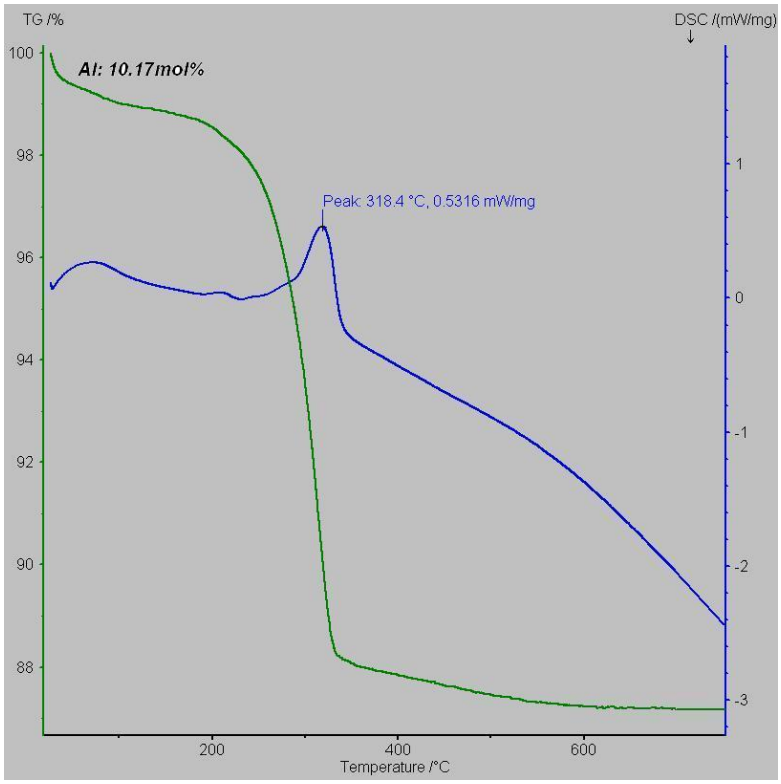

(D) TG/DTA curves for Al-goethite with 10.17 mol% Al substitution

Figure 5.1 TG/DTA curves of Al-goethite samples with varying substitution of Al^{3+}. From top to bottom: Al substitution: 0, 3.34, 3.83, 8.01 mol %.

5.2.2 Impact of Al substitution on the thermal treatment of Al-goethite

5.2.2.1 Impact on the de-hydroxylation temperature

The maximum temperature of the main endothermic peak as a function of Al substitution is given in **Figure 5.2**, which clearly shows that the maximum temperature increases as a result of increasing Al substitution. The relationship between maximum temperature and Al substitution has been mostly accepted as a linear function (**Figure 5.2 a**) (Ruan *et al.*, 2002b), while a second order function may be applied in this study (**Figure 5.2 b**). However, a conclusion is hard to be drawn before substantial amount of data is obtained to carry out a statistical F test to determine which model describes the relationship better.

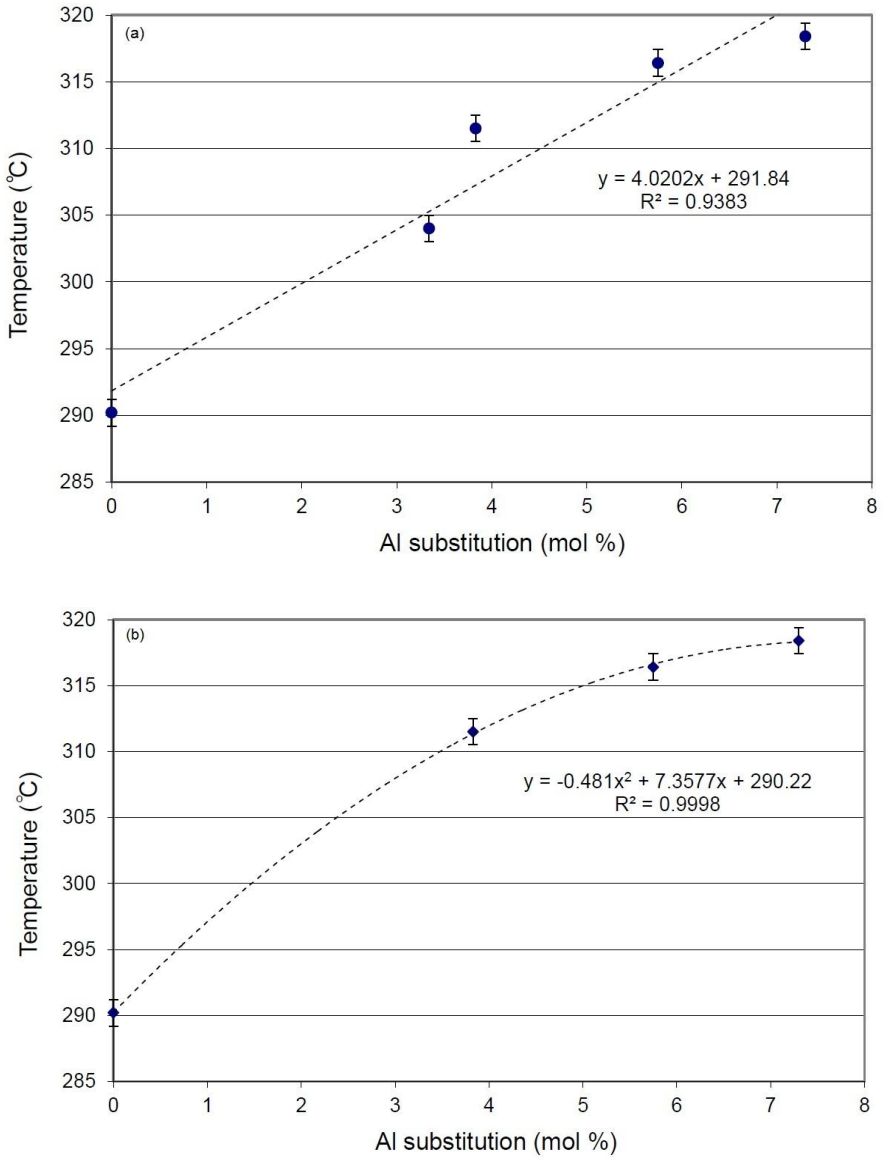

Figure 5.2 The de-hydroxylation maximum temperature as a function of Al substitution. (a) linear function; (b) second order function.

The increase of the maximum temperature for the main endothermic peak as a result of increasing Al substitution is correlated to the distortion of the goethite structure due to the substitution of the smaller Al^{3+} for Fe^{3+}. The original Fe-O-H structure is thus forming a coexistent structure of Fe-O-H and Al-O-H, which inevitably causes the mismatch between the pair. Therefore, more energy for thermal transformation of Al-goethite is required than that for pure goethite to break the elevated barrier due to the structural distortion.

5.2.2.2 Impact on the mass losses

Thermal analysis, in particular thermogravimetry (TG), provides the information of weight losses related to the corresponding peaks. The process that forms the corresponding peaks can sometimes be deducted through the interpretation of the mass losses. However, it is suggested that the mass losses measured by TG sometimes show inconsistency with the stoichiometric mass losses due to potential complication caused by the components in the testing samples. In such cases, the indication of the difference between the measured and stoichiometric values is most likely to be valuable.

Table 5.1 demonstrates the mass losses extracted from TG results with reference to the theoretical mass loss calculated from the Equation 5.1:

$$2Fe_{1-x}AlxOOH \rightarrow Fe_{2(1-x)}Al_{2x}O_3 + H_2O \quad \textbf{(5.1)}$$

The theoretical mass loss of Al-goethite for a complete dehydration beyond the temperature 400 ℃ can be obtained from the dehydration during the process as follows:

$$\%H_2O = \frac{M_{H_2O}/2}{M_{Fe(1-x)AlxOOH}} \times 100\% \quad \textbf{(5.2)}$$

where M_{H2O} and $M_{Fe1\text{-}xAlxOOH}$ are the molecular mass for water and Al-goethite; x is the mole ratio of Al substituted into the goethite structure.

Table 5.1 Comparison of theoretical and measured mass losses for Al-goethite samples

Sample ID	Al/(Al+Fe) (mol %)	Theoretical mass loss (%)	Mass loss from TG (%)
ALGOE-1	0	10.11	10.04
ALGOE-3	3.83	10.24	11.44
ALGOE-4	5.75	10.31	11.53
ALGOE-7	10.17	10.46	11.67

To investigate the correlation between Al substitution and the mass loss during the thermal treatment for Al-goethite, a plot of mass loss as a function of Al substitution is shown in **Figure 5.3**. It is found that the mass loss rises as the content of Al substitution in the goethite increases, which is in agreement with the trend of theoretical mass loss for Al-goethite. It is, however, also suggested from both **Figure 5.3** and **Table 5.1** that the observed mass loss for the samples seems mostly greater than the theoretical mass loss although all the samples were oven dried at 100 ℃ overnight prior to measuring. For example, the theoretical mass losses from the stoichiometric calculation are 10.24, 10.31 and 10.46 % for 3.83, 5.75 and 10.17 mol % Al-goethite respectively; while the real mass losses from thermal analysis correspondingly increase to 11.44, 11.53 and 11.67%. It should be noted that there appears to be a linear relationship between the observed weight loss and Al substitution if the pure goethite is excluded from consideration. The differences between the pair weight losses for Al-goethite samples are very consistent with a nearly parallel line to the theoretical value line. This linear relationship was also reported by Ruan (2002b).

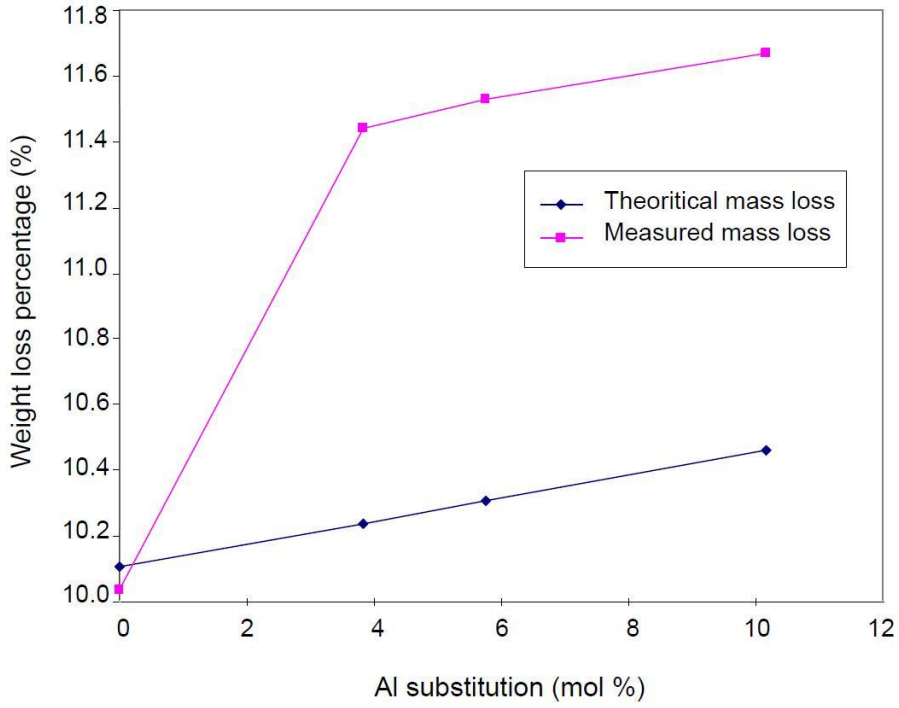

Figure 5.3 Mass loss (%) of thermal treatment of Al-goethite measured from TGA against Al substitution (mol %).

The consistent differences between theoretical mass loss and TG results arise from adsorbed water, which can be detected occasionally in some of the samples (**Figure 5.1**), and is more likely to be perceptible in Al-substituted samples in which increasing surface area caused by the Al substitution gives rise to the adsorption. Another explanation for this phenomenon is associated with the excess structural OH^- existing in the Al-substituted goethite. It is considered that the compensation of excess hydroxyl structural OH^- possibly occurs due to the cation deficient sites caused by the Al for Fe substitution in the goethite structure. Thus, the general formula for Al-substituted goethite was suggested as $(Fe_{1-x}Al_x)_{1-y/3}O_{1-y}(OH)_{1+y}$ (Wolska and Schwertmann, 1993), in which y is referred to as the excess proportion of OH^- and the value of y may be as high as 0.25 (Cornell and Schwertmann, 2003). In such case, the water that can be expelled from the goethite structure is much more than the theoretical value calculated from the common Al-goethite formula, $(Fe_{1-x}Al_x)O(OH)$.

5.2.3 XRD and TEM study on thermal transformation

The temperature range of the thermal transformation of Al-goethite to hematite and the mass losses accompanied with the transformation have been investigated. Thus, the fundamental elements for the thermal transformation have been established with transformation temperatures widely ranging from ~ 250 ℃ to nearly 400 ℃ for goethite or Al-goethite. It, however, raises another concern as to what the mechanism of the thermal transformation is and whether the crystal morphology turns out to be different during the thermal treatments, which are crucial for practical application in consideration of the problem caused by the physical properties of goethite, such as particle size and surface area. In order to investigate the mechanism of thermal transformation and the morphology changes during the transformation, the analytical techniques of XRD and TEM were employed to conduct the study.

5.2.3.1 XRD study of the phase change

Commercial pure goethite was used in this mechanism study. According to the thermal analysis results, several key temperatures, 300, 400, 600, 800 and 1000 ℃, were adopted to implement the thermal treatment and the subsequent XRD and TEM analysis. The operation initially started from the thermal treatment of pure synthetic goethite at the set-up temperature in the furnace for 1 hour (See the detailed description of the treatment in Section 3.2.2.1). The residues were then assessed with XRD for phase determination and TEM for the morphological study.

The findings from the thermal treatment for pure goethite greatly tally with the result from the thermal analysis. For example, hematite, the product of de-hydroxylation of goethite, was the only phase at temperature $T \geq 300$℃ in the XRD patterns, while at temperature 200 ℃ goethite was the only phase in the XRD patterns. This further identifies that the thermal transformation for pure goethite takes place between 200 and 300 ℃, which is consistent with the thermal analysis as well as other literature on this issue (Walter *et al.*, 2001; Fan *et al.*, 2006; Gialanella *et al.*, 2010). Despite hematite being the dominant phase for the thermal treated residues at temperatures over 300 ℃, the extent of crystallization and the intensity of different crystal plane varies from residue to residue. **Figure 5.4** shows the XRD patterns of raw goethite and the goethite samples thermal treated at temperatures of 400 ℃ and 1000 ℃ respectively. The XRD patterns show that raw goethite samples were completely transformed to hematite, the only phase observed in XRD patterns, when thermal treated at temperatures 400 ℃ and

1000 ℃ for 1 hour. However, differences can be easily found in the two patterns. The residue heat-treated at 1000 ℃ appears well crystallized with fairly sharp XRD peaks, while the residue treated at 400 ℃ shows a relatively poorly crystal phase of hematite with broader peaks than that in the 1000 ℃ pattern. This broadening of the peaks at relatively lower temperatures is in agreement with the previous study (González *et al.*, 2000) and can be associated with structural change during the goethite to hematite transformation.

Another difference observed from the XRD analysis for 400 and 1000 ℃ residues is the intensity of some of the peaks. The intensity of some of the peaks, for instance $(110)_H$, $(113)_H$, $(116)_H$ and $(330)_H$, where subscript 'H' represents hematite, in the 400ºC XRD are unusually strong when compared to the standard hematite XRD intensity, while the 1000 ℃ sample XRD compares well to the standard hematite peak. The peaks with unusual intensities could be attributed to the overlapping peaks in raw goethite:, $(110)_H/(101)_G$ at 2.52Å, $(113)_H/(140)_G$ at 2.20Å, $(116)_H/(240)_G$ at 1.69Å and $(300)_H/(061)_G$ at 1.45Å, where subscript 'H' and 'G' respectively represent hematite and goethite. Therefore the stronger than usual intensities present in the 400 ℃ belong to those integrated intensities, which means that the residue heat-treated at this temperature still remains part of the goethite structure. It should also be noted that some of the peaks appear to be broadened more than others. This selective peak broadening could be due to the porous structure of the transitional hematite which retains overall smaller dimensions in certain directions. As the temperature increases further to 1000 ℃, a completely transformed hematite phase appears in the XRD pattern.

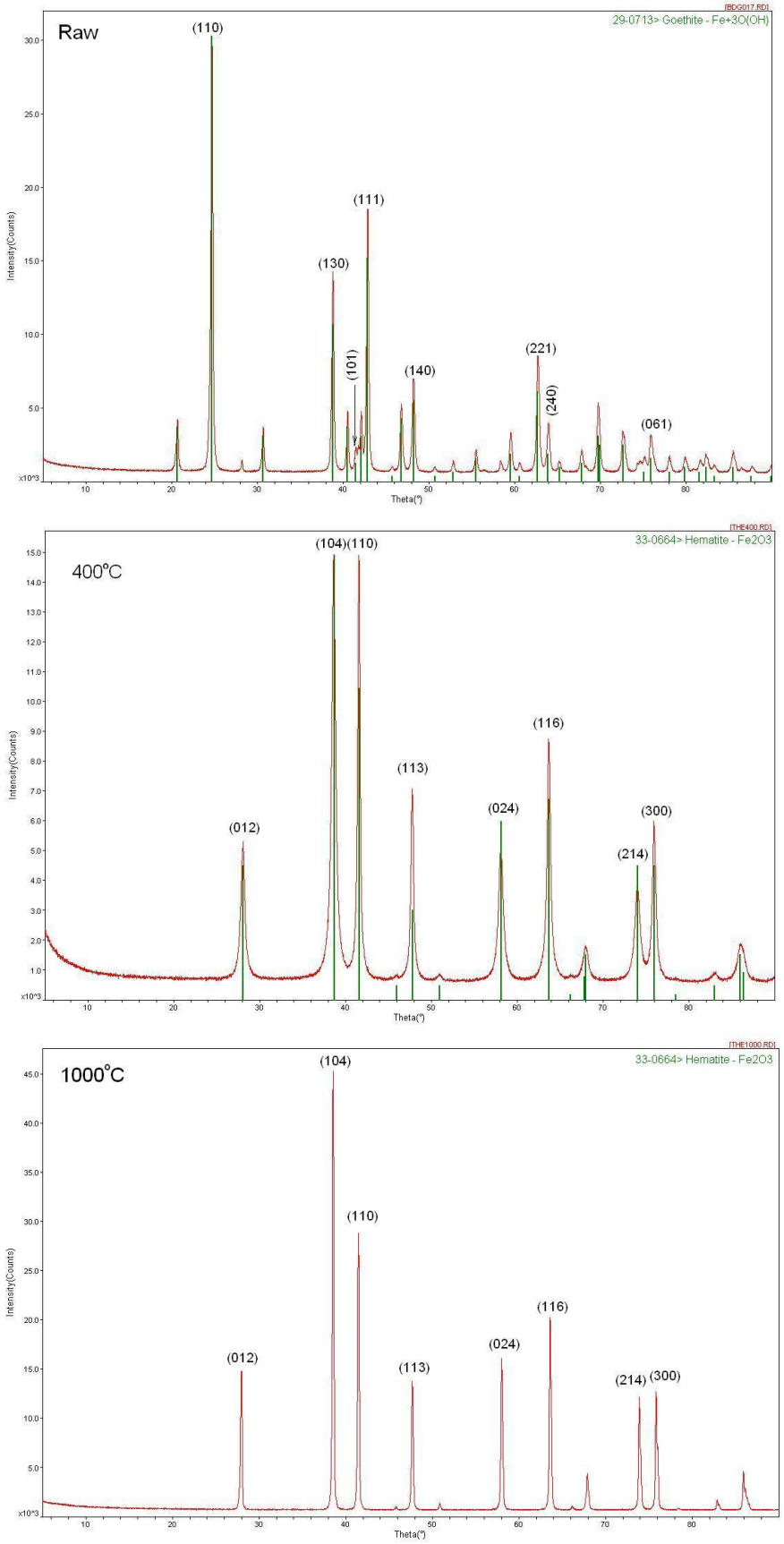

Figure 5.4 XRD patterns for thermal treated goethite samples at different temperatures. From top to bottom: raw goethite, 400 ℃, 1000 ℃.

5.2.3.2 TEM study on the morphological change

In order to understand the differences observed in the XRD patterns for annealing treated residues, TEM analysis was conducted to monitor the morphological change during the process. **Figure 5.5** shows the TEM images of raw goethite and the residues thermally treated at 400 ℃ and 1000 ℃. The untreated raw goethite sample clearly has the characteristic goethite structure with elongated acicular grains and parallel domains (**Figure 5.5 (A)**). Annealing the goethite at either 400 ℃ or 1000 ℃ can cause complete mineral phase transition from goethite to hematite, as evidenced by the XRD profiles of thermally treated residues. However, this mineral chemistry/phase transformation is not completely in sync with their morphological changes. It is revealed from **Figure 5.5 (B)** that the morphology and the crystallographic structure of the thermally treated residue at 400 ℃ for 1 hour remains unexpectedly similar to those of pure goethite although the de-hydroxylation of goethite to hematite is apparently underway at this stage according to the previous XRD and Thermal analyses. The only difference between the morphology of untreated goethite and that of thermally treated residue at 400 ℃ is that the later has a more porous appearance. This porous microstructure can be seen on the goethite-like grains in **Figure 5.5 (B)**. The increase in porosity is associated with a loss of water. It is therefore concluded that the dehydration of goethite has taken place at 400 ℃ which is in close agreement with the XRD data. However, the microstructure change induced by dehydration at 400 ℃ is not significant enough to trigger a large scale break-down of the goethite-like acicular morphology. A higher annealing temperature (**Figure 5.5 (C)**) is needed for this drastic morphological evolution to take place. The goethite structure at this stage starts to fall apart into small irregular hematite fragments. As temperature further increases, the recrystallization of hematite gradually takes place. **Figure 5.5 (D)** shows that this goal is achieved by annealing goethite at 1000 ℃ for 1 hour, which produces irregular but crystallised hematite.

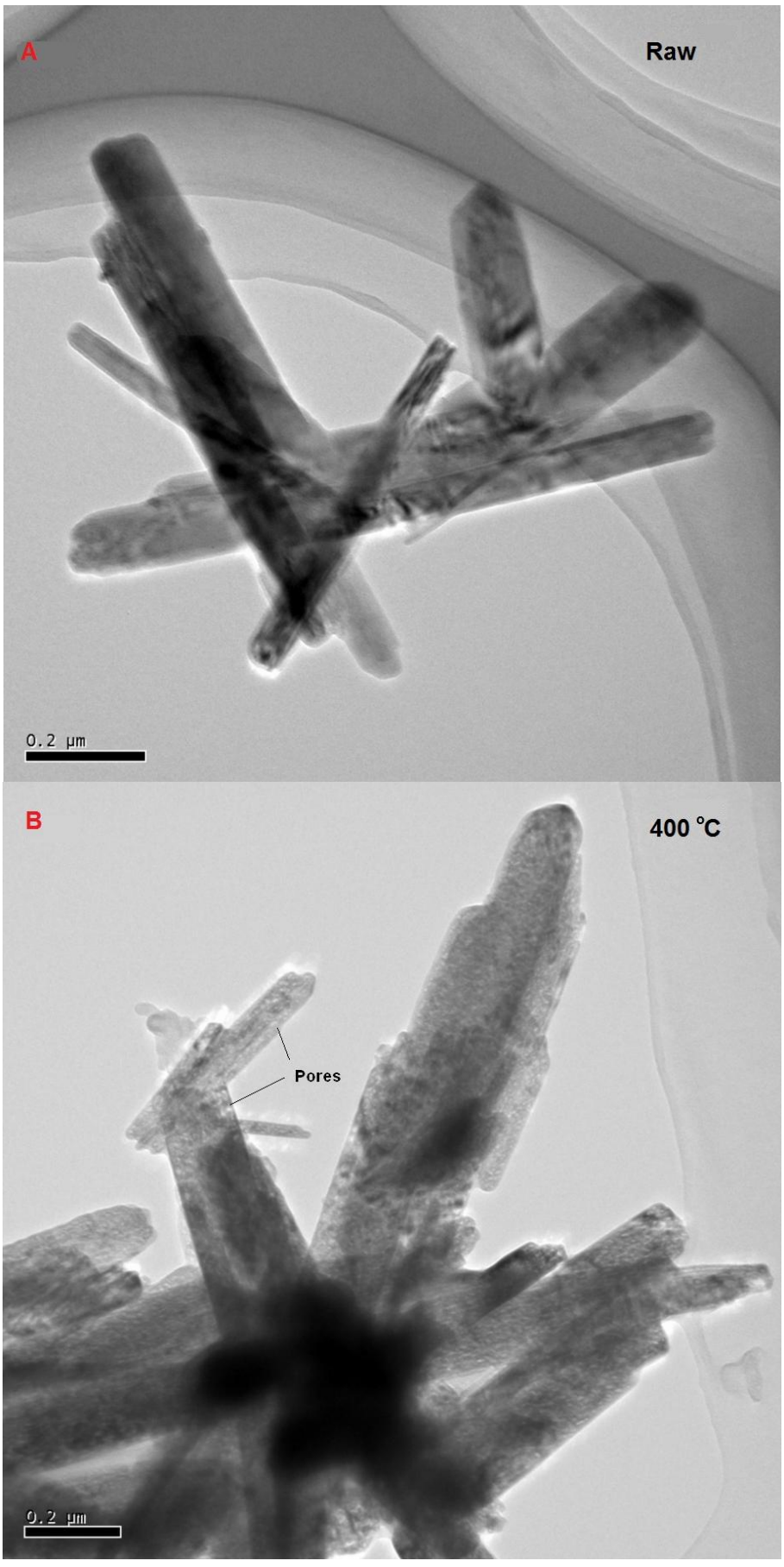
A
Raw
0.2 µm
B
400 °C
Pores
0.2 µm

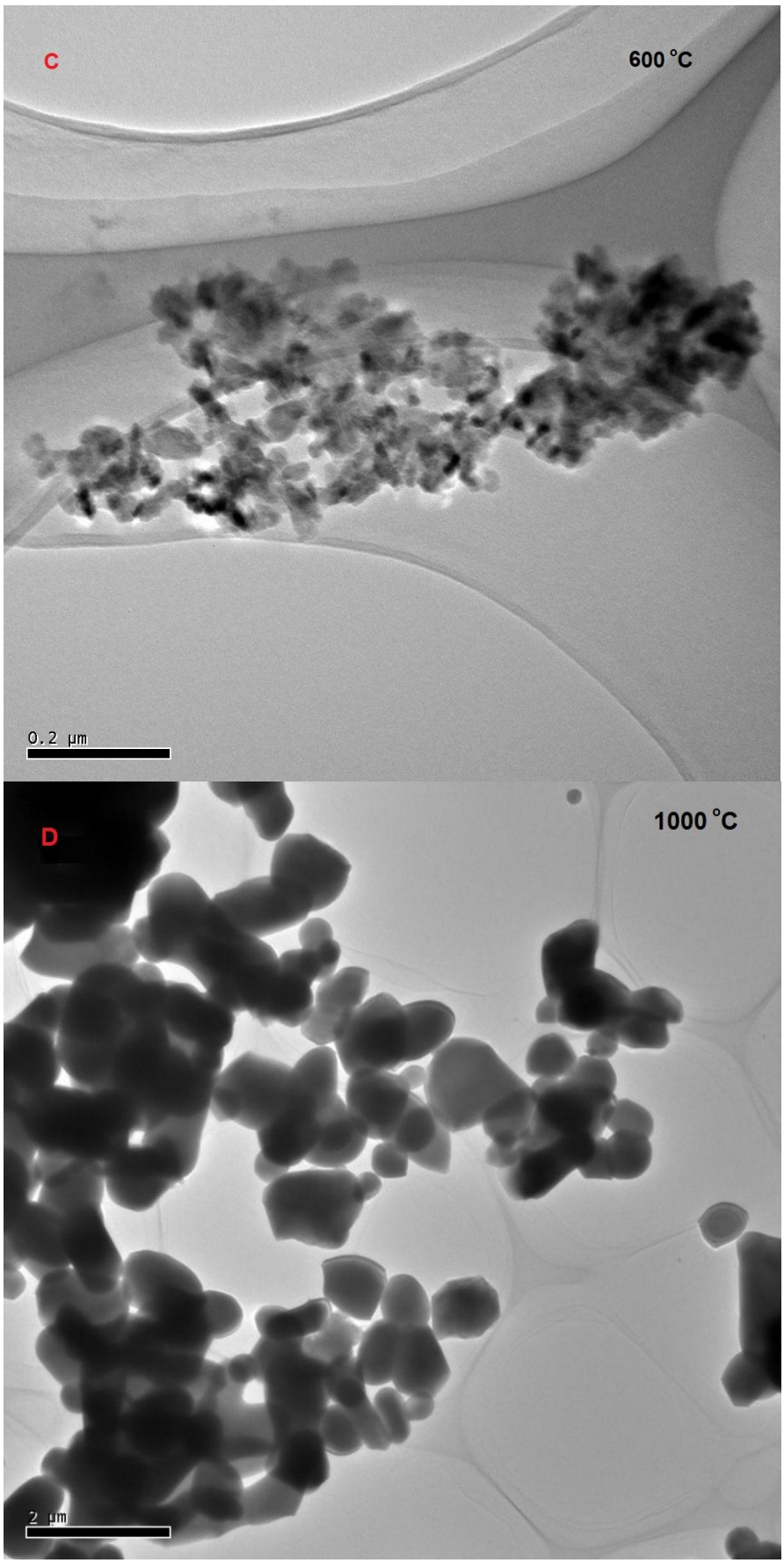

Figure 5.5 TEM for thermal treated goethite samples at different temperatures. A: raw goethite; B: 400 ℃; C: 600 ℃; D: 1000 ℃.

5.2.4 Mechanism of thermal transformation of goethite to hematite

As indicated from the above discussion, the thermal transformation of goethite to hematite is a topotactic process, which is in agreement with the study conducted by Gonzalez et al. (2000) and Watari et al. (1983). The process experiences a phase change from goethite to hematite due to de-hydroxylation, a process that releases OH- from goethite crystal, without morphological change in the original goethite-like appearances during the early transformation stage (annealing temperature below 600 ℃). The morphological change cannot occur until the temperature further increases to over 800 ℃. To demonstrate the process, a schematic diagram of the thermal transformation of goethite to hematite is shown in **Figure 5.6**, in which the thermally induced transformation of goethite to hematite is divided into three zones, inert zone, de-hydroxylation zone and recrystallization zone, according to the residues' morphological change in the temperature range of 0 - 1000 ℃.

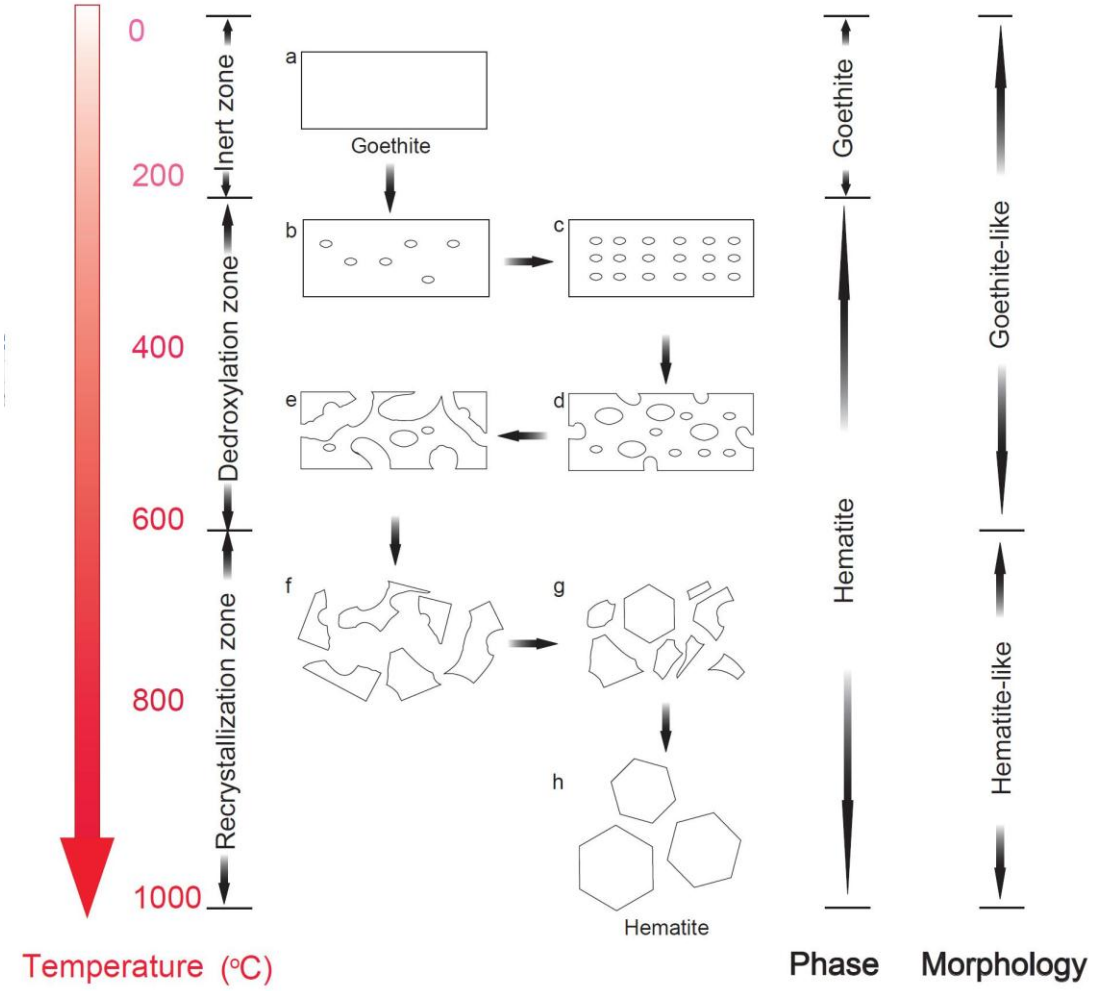

Figure 5.6 Schematic diagrams for the mechanism of thermal induced transformation of goethite to hematite. **Note:** (*h*) simply outlines general hexagonal morphology of hematite. Sintered hematite may be irregular in shape.

Inert Zone: in the temperature range of 0 to 200 ˚C, goethite→ hematite transition does not occur. Therefore, both mineral chemistry/phase and morphology remain unaltered.

De-hydroxylation zone: the transformation of goethite to hematite starts at a temperature near 200 ℃. It is in fact a process of de-hydroxylation, release of OH^-, as seen in **Figure 5.6b**. At this early de-hydroxylation stage part of the OH^- was expelled as the result of increasing temperature, which gives rise to the presence of de-hydroxylation pores in the parent goethite structure. As temperature increases, all the available OH^- gradually leaves the structure and relative regular pores consequently form within the goethite structure (**Figure 5.6c**). The goethite by far has been

completely transformed to hematite in terms of mineral chemistry/phase, which can be observed from XRD results in **Figure 5.4B**. However, it should be more carefully noticed that this transformation only happens within the goethite-like structure. In other words, the strains caused by the de-hydroxylation pores during the departure of OH^- are not strong enough to induce the beak-down of parent goethite crystal. As a result, the thermally treated goethite at a temperature even as high as 400 °C still shows goethite-like shape with a number of visible de-hydroxylation pores in the TEM image from **Figure 5.5B**. It is necessary to emphasize that de-hydroxylation temperature for goethite/Al-goethite varies from sample to sample depending on the particle sizes of the raw goethites and the extent of Al substitution in the goethite. Smaller particle sizes and higher Al substitutions warrant higher transformation temperatures.

If further increased the temperature up to ~600 °C, the dehydration pores tend to coalesce to form larger voids since the increasing temperature accelerates the migration of pores in each other's vicinity (**Figure 5.6d**). It is not until this stage that the strains in the goethite crystal grow large enough to initiate the breakage of the parent goethite structure (**Figure 5.6e and Figure 5.5C**).

Recrystallization zone: in the temperature range of 800 to 1000 °C, the recrystallization process is evident in the TEM images. The whole goethite crystal thoroughly breaks into small hematite grains by the progressive force within the crystal structure (**Figure 5.6f**). Further increase in temperature gives rise to the recrystallization of hematite initially between some of the hematite grains. At temperatures close to ~1000 °C the hematite recrystallization completes by exhibiting typical hexagonal or irregular shape of hematite (**Figure 5.6h** and **Figure 5.5D**).

Similar observations and discussions in relation to the de-hydroxylation and recrystallization process have been mentioned in the previous studies (Watari *et al.*, 1983; Pomiès *et al.*, 1999; González *et al.*, 2000; Gialanella *et al.*, 2010). The mechanism proposed in this study has the similar outcome in terms of the de-hydroxylation and recrystallization process; however, some deviations between studies regarding the detailed process obviously exist, which could be attributed to the variation in treatment methods, heating and grinding, and treatment time ranging from 5 minutes (Gialanella *et al.*, 2010) to as long as 104 hours (González *et al.*, 2000) adopted by the different studies. Nevertheless, this proposed mechanism reflect the fact (observed in the current study) that the thermal transformation of goethite to hematite is a process

without forming any intermediate produces mentioned in some of the previous studies (Mendelovici and Yariv, 1981; Wolska *et al.*, 1994). The mismatch between mineral chemistry/phase change and the morphological change during the goethite→hematite transition could contribute to the discrepancies.

5.3 Hydrothermal transformation

It has been proposed that the hydrothermal transformation of goethite to hematite experiences a dissolution/re-precipitation mechanism in caustic solution (King, 1971; Basu, 1983; Murray *et al.*, 2009). The transformation begins with the dissolution of goethite where the difference of solubility between goethite and hematite is the driving force (Cornell and Schwertmann, 2003). An intermediate phase, referred to as sodium ferrate or ferrite, is then formed and further crystallize as hematite (Basu, 1983). A number of studies have been carried out at a temperature range from 150 to 260 ℃ by both *ex-situ* and *in-situ* methods to establish the important factors, kinetics and mechanism of the hydrothermal transformation of goethite to hematite in the Bayer digestion step. From these studies increasing temperature, caustic soda concentration and the presence of hematite seeding was found to enhance the process while the presence of anatase has a detrimental effect on the conversion (Murray *et al.*, 2009). However, differences in details between the studies have also been found. For instance, goethite converts to hematite in a Bayer liquor at 250 ℃ in 30 minutes regardless of the presence of hematite seeding in Basu's (Basu, 1983) study, however, Murray et al. (2009) found that, under the same conditions, hematite seed was required. Thus, the aim for the following section is to acquire accurate data for the hydrothermal transformation under the Bayer digestion conditions and understand the mechanism of the transformation. When these results are combined with the valuable data from previous studies, this will aid the study of the hydrothermal transformation of goethite/Al-goethite in natural bauxites in the Bayer process which will be discussed in Chapter 6.

5.3.1 Experiments and data analysis

5.3.1.1 Experiments and materials

The detailed description of the methods and characterisations used in the study of hydrothermal transformation of goethite to hematite can be found in Chapter 3. The digestion reactions were carried out in a Gas Fired Reactor (GFR) with a bomb

digestion vessel at required temperatures. For a regular experiment, ~2 g goethite, which is equivalent to a 160 g/L charge of bauxite with a 10% goethite content, were mixed in 150 mL of either pure caustic soda or Bayer liquor for the desired period of time at the given temperature. The residues are then collected after pressure filtration and washing. In this part of the study, LOI (Loss on ignition) is used to examine the weight loss of the residues in order to calculate the conversion percentage of goethite and XRD (X-ray diffraction) is carried out to monitor the phase change.

The experimental materials used in the hydrothermal transformation experiments are mainly goethite, hematite, caustic soda solution and synthetic Bayer liquor (sodium aluminate solution). Pure goethite and hematite were also used to minimize the interference that could be potentially caused by impurities. Various concentrations of synthetic Bayer liquor (with and without dissolved alumina) were freshly made up in the laboratory. All the sodium aluminate solutions in the experiments were made up with 240 g/L (as Na_2CO_3) NaOH solution. The composition of solutions used in the experiments is shown in **Table 5.2**. Titration was employed to determine the content of alumina and caustic in the liquors.

Table 5.2 Composition of solutions used

Solution	Al_2O_3 (g/L)	Total Caustic $NaAl(OH)_4$ +NaOH as Na_2CO_3 (g/L)	A/C ratio	Free caustic NaOH as Na_2CO_3 (g/L)
Caustic solutions	0	100	0	100.00
	0	115	0	115.00
	0	140	0	140.00
	0	150	0	150.00
	0	165	0	165.00
	0	240	0	240.00
Bayer liquor	168	240	0.70	65.41
	156	240	0.65	77.88
	144	240	0.60	90.35
	132	240	0.55	102.82
	96	240	0.40	140.24
	72	240	0.30	165.18
	48	240	0.20	190.12

5.3.1.2 Calculation of goethite to hematite conversion extent

The extent of goethite to hematite conversion can be determined in several ways, of which Loss on ignition (LOI) is an economic and efficient way to calculate the degree of conversion of goethite based on weight loss during thermal treatment of *pure* mixture

of goethite and hematite. However, the transformation of goethite to hematite cannot be assessed by LOI when *impurities*, such as those in bauxite, are involved in the process. The weight loss in such cases could result from various species in the samples. XRD in this scenario was introduced to follow up the transformation, for example, determination of goethite conversion in natural bauxite in Chapter 6. In this chapter, LOI is used as the major method to evaluate the conversion degree of goethite to hematite and XRD determination as reference is also performed on randomly selected samples.

The extent that goethite converts to hematite can be determined by the 'Loss on Ignition' measure (LOI) in which the hematite to goethite ratio is directly related to the weight loss of the leached residue in the ignition test. As shown in Equation 5.3 and 5.4, a 10.14 wt% loss should arise following the complete decomposition of goethite.

$$FeOOH \rightarrow 0.5Fe_2O_3(s) + 0.5H_2O \uparrow \quad \textbf{(5.3)}$$

$$wt\%\ Loss = \frac{0.5MH_2O}{1MFeOOH} \times 100\% = \frac{0.5 \times 18}{1 \times 89} = 10.14\% \quad (\textbf{5.4})$$

Assuming the leached residue contains only goethite and hematite and only goethite undergoes further decomposition in the ignition test according to the Eq. (5.3), the initial goethite and hematite contents in the leach residue are easily calculated as follows:

$$wt\%\ Hematite\ in\ leach\ residue\ (wt\%H) = (1 - \frac{LOI}{10.14\%}) \times 100\% \quad (\textbf{5.5})$$

$$wt\%\ Goethite\ in\ leach\ residue\ (wt\%G) = (\frac{LOI}{10.14\%}) \times 100\% \quad (\textbf{5.6})$$

where LOI is the 'Loss on ignition' result, the overall weight loss in percentage of the digestion residue after ignition tests.

The goethite conversion extent during digestion is consequently calculated as:

$$\frac{2 \times \frac{wt\%H}{HMW}}{2 \times \frac{wt\%H}{HMW} + \frac{wt\%G}{GMW}} \times 100\% \quad (\textbf{5.7})$$

where HMW and GMW are the molecular weights of hematite and goethite respectively.

5.3.1.3 An adjustment for weight loss - surface adsorbed water

The Equations 5.3 to 5.7 are based on the assumption that the adsorbed water on the surfaces of leached residue is negligible. However, small amount of moisture was invariably adsorbed and observed on leached residue in the current study. The raw materials used in the digestion test consists of the laboratory pure hematite and goethite. These materials are not chemically/physically homogenous and may vary in adsorbed water. As a result, the weight loss observed was more than the theoretical value for goethite although the samples were oven dried at 100 ℃ over night. The difference between the LOI result and the theoretical value of weight loss is attributed absorbed water and detectable for samples with fine particle size (<80 nm) (Sudakar *et al.*, 2004b).

The weight losses of the pure hematite and goethite in isothermal conditions are used as the baseline water loss for the corresponding digestion tests. Since the hematite (Fe_2O_3) molecule contains no structural water, the weight loss observed in current experiments must be attributed to the adsorbed surface moisture in the initial pure hematite samples. A similar weight loss was observed with the pure goethite samples upon ignition. Up to 17.51wt% of weight loss observed was observed in the goethite LOI test compared to the theoretical 10.14 wt% loss shown in Equation 5.4. Therefore, an adjustment to the Equation 5.3 to 5.7 is needed to account for the moisture adsorption of the digestion residue prior to the Ignition Test.

$$\textit{Adjusted wt\% Hematite in leach residue (wt\%H')} = \left(\frac{wt\%LPG - LOI}{wt\%LPG - wt\%LPH}\right) \times 100\% \quad \textbf{(5.8)}$$

$$\textit{Adjusted wt\% Goethite in leach residue (wt\%G')} = \left(1 - \frac{wt\%LPG - LOI}{wt\%LPG - wt\%LPH}\right) \times 100\% \quad \textbf{(5.9)}$$

where the wt%LPG and wt%LPH are respectively the measured weight losses of pure goethite and hematite upon ignition.

The adjusted goethite conversion extent during leaching is:

$$\frac{2\times\frac{[wt\%H'\times(100-wt\%LPH)]}{HMW}}{2\times\frac{[wt\%H'\times(100-wt\%LPH)]}{HMW}+\frac{[wt\%G'\times(100+10.14-wt\%LPG)]}{GMW}}\times 100\% \qquad \textbf{(5.10)}$$

It should be borne in mind that the baseline water loss for goethite and hematite adopted in this study may vary from batch from batch as mentioned earlier. To assure accurate calculation results, blank LOI tests for both pure goethite and hematite were simultaneously conducted with the LOI test on residues. Thus, a baseline for each batch has been indicated with the data shown in the following discussion. In this study, the calculated result of goethite-to-hematite conversion between ~95 to 100% is recognised as a complete transformation due to the allowable error.

5.3.2 The factors that affect the hydrothermal transformation

5.3.2.1 The influence of temperature

It is well understood that higher digestion temperature promotes goethite to hematite conversion in caustic liquor. This is confirmed in this study. **Figure 5.7** shows the XRD patterns of digested residues of goethite at different temperatures. It is clearly demonstrated that goethite remains in the digested residues as the only phase when the digestion takes place at 180 ℃ for 15 min. The transformation is yet to happen at this temperature. As temperature increases to 220 ℃, goethite and hematite can be both found in the XRD pattern of the residue, which suggests the transformation of goethite to hematite occurs. Further increases in the temperature to 250 ℃ shows that hematite is the dominant phase in the residue. Therefore, the XRD patterns indicate that the extent of hydrothermal transformation of goethite to hematite greatly depends on the increasing digestion temperature.

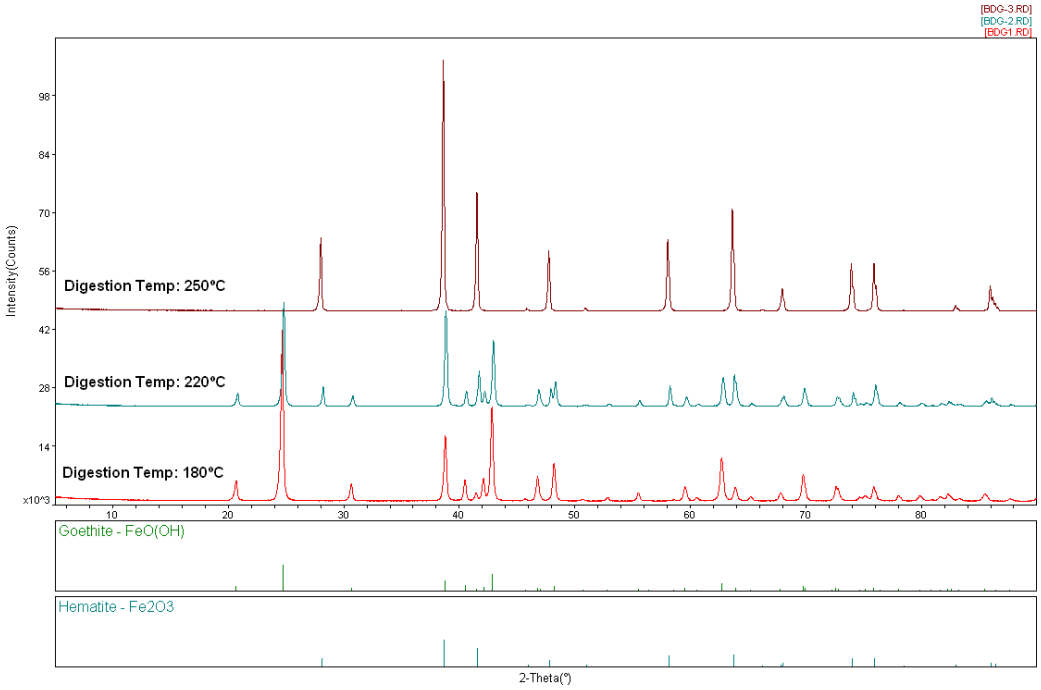

Figure 5.7 XRD patterns of digested residues of goethite in caustic soda at different temperatures. Digestion temperature from bottom to top are 180, 220 and 250 ℃ respectively, the digestion time is 15 minutes and the caustic soda concentration C=240 g/L.

The reaction extent, however, is not linear with respect to the increasing digestion temperature. To quantify the relationship between digestion temperature and goethite to hematite conversion, a series of experiments were conducted under the digestion conditions listed in **Table 5.3**. All digestion parameters were kept constant (e.g. digestion time = 15min, free caustic = 240 g/L) except for the holding temperatures, which varied from 180 to 280^{o}C. A plot of adjusted weight percentages of goethite and hematite in the residues after digestion is shown in **Figure 5.8**. The figure shows that hematite increases at the expense of goethite in the temperature range T < 200^{o}C (marked as 'Linear zone' in **Figure 5.8**). When the digestion temperature reaches 230^{o}C, however, the goethite to hematite conversion accelerates and the reaction extent appears to follow a more exponential trend. This temperature range, 230-250^{o}C, is marked in **Figure 5.**8 as the 'Accelerating zone'.

Table 5.3 The impact of temperature on the extent of goethite to hematite conversion under the conditions listed

Digestion Conditions					Results				
Goethite (g)	Hematite (g)	Temp (℃)	Time (min)	Caustic (g/L)	LOI (%)	XRD	wt% H'	wt% G'	%GCE
2.2579	0.0000	180	15	240	14.79	G	6.42	93.58	7.35
2.0071	0.0000	220	15	240	10.41	H, G	38.39	61.61	41.89
2.0532	0.0000	250	15	240	2.98	H	92.63	7.37	93.56
2.0592	0.0000	280	15	240	2.89	H	93.28	6.72	94.14

Note:
- G, H in XRD results represents goethite and hematite respectively.
- % GCE is the extent of goethite conversion.
- The measured weight losses of 'pure' goethite and hematite upon ignition in this batch are wt% LPG=15.67% and wt% LPH=1.97% respectively.

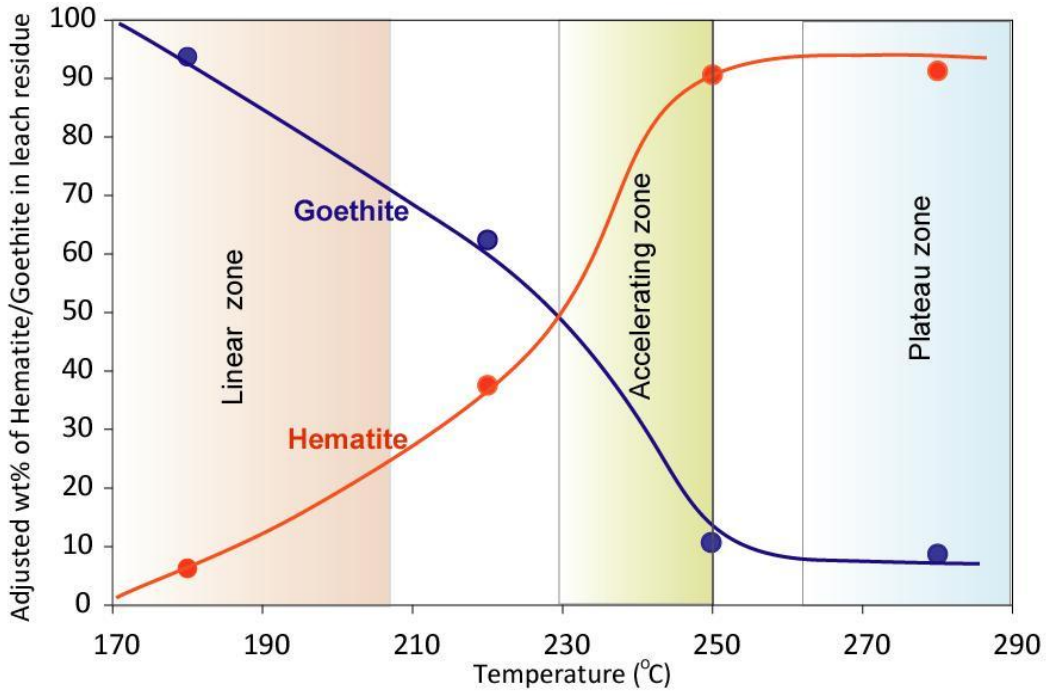

Figure 5.8 The weight percentage of goethite and hematite in leached residues after digestion at various temperatures ranging from 180-280 ℃. Caustic in the digestion is 240 g/L, the duration of digestion is 15 minutes, no hematite seeding.

In the ‘Accelerating zone’, the reaction of goethite to hematite becomes more sensitive to temperature, identified by a sudden increase in hematite content in the residue after digestion. The goethite to hematite conversion curve is plotted against temperature in **Figure 5.9(A)**. It should be noticed that this conversion curve is not the same as the hematite formation curve in **Figure 5.8**, although the trends against temperature of both processes are very similar. However, they are close reflections of each other and one curve can be derived from the other through the following mathematical manipulation.

In **Figure 5.9(A),** the goethite conversion extent (%GCE) is an ‘S’ shape function of temperature. The reaction apparently accelerates near the temperature 230^{o}C and plateaus at temperatures above 250^{o}C. To determine the most temperature sensitive region, a derivative of %GCE against temperature is plotted in **Figure 5.9(B)**. The maximum derivative, dGCE/dT is found near temperature 230^{o}C, which coincides with the most sensitive temperature for goethite to hematite transformation.

The practical value of this finding is to provide guidance in evaluating the goethite to hematite transformation at various temperatures, given that the reaction suddenly becomes very fast when the digestion temperature exceeds 230^{o}C. As shown in **Table 5.3**, the goethite to hematite conversion is significantly slower in the temperature range T < 230^{o}C, with 41.89% goethite conversion in 15 min at 220^{o}C, compared to the 93.56% goethite conversion within the same time frame at 250^{o}C.

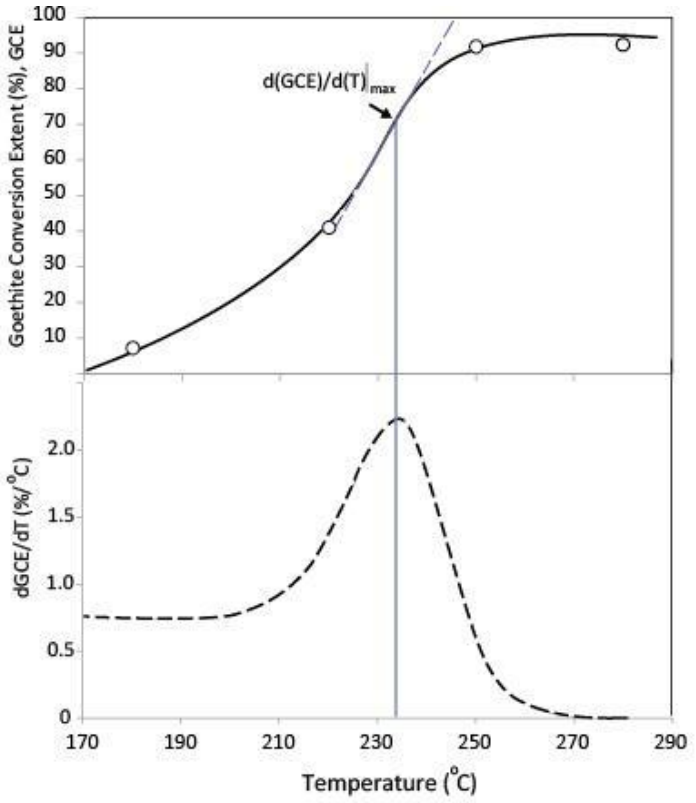

Figure 5.9 (**A**) The relationship between goethite to hematite conversion extent and digestion temperature. (**B**) The derivative of goethite to hematite conversion extent against temperature (*d*GCE/*d*T), giving the reaction sensitivity towards temperature variation.

The 'Plateau zone' in **Figure 5.8** is the area that the digestion temperatures are above 260^{o}C. In this zone goethite to hematite conversion is so fast that near complete conversions are observed within minutes. This region is named the 'Plateau zone' because goethite to hematite conversion proceeds to near completion and appears independent of further increases in digestion temperature. The practical value of the 'Plateau zone' is to show that at temperatures above 260^{o}C little gain in goethite conversion can be achieved by increasing digestion temperature.

5.3.2.2 The influence of free caustic concentration

Basu (1983) and Murray et al. (2009) have reported that the caustic soda concentration positively enhances the goethite transformation in the sodium aluminate solution. They found that higher free caustic concentration or caustic soda concentration leads to a faster transformation. In this study, we found that it is the increasing free caustic soda concentration that is more likely to contribute to the faster transformation.

Table 5.4 The influence of free caustic (with varying A/C ratio) on the goethite to hematite conversion

Goethite (g)	Hematite (g)	Digestion Conditions				Result		
		Temp(℃)	Time (min)	A/C	Free Caustic	wt% H'	wt% G'	%GCE
2.0172	0.0000	250	15	0.60	90.35	0.00	100.00	0.00
2.0264	0.0000	250	15	0.55	102.82	6.27	93.73	7.39
2.0383	0.0000	250	15	0.40	140.24	19.18	80.82	22.07
2.0532	0.0000	250	15	0.00	240.00	90.19	9.81	91.65

Note:
- % GCE is the conversion of goethite to hematite.
- The measured weight losses of 'pure' goethite and hematite upon ignition in this batch are wt% LPG=17.51% and wt% LPH=1.67% respectively.

Table 5.4 lists the digestion conditions that were used to investigate the influence of free caustic (with varying A/C ratio in the same caustic concentration 240 g/L) on the goethite transformation at 250^{o}C. The caustic soda concentration (C) for all the solutions stayed at the same level but free caustic varied from 90.35 to 240 g/L. The digestion time was 15 min. **Figure 5.10(A)** shows the adjusted weight percentages of hematite and goethite in digestion residues, calculated using **Equation 5.5** and **5.6**. The hematite forms at the expense of goethite. This process is relatively slow at free caustic levels less than 110 g/L (see **Figure 5.10**). The reaction starts to accelerate in the free caustic region of 110-140 g/L. After the free caustic exceeds 140 g/L, the reaction extent increases steadily with free caustic concentration to over 90% at 240 g/L free caustic. Given the same caustic soda concentration (C: 240 g/L), this increase of transformation extent (from 22.07% to 91.65%) is apparently due to the increase of free caustic soda concentration from 90.35 g/L to 240 g/L.

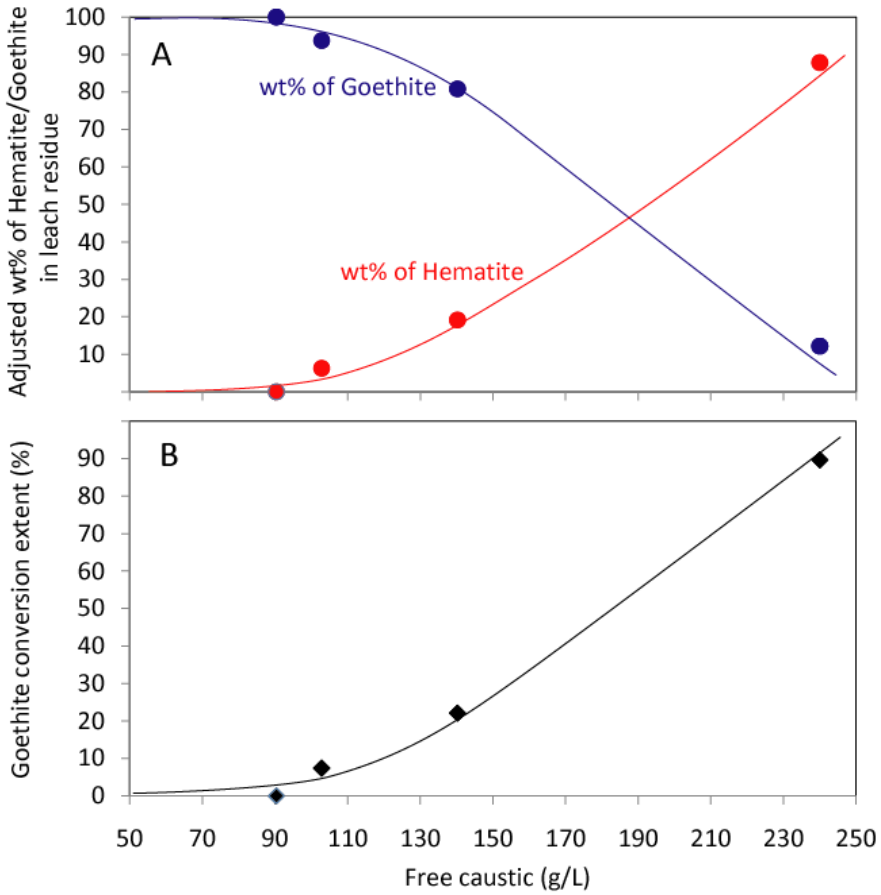

Figure 5.10 (**A**) The adjusted weight percentages of hematite and goethite in digestion residues after digestions in liquors with various free caustic ranging from 90.35-240 g/L. (**B**) The influence of free caustic on goethite to hematite conversion process. A/C ratio ranges from 0 (free caustic =240 g/L) to 0.6 (free caustic = 90.35 g/L). The digestion time is 15 min at 250 °C. No hematite seeding in digestions.

The study clearly shows the enhancement of increasing free caustic soda concentration to the transformation although the caustic soda concentrations for all the solutions remain the same. It is strongly suggest that the free caustic soda concentration, rather than the caustic soda concentration, is a stimulant to the hydrothermal transformation of goethite to hematite.

5.3.2.3 The influence of alumina content in caustic liquor

The early work by Basu (1983) and King (1971) provides the foundation of studying the goethite to hematite transformation process. These studies proposed a 'Dissolution/re-precipitation' mechanism, which is shown in **Figure 5.11** relying on the solubility difference between goethite and hematite in caustic liquor. Initially, the octahedral [FeO_4] units disassociate from the goethite crystal lattice and form part of the intermediate product, sodium ferrate (Na_4FeO_4), by interacting with Na^+ in solution; the sodium ferrate further aggregates around the hematite crystal embryos (or seeds) in solution, leading to the formation and growth of hematite crystals (King, 1971; Crombie *et al.*, 1973). Although the dissolution/re-precipitation has been widely recognised as the fundamental mechanism for hydrothermal transformation of goethite to hematite, the formation of the sodium ferrate intermediate is not sound. The formation of sodium ferrate in solution, in fact, is extremely harsh and requires strongly oxidising conditions (Ockerman and Schreyer, 1951; Jeannot *et al.*, 2002) and these conditions cannot be met with under the Bayer digestion conditions. It is convincingly suggested by Cornell and Schwertmann (2003) that the driving force for this dissolution/re-precipitation is the lower solubility and greater thermodynamic stability of hematite compared with that of goethite.

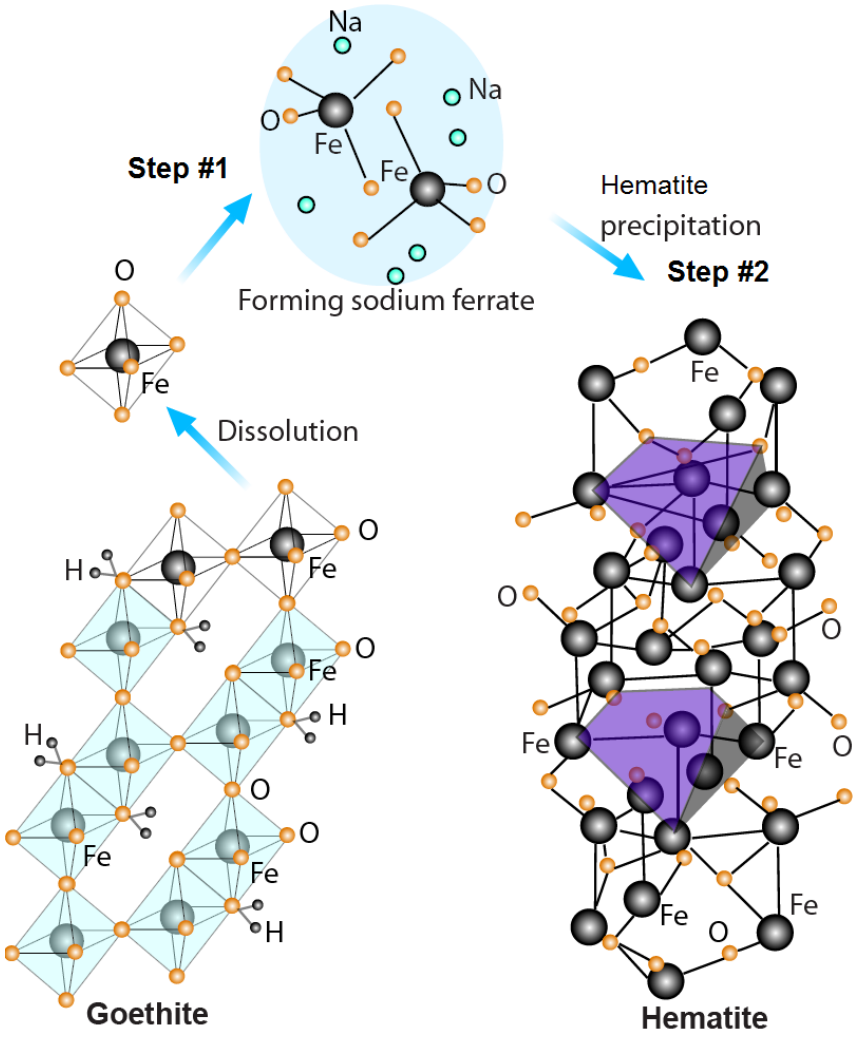

Figure 5.11 Schematic diagram of proposed mechanism for hydrothermal transformation of goethite to hematite (drawn after King (1971), Basu (1986) and Murray et al. (2009)). The goethite crystal structure was drawn according to the description from Burgina et al. (2000) and the hematite crystal structure was from Okinaka and Maekawa (2001).

Basu (1983) further suggested that the goethite transformation rate in pure caustic solution is faster than in sodium aluminate solutions for a given free caustic concentration. Whether the aluminium ions inhibit the goethite dissolution step or the hematite precipitation step remains unclear. A series of experiments was, therefore, conducted to compare the goethite to hematite conversion extent at various A/C levels (including A/C=0). The digestion temperature was set at 250 ℃. The study shows the existence of aluminium ions in caustic liquor severely retards the goethite conversion to hematite as shown in **Figure 5.12**, which is in agreement with Basu (1983). For pure caustic soda solution digestion, goethite transforms to hematite even in an extremely

low caustic concentration (lower than 10g/L) and the transformation rapidly approaches completion with as low as ~80 g/L free caustic. However, digestion in Bayer liquor is a different scenario, in which the transformation does not proceed until the free caustic soda increases to 100 g/L and then the conversion sluggishly rises. The transformation is eventually close to complete when the free caustic soda concentration further increases to ~ 190 g /L (A/C=0.2). A huge gap in the extent of transformation of goethite occurs between pure caustic digestion and Bayer liquor digestion even with the same free caustic soda concentration (when free caustic soda concentration is lower than ~150g/L).

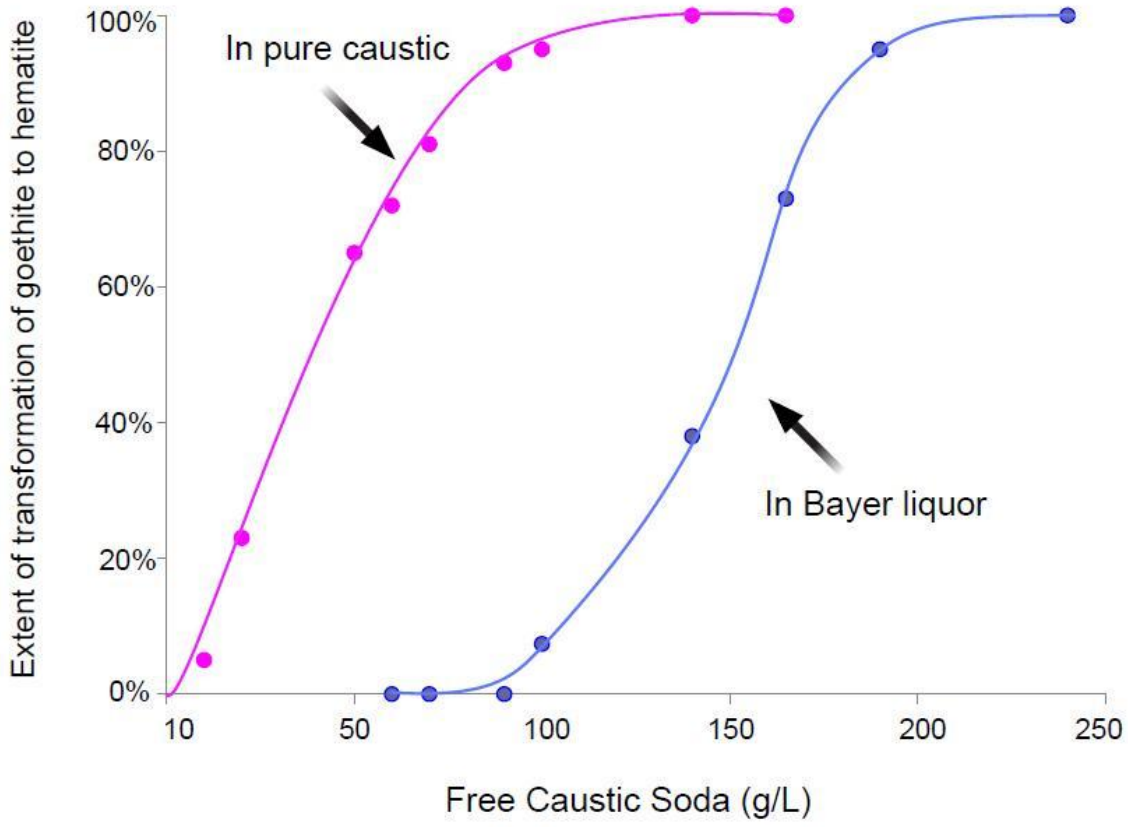

Figure 5.12 The effect of alumina content (gibbsite) to the hydrothermal transformation through the relationship between the extent of transformation and free caustic in both pure caustic (pink curve) and Bayer liquor (blue curve). Temperature: 250 ºC and holding time: 30 minutes. For pure caustic: C is equivalent to free caustic soda concentration; for Bayer liquor, C = 240 g/L.

To further identify the retardation of the presence of alumina content to the transformation, the extent of goethite transformation in pure caustic soda (A/C=0, C=240g/L) and in sodium aluminate solution (A/C=0.7, C=240g/L) in different digestion time was also conducted. As shown in **Figure 5.13**, the goethite almost completely converts to hematite within minutes (< 5min) in the caustic liquor free of aluminium ions (A/C = 0) at 250^{o}C. In the caustic liquor with A/C =0.7, the goethite conversion significantly reduced. Very little goethite to hematite conversion was observed in the first 30 min of digestion under this condition. The reaction rate was so slow that only 20.75% goethite converted to hematite after 60 min digestion (**Figure 5.13**), which is much longer than most Bayer digestion holding times at this temperature.

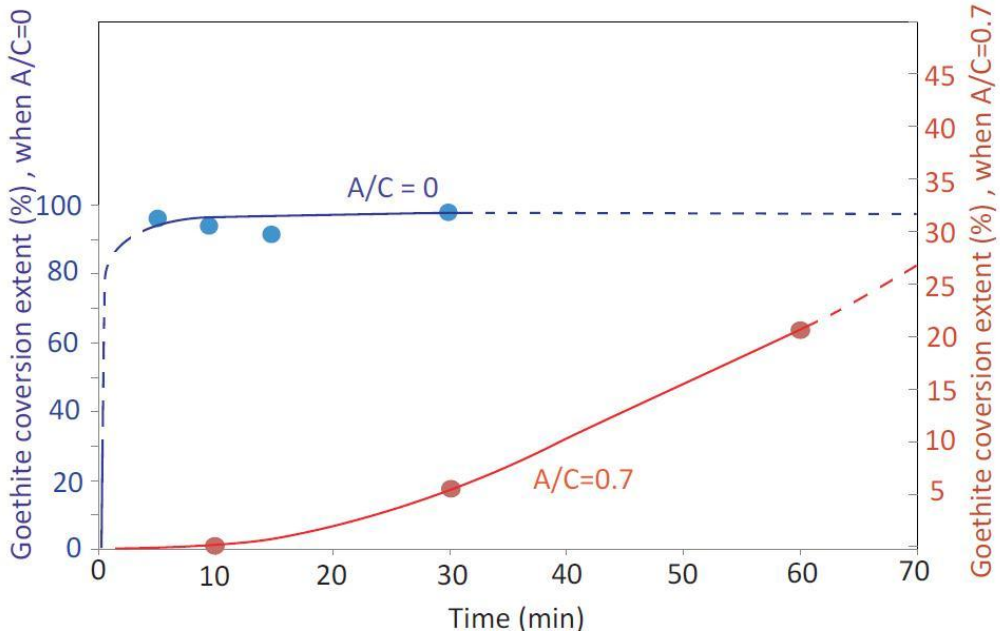

Figure 5.13 A comparison of the kinetic behaviours of goethite to hematite conversion under the condition of A/C = 0 with that under the condition of A/C = 0.7 against holding time. All digestions were carried out at 250 °C. Samples were taken from digestion time ranging from 5-60 min. No hematite seeding was used in the digestion.

It appears that the reduction in conversion extent is attributed to (i) the reduced free caustic concentration from 240 g/L (pure caustic) to 65.43 g/L (A/C = 0.7, C=240 g/L) (as shown in **Figure 5.13**) and (ii) the presence of aluminium ions in caustic liquor (as shown in **Figure5.12**). Therefore, the concentration of both free caustic and alumina content are important in the goethite to hematite transformation process.

In terms of alumina content, a new intermediate bearing both Al and Fe could be formed with the involvement of alumina content in the sodium aluminate solution rather than sodium ferrate (Na_4FeO_4) as mentioned in the mechanism of the transformation. In conjunction with the proposed mechanism, possible structure of the new intermediate species, [Na-Al-Fe-O] is illustrated in **Figure 5.14** compared to the intermediate species [Na-Fe-O] in pure caustic soda. This is able to explain the retardation of the transformation in sodium aluminate solution even with the same level of free caustic soda concentration as a caustic soda solution. It could be more difficult for the intermediate with Al incorporated in the structure than Na_4FeO_4 to precipitate as hematite due to more energy needed to conquer the barrier.

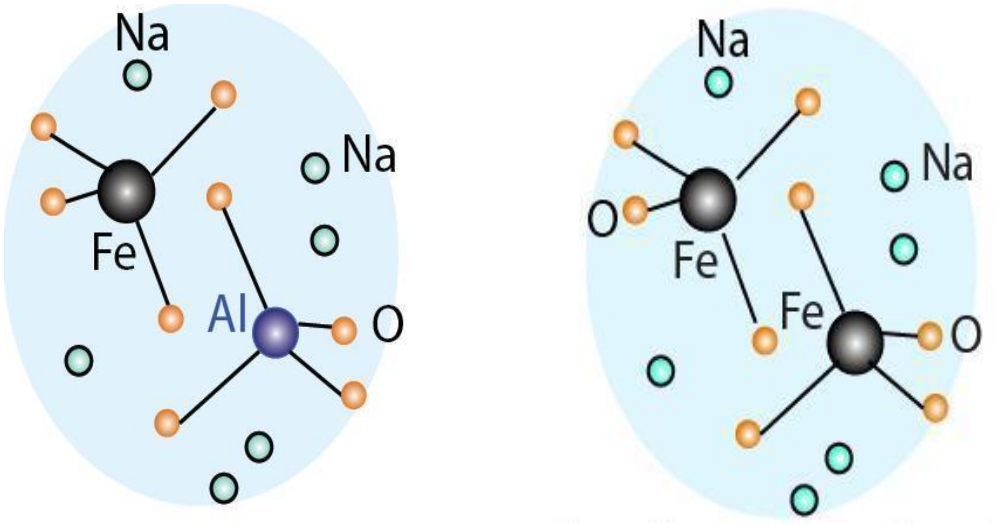

(a) Species possibly present in sodium aluminate solution.

(b) Species present in the pure caustic soda solution.

Figure 5.14 Possible intermediate species present in Bayer liquor for hydrothermal transformation of goethite to hematite. (a) In sodium aluminate solution (Bayer liquor); (b) In pure caustic soda

The following TEM-EDS (**Figure 5.15**) could provide evidence for the presence of [Na-Al-Fe-O] intermediate species during the hydrothermal transformation of goethite to hematite. Al in the goethite structure was detected by TEM-EDS technique as shown in **Figure 5.15**. Analysis of this digested residue found 2.17 mol% Al presents in the goethite structure. However the structure of this intermediate remains unclear at this stage although an Al-goethite-like structure has been suggested by Basu (1983).

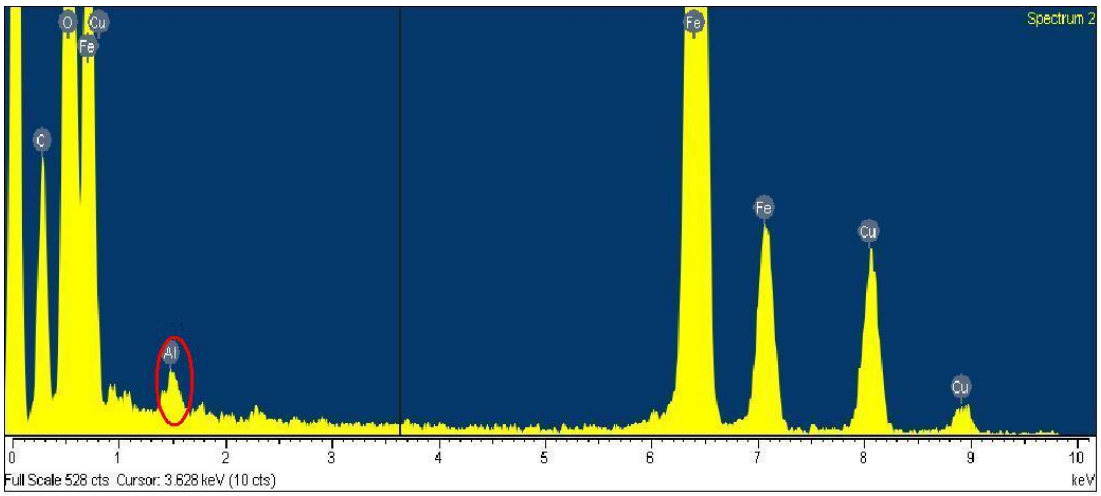

Element	Weight %	Atomic %	Al/(Al+Fe) mol %
O	44.22	73.23	2.17
Al	0.59	0.58	
Fe	55.19	26.18	
Totals	100.00	99.99	

Figure 5.15 TEM-EDS spectra and report to show 2.17 mol% Al incorporated in the goethite particle in one of the digested residues. The residue was obtained by digesting pure goethite in sodium aluminate solution with C = 240 g/L, A/C = 0.4 at 250 ºC for 30 minutes.

5.3.2.4 The influence of hematite seeding

In the seeding experiments conducted, all digestions were carried out at 250^{o}C due to low reactivity ~140 ℃. In this high digestion temperature state, the majority of the goethite transforms to hematite given sufficient digestion time and conditions (e.g. free caustic in digestion liquor).

To formulate the function of goethite to hematite conversion against H/G molar ratio, a series of digestions were conducted under the conditions listed in **Table 5.5**. The digestion conditions are adopted as close as possible to real Bayer process conditions. For example, the A/C ratio maintained at 0.7 and the free caustic is 65.41 throughout the seeding tests. The only variable in these tests is the molar ratio H/G ranging from 0 to 2.0.

Table 5.5 The impact of hematite seeding on the goethite to hematite conversion

Digestion Conditions							Results			
Goethite (g)	Hematite (g)	H/G	Temp (℃)	Time (min)	A/C	Free Caustic (g/L)	LOI (wt%)	wt% H'	wt% G'	%GCE
2.0040	7.2060	2.00	250	30	0.70	65.41	6.23	70.08	29.92	73.50
2.0123	3.5969	0.99	250	30	0.70	65.41	3.43	87.43	12.57	88.94
2.0113	2.5712	0.71	250	30	0.70	65.41	1.97	98.03	1.97	98.33
2.0153	1.2010	0.33	250	30	0.70	65.41	5.70	73.56	26.44	76.71
2.0040	0.4024	0.11	250	30	0.70	65.41	8.21	53.29	46.71	56.88
2.0271	0.0000	0.00	250	30	0.70	65.41	16.17	4.95	95.05	5.81

Note:
- H/G is the molar ratio of hematite to goethite in the prepared material prior to digestion.
- % GCE is the conversion of goethite to hematite.
- The measured weight losses of 'pure' goethite and hematite upon ignition in this batch are wt% LPG=16.91% and wt% LPH=1.67% respectively.

A plot of the goethite to hematite conversion extent (%) as a function of H/G ratio is shown in **Figure 5.16**. The conversion increases with the extent of hematite seeding to a maximum value of H/G 0.7. With H/G beyond this value, more hematite seeding does not support greater conversion. Hematite seeding under this value shows a potential linear relationship with the conversion. As shown in **Figure 5.17**, %GCE increases linearly with respect to the amount of hematite seeding added when the H/G molar ratio is under the value that can almost get goethite fully transformed to hematite. It would be of value to the industrial practice if this possible linear relationship does exist. The 'Least square regression' method was used to formulate the trend line, showing the potential linear relationship between the reaction extent and hematite seeding:

$$\%GCE = 62.369\ H/G + 56.116 \qquad \textbf{(5.11)}$$

It is worth noting that the amount of hematite is of course linearly related to the total hematite surface area, which can act as seed for hematite crystallisation.

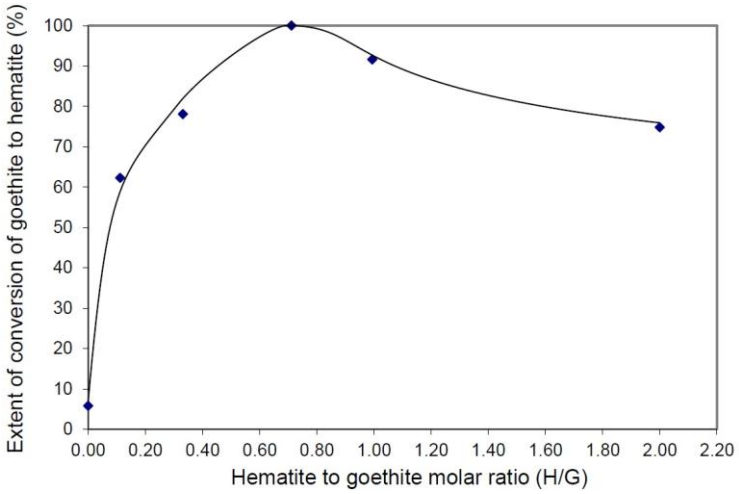

Figure 5.16 The relationship between goethite to hematite conversion and hematite seeding. All digestions were conducted at 250 °C for the period of 30 minutes. A/C = 0.7. The free caustic is 65.41 g/L.

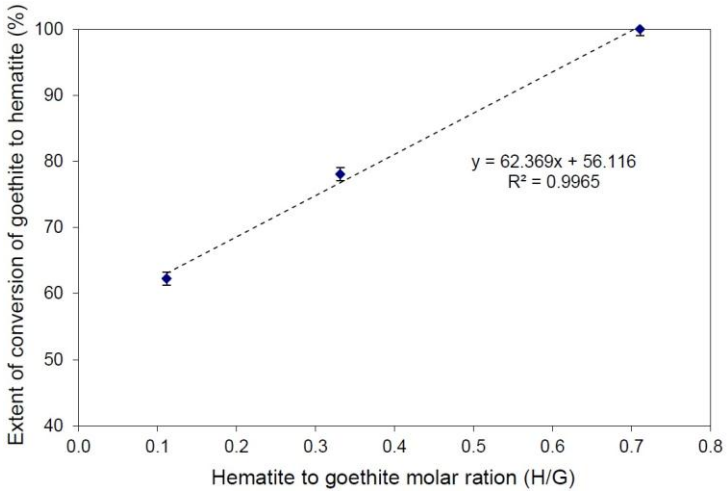

Figure 5.17 The linear relationship between hematite seeding and the goethite to hematite conversion when H/G ranging between 0 and 0.7. All digestions were conducted at 250 °C for the period of 30 minutes. A/C = 0.7. The free caustic is 65.41 g/L.

It has been widely suggested that hematite seeding improves the performance of goethite to hematite conversion in the Bayer digestion. The conclusion from this study confirmed that hematite seeding linearly enhances the transformation when H/G lies between 0.1 and 0.7. However, it seems that this conclusion is only valid under a maximum value for H/G at 0.7. More hematite seeding than that ratio, on the contrary, does not support a better performance.

5.3.3 Mechanism of hydrothermal transformation

It has long been believed that the hydrothermal transformation of goethite to hematite experiences a two-step mechanism, dissolution of goethite and precipitation of hematite (King, 1971; Basu, 1983; Murray *et al.*, 2009). The conclusion in this study is in agreement with the mechanism in explaining the phenomena such as the retardation by the alumina content and the enhancement of hematite seeding to the hydrothermal transformation.

The driving force of the proposed mechanism is attributed to the difference of the solubility between goethite and hematite in the Bayer liquor. An attempt was made to investigate the solubility performance of both goethite and hematite in Bayer. However, the experiments were severely affected by the extremely low solubility of goethite and hematite in both the caustic soda and the Bayer liquor. The trends from the test show that goethite seems more soluble in the caustic soda solution than hematite, which is in agreement with expectation; meanwhile, both goethite and hematite are easier to dissolve in the caustic soda than in the sodium aluminate solution, which provides further evidence as for why the presence of alumina content is an inhibitor to the transformation. This data, however, needs to be replicated in a manner with smaller experimental errors. As such, no definitive conclusions with regard to solubility are made here.

References

Authier-Martin, M., Forte, G., Ostap, S. & See, J. (2001) The mineralogy of bauxite for producing smelter-grade alumina. *Journal of Mineralogy,* 53**,** 36-40.

Basu, P. (1983) Reaction of iron minerals in sodium aluminate solutions. IN ADKINS, E. M. (Ed.) *Light Metals.* New York, The Metallurgical Society of AIME.

Basu, P., Nitowski, G. A. & The, P. J. (1986) Proceedings of the International Symposium on Iron Control Hydrometallurgy. IN Ellis Horwood Limited, Chichester, UK. 223-244

Burgina, E. B., Kustova, G. N. , Tsybulya, S. V., Kryukova, G. N., Litvak, G. S., Isupova, L. A. & Sadykov, V. A. (2000) Structure of the metastable modification of iron (III) oxide. *Journal of Structural Chemistry,* 41**,** 396-402.

Cornell, R. M. & Schwertmann, U. (2003) *The Iron Oxides: Structure, Properties, Reactions, Occurrences and Uses,* Weinheim:Wiley-VCH.

Crombie, T., Davis, M. & Laurie, J. E. (1973) Method of digesting bauxite via the Bayer process with the addition of reducing agents. United States Patent 4059672.

Fey, M. V. & Dixon, J. B. (1981) Synthesis and properties of poorly crystalline hydrated aluminous goethite. *Clays and Clay Minerals,* 29**,** 91-100.

Frost, R. L., Ding, Z. & Ruan, H. D. (2003) Thermal analysis of goethite. *Journal of Thermal Analysis and Calorimetry,* 71**,** 783-797.

Gialanella, S., Girardi, F., Ischia, G., Lonardelli, I., Mattarelli, M. & Montagna, M. (2010) On the goethite to hematite phase transformation. *Journal of Thermal Analysis Calorimetry,* 102**,** 867-873.

González, G., Sagarzazu, A. & Villalba, R. (2000) Study of the mechano-chemical transformation of goethite to hematite by TEM and XRD. *Materials Research Bulletin,* 35**,** 2295-2308.

Jeannot, C., Malaman, B., Gérardin, R. & Oulladiaf, B. (2002) Synthesis, Crystal and Magnetic Structures of the Sodium Ferrate (IV) Na_4FeO_4 Studied by Neutron Diffraction and Mössbauer Techniques. *Journal of Solid State Chemistry,* 165**,** 266-277.

King, W. R. (1971) The iron minerals in Jamaican bauxites. IN The Metallurgical Society of AIME, Light metals. New York, 18-20

Li, L. Y. (2001) A study of iron mineral transformation to reduce red mud tailings. *Waste Management,* 21**,** 525-534.

Majzlan, J. & Navrotsky, A. (2003) Thermodynamics of the goethite-diaspore solid solution. *Eur. J. Mineral,* 15, 495-501.

Mendelovici, Efraim & Yariv, Shmuel (1981) Interactions between the iron and the aluminum minerals during the heating of Venezuelan lateritic bauxites. I. Infrared spectroscopy investigation. *Thermochimica Acta,* 45**,** 327-337.

Murray, J., Kirwan, L., Loan, M. & Hodnett, B. K. (2009) In-situ synchrotron diffraction study of the hydrothermal transformation of goethite to hematite in sodium aluminate solutions. *Hydrometallurgy,* 95**,** 239-246.

Ockerman, L. T. & Schreyer, J. M. (1951) Preparation of Sodium Ferrate (VI). *Journal of American Chemistry Society,* 73**,** 5478.

Okinaka, K. & Maekawa, M. (2001) Spindle-shaped goethite particles, sindle-shaped hematite particles and magnetic sindle-shaped metal particles containing iron as main component. US Patent 6309479.

Pomiès, M. P., Menu, M. & Vignaud, C. (1999) TEM observations of goethite dehydration: application to archaeological samples. *Journal of the European Ceramic Society,* 19**,** 1605-1614.

Prasad, P. S. R., Shiva Prasad, K., Krishna Chaitanya, V., Babu, E. V. S. S. K., Sreedhar, B. & Ramana Murthy, S. (2006) In situ FTIR study on the dehydration of natural goethite. *Journal of Asian Earth Sciences,* 27**,** 503-511.

Ruan, H. D., Frost, R. L. & Kloprogge, J. T. (2001) The behavior of hydroxyl units of synthetic goethite and its dehydroxylated product hematite. *Spectrochimica Acta Part A: Molecular and Biomolecular Spectroscopy,* 57**,** 2575-2586.

Ruan, H. D., Frost, R. L., Kloprogge, J. T. & Duong, L. (2002) Infrared spectroscopy of goethite dehydroxylation. II. Effect of aluminium substitution on the behaviour of hydroxyl units. *Spectrochimica Acta Part A: Molecular and Biomolecular Spectroscopy,* 58**,** 479-491.

Schwertmann, U. & Cornell, R. M. (2000) *Iron Oxides in the Laboratory: Preparation and Characterization,* Weinheim, Wiley-VCH.

Sudakar, C., Subbanna, G. N. & Kutty, T. R. N. (2004) Effect of cationic substituents on particle morphology of goethite and the magnetic properties of maghemite derived from substituted goethite. *Journal of Materials Science,* 39**,** 4271-4286.

Walter, D., Buxhaum, G. & Laqua, W. (2001) The mechanism of the transformation from goethite to hematite. *Journal of Thermal Analysis and Calorimetry,* 63**,** 733-748.

Wolska, E. & Schwertmann, U. (1993) The mechanism of solid solution formation between goethite and diaspore. 213-223.

Wolska, E., Szajda, W. & Piszora, P. (1994) Mechanism of Al- for Fe-substitution during the α-(Fe, Al) OOH to γ-(Fe, $Al)_2O_3$ transformation. *Solid State Ionics,* 70/71**,** 537-541.

Chapter 6
Al-substituted Goethite in the Bayer Digestion Process

6.1 Overview

The hydrothermal transformation of synthetic goethite to hematite was investigated in the previous Chapter 5 and the optimized conditions which encourages the transformation were developed. In this chapter, the aim is to examine the applicability of these conditions to natural Al-goethite to hematite transformation. Significant differences in digestion conditions will be expected between synthetic goethite and natural Al-goethite in bauxite due to possible interference from its complexities and impurities in natural bauxite.

The aim of this chapter is to investigate the hydrothermal transformation behaviour of Al-goethite in Jamaican bauxite based on the results obtained from transformation study of synthetic goethite in Chapter 5. Due to the complexity of interactions imparted by the impurities in bauxite, the study is designed as a stepwise process. It investigates one impact factor at a time for its effects on the aluminous goethite to hematite transition. This is achieved by altering one parameter while other parameters are kept relatively constant to minimize the numbers of variables that may complicate the study.

The schematic demonstration of bauxite preparation and their use in this chapter is shown in **Figure 6.1**. Firstly, to minimize the interference caused by the impurities, a pre-treatment to the Jamaican bauxite was carried out by mildly digesting the bauxites in low concentration caustic soda to remove gibbsite and eliminate its impact on the transformation. The digestion of pre-treated bauxite was then conducted to determine the factors that influence goethite to hematite conversion. Secondly, a transformation test on raw bauxite was subsequently performed to examine the digestion of Al-goethite in natural bauxite. The problems arose from Al-goethite transformation in raw bauxite were carefully investigated.

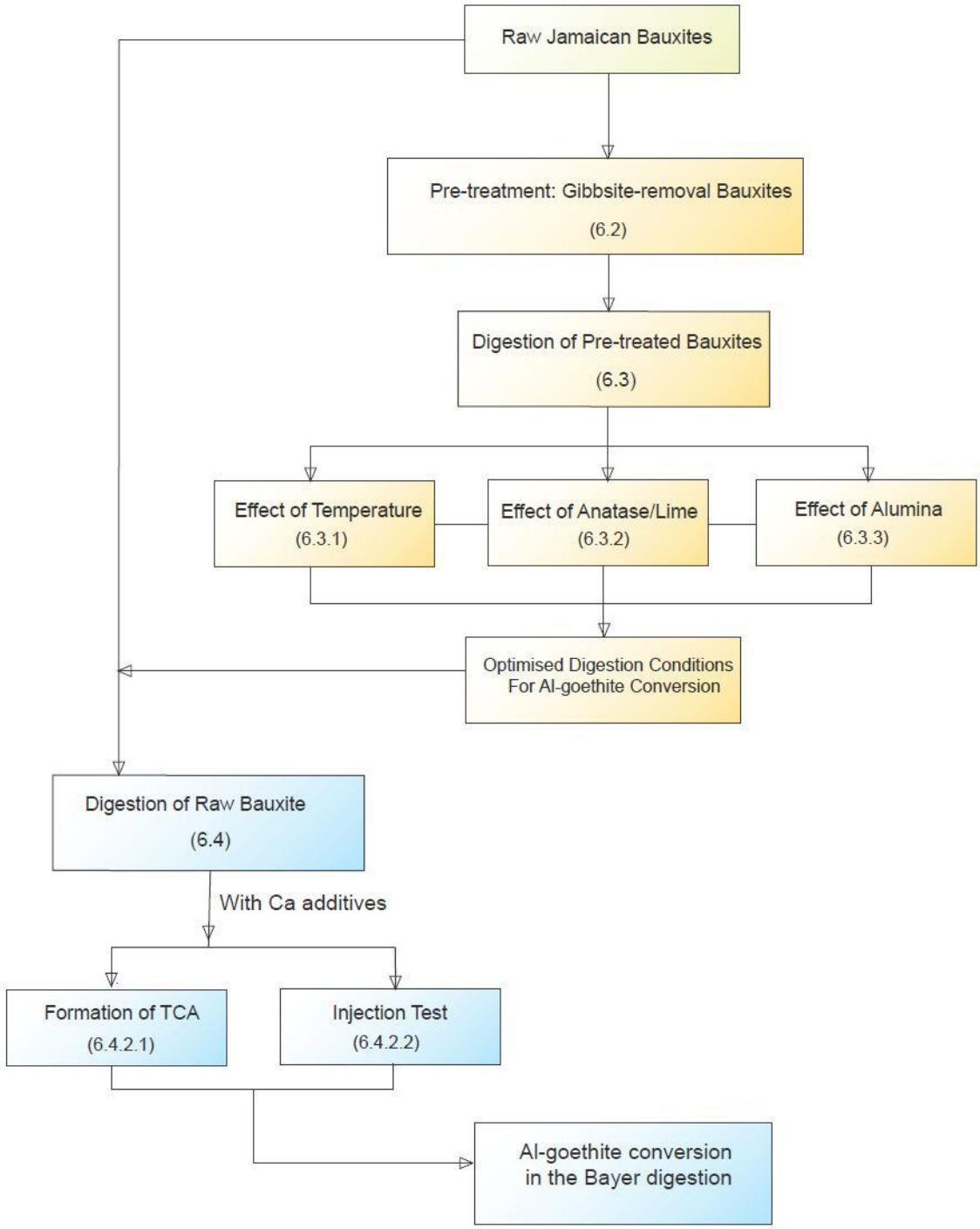

Figure 6.1 Schematic diagram of the outline for the Chapter

6.2 Pre-treatment of Jamaican bauxite

Twelve Jamaican bauxites provided by Alcoa World Alumina were used in this study. The list of mineral compositions of the raw (untreated) bauxites are shown in **Table 6.1** and Appendix C. It should be noted that the high gibbsite content in the Jamaican bauxite is likely to overshadow the evidence of Al-goethite to hematite transformation,

and makes the study of the underlying mechanisms more difficult. (see Section 5.3.2.2). The presence of gibbsite interferes with this study as some of its XRD peaks overlap with that of goethite and hematite. This makes it difficult to accurately calculate the aluminium substitution in both goethite and hematite. Therefore, pre-treatment of Jamaican bauxites was conducted to eliminate the influence of gibbsite.

6.2.1 Pre-treatment of Jamaican bauxite

The detailed description of pre-treatment of Jamaican bauxite can be seen in Section 3.2.3.1. The pre-treated residues were characterised by X-ray diffraction (XRD) to ensure adequate removal of gibbsite. The proportion of goethite to hematite G/(G+H) and the extent of Al substitution in both goethite and hematite are summarised in **Table 6.1**. The operation of the pre-treatment of raw Jamaican bauxites was described and demonstrated in Section **3.2.3.1**.

Table 6.1 Chemical and mineral composition in Jamaican bauxites

Sample	Main compositions, % (XRF)						Minerals (XRD)	SiO_2 after pre-treatment, %	G/(G+H)	Selected samples
	Al_2O_3	av. Al_2O_3	Fe_2O_3	SiO_2	TiO_2	CaO				
JCB-BLM	48.2	45.9	18.9	1.9	2.42	0.04	Gi,Bo,He,Go,An,Ka	0.60	0.20	X
JCB-GPM	47.5	43.8	19.3	2.32	2.56	0.06	Gi,Bo,He,Go,An,Ka	0.78	0.34	X
JCB-PAT	49.7	46.3	17.5	0.8	2.11	0.31	Gi,Bo,He,Go,An,Ka	0.46	0.21	V
JCB-ASI	49.5	44.1	18.2	1.12	2.27	0.04	Gi,He,Go,An,Ka	0.38	0.23	V
JCB-218	48.2	41.8	17.5	0.99	2.31	0.54	Gi,Bo,Go,An	0.48	0.97	X
JCB-090	48.0	39.9	17.6	0.87	2.35	0.65	Gi.Bo.Go.An	0.32	1.00	X
JCB-270	49.8	41.3	17.4	0.12	2.48	0.07	Gi,Bo,Go,An	0.00	1.00	V
JCB-BST	46.6	39.8	18.2	4.57	2.34	0.15	Gi,Bo,Go,He,An,Ka	2.83	0.72	X
JCB-WRP	47.9	42.4	18.9	0.56	2.65	0.24	Gi,Bo,Go,He,An,Ka	0.28	0.84	V
JCB-BTM	50.9	49.1	17.3	0.28	2.25	0.03	Gi,Go,He,An,Ka	0.07	0.15	V
JCB-RBM	48.6	46.6	18.8	2.42	2.33	0.06	Gi,Bo,He,Go,An,Ka	1.00	0.23	X
JCB-HAM	48.9	42.9	16.8	3.95	2.33	0.06	Gi,Bo,He,Go,An,Ka	1.06	0.24	X

Note:

1. Gi - gibbsite, Bo - boehmite, He - Hematite, Go - goethite, An – anatase, Ka-kaolinite.
2. The analysis of available Al_2O_3: 1g of sample was digested in 20g of 80g/L caustic soda at 80~90 ℃ for 2hours. The digested solution was titrated to calculate the available Al_2O_3.
3. G/(G+H): Calculated by XRD results. Peaks used were goethite (110, *d*=0.4183) and hematite (110, *d*=0.2519).

6.2.2 Selection and digestion of Jamaican bauxites

Table 6.1 shows the chemical and mineral composition of the raw bauxites. Combined XRD with XRF results for the total 12 bauxites (see detailed information in Appendix C) show gibbsite as the dominant alumina mineral in all the samples. A trace amount of boehmite is also present in most of the bauxites used in the study. Goethite and hematite are the main iron oxides, but the goethite content varies extensively from ~ 20% of total iron in half of the samples to nearly 100% of total iron in JCB-090, JCB-218 and JCB-270.

Five bauxites, JCB-ASI, JCB-PAT, JCB-270, JCB-WRP and JCB-BTM, were selected for further digestion tests. The reason for this selection can be found in Section 6.4.1. The compositions of the five bauxites are also shown in **Table 6.1**. These bauxites typically have a varying content of goethite and hematite with G/(G+H) ranging from 0.15 to 1.00 and low silica content (<0.5%). The effects of varying bauxite compositions in the five chosen bauxites can be representative by comparing their digestion outcomes. The experimental results derived from these bauxite samples are therefore, likely to produce information that is more relevant and useful in guiding an industrial process.

The digestion of pre-treated bauxite and raw Jamaican bauxite in the following discussion were both performed in bomb digestion vessels. Bomb digestion was carried out using a gas-fired reactor system (250mL capacity) with rapid rates of heat-up (~35 ℃/min) and cool-down (~70 ℃/min). Approximately 5g pre-treated bauxite or ~15 g raw bauxite, which is equivalent to ~80 g/L loading of raw bauxite were mixed in 150 mL pure caustic soda or Bayer liquor for a desired period of time at defined temperatures. The reactor was rotated horizontally during the digestion to ensure sufficient mixing of the reactants. The cooled slurry was pressure filtered through a 0.45 μm membrane filter. The residues were washed with deionised water several times and then dried at 100 ℃ overnight. The samples were characterised by XRD to determine phase changes and by XRF to determine elemental composition. The exit filtrate was analysed by titration for A/C ratio using the Gluconate Method (Connop 1996) and ICP for the chemical composition.

6.2.3 Methods of estimation of Al substitution in goethite and hematite

The extent of aluminium substitution for iron in Al-goethite and Al-hematite in bauxites by the chemical method is not ideal. The presence of a variety of other minerals in the bauxites such as gibbsite or boehmite greatly impacts the accuracy of chemical determination of Al substitution in goethite and hematite. As a result, the estimation of Al substitution in both goethite and hematite was alternatively achieved from the change in their XRD patterns, secondary to the crystal lattice distortion caused by ion exchange. However, it should be noted that the calculation for goethite/hematite in bauxite is slightly different from that in synthetic Al-goethite mentioned previously due to the possible effects caused by other accompanying minerals in natural bauxites. The methods described by Zwingmann et al. (2008) and Schulze (1984) were employed in this chapter to calculate Al substitution. It is worth noting that significant peak overlaps are more likely to happen between gibbsite and goethite/ hematite in XRD patterns. Therefore, the XRD patterns used to calculate the Al substitution in goethite or hematite were those of pre-treated gibbsite-removal bauxites. The Al substitution for goethite and hematite in the Jamaican bauxites calculated by these methods are listed in **Table 6.2**. Al substitution in goethite ranges between 9 and 28 mol %. Cornell and Schwertmann (2003) revealed that Al substitution in goethite can be up to 33 mol % in nature. Al substitution for all the 12 bauxites used in this research is within that range. Al substitution for hematite ranges from 0 to 14 mol %.

6.2.3.1 Estimation of Al substitution in goethite

In this chapter, the following two methods were used to estimate the Al substitution under different conditions (Zwingmann *et al.*, 2008).

Method 1: Neither gibbsite nor anatase is present in the bauxites. In this case, there are no anatase XRD diffraction peaks that overlap with goethite peaks. The relationship (Equation 6.1) between *c* (the unit cell length of goethite along the *c* axis) and Al substitution (mol %) described by Schwertmann and Carlson (1994) was used to estimate the extent of substitution in soil goethite.

$$\text{Al substitution in goethite (mol \%)} = 1468\text{-}483.1c \qquad \textbf{(6.1)}$$

where *c*, the unit cell length of goethite along the *c* axis, can be calculated using Equation 6.2 (Schulze, 1984).

$$c = \frac{1}{\sqrt{\left(\frac{1}{d_{111}}\right)^2 - \left(\frac{1}{d_{110}}\right)^2}} \quad \textbf{(6.2)}$$

where the distance between planes, d_{111} (d = 0.245 nm) and d_{110} (d = 0.418 nm) for Al substituted goethite, are obtained from XRD patterns.

Method 2: Anatase is present, but no gibbsite is present in the bauxites. The relationship (Equation 6.1) was also used in this case. However, the anatase peak d_{103} (d = 0.243 nm) overlaps with goethite peak d_{111} (d = 0.245 nm). Therefore, an alternative Equation 6.3 was used to calculate the value of the c dimension instead (Zwingmann *et al.*, 2008).

$$c = \frac{1}{\sqrt{\left(\frac{1}{d_{021}}\right)^2 - \left(\frac{1}{d_{020}}\right)^2}} \quad \textbf{(6.3)}$$

where substituting value of d_{021} (d = 0.258 nm) and d_{020} (d = 0.498 nm) were used instead of d_{111} and d_{110} in Equation (6.2).

6.2.3.2 Estimation of Al substitution in hematite

Estimation of Al substitution in hematite has been widely studied and various calculation methods in regards to the estimation are established. Some of the methods are concentrated on the relationship between Al substitution and the unit cell a (Schwertmann and Kampf, 1985; Schwertmann, 1987; Schwertmann, 1988). For the others however, a combination effect of a dimension and the loss of ignition (LOI) has been considered by Stanjek and Schwertmann (1992). The aluminium substitution in hematite causes a reduction in the unit cell length along the a axis. The more extensive the Al-Fe substitution is, the greater the reduction of the unit cell length along the a axis will be. The schematic diagram showing the phenomenon is shown in **Figure 6.2**.

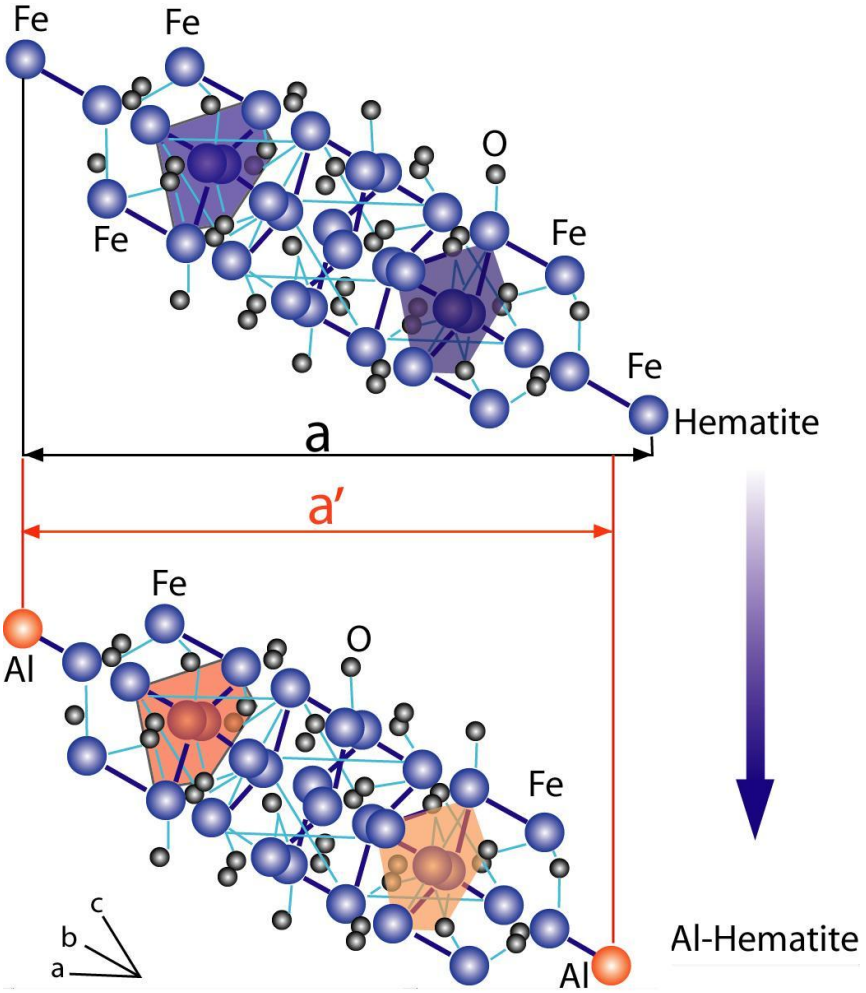

Figure 6.2 A schematic diagram showing unit cell reduction along the *a* axis with aluminium substitution in hematite. *a* and *a'* are the unit cell lengths of Al-hematite and hematite along their *a* axis respectively (*a'* < *a*).

Given that Al-hematite used in this chapter is a component of natural bauxites rather than pure synthetic hematite (LOI is not applicable), the relationship between Al substitution and unit cell dimension a for hematite proposed by Schwertmann and Kampf (1985) was used in the study (Equation 6.4).

Al substitution in hematite (mol %) = 3109-617.1*a* **(6.4)**

where *a*, the unit cell of hematite, can be calculated from the shifted peak position of the *d*(110) in XRD patterns for hematite (Equation 6.5). That is,

$$a = 2d_{110} \quad \textbf{(6.5)}$$

where d_{110} is the d spacing along the (110) crystal plane.

Equation 6.5 was derived from Equation 6.6 described by Klug and Alexander (1974).

$$d_{hkl} = \frac{a}{\sqrt{\frac{4}{3}\left(h^2 + hk + k^2\right) + \left(\frac{l}{c}\right)^2}} \rightarrow d_{110} = \frac{a}{\sqrt{\frac{4}{3}\left(1^2 + 1\times 1 + 1^2\right) + \left(\frac{0}{c}\right)^2}} \rightarrow d_{110} = \frac{a}{2} \qquad \textbf{(6.6)}$$

where *h, k, l* are the Miller indices of the crystal, while a, c are the unit cell lengths along *a* and *c* axes for Al-substituted hematite (which can be obtained from XRD patterns).

6.2.3.3 G/(G+H): Goethite to total iron oxides

The proportion of goethite to the total iron oxides, G/(G+H), was employed to present the extent of the goethite transformation to hematite. The goethite (110) peak from XRD patterns along with the hematite (110) peak was used to calculate the value of G/(G+H) (Equation 6.7). Intensities were calculated from areas under the peaks.

$$\text{G/(G+H)} = \frac{I_{(goethite,110)}}{I_{(goethite,110)} + I_{(hematite,110)}} \qquad \textbf{(6.7)}$$

where *I* is the intensity of the corresponding goethite or hematite peak at crystal plane (110).

Table 6.2 Aluminium substitution in goethite and hematite in the Jamaican bauxite samples

Sample	G/(G+H)	Al substitution in goethite[1]	Al substitution in hematite[2]	Selected samples
JCB-BLM	0.20	14	6	X
JCB-GPM	0.34	19	6	X
JCB-PAT	0.21	21	14	V
JCB-ASI	0.23	11	12	V
JCB-218	0.97	12	- (No hematite)	V
JCB-090	1.00	28	- (No hematite)	V
JCB-270	1.00	25	- (No hematite)	V
JCB-BST	0.72	17	9	X
JCB-WRP	0.84	20	0	V
JCB-BTM	0.15	11	10	V
JCB-RBM	0.23	11	4	X
JCB-HAM	0.24	9	7	X

Note:

1. Al substitution in goethite (mol %) = 1468-483.1c

   where $c = \dfrac{1}{\sqrt{\left(\dfrac{1}{d_{111}}\right)^2 - \left(\dfrac{1}{d_{110}}\right)^2}}$ if anatase is not present, $c = \dfrac{1}{\sqrt{\left(\dfrac{1}{d_{021}}\right)^2 - \left(\dfrac{1}{d_{020}}\right)^2}}$ if anatase is present in the bauxite.

   d values obtained from XRD results.

2. Al substitution in hematite (mol %) = 3109-617.1a, where $a = 2d_{110}$, d_{110} is obtained from XRD results.

6.3 Hydrothermal transformation of goethite in gibbsite-removed bauxites under Bayer conditions

A series of digestion experiments based on the results obtained from digestion on synthetic goethite in chapter 5 was conducted to investigate if the optimised conditions derived from the synthetic samples still applies to the pre-treated natural goethite. If not, what is responsible for the difference and what could be done to address this problem.

Table 6.3 Hydrothermal transformation of goethite in pre-treated bauxites in high temperature digestion (≥230 ºC)

Bauxite	Initial					Result	
	Temperature (℃)	Time (min)	A/C*	CaO added	Initial G/(G+H)**	Final G/(G+H)**	Exit A/C
JCB-270	230	30	0		1.00	0.97	0.017
	250	30	0			1.00	0.018
	280	30	0			0.96	0.020
	250	30	0.56			0.98	0.018
	250	30	0	CaO***		0.12	0.025
JCB-WRP	230	30	0		0.84	0.76	0.012
	250	30	0			0.69	0.013
	280	30	0			0.52	0.015
JCB-ASI	230	30	0		0.23	0.21	0.008
	250	30	0			0.19	0.006
	280	30	0			0.15	0.004
	250	30	0.56			0.22	0.004
JCB-BTM	230	30	0		0.15	0.13	0.006
	250	30	0			0.15	0.003
	280	30	0			0.11	0.023
JCB-PAT	230	30	0		0.21	0.15	0.024
	250	30	0			0.10	0.025
	280	30	0			0.00	0.026

Note:

* A/C: ratio of alumina to caustic soda.

** G/(G+H) is goethite to (goethite + hematite) ratio in bauxites. It is calculated by XRD results. Peaks used were goethite (110, *d*=0.4183) and hematite (110, *d*=0.2519).

***CaO added in the experiments were 1%, 2% and 3% (wt. %) of total weight of pre-treated bauxite respectively. However, the charge of CaO show little effect on the final results with the final G/(G+H) and exit A/C remain unchanged.

In chapter 5, the digestion conditions that affect the performance of hydrothermal transformation were studied on relatively pure samples. However, when natural bauxites with more complex mineral constituents are used, the optimum digestion conditions could change dramatically in response to the impurities introduced. **Table 6.3** shows the hydrothermal transformation of goethite/Al-goethite to hematite in

different pre-treated Jamaican bauxites under high digestion temperatures (≥230ºC). The detailed analysis with the data shown in the table is discussed further in the latter part of this chapter.

6.3.1 Effect of temperature

Three temperatures 230 ℃, 250 ℃ and 280 ℃ were investigated for the five selected pre-treated Jamaican bauxites. The proportion of goethite to the overall iron oxides, G/(G+H), in the digested residues are shown in **Table 6.3** and were determined by XRD patterns to identify the extent of the conversion. **Figure 6.3** shows the change of G/(G+H) as a function of digestion temperature. The holding time for the digestion is 30 minutes and the concentration of caustic soda (C) is 240g/L. Overall, increasing temperature benefits the transformation of Al-goethite to hematite as expected (JCB-WRP, JCB-ASI and JCB-PAT), particularly in JCB-PAT with complete conversion and a 30% reduction of goethite in JCB-WRP at 280 ℃. However, transformation of goethite in JCB-270 and JCB-BTM are considerably lower with nearly no change in G/(G+H) at elevated temperatures even up to 280 ℃. Overall, there is a positive effect of increasing temperature on the transformation and this is consistent with that of the pure goethite digestion although the digestion temperature (250-280 ℃) is apparently higher than that (230-250 ℃) for pure goethite.

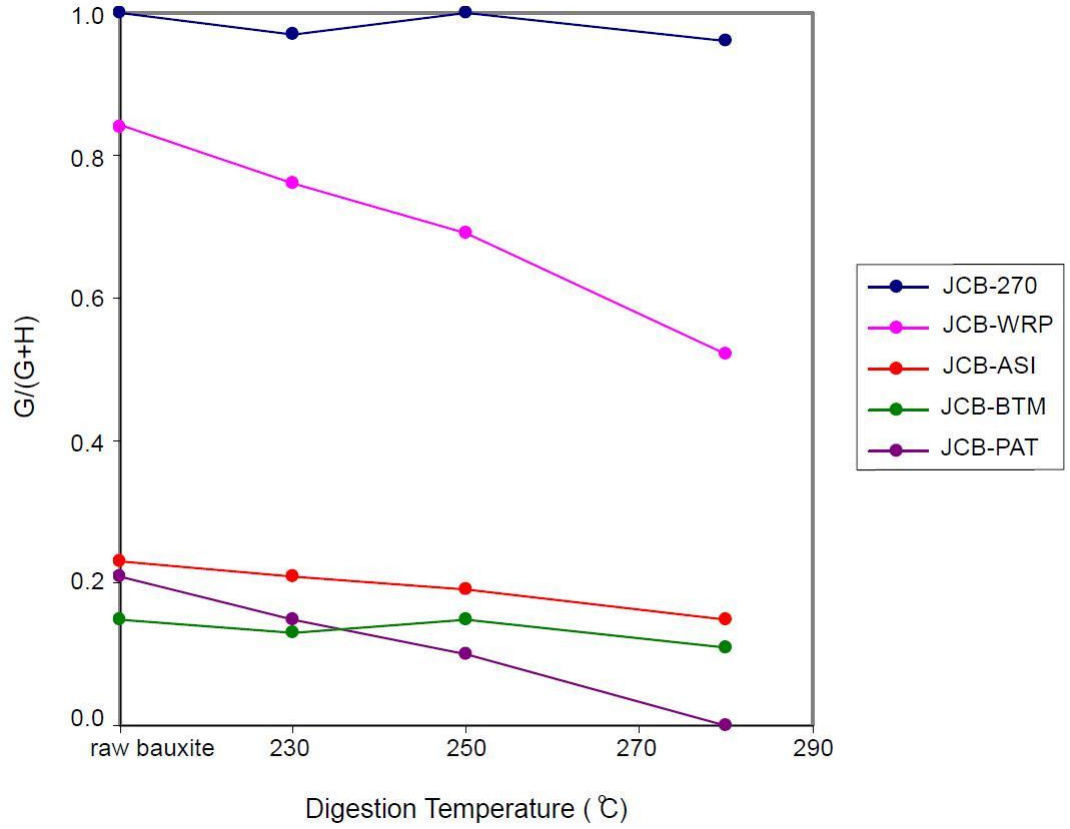

Figure 6.3 Hydrothermal transformation of Al-goethite to hematite in Jamaican bauxites in the Bayer digestion process at digestion temperatures 230 ℃, 250 ℃ and 280 ℃. Caustic soda concentration C = 240 g/L, holding time = 30 minutes.

6.3.2 Effect of anatase and lime

According to the results observed in Chapter 5, increase in digestion temperature can greatly enhance the transformation of goethite to hematite. However, such enhancement is not obvious in the three pre-treated bauxites, namely JCB-270, JCB-BTM and JCB-ASI (as described above). For these samples, temperature appears to become a less significant factor with respect to goethite transformation. Apparently, different natural goethite samples respond to temperature increases differently. Since the main difference between goethite samples are their impurity levels, finding the relationship between the transformation rate of goethite and the amount of impurities contained in goethite samples (mainly anatase and lime) becomes one of the major tasks in this study. For the temperature-insensitive samples (e.g. JCB-270), it is not the temperature itself that loses its role in the goethite-to-hematite transformation, but the 'impurities' contained within these samples that are causing the problem. This is supported by the XRD analysis of

the digested bauxite residues as shown in **Figure 6.4**. The pre-treated bauxite samples were digested in caustic soda (C=240 g/L) at 280 ℃ for 30 minutes. A broad XRD reflection at 8.1-8.3 Å appears only in three samples, JCB-270, JCB-BTM and JCB-ASI, which are the samples that are barely respond to the increasing digestion temperature. The reflection at 8.1-8.3 Å in those three samples belongs to sodium titanate. Practically, it is difficult to identify sodium titanate (e.g. Na_2TiO_3) in XRD patterns due to its lack of crystallinity. Apart from consuming caustic soda, sodium titanate has also been long believed to inhibit the transformation of goethite to hematite (Malts, 1991; Croker *et al.*, 2009; Xu *et al.*, 2010).

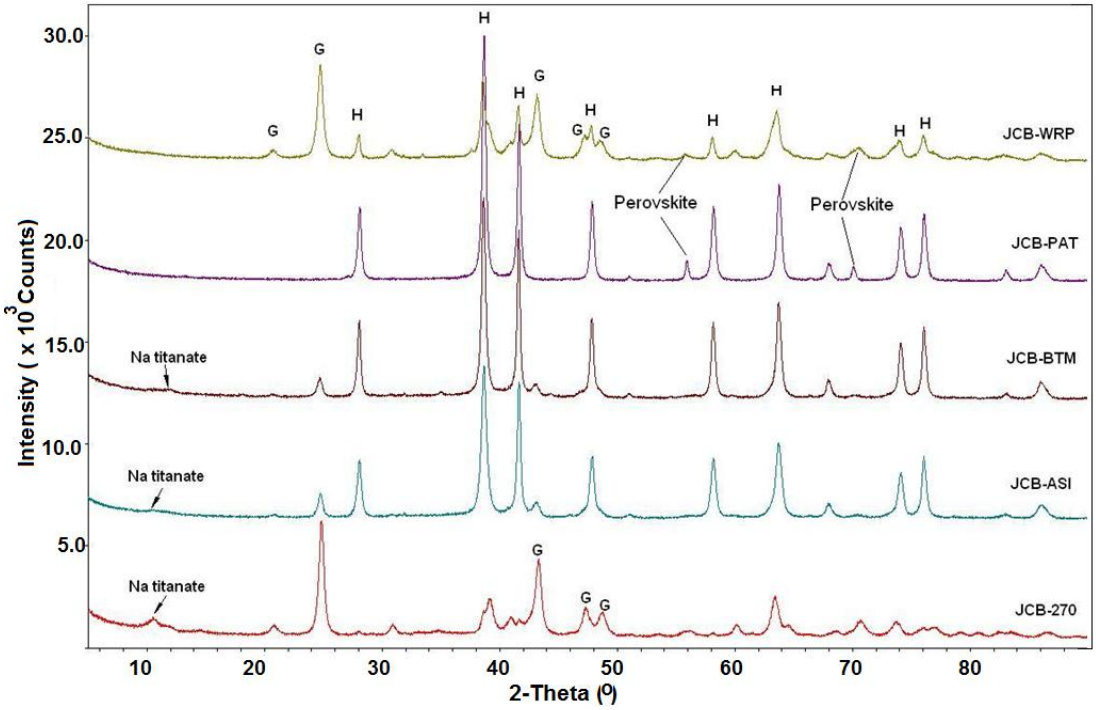

Figure 6.4 XRD patterns for digested Jamaican bauxite samples at 280 ℃ for 30 minutes. Sodium titanate peaks appear in three samples, JCB-BTM, JCB ASI and JCB-270, which are the three samples not responding to the elevated digestion temperature.

To investigate the formation of the sodium titanate, the XRF analysis for the pre-treated bauxites was carefully studied. It is shown in **Table 6.4** that all the selected Jamaican bauxites used in the study contain similar level of anatase (TiO_2). Therefore, the formation of the sodium titanate is more likely attributed to the reaction of anatase with caustic soda at high temperatures (>230 ℃) in the Bayer digestion. Sodium titanate is an umbrella term for a various forms of minerals in the Na-Ti-O system. It has been

widely reported that sodium titanate is formed in the Bayer digestion step following different digestion conditions (Croker *et al.*, 2006). Nevertheless, the adsorption or coating of sodium titanate (regardless of its forms) on the surface of goethite and boehmite results in a low alumina extraction and poor mud settling with problematic scaling formation (Malts, 1991; Xu *et al.*, 2010).

Table 6.4 Minerals and components in the selected Jamaican bauxites

Sample	Main compositions, % (XRF)						Minerals[2]	G/(G+H)[3]
	Al_2O_3	av. Al_2O_3 [1]	Fe_2O_3	SiO_2	TiO_2	CaO		
JCB-PAT	49.7	46.3	17.5	0.8	2.11	0.31	Gi,Bo,He,Go,An,Ka	0.21
JCB-ASI	49.5	44.1	18.2	1.12	2.27	0.04	Gi,He,Go,An,Ka	0.23
JCB-270	49.8	41.3	17.4	0.12	2.48	0.07	Gi,Bo,Go,An	1.00
JCB-WRP	47.9	42.4	18.9	0.56	2.65	0.24	Gi,Bo,Go,He,An,Ka	0.84
JCB-BTM	50.9	49.1	17.3	0.28	2.25	0.03	Gi,Go,He,An,Ka	0.15

Note:

1. The analysis of available Al_2O_3: 1g of sample was digested in 20g of 80 g/L caustic soda at 80~90 ℃ for 2 hours. The digested solution was titrated to calculate the available Al_2O_3.
2. Gi: gibbsite, Bo: boehmite, He: Hematite, Go: goethite, An: anatase, Ka: kaolinite.
3. G/(G+H): Calculated from XRD results.

It is interesting to notice that sodium titanate did not form in two of the five samples (JCB-WRP and JCB-PAT). In these samples, the titanium-containing mineral formed in the digestion residues is perovskite, a type of calcium titanate ($CaTiO_3$). The Bragg reflections at 1.91Å and 1.55Å specific for perovskite are clearly shown in the XRD patterns instead of sodium titanate's characteristic peaks at 8.1-8.3 Å (shown in **Figure 6.3**). Both perovskite and sodium titanate are titanium minerals formed during bauxite digestion, but their effects on the goethite → hematite transformation are distinctly different. Perovskite, unlike sodium titanate, has little detrimental effect on the transformation of goethite to hematite during high temperature Bayer digestion. This is in contrast to the readily observed thin titanate coating that impedes goethite's reactivity (Wohlfarth and Buschow, 1980). The XRF results for the bauxites in **Table 6.4** also indicate that the content of lime (CaO) in JCB-PAT and JCB-WRP is relatively higher with 0.31% in JCB-PAT and 0.24 % in JCB-WRP while less than the CaO level of 0.07% in the other three bauxites, in which no perovskite was produced during the digestion. Numerous studies have suggested that the presence of lime in bauxites is beneficial to the Bayer process (Croker *et al.*, 2009). In the course of perovskite

formation, anatase preferentially reacts with CaO to form $CaTiO_3$ and consequently avoids the reaction between anatase and Na_2O to form sodium titanate (Xu *et al.*, 2010). This formation of perovskite in the presence of lime has also been reported in the literature (Croker *et al.*, 2009).

The beneficial effect of lime on goethite conversion was further investigated by purposely adding CaO to the digestion system. An extra 3 wt. % CaO was added into the JCB-270 and then the mixture was digested at 250 ºC for 30min. The G/(G+H) shown in **Table 6.3** dramatically dropped by nearly 90% from 1.00 without CaO to 0.12 with CaO. The titanium mineral in the digestion residue of JCB-270 was sodium titanate, however it becomes perovskite once CaO is added. This is proven by the XRD patterns shown in **Figure 6.5**. These XRD patterns also demonstrate that perovskite does not form without an adequate amount of CaO in the bauxite, leading to a sodium titanate coated goethite surface (marked in **Figure 6.5**).

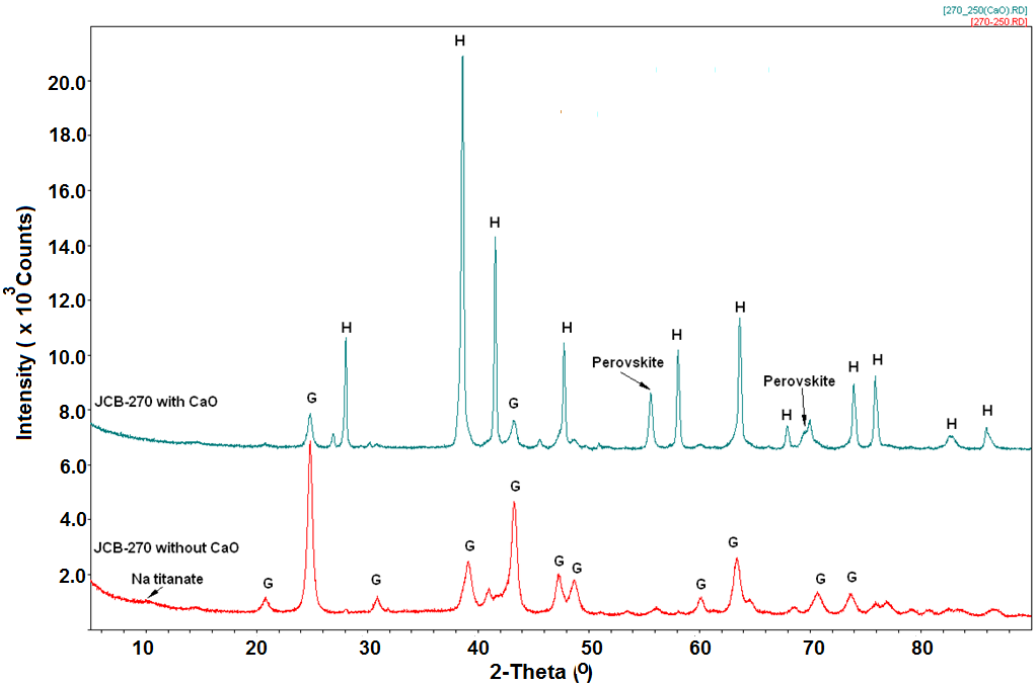

Figure 6.5 XRD patterns for JCB-270 digested at 250 ℃ for 30mins with (top) and without CaO (bottom).

In summary, the formation of sodium aluminate or perovskite during the high temperature digestion can be described as follows:

1. Sodium titanate, formed by interaction between caustic soda and anatase is an inhibitor to the transformation of goethite to hematite in high temperature digestion (≥230°C) by coating or producing a film on the goethite surface.

2. Perovskite ($CaTiO_3$), which is produced through the reaction of lime (CaO) and anatase (TiO_2) in the caustic solution, is favoured in the Bayer process. More importantly, the consumption of TiO_2 in bauxites to form perovskite is likely to avoid the formation of sodium titanate and therefore eliminate the negative effects caused by sodium titanate.

3. The selectivity of formation either sodium titanate or perovskite greatly relies on the composition of the bauxites used in the digestion. Sodium titanate is formed if CaO is absent or present in only trace amounts, while perovskite is preferentially generated if sufficient amount of CaO is present in the bauxite.

Experimental results suggest that the process described above is independent of the A/C ratio used in a Bayer liquor.

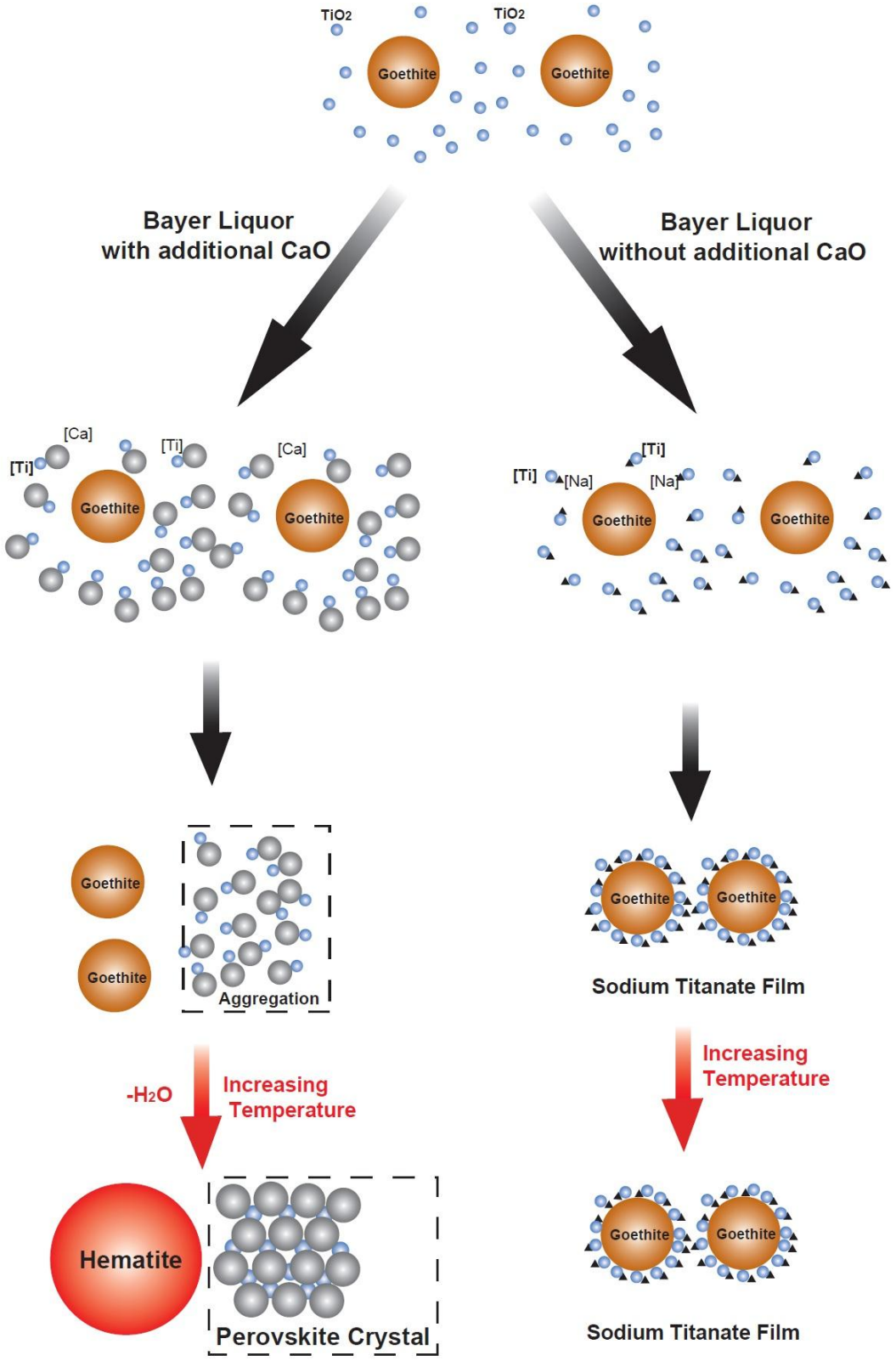

Figure 6.6 The schematic diagram for the effects of anatase (TiO_2) and lime (CaO) on the transformation of goethite to hematite in the Bayer process.

According to the above analysis, a schematic diagram for the formation of perovskite ($CaTiO_3$) and sodium titanate and their effects on the transformation of goethite to hematite is proposed in **Figure 6.6**. In Bayer liquor, the dissolved TiO_2 exists in the form of sodium titanate and is preferentially absorbed onto goethite particles. The surfaces of goethite in a caustic digestion condition are covered by abundant defects of high energy states, which absorb sodium titanate to reduce overall surface tensions. This conforms to the classic physical chemistry model of 'surface tension reduction' (Hu *et al.*, 1999). The absorbed sodium titanate, therefore, covers the goethite surfaces, forming a film that acts as a barrier to stop further contact of the inner core of goethite with the caustic solution. This mechanism explains the reason why the sodium titanate coated goethite is relatively unresponsive to temperature increases and not converting to hematite, despite that fact that hematite is thermodynamically more stable than goethite.

It is a totally different scenario when CaO is added to the Bayer liquor. The reaction between CaO and anatase subsequently produces perovskite crystals. This is evident via XRD diffraction in all titanium containing samples with added CaO. The detrimental sodium titanate is therefore, removed by forming a new mineral (namely perovskite) with CaO. Without the interference of sodium titanate film on the surface of goethite particles, the transformation from goethite to hematite occurs more or less as predicated by the common law of thermodynamics (see **Figure 6.6**).

6.3.3 Effect of alumina content

Alumina present in the system has been identified as an inhibitor to the hydrothermal transformation of synthetic goethite to hematite under the Bayer digestion conditions in the previous discussion in Chapter 5. In order to investigate the effect of alumina on the transformation of goethite to hematite in natural bauxite digestion, the pre-treated bauxites, JCB-270 and JCB-ASI were selected to conduct a digestion test with pure caustic soda and sodium aluminate solution. JCB-270 and JCB-ASI were selected for in-depth investigations, as they represent the two distinct groups of Jamaican bauxites (shown in **Table 6.5**). JCB-270 represents the group of goethite-rich bauxites containing both gibbsite and boehmite, whereas JCB-ASI represents the group with low goethite content and containing only gibbsite type of alumina. .

Table 6.5 Selected bauxites used in the investigation into impact of alumina and relevant bauxites that they represent separately

Selected Bauxite	G/(G+H)	Represented bauxites	Type of alumina	Represented bauxites
JCB-270	1.00	**High goethite content (>0.70)**, including JCB-090, 218 and BST	Gibbsite, boehmite	JCB-090, 218, BST, BLM, GPM, PAT, RBM and HAM
JCB-ASI	0.23	**Low goethite content (<0.30)**, including JCB-BLM, GPM, PAT, BTM, RBM and HAM	Gibbsite	JCB-BTM and ASI

The alumina content present in the bauxite appears to retard the goethite to hematite conversion regardless of the feeding material in digestion being synthetic pure goethite or naturally occurring goethite in bauxites (data relating to synthetic goethite refer to Chapter 5). However, to what extent this retardation will manifest depends on whether or not a pure goethite is used. For a given sample, a change in the extent of goethite to hematite conversion leads to a corresponding change in its G/ (G+H) value (see **Table 6.3**). It is apparent that the reduction in goethite to hematite conversion in natural bauxite digestion is much less prominent than that observed during the synthetic goethite digestion. This phenomenon translates to a more or less unchanged G/(G+H) value in the bauxite samples (JBC-270 and JBC-ASI) throughout the digestion using either pure caustic soda liquors or a typical Bayer liquor with A/C of 0.56. In pure caustic soda digested residue of JBC-270, the G/(G+H) is a constant value of 1.0 before and after digestion. Although the G/(G+H) value slightly reduces to 0.98 when JBC-270 is digested in sodium aluminate, such change is not significant. The G/(G+H) of JBC-ASI digested in pure caustic soda decreases from 0.23 to 0.19. This is consistent with a small degree of goethite to hematite transforms. JBC-ASI digested in the sodium aluminate solution gives a G/(G+H) value of 0.22. This value is only marginally reduced from the G/(G+H) value of 0.23 in the undigested JBC-ASI.

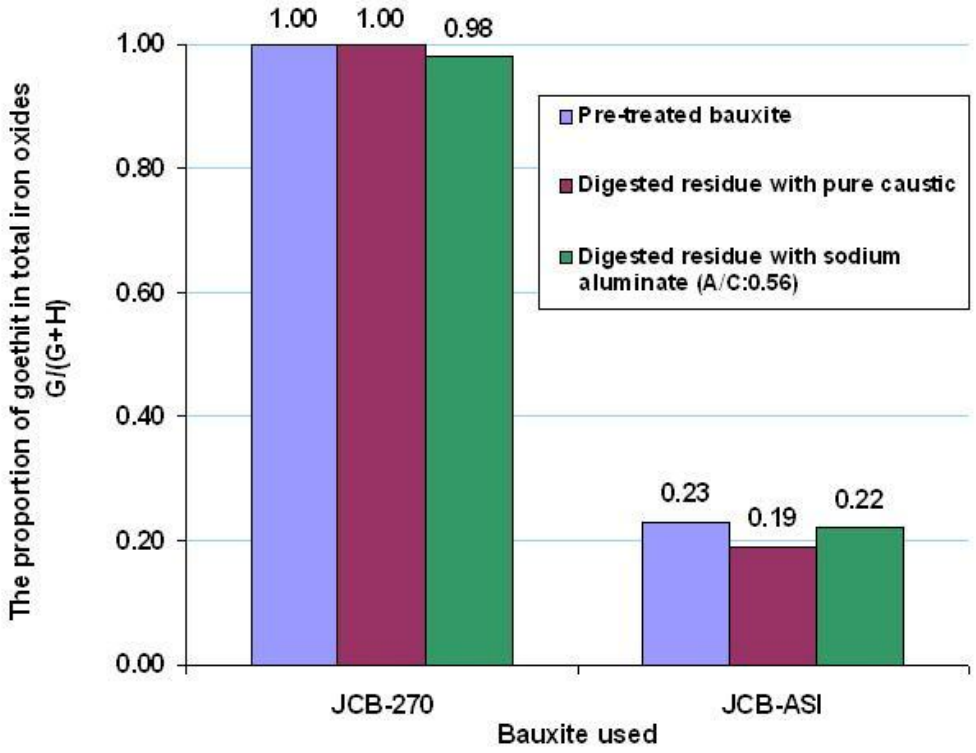

Figure 6.7 Effect of alumina content to the goethite transformation in natural bauxite (pre-treated with caustic to remove gibbsite) with different digestion solutions. Temperature of digestion: 250 ^{o}C; holding time: 30 minutes.

It is evident that the pre-treated JCB-ASI is more sensitive to the alumina level in the digestion liquor than the pre-treated JCB-270. This discrepancy is caused by the different aluminous mineral contents in these two samples. The untreated JBC-ASI contains gibbsite, whereas JCB-270 contains both gibbsite and boehmite. On completion of the 'pre-treatment', JCB-ASI is more or less free of alumina. In sample JCB-270, however, the boehmite is not removed under the mild condition of 'pre-treatment'. Therefore, the pre-treated JCB-270 is still capable of releasing alumina (from boehmite) to the digestion liquor, as opposed to the pre-treated JCB-ASI. Thus, boehmite-containing bauxite, JCB-270, is no longer sensitive to alumina content in digestion solution and the goethite conversion is naturally inhibited even with pure caustic soda digestion (experimental evidence see G/(G+H) values in **Table 6.3**).

In theory, alumina's retardation effects on goethite → hematite conversion still exist in natural bauxites. However, alumina level in digestion liquors is rarely considered as a factor that influences the rate of hematite formation in a commercial Bayer plant. As explained in Chapter 5, even a small amount of alumina in the digestion liquor will

significantly reduce the pure goethite to hematite transformation. In a Bayer plant, it is impossible to have alumina free digestion liquors. Even if a pure caustic soda is used the gibbsite and/or boehmite in bauxite ores will readily release alumina to the liquor as soon as the digestion process begins. The alumina level is especially high in saturated digestion liquors. Therefore, whether or not a pure caustic soda is used to digest natural bauxite makes little difference in the goethite → hematite conversion.

6.4 Hydrothermal transformation of Al-goethite in raw Jamaican bauxite

The effects of the impurities in Jamaican bauxites such as lime and anatase, and the digestion conditions on Al-goethite to hematite transformation were examined. The results have been discussed. However, those conclusions have been reached under the condition that gibbsite in the bauxites was pre-removed prior to the digestion. Thus, the concern has been raised as to whether the conclusion can be also applied to the raw bauxites without the prerequisite for gibbsite removal. In this part, the digestion of selected raw Jamaican bauxite has been studied under desired conditions obtained with the pre-treated bauxites. It aims to verify the applicability of the conclusions made in the previous research to raw bauxites. In addition, it further optimizes the reaction conditions and additives which tend to enhance the hydrothermal transformation of Al-goethite to hematite and thus improve the alumina recovery from the transformation.

6.4.1 Selection of the Jamaican bauxites, the digestion conditions and the additives

Selection of the Jamaican bauxite: The raw Jamaican bauxite, JCB-270, was investigated to understand its digestion behaviour, transformation performance of goethite to hematite, and the quantitative relationship between the extent of transformation and the concentration of calcium-containing compounds in bauxites. Careful consideration has been given regarding the selection of JCB-270. Firstly, goethite is the only iron oxide present eliminating any interference from hematite seeding. In other words, the outcome from the research will be more likely to be practically applicable to bauxites with or without hematite. Secondly, the alumina content in JCB-270 comprises both gibbsite and boehmite, which means that the

complication of various alumina species can be investigated. Lastly, it would be much easier to observe the transformation of goethite to hematite in terms of change of morphology given that goethite is the only iron oxide in the bauxite.

15 g natural bauxite sample in a 150 ml Bayer liquor gives a mixture consisting of 100 g/L natural bauxite with a 18% goethite content. This is consistent with the previous operation using pure synthetic goethite (160 g/L charge of bauxite containing 10% goethite) and the gibbsite-removed bauxite (35 g/L charge of gibbsite-removed bauxite containing 50% goethite).

Selection of digestion conditions: The digestion conditions used in this study fall in the typical range recommended for digesting boehmite-containing bauxite. In terms of digestion temperature, **Table 6.6** lists the reference ranges for bauxite digestion, goethite transformation and the temperature chosen in this study. 250 ℃ was chosen as the digestion temperature since this is characteristic both of boehmite digestion and goethite to hematite transformation.

Table 6.6 List of temperature ranges for bauxite digestion, goethite transformation and chosen temperature in this study

	Digestion		Goethite transformation		Temperature used in the study (boehmite bauxite)
	Gibbsite-bauxite	Boehmite-bauxite	Goethite	Al-goethite	
Temperature	145-155 ºC[1]	220-270 ºC[1]	225-275 ºC[2]	230-320 ºC[3]	250ºC

Note:
1. (Hudson, 1987; Whittington, 1996; Smith, 2009)
2. (Crombie *et al.*, 1973; Brown and Tremblay, 1974; Li, 2001; Murray *et al.*, 2009)
3. (Suss and Maltz, 1992)

Different digestion holding times, including 30, 60 and 120 mins, have been investigated to establish the relationship between the Al-goethite → hematite transformation performance in the natural bauxite and the overall digestion time.

A Bayer liquor with A/C ratio of 0.29-0.56 and pure caustic soda were used in the investigation. Pure caustic soda and the Bayer liquor with lower A/C ratio (~0.3) were prepared in the main laboratory with the procedure described in Chapter 3. For the Bayer liquor with higher A/C ratios, commercial concentrated Bayer liquor was used to make up the solution with desired A/C ratio. More details of this procedure are given in Chapter 3.

Selection of Additives: It has been shown that adding calcium oxide in the digestion system greatly improves the extent of goethite to hematite transformation in pre-treated bauxite. As anatase is also in the natural bauxite, calcium treated as an enhancement factor to the Al-goethite transformation is also investigated.

In natural bauxite, the existence of gibbsite may complicate calcium oxide's role in promoting goethite to hematite transformation. In such cases, a number of calcium-additives should be adopted to compare their effects on the goethite to hematite transformation process. For example, either calcium hydroxide [$Ca(OH)_2$] or calcium carbonate [$CaCO_3$] is an alternative to CaO.

6.4.2 Hydrothermal transformation of Al-goethite during the digestion of natural raw bauxites

The tests for digestion of natural bauxite JCB-270 were first conducted in Bayer liquor at 250 ºC for different holding times, 30, 60 and 120 minutes without any additives. As seen in **Table 6.7**, the proportion of goethite to the total iron oxides stays unchanged at 1.00 which suggests that there is no Al-goethite transformed to hematite under the conditions even with longer holding times stretching to 120 minutes. This is to be expected from the results in **Figure 6.3**. The broad reflection peak at ~8.3 nm of sodium titanate has been detected in the XRD patterns of digested natural bauxite JCB-270 residue. The formation of sodium aluminate significantly prevents Al-goethite from transforming to hematite via the generation of an amorphous film-like layer on the surface of Al-goethite.

It has been suggested in the digestion of gibbsite-removed bauxite that lime (CaO) as an additive to the digestion effectively improves the Al-goethite to hematite conversion by almost 90% through the formation of perovskite ($CaTiO_3$).

Table 6.7 The transformation of Al-goethite in the natural bauxite JCB-270 during digestion at 250 ºC with different calcium-containing additives. The Bayer liquor: A/C = 0.30, C = 240 g/L, digestion temperature: 250 ºC.

Additive	**Reaction Conditions**		**G/(G+H)**
	Temperature/ ℃	**Time/ mins**	
Nil	250	0	1.00
	250	30	1.00
	250	60	1.00
	250	120	1.00
CaO (2%)	250	0	1.00
	250	30	0.94
	250	60	0.92
	250	120	0.82
$Ca(OH)_2$ (equ. 2% CaO)	250	0	1.00
	250	30	0.96
	250	60	0.96
	250	120	0.91
$CaCO_3$ (equ. 2% CaO)	250	0	1.00
	250	30	1.00
	250	60	0.93
	250	120	0.94

Lime (at 2 wt. % in various forms) was added to the digestion of JCB-270. As expected, the transformation of Al-goethite to hematite has been enhanced. This is reflected by the change of G/(G+H) from 1.00 to 0.94 in 30 minutes of digestion, further reduced to 0.92 in 60 minutes, and then 0.82 in 2 hours. This enhancement observed in the gibbsitic bauxite digestion are relatively modest compared to that observed in the digestion of gibbsite-removed bauxite in **Table 6.3**. The only difference between these two types of digestions is that the former uses gibbsite containing head feed, whereas the later uses gibbsite free head feed. Therefore, the very existence of gibbsite in the digestion feed may be the cause for the ineffectiveness of CaO in promoting the goethite → hematite conversion. In the previous digestion of gibbsite-removed bauxite the extent of goethite → hematite conversion reaches nearly 88% when lime is added, compared to the 2% conversion rate without lime addition (data see **Table 6.3**). This is in contrast to the rather mild increase in goethite → hematite conversion when gibbsitic bauxite is used. In the gibbsitic bauxite digestion residue, the goethite → hematite conversion was observed to be 18%, compared to 0% without lime addition.

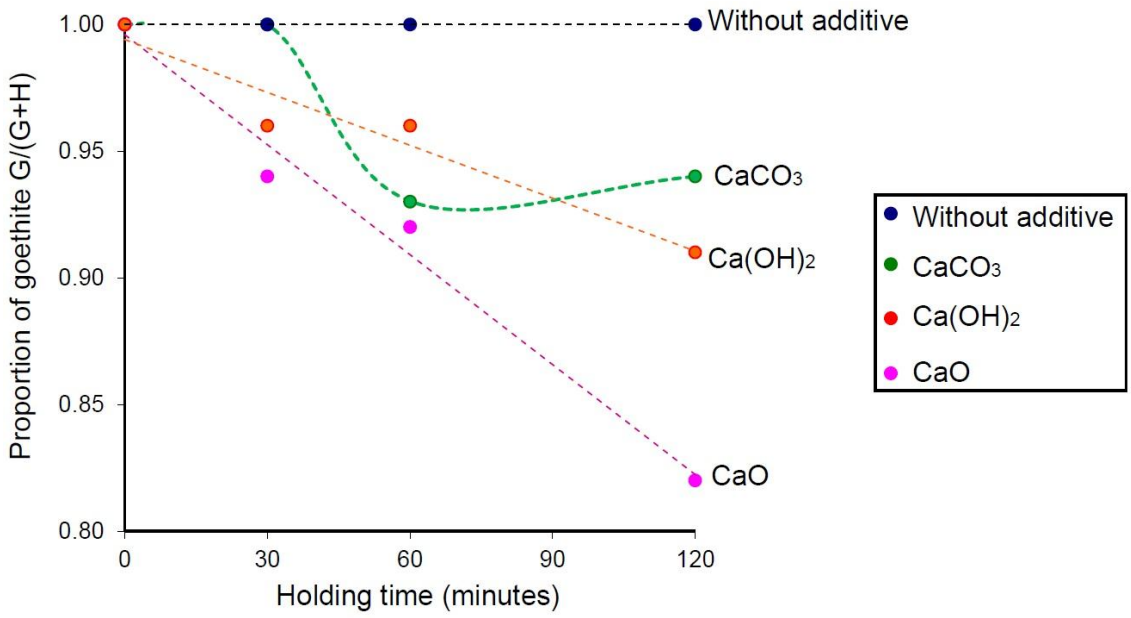

Figure 6.8 The comparison of G/(G+H) against digestion time in the digested JCB-270 residue with various calcium-containing additives. The straight dash lines are linear fits using Least Square Method; however, a linear fit for the data from digestion with $CaCO_3$ is not available.

Additional calcium-containing additives, calcium carbonate $CaCO_3$ and calcium hydroxide $Ca(OH)_2$ have been also investigated to observe the effect on the transformation. **Figure 6.8** shows a comparison of G/(G+H) in the digested JCB-270 residues with these three additives added to the digestion. Key points from the figure can be concluded: 1) Transformation is encouraged by lime; 2) Lime type appears to be important; 3)Transformation is largely retarded in raw bauxite with maximum to ~10 % transformation even after 2-hour digestion compared to that in gibbsite-removed bauxite (~90% transformation).

This retardation is most likely to be attributed to the reaction with lime to perovskite competing with other reactions, e.g. TCA (tri-calcium aluminate hexahydrate, $Ca_3Al_2(OH)_{12}$). Croker et al. (Croker *et al.*, 2006; Croker *et al.*, 2009) reported calcium titanate formation, as a result of the reaction between TiO_2 and calcium compounds, preferentially occurs in the high temperature Bayer process. At lower temperature the formation of perovskite could be interfered by the competition of gibbsite in bauxite. It is more likely that the formation of the desirable calcium titanate, $CaTiO_3$, does not occur in the natural bauxite digestion with the addition of a calcium compound in the raw bauxite JCB-270 according to **Figure 6.8**.

6.4.2.1 The formation of TCA

In order to identify the process occurring during the high temperature digestion, XRD patterns for the digested residues with different calcium-containing additives at the same digestion conditions have been studied. A comparison of XRD patterns for raw and digested JCB-270 residues (without Ca additives, with CaO, $Ca(OH)_2$ and $CaCO_3$ respectively) at 250 ℃ in 30 minutes have been shown in **Figure 6.9**. Unexpectedly it is found that the typical broad reflection peak at d = ~8.3 nm for sodium titanate emerges in all four digested residues, which suggests that the added calcium compound does not react with anatase as expected, to form perovskite. Meanwhile, when comparing the residues with and without addition of calcium-containing compounds it is revealed that a new phase(s) is generated in those residues digested with CaO, $Ca(OH)_2$ and $CaCO_3$ (see **Figure 6.9**). The new phase belongs to tri-calcium aluminate hexahydrate which is normally referred to as TCA in the Bayer industry. Tri-calcium aluminate hexahydrate (TCA) has been widely used within the Bayer process, more specifically as a filter aid during green liquor clarification or as a desilicating agent during pre-desilication/digestion (Whittington, 1996; Whittington and Cardile, 1996). The formation of TCA in the Bayer process has also been frequently reported when lime is added to Bayer liquor (Suarez *et al.*, 1990; Perotta and Williams, 1995; Whittington, 1996).

With the formation of TCA during the digestion of natural bauxite in the Bayer liquor, it is understandable why the formation of the desirable perovskite hardly happens even with addition of lime. Lime and the other calcium-containing additives tend to react with sodium aluminate solution to form TCA which prevents the formation of perovskite by consuming those calcium-containing additives. It is reported in a number of publications that the formation of TCA in Bayer digestion happens in a relatively mild environment with temperature ranging from 25 ℃ (Xu, 1991) to 100 ℃ (Whittington and Cardile, 1996) within very short period of time (2 to 30 minutes) (Perotta and Williams, 1995; Whittington and Cardile, 1996). On the other hand, the formation of perovskite requires extremely high temperature (~250 ℃) in the Bayer process. The addition of lime and the other calcium-containing additives favours the formation of TCA within a short time. In such cases, the calcium compound is consumed by the formation of TCA even prior to appropriate temperature reached for formation of perovskite.

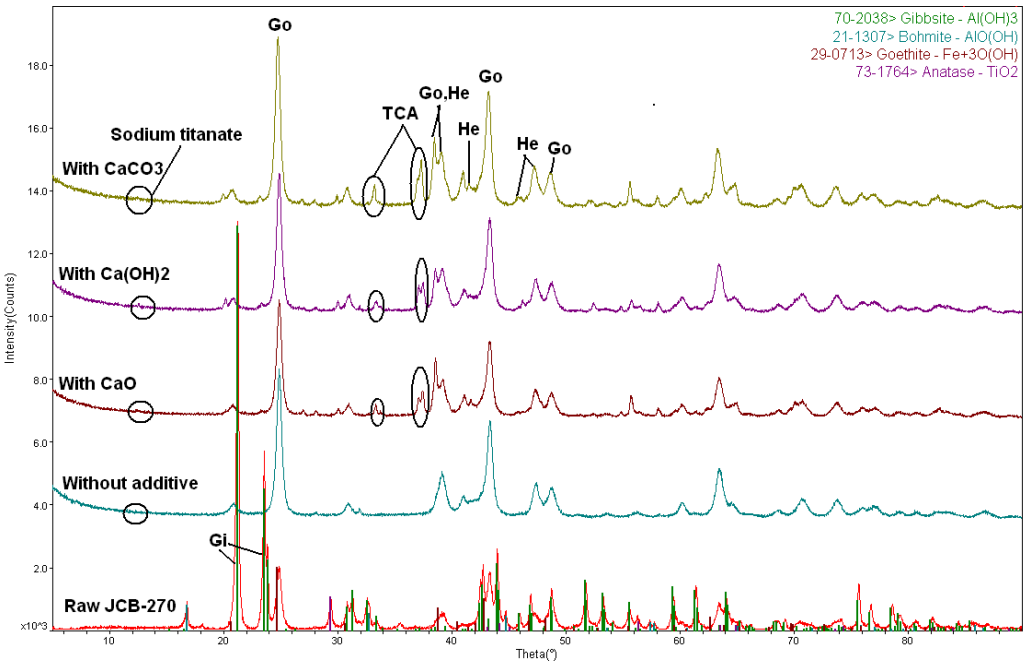

Figure 6.9 XRD patterns for raw JCB-270 and digested residues with different additives. The reaction conditions: C = 240 g/L; A/C = 0.3; digestion temperature: 250 ºC; time: 30 minutes. In the patterns, abbreviation 'Go' represents goethite, 'He' for hematite, 'Gi' for gibbsite. It should be noted that the remainder of the phases are marked by the coloured lines which can be referred to the top right for the corresponding minerals.

In the previous study for the gibbsite-removed bauxite digestion, the absence of gibbsite in the natural bauxite contributes to the occurrence of the reaction of lime and anatase at high temperature (250 ℃). Once gibbsite is present in natural bauxite, lime is more likely to form TCA with within minutes under an alkaline environment. A number of processes for the reactions between gibbsite and lime (or the other calcium-containing additives) in alkaline conditions have been reported (Xu, 1991; Perotta and Williams, 1995; Whittington and Cardile, 1996). The fundamental paths for the reactions can be described in the following formulas:

Formation of TCA via CaO:

$$3CaO + 2Al(OH)_3 + 3H_2O \rightarrow Ca_3Al_2(OH)_{12} \qquad \textbf{(6.1)}$$

Gibbsite TCA

Formation of TCA via $Ca(OH)_2$:

$$3Ca(OH)_2 + 2Al(OH)_3 \rightarrow Ca_3Al_2(OH)_{12} \quad \textbf{(6.2)}$$

Gibbsite TCA

$$3Ca(OH)_2 + 2AlOOH + 2H_2O \rightarrow Ca_3Al_2(OH)_{12} \quad \textbf{(6.3)}$$

Boehmite TCA

Formation of TCA via $CaCO_3$:

$$3CaCO_3 + 2Al(OH)_3 + 6OH^- \rightarrow Ca_3Al_2(OH)_{12} \quad \textbf{(6.4)}$$

Gibbsite TCA

It is obvious that the process of perovskite ($CaTiO_3$) formation at high digestion temperature ~250 ℃ has been interrupted by the formation of TCA at much lower temperature (<100 ℃) if lime or other calcium-containing compounds is initially added to raw bauxite. The improvement of Al-goethite transformation cannot be achieved without the formation of perovskite. In such cases, the adding point of lime or additives is more likely to play an important role in accelerating the transformation of Al-goethite to hematite.

6.4.2.2 Injection point tests

As discussed earlier, adding lime to a digestion process can promote the formation of perovskite through the reaction of lime with anatase. However, this does not occur when alumina is present in the liquor or from the bauxite resulting in the formation of TCA. This consumption occurs mostly during the early temperature-increasing stage of digestion. Therefore, the lime depleted digestion liquid will not be able to provide the CaO needed for perovskite formation. Since TCA forms at low temperatures, lime or calcium-containing additives, such as such as $Ca(OH)_2$ and $CaCO_3$ in this study, was added at digestion temperature to allow direct competition of Al and Ti for lime.

The autoclave digestion tests, to investigate the effect of the injection point of lime or other calcium-containing additives to the Al-goethite transformation during the digestion, have been conducted. The injection tests were designed to add the additives to the system only when the major digestion temperature zone has reached the desired temperature of 250 ℃. The formation of TCA at low temperatures tends to be accordingly avoided as a result of late injection of the additives. The detailed

description of the injection tests can be found in the Methodology part in this thesis. In comparison with the results from head feeding, the same calcium compounds as those for the previous study, CaO, $Ca(OH)_2$ and $CaCO_3$, have been used. The reaction conditions also remain the same as digestion temperature at 250 ℃ with holding time of 30 minutes as well as the same concentration for the Bayer liquor (C=240 g/L, A/C = 0.30). However, charge of the solution and the solids was scaled up to accommodate the volume capacity of the autoclave. The Bayer liquor was charged three times larger than that in the bomb digestion from 150 mL to 600 mL and the dosage of raw bauxite JCB-270 correspondingly increased from 15 g to 60 g. Lime equivalent to 2 wt. % of bauxite (equivalent 2 wt. % CaO in bauxite for calcium compounds) was added into the injector and pressure injected to the main reactor once the set temperature is reached. The collected slurry is then pressure filtered. Characterisations for both spent liquor and residues including XRD (see Figure 6.9), XRF and titration are carried out for further analyses.

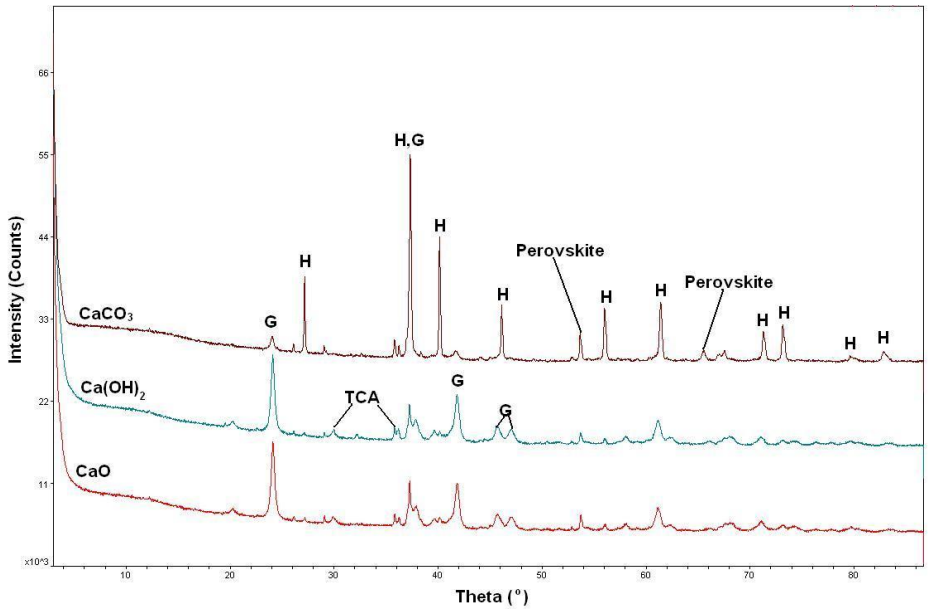

Figure 6.10 XRD patterns for the JCB-270 residues upon digestion in the presence of calcium compounds in the digestion zone. G: goethite; H: hematite; TCA: tri-calcium aluminate.

The XRD and XRF (**Figure 6.10** and **Table 6.8**) results demonstrate that introducing calcium in the head feed does not improve goethite to hematite conversion regardless of the type of calcium compounds used (namely $CaCO_3$, CaO, and $Ca(OH)_2$). Addition of CaO, or $Ca(OH)_2$, to the digestion zone at 250 ℃ did not prevent the formation of

sodium titanate or aid in the transformation of goethite to hematite. However, adding $CaCO_3$ when the temperature reaches 250 °C (instead of at room temperature with head feed of bauxite) shows almost complete conversion of goethite to hematite. A summary of the results are shown schematically in **Figure 6.11**.

Table 6.8 Products observed upon digestion of bauxite JCB-270

	Injection point	Dominant iron oxide	G/(G+H)	Al substitution	TiO_2 products	CaO products
No additive	-	Goethite	1.00	24	Sodium titanate	-
2% CaO	Head feed	Goethite	0.94	24	Sodium titanate	TCA
	Digestion zone	Goethite	0.94	24	Sodium titanate	TCA
$Ca(OH)_2$	Head feed	Goethite	0.96	25	Sodium titanate	TCA
	Digestion zone	Goethite	0.95	24	Sodium titanate	TCA
$CaCO_3$	Head feed	Goethite	1.00	25	Sodium titanate	TCA
	Digestion zone	Hematite	0.10	6 (hematite)	Perovskite, trace TCA	

*Charge of $Ca(OH)_2$ or $CaCO_3$ is equivalent to 2% CaO in bauxite.
**The digestion temperature is 250 ℃, holding time 30 minutes.

The goal is to produce the desirable titanium residue perovskite, as the alternative titanium digestion product, sodium titanate is detrimental to the goethite to hematite conversion. The experimental results show that $CaCO_3$ preferentially reacts with TiO_2 at 250^{o}C, whereas CaO and $Ca(OH)_2$ preferentially react with sodium aluminate (**Figure 6.10** and **Table 6.8**) . Adding $CaCO_3$ at 250 °C not only converts most Al-goethite to Al-hematite, it also promotes the release of extra alumina into the Bayer liquor. The preference for reaction to TCA or perovskite is dependent on thermodynamics and kinetics. By adding $CaCO_3$ at 250 °C in lieu of CaO and $Ca(OH)_2$ at the same temperature, the desired digestion residues (perovskite and hematite) can be achieved. This is likely attributed to the dissolution of $CaCO_3$ in slow giving Ca^{2+} the opportunity to compete for either titanium in solution or alumina.

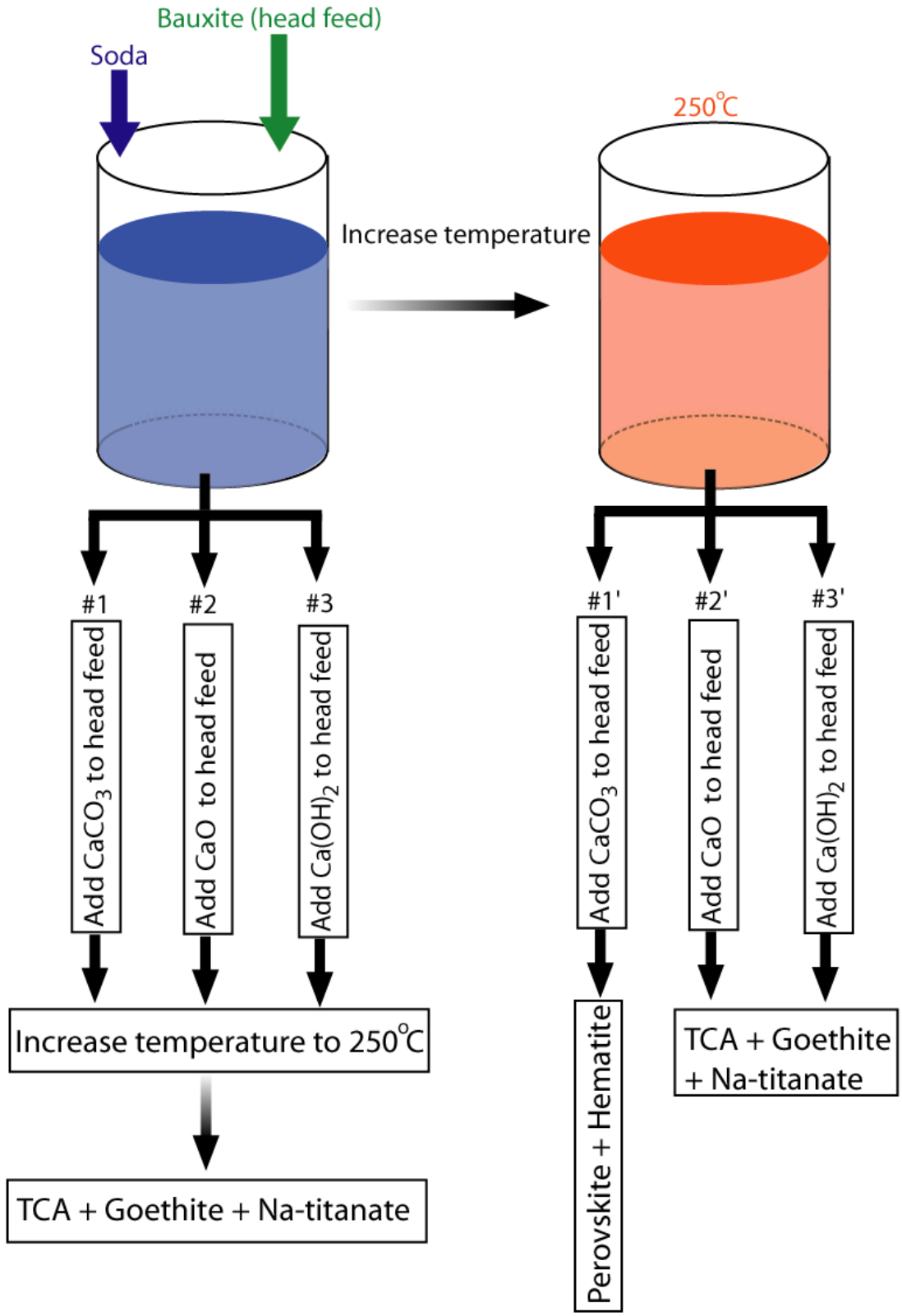

Figure 6.11 Digestion of bauxite JBC-270 with different schemes of calcium introduction. In schemes #1-3, calcium was added to the head feed as $CaCO_3$, CaO, and $Ca(OH)_2$ respectively. In schemes # 1'-3', these calcium compounds were added at 250 °C. For simplicity, only the Ca, Al, and Ti containing digestion residues are shown in this diagram.

References

Brown, N. & Tremblay, R. J. (1974) Some studies of the mineral transformations during high temperature digestion of Jamaican bauxite. *Light Metals,* 3**,** 825 - 844.

Connop, W. L. (1996) A new procedure for the determination of alumina caustic and carbonate in Bayer liquors. *Fourth International Alumina Quality Workshop,* Darwin, Austrlia. 321-330.

Cornell, R. M. & Schwertmann, U. (2003) *The Iron Oxides: Structure, Properties, Reactions, Occurrences and Uses,* Weinheim:Wiley-VCH.

Croker, D., Loan, M. & Hodnett, K. (2006) Sodium titanate formation in high temperature Bayer digestion. *TRAVAUX,* 33**,** 154-165.

Croker, D., Loan, M. & Hodnett, B. K. (2009) Kinetics and mechanisms of the hydrothermal crystallization of calcium titanate species *Crystal Growth and Design,* 9**,** 2207-2213.

Crombie, T., Davis, M. & Laurie, J. E. 1973. *Method of digesting bauxite via the Bayer process with the addition of reducing agents*. United States patent application 346736.

Dudek, K., Jones, F., Radomirovic, T. & Smith, P. (2009) The effect of anatase, rutile and sodium titanate on the dissolution of boehmite and gibbsite at 90 ^{o}C. *International Journal of Mineral Processing,* 93**,** 135-140.

Hind, A. R., Bhargava, S. K. & Grocott, S. C. (1999) The surface chemistry of Bayer process solids: a review. *Colloids and Surfaces A: Physicochemical and Engineering Aspects,* 146**,** 359-374.

Hudson, L. K. (1987) Alumina Production. *In:* BURKIN, A. R. (ed.) *Production of Aluminium and Alumina.* Chichester: John Wiley and Sons.

Klug, H. P. & Alexander, L. E. (1974) *X-ray Diffraction Precedures for Polycrystalline and Amorphous Materials,* New York, Wiley.

Li, L. Y. (2001) A study of iron mineral transformation to reduce red mud tailings. *Waste Management,* 21**,** 525-534.

Lide, D. R. (2010) *CRC handbook of chemistry and physics: a ready-reference book of chemical and physical data,* Colorado, CRC Press.

Malts, N. S. (1991) Efficiency of lime use in Bayer alumina production. *Light Metals***,** 257-262.

Murray, J., Kirwan, L., Loan, M. & Hodnett, B. K. (2009) In-situ synchrotron diffraction study of the hydrothermal transformation of goethite to hematite in sodium aluminate solutions. *Hydrometallurgy,* 95**,** 239-246.

Perotta, A. J. & Williams, F. (1995) Hydrocalumite formation in Bayer liquor and its promotional effect on oxalate precipitation. *Light Metals***,** 77-87.

Schultze-Rhonof, E. & Winkhaus, G. (1972) On the chemistry of bauxite extraction I. Studies in the system Na_2O-CaO-Al_2O_3-TiO_2-H_2O at 100°C and atmospheric pressure. *Z. Anorg. Allg. Chem.,* 390**,** 97-103.

Schultze-Rhonof, E. (1973) On the chemistry of bauxite extraction II. Studies in the system Na_2O-CaO-Al_2O_3-TiO_2-H_2O between 100°C and 275°C. *Z. Anorg. Allg. Chem.,* 396**,** 303-307.

Schulze, D. G. (1984) The influence of aluminum on iron oxides. VIII. Unit cell dimensions of Al-substituted goethites and estimation of Al from them. *Clays and Clay Minerals,* 32**,** 36-44.

Schulze, D. G. & Schwertmann, U. (1984) The influence of aluminium on iron oxides. X. Properties of Al-substituted goethites. *Clay Minerals,* 19**,** 521-539.

Schwertmann, U. & Kampf, N. (1985) Properties of goethite and hematite in kaolinitic soils of Southern and Central Brazil. *Soil Science,* 139**,** 344-350.

Schwertmann, U. (1987) Goethite and hematite formation in the presence of clay minerals and gibbsite at 25°C. *Soil Science Society American Journal,* 52**,** 288-291.

Schwertmann, U. (1988) Some properties of soil and synthetic iron oxides. . *In:* STUCKI, J. W., GOODMAN, B. A. & SCHWERTMANN, U. (eds.) *Iron in soils and clay minerals.* Dordrecht: D. Peidel Publishing Company.

Schwertmann, U. & Carlson, L. (1994) Aluminum influence on iron oxides: XVII. Unit-cell parameters and aluminum substitution of natural goethites. *Soil Science Society of American Journal,* 58**,** 256-261.

Smith, P. (2009) The processing of high silica bauxites -- Review of existing and potential processes. *Hydrometallurgy,* 98**,** 162-176.

Stanjek, H. & Schwertmann, U. (1992) The influence of aluminum on iron oxides. Part XVI: hydroxyl and aluminum substitution in synthetic hematite. *Clays and Clay Minerals,* 40**,** 347-354.

Suarez, C. E., Sulpizi, E., Peleato, F. & Saraullo, A. (1990) Application of the philosophy of expert systems to red mud thickeners overflow quality monitoring. *Ligh Metals***,** 79-84.

Suss, A. G. & Maltz, N. S. (1992) Aluminium and chromium containing goethite: composition, properties, behaviour in soda aluminate liquors in presence of silicon, titanium and calcium conpounds. *Light Metals***,** 1343-1347.

Whittington, B. I. & Cardile, C. M. (1996) The chemistry of tricalcium aluminate hexahydrate relating to the Bayer industry. *International Journal of Mineral Processing,* 48**,** 21-38.

Wohlfarth, E. P. & Buschow, K. H. J. (1980) *Ferromagnetic materials: a handbook on the properties of magnetically ordered substances,* North Holland, Elsevier.

Xu, B. (1991) *Lime chemistry in the Bayer process.* Ph.D., Murdoch University.

Xu, B., Smith, P., Wingate, C. & Silva, L. D. (2010) The effect of anatase and lime on the transformation of sodalite to cancrite in Bayer digestion at 250C. *Light Metals***,** 81-86.

Zwingmann, N., Gilkes, R. J. & Swash, P. M. 2008. Iron oxyhydroxide characterisation and modification in bauxite: tools for predicting and improving Bayer performance. Perth: Minerals and Energy Research Institute of Western Australia.

Chapter 7
Alumina Recovery and Improved Settling Rate

The hydrothermal transformation of both synthetic goethite and aluminous goethite in natural bauxites in a Bayer digestion environment has been comprehensively investigated. The results have elucidated the digestion reactions, the effects of impurities ascertained, and improvement of transformation with additives. In addition, the reaction mechanisms and kinetics associated with goethite to hematite conversion have also been proposed. The Al-goethite to Al-hematite conversion has been achieved at digestion temperature of 250 ℃ in 30 minutes with the addition of $CaCO_3$ directly to the digestion zone. This promising outcome would greatly benefit the industrial practice in terms of eliminating the negative effects of Al-goethite to the Bayer circuit. However, the two key issues that this project intends to address still remain unclear at this stage: how much alumina can be recovered from Al-goethite and to what extent the settling rate of red mud has been improved as a result of the hydrothermal transformation of Al-goethite to hematite.

In this chapter, alumina recovery from aluminous goethite and enhancement of settling rate by hydrothermal transformation of Al-goethite in natural bauxite were investigated and the corresponding data have been analyzed to determine the positive outcomes from the project.

7.1 Alumina recovery

Table 7.1 shows the XRF results for the digested residues with/without additives under the same digestion conditions (Digestion temperature: 250 ℃, time: 30minutes, C: 240 g/L and A/C: 0.30). In order to ensure data reliability, duplicate XRF analyses on each digested JCB-270 sample (under various digestion conditions) have been undertaken.

As predicted, the contents of Al_2O_3 and Fe_2O_3 in all of the residues, except the residue with the addition of $CaCO_3$ in the digestion zone, are at very similar levels (11.7 ± 0.6 %). This is in agreement with the analyses obtained in the XRD results, that is, only trace amount of Al-goethite was transferred to Al-hematite. In addition, the Al substitution level stays unchanged at ~25 mol% for the Al-goethite. However, the

content of Al_2O_3 in the residue digested with the addition of $CaCO_3$ in the digestion zone dramatically decreases to a considerably low level of 2.99%. More importantly, the corresponding Al substitution in the hematite structure also reduces to 5-6 mol%. Hematite has less capacity to accommodate alumina in the structure than goethite, which would allow part of the alumina in the goethite to be released to the spent liquor. As a result, the alumina recovery tends to be increased by the Al-goethite to Al-hematite transformation.

Table 7.1XRF analyses for the digested JCB-270 residues with/without additives

Sample	Injection point	XRF Result							Al substitution
		SiO_2	Al_2O_3	CaO	Fe_2O_3	Na_2O	P_2O_5	TiO_2	
Units		%	%	%	%	%	%	%	mol %
no additive	-	0.48	12.3	0.29	61.3	1.47	0.37	8.77	24
2 % CaO	Head feed	0.37	11.1	6.47	56.4	1.42	2.1	8.11	24
	Digestion zone	0.37	11.4	6.23	56.4	1.29	2.3	8.15	24
$Ca(OH)_2$	Head feed	0.68	12.1	5.63	55.4	1.23	2.06	7.87	26
	Digestion zone	0.55	11.4	6.4	56.3	0.79	2.21	8.02	24
$CaCO_3$	Head feed	0.43	11.7	6.49	55.3	1.65	1.85	7.77	25
	Digestion zone	0.15	2.99	8.84	68.4	0.48	3.12	10.16	6

*The charge of the $Ca(OH)_2$ or $CaCO_3$ is equivalent to the 2% CaO in the bauxite.
** The digestion temperature: 250 ℃, time: 30minutes, C: 240 g/L and A/C: 0.30.

The enhancement of the alumina recovery can also be evaluated by the percentage of alumina extracted from the bauxite. **Figure 7.1** shows the percentage of alumina extracted from bauxite JCB-270 by the different digestion processes. The alumina extracted can be calculated by the following equation:

$$\%\ Al_2O_3\ \text{extracted} = \frac{Al_2O_3\_in\_bauxite - Al_2O_3\_in\_digested\_residue}{Al_2O_3\_in\_bauxite} \times 100\% \qquad \textbf{(7.1)}$$

where Al_2O_3 in bauxite (refer to Appendix C) and Al_2O_3 in digested residue (listed in **Figure 7.1**) are the corresponding analytical results from XRF analyses.

A near completion of conversion of Al-goethite to hematite has been achieved by directly adding $CaCO_3$ to the digestion zone at 250 ℃. The figure apparently shows that the alumina extracted from the bauxite fluctuates between 75.3% and 77.7% but the only substantial increase of alumina recovery to 94.0% occurs in the digestion with adding $CaCO_3$ directly to the digestion zone. This is due to the near complete transformation of Al-goethite to Al-hematite which releases most of the alumina in the goethite to the spent liquor. The improvement of alumina recovery by adding the calcium-containing additive was also reported by Solymar et al. (1992) and Suss et al. (Suss and Maltz, 1992; Suss *et al.*, 2010). The outcome from Solymar et al. (1992) recorded a similar 92% alumina reversion during digestion of the Weipa/Bokéor Jamaican bauxites in the presence of lime. However, no details are provided as to the composition of Bayer liquor, the form of calcium-additives added or the injection point.

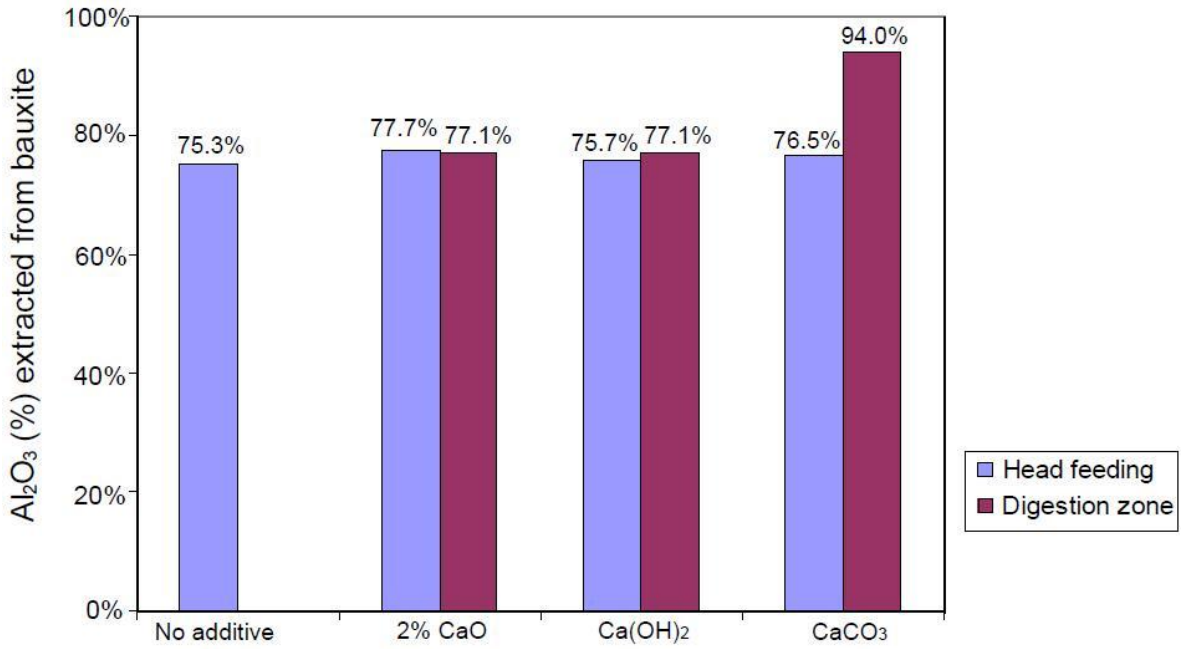

Figure 7.1 Alumina recoveries from Jamaican bauxite JCB-270 when digested with/without calcium additives at digestion temperature 250 ℃ in 30 minutes and the Bayer liquor concentration 240 g/L. Blue bars represent head feed of additives to the raw bauxite and red bars refer to the digestion with addition of lime/ Ca compounds directly to the digestion zone. The charge of lime is 2 wt. % of the bauxite and the dosage of $Ca(OH)_2$ or $CaCO_3$ is equivalent to the 2 wt. % CaO in the bauxite.

In summary, the alumina initially substituted in the goethite structure can be mostly released from aluminous goethite to the spent liquor as a result of nearly completed transformation of Al-goethite to Al-hematite during the Bayer digestion where $CaCO_3$ (equivalent to ~ 2 wt.% CaO) is directly added to the digest zone. This would greatly improve the productivity of alumina in the Bayer circuit.

7.2 Improvement of settling rate

The other concern that has been raised for Al-goethite bauxite is related to the settling problem. The settling difficulty caused by goethite present in red mud is associated with its physical properties, in particular its relatively smaller particle size and larger specific surface area compared to those of hematite.

The improvement in settling behavior of red mud by transformation of Al-goethite to hematite has been verified by two pathways: physical properties and settling rate. Two residues involved in this settling behavior test are the digested JCB-270 residues, one without additives and the other one with $CaCO_3$ directly added to the digestion zone (250 ºC) but the digestion conditions are otherwise the same with temperature at 250 ℃ in 30 minutes in the same level of sodium aluminate solution (C = 240 g/L, A/C = 0.30).

In terms of physical properties, particle size distribution (PSD) and specific surface area (SSA) are the two key parameters to decide the settling performance of red mud. Generally finer particle size and larger surface area is more likely to give rise to a slower settling rate. The particle size distribution analysis is designed to determine the information about the size and range of a set of particles representative of the measured sample. In order to exclude interference of particle sizes of additives, ultra-fine particles of three additives have been used in this study. In addition, a tiny amount of additives (1~3 wt.% of total solids) were involved in the experiments which should not substantially affect the physical properties of the solids in the process.

Figure 7.2 shows the particle size distributions for the digested JCB-270 residues. The particle size distribution of the residue digested with $CaCO_3$ is increased from ~1 μm for the digested residue without Ca additive to ~10 μm.

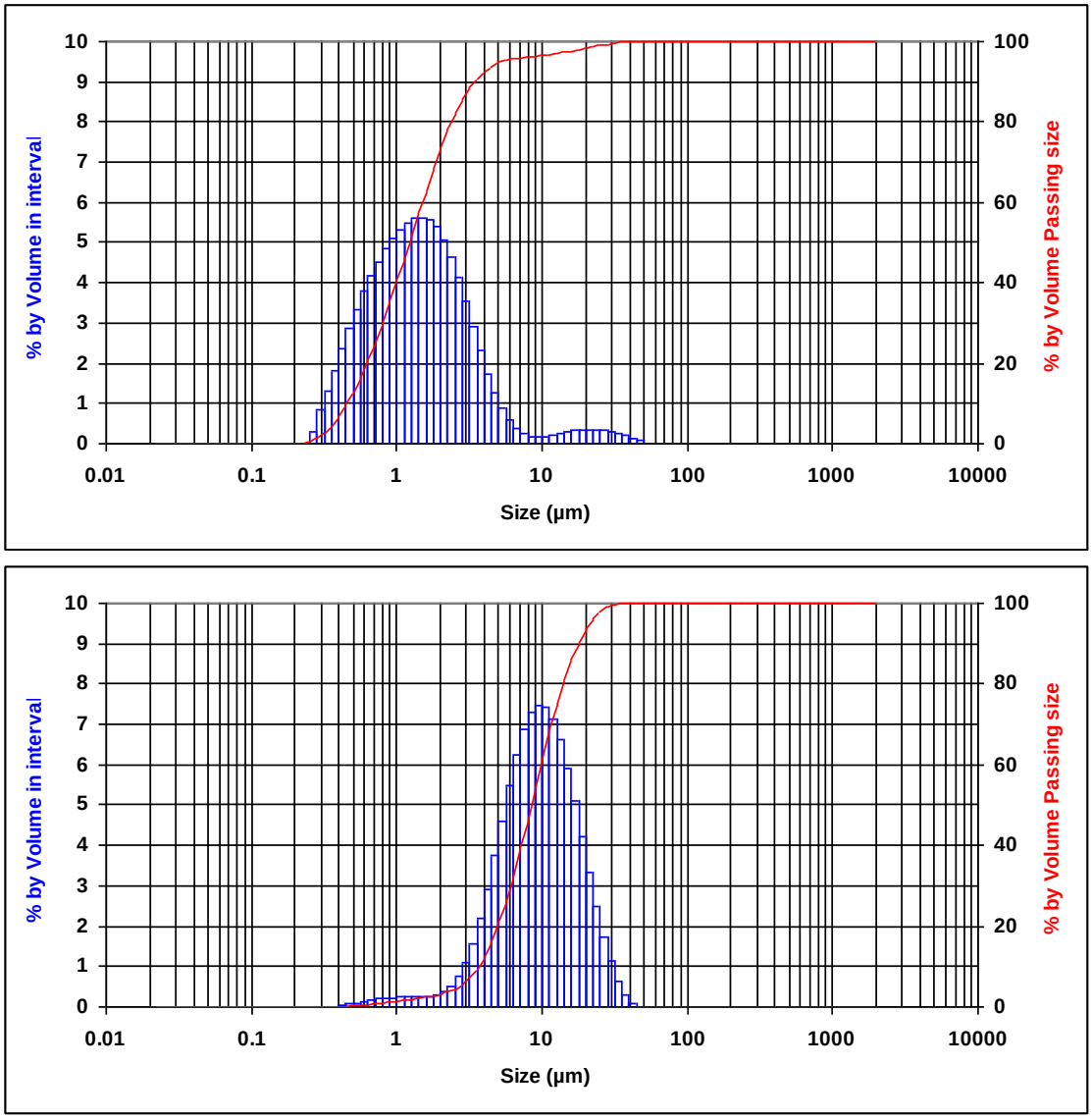

Figure 7.2 Particle size distributions of the digested JCB-270 residues. Digestion conditions: Temp = 250 ºC, holding time = 30 minutes, C (as Na_2CO_3) = 240 g/L and A/C = 0.3. Top: without additives; bottom: with $CaCO_3$ (equivalent to 2 wt. % CaO in the solids) as additive directly added to the digestion zone.

Specific surface area, listed in **Table 7.2**, also reduces from 6.737 to 1.144 m^2/g as a result of the transformation of Al-goethite to hematite. The XRD pattern for the residues proves that hematite is the dominant iron oxides in the $CaCO_3$ present digestion process, which explains the significant reduction of specific surface area. The settling behavior of red mud can be greatly improved by the increased particle sizes and specific surface area.

Table 7.2 The comparison of the settling behaviors for the two digested bauxite residues.

Digestion of JCB-270	Dominant iron oxides	Physical properties		Settling rate (m/h) at 60g/L solids concentration (*Flocculant dose 39.9 g/t)
		Particle size (μm)	Surface area (m^2/g)	
Without additives	Goethite	~1	6.737	0.26
With $CaCO_3$ directly added to the digestion zone	Hematite	~10	1.144	1.96

Finally, the settling performance tests for the two residues were conducted with the assistance of synthetic flocculant. The settling rate for the goethite-transformed slurry (1.96 m/h) is around six times faster than the untransformed slurry (0.26 m/h).

In conclusion, both alumina recovery from Al-goethite and the settling rate has been greatly enhanced by the hydrothermal transformation of Al-goethite to Al-hematite through addition of $CaCO_3$ directly to the digestion zone. Alumina recovery significantly increases by approximately 20% from ~75% for the digestion without additives to 94% for digestion with addition of $CaCO_3$ to the digestion zone. The settling rate also improves from a relatively slower 0.26 m/h to a considerable faster 1.96 m/h. The ultimate objectives of this project, the improvement of alumina recovery from Al-goethite and settling rate of red mud via hydrothermal transformation of Al-goethite to hematite/Al-hematite under the Bayer digestion conditions, have been achieved.

References

Solymar, K., Sajo, I., Steiner, J. & Zoldi, J. (1992) Characteristics and separability of red mud. *Light Metals***,** 209-223.

Suss, A. G. & Maltz, N. S. (1992) Aluminium and chromium containing goethite: composition, properties, behaviour in soda aluminate liquors in presence of silicon, titanium and calcium conpounds. *Light Metals***,** 1343-1347.

Suss, A., Fedyaev, A., Kuznetzova, N., Damaskin, A., Kuvyrkina, A., Panov, A., Paromova, I. & Lukyanov, I. (2010) Technology solutions to increase alumina recovery from aluminogoethitic bauxites. *Light Metals*.

Chapter 8
Conclusions and Future Work

8.1 Conclusions

8.1.1 Characterisation of synthetic Al-substituted goethite

Laboratory synthesis of Al-substituted goethite has been achieved in this study. Ageing $Fe(NO_3)_3$ and $Al(NO_3)_3$ in KOH solution at 70℃ for 14 days was employed to synthesize goethite with relatively low Al substitution. The advantage of this method is that pure and well-crystallized Al-substituted goethite can be obtained. However, the drawback is that higher than 12 mol % Al substitution is not achievable. In order to prepare goethite with higher Al substitution, slow air oxidation of $FeCl_2$ and $AlCl_3$ in an alkaline environment at room temperature for 3 months was conducted. The maximum Al level incorporated in the goethite structure was 28 mol %, similar to natural samples. Although a much more Al enriched goethite can be synthesized by this method, it has associated disadvantages including higher amounts of impurities in the final product and poorly crystallized goethite. Monitoring this synthetic process tends to be very difficult due to the long holding time and the impact from the ambient environment.

The study on the synthetic method indicates that the synthesis of Al-goethite from Fe^{3+} in a KOH solution is a promising method due to the formation of pure and well crystallised solid. Kinetic studies on the effects of temperature on the preparation reveals that in the range of 25-90 ℃, the reaction temperature of 70 ℃ is the most appropriate because products with more predictable Al substitution were generated.

Multiple characterisation methods were used to evaluate the synthetic aluminous goethite samples. XRD was employed to determine the mineral phases present and to calculate the degree of Al substitution in the Al-goethite according to the shift in its characteristic XRD peaks. Morphology of Al-goethite was thoroughly investigated using TEM and the structure change was monitored by IR spectroscopy. Thermal analysis (e.g. DSC and TG) was primarily adopted to establish the thermal behaviour of Al-goethite as well as obtain the thermodynamic data.

The understanding of synthetic Al-goethite from an Fe^{3+} system in this study has been established by the various characteristic technologies. The goethite structure appears to

be acicular in shape at zero Al substitution, however with increasing Al content it gradually becomes rod shaped, which is the fundamental shape for diaspore. The particle size simultaneously shrinks along the *c*-axis from 1500nm in pure goethite to 300nm in goethite that contains 10.17 mol % Al. This predictable change along the *c*-axis provides a valuable correlation between Al substitution and the change in *c* value in an Al-substituted goethite.

A study of the IR spectra of Al-goethite shows an obvious shift in peaks from the characteristic goethite frequencies to the diaspore spectrum to higher frequencies with increasing Al substitution. This is associated with the structure strain that is caused by the replacement of Fe^{3+} with the smaller Al^{3+} in Al-goethite. However, this shift does not occur when further increasing the Al substitution from 10 mol % to 25 mol %. Instead, broader IR peaks were observed in the 25 mol % Al-goethite, compared to the relatively narrow peaks of the sample containing 10 mol % Al. The peak widening (without obvious peak shift) indicates heterogeneity of morphology rather than structural strain secondary to the Al substitution for Fe in goethite.

Enthalpy of mixing (ΔH_{mix}) for the goethite-diaspore solid solution has confirmed that the Al-goethite with Al > ~10 mol% enters the metastable zone with ΔH_{mix} = 20-25kJ/mol. Solid solutions in this metastable zone are unlikely to persist for a long time or cannot be formed at all (Majzlan and Navrotsky, 2003).

A proposed model for the diaspore-goethite solid solution was preliminarily developed according to the results from IR, DSC and IR. Firstly, a substitution gap between initial concentration of Al^{3+} in the synthetic system and the incorporated Al-goethite exists in synthetic Al-goethite. However, the degree of the discrepancy in the synthesis varies from method to method. Secondly, the model suggests a limit for Al for Fe substitution at 10-12 mol % but further aluminium is more likely to simply adhere on the surface of the Al-goethite particles as diaspore. This was confirmed by TEM investigation on the goethite sample with higher Al substitution, in which a diasporic coating was observed.

8.1.2 Transformation of synthetic goethite to hematite

Thermal transformation:

Thermal transformation of goethite to hematite occurs at temperatures ranging from 200 to 300 ℃. However, the transformation further shifts to a higher temperature zone up to 400 ℃ for Al-substituted goethite. The transformation temperature for Al-goethite depends on the extent of Al-substitution, which elevates with increasing Al substitution.

From the morphological and structural perspectives (shown in XRD and TEM analysis), goethite does not completely transform to hematite until reaching extremely high temperature (800-1000ºC), below which the derived "hematite" after heat treatment still remains in the parent "goethite" phase. The recrystallization of hematite takes place only above 800 ℃ or higher.

The mechanism of thermal transformation from goethite/Al-goethite to hematite is a topotactic reaction process. It is suggested that the dehydration takes place in the parent goethite phase from the surface without structural change at the starting stage. As temperature increases, dehydration channels gradually form inside the goethite phase and eventually coalesce, which gives rise to the fracture of goethite-like crystal. Recrystallization between the fragments is finally complete with further increasing the temperature to ~1000 ℃. There is no new species generated through the whole process except for the constant change of structure and morphology. It is therefore concluded that the thermal transformation of goethite to hematite is a direct process without production of any intermediate.

In summary, the thermal transformation of goethite/Al-goethite to hematite takes place under relative high temperatures and does not form the desired hematite phase unless extremely high temperature (~1000 ℃) applies. The problems that goethite has caused to the Bayer process are primarily related to the physical properties, such as small particle size and large surface area. However, the thermal transformation cannot bring benefits to combat those problems due to the topotactic mechanism. Thus, it is not difficult to reach the conclusion that thermal transformation of goethite/Al-goethite to hematite is not practical for the Bayer circuit. However, it can still be adopted as a pre-treatment of bauxite or processing method of red mud. Since this thermal transformation can be

achieved within very short period of time at certain given temperature (800 – 1000 ℃), it would be an economic and practical way for pre-treatment of bauxite.

Hydrothermal transformation:

The hydrothermal transformation of goethite to hematite under Bayer digestion conditions is mainly influenced by digestion temperature, free caustic, soda concentration, the presence of alumina and hematite seeding in the solution.

Increasing digestion temperature favours goethite to hematite transformation. The transformation occurs at temperatures ranging from 180 to 280 ºC. A sensitive digestion temperature near 230 ℃ has been mathematically obtained which, to the best of our knowledge, has not yet been seen in other studies.

Three temperature zones can be said to affect the hydrothermal transformation of goethite to hematite, namely the linear zone, the accelerating zone and the plateau zone respectively. This provides practical guidance to the operation of the goethite to hematite conversion in the Bayer digestion.

The hydrothermal transformation can also be enhanced by increasing the free caustic soda concentration and/or by adding hematite seed (H/G ratio ≤ 0.7). However, the presence of aluminate in the Bayer liquor severely retards the transformation due to the formation of a possible intermediate bearing [Na-Fe-Al-O] in the system, which requires more energy to complete the transformation.

This study supports the mechanism, dissolution of goethite and precipitation of hematite, proposed by a number of previous studies.

In terms of the practical application of the hydrothermal transformation, it is most likely to be employed to combat the problems caused by goethite in the Bayer digestion process due to the operational temperature range. More importantly, the investigation suggests this process leads to complete transformation with not only a phase (goethite to hematite) change but also a particle size change at the same time.

8.1.3 Al-goethite in natural bauxite under the Bayer digestion environment

Hydrothermal transformation of Al-goethite to hematite in natural bauxite in the Bayer digestion is more complicated than that of synthetic goethite/Al-goethite to hematite. The extent of the transformation greatly depends on the types of impurities present in the natural bauxites. Anatase (TiO_2) present in bauxite tends to react with Bayer liquor to form sodium titanate, which is generally referred to as a series of minerals comprising of Na-Ti-O, at high temperature digestion (~250 ℃) in the absence of CaO. The transformation of goethite to hematite is inhibited by the formation of a sodium titanate coating on the Al-goethite surface. However, the presence of CaO in the bauxite or addition of CaO to the digestion system could prevent the formation of sodium titanate as a result of the competitive formation of perovskite $CaTiO_3$ via reactions between CaO and TiO_2 at relatively high digestion temperature (~250 ℃). Purposely adding CaO to the bauxite proves that lime feeding greatly promotes the transformation of goethite to hematite when digesting the gibbsite free bauxite (from nearly no transformation to ~90% goethite conversion).

It should be noted the advantages of adding CaO to the transformation only occurs when lime is directly added to the digestion zone (250 ℃) rather than the head feeding in raw bauxite (without pre-removal of gibbsite from the bauxite). In other words, the adding point of CaO, also referred to as the injection point, is crucial to the formation of perovskite. If CaO (or other calcium-containing additives, such as $Ca(OH)_2$ and $CaCO_3$) is added to the head fed of raw bauxite it will be consumed by gibbsite to form tri-calcium aluminate (TCA) at a relatively low temperature range (~100 ℃) within minutes. Although some CaO is likely to be released from TCA to the digestion liquor with longer holding times of greater than to 2 hours, the performance of the transformation of Al-goethite still cannot reach its maximum potential. Thus lime or calcium compounds added directly to the digestion zone to avoid the formation of TCA using the autoclave reaction system are preferred. In such a setting, the transformation of Al-goethite to hematite was greatly improved with the addition of $CaCO_3$. The dominant iron oxide in the digested residue treated by this method is hematite. However, the addition of CaO or $Ca(OH)_2$ does not show a similar improvement with goethite remaining the dominant iron oxide in the digested residues.

8.1.4 Improvement of alumina recovery and settling rate

The hydrothermal transformation of part or all of Al-goethite in natural bauxite to hematite under Bayer digestion conditions has been achieved by directly adding $CaCO_3$ to the digestion zone. The improvement of this transformation to the Bayer process was evaluated by two parameters: alumina recovery from Al-goethite and settling rate of the red mud.

The alumina extracted from the experimental bauxite sharply increases from a 75 – 77% recovery for the common digestion (no additives involved or head feeding of calcium-containing additives) to a 94% recovery for digestion under the same digestion conditions with the addition of $CaCO_3$ directly to the digestion zone. Meanwhile, the settling performance for the red mud from this improved process has been greatly enhanced by nearly 6 times from only 0.26 m/h to nearly 2 m/h.

The improvement achieved in the current study in terms of more alumina recovery and faster settling rates performance than those reported by Solymar *et al.* (1992) and Suss *et al*. (2010).

8.2 Future Work

Substantial improvement in alumina recovery and settling rate has been achieved with this project as mentioned in the Conclusions. However, some concerns raised during the study should be the focus of the future research in relation to aluminous goethite in the Bayer process.

1. Use of Electron Energy Loss Spectroscopy (EELS) and High Resolution Transmission Electron Microscopy (HRTEM) on the proposed model of synthetic Al-goethite samples should be taken into account. These techniques would be able to verify the proposed hypothesis on the morphology of synthetic Al-goethite. In addition, the same techniques should also be applied to investigating the sodium titanate coating on the hydrothermal transformation of Al-goethite in the natural bauxite.

2. *In-situ* XRD monitored digestion processes can be employed to track the possible reactions and the change of mineral phases during the digestion in real time.

3. The chemistry of aluminous goethite in the Bayer digestion process will require more study. Firstly, the mechanism of the formation of sodium titanate and its impact on Al-goethite transformation during the digestion process has not been fully established; the morphological and kinetics study on the sodium titanate would be of great help to the mechanism study. Secondly, the competition between the formation of TCA and perovskite when calcium compounds are present during digestion requires elucidation.

4. Detailed thermodynamic and kinetic studies should be carried out in finding plausible reaction mechanisms for the calcium compound reactions.

Reference (Full version)

Anand, R. R., Gilkes, R. J. & Roach, G. I. D. (1991) Geochemical and mineralogical characteristics of bauxites, Darling Range, Western Australia. *Applied Geochemistry,* 6**,** 233-248.

Atasoy, A. (2005) An investigation on characterization and thermal analysis of the Aughinish red mud. *Journal of Thermal Analysis and Calorimetry,* 81**,** 375-361.

Atkinson, R. J., Posner, A. M. & Quirk, J. P. (1968) Crystal nucleation in Fe(III) solutions and hydroxide gels. *Journal of Inorganic and Nuclear Chemistry,* 30**,** 2371-2381.

Authier-Martin, M., Forte, G., Ostap, S. & See, J. (2001) The mineralogy of bauxite for producing smelter-grade alumina. *Journal of Mineralogy,* 53**,** 36-40.

Bardossy, G. (1982) Karst Bauxites. Bauxite deposits on carbonate rocks. *Elsevier,* 14**,** 441.

Bardossy, G. & Aleva, G. J. J. (1990) Lateritic Bauxites. *Developments in Economic Geology,* 27**,** 624.

Basu, P. (1983) Reaction of iron minerals in sodium aluminate solutions. *In:* ADKINS, E. M. (ed.) *Light Metals.* New York: The Metallurgical Society of AIME.

Basu, P., Nitowski, G. A. & The, P. J. (Year) Proceedings of the International Symposium on Iron Control Hydrometallurgy. *In:* J. E. DUTRIZAC, A. J. M., ed., 1986. Ellis Horwood Limited, Chichester, UK, 223-244.

Blanch, A. J., Quinton, J. S., Lenehan, c. E. & Pring, A. (2008) The crystal chemistry of Al-bearing goethites: an infrared spectroscopic study. *Mineralogical Magazine,* 72**,** 1043-1056.

Brown, N. & Tremblay, R. J. (1974) Some studies of the mineral transformations during high temperature digestion of Jamaican bauxite. *Light Metals,* 3**,** 825 - 844.

Burgina, E. B., Kustova, G. N., Tsybulya, S. V., Kryukova, G. N., Litvak, G. S., Isupova, L. A. & Sadykov, V. A. (2000) Structure of the metastable modification of iron (III) oxide. *Journal of Structural Chemistry,* 41**,** 396-402.

Burke, J. (1965) *The kinetics of phase transformations in metals,* Oxford, Pergamon Press.

Cornell, R. M. & Schwertmann, U. (2000) *The Iron Oxides: Structure, Properties, Reactions, Occurrences and Uses,* Weinheim, Wiley-VCH.

Cornell, R. M. & Schwertmann, U. (2003) *The Iron Oxides: Structure, Properties, Reactions, Occurrences and Uses,* Weinheim:Wiley-VCH.

Croker, D., Loan, M. & Hodnett, K. (2006) Sodium titanate formation in high temperature Bayer digestion. *TRAVAUX,* 33**,** 154-165.

Croker, D., Loan, M. & Hodnett, B. K. (2009) Kinetics and mechanisms of the hydrothermal crystallization of calcium titanate species *Crystal Growth and Design,* 9**,** 2207-2213.

Crombie, T., Davis, M. & Laurie, J. E. 1973. *Method of digesting bauxite via the Bayer process with the addition of reducing agents*. United States patent application 346736.

Davies, P. K. & Navrotsky, A. (1983) Quantitative correlations of deviations from ideality in binary and pseudobinary solid solutions. *Journal of Solid State Chemistry,* 46**,** 1-22.

Davis, C. E. (Year) The mineralogy of Jamaican bauxites. . *In:* The Journal of Geological Society of Jamaican Proceedings of Bauxite Symposium II, 6-20 October 1973.

Diakonov, I., Khodakovsky, I., Schott, J. & Sergeeva, E. (1994) Thermodynamic properties of iron oxides and hydroxides. I. Surface and bulk thermodynamic properties of goethite up to 500 K. *European Journal of Mineralogy,* 6**,** 967-983.

Diamandescu, L., Mihãil à-Tãrãbãsanu, D. & Feder, M. (1993) On the solid phase transformation goethite --> hematite. *Materials Letters,* 17**,** 309-311.

Ewing, F. J. (1935) The crystal structure of diaspore. *Journal of Chemical Physics,* 3**,** 203-207.

Fan, H., Song, B. & Li, Q. (2006) Thermal behavior of goethite during transformation to hematite. *Materials Chemistry and Physics,* 98**,** 148-153.

Fey, M. V. & Dixon, J. B. (1981) Synthesis and properties of poorly crystalline hydrated aluminous goethite. *Clays and Clay Minerals,* 29**,** 91-100.

Frost, R. L., Ding, Z. & Ruan, H. D. (2003) Thermal analysis of goethite. *Journal of Thermal Analysis and Calorimetry,* 71**,** 783-797.

Garing, M. L., Wright, J. R., Featherston, R. H. & Fischer, J. P. 1980. *Lime Feeding for Bayer Process*. United States of America patent application 305922. 1980-07-29.

Gialanella, S., Girardi, F., Ischia, G., Lonardelli, I., Mattarelli, M. & Montagna, M. (2010) On the goethite to hematite phase transformation. *Journal of Thermal Analysis Calorimetry,* 102**,** 867-873.

Gonzâlez, G., Sagarzazu, A. & Villalba, R. (2000) Study of the mechano-chemical transformation of goethite to hematite by TEM and XRD. *Materials Research Bulletin,* 35**,** 2295-2308.

Grubbs, D. K., Libby, S. C., Rodenburg, J. K. & Wefers, K. A. (1980) The geology, mineralogy and clarification properties of red and yellow Jamaican bauxites. *Journal of the Geological Society of Jamaican Proceeding of Bauxite Symposium IV***.,** 176-186.

Gualtieri, A. F. & Venturelli, P. (1999) In situ study of the goethite-hematite phase transformation by real time, synchrotron powder diffraction, Sample at T = 25 C *American Mineralogist,* 84**,** 895-904.

Hahn, T. (ed.) 1996. *International Tables for Crystallography, Vol. A: Space-group Symmetry,* Dordrecht, The Netherlands: Kluwer Academic Publisher.

Hass, H. (1972) Diaspore-corrundum equilibrium determined by epitaxis of diaspore on corundum. *American Mineralogist,* 157**,** 1375-1385.

Hind, A. R., Bhargava, S. K. & Grocott, S. C. (1999) The surface chemistry of Bayer process solids: a review. *Colloids and Surfaces A: Physicochemical and Engineering Aspects,* 146**,** 359-374.

Hu, Y., Lv, R., Liu, G. & Ye, R. (1999) *Physical Chemistry (Chinese),* Beijing, Higher Education Press.

Hudson, L. K. (1987) Alumina Production. *In:* BURKIN, A. R. (ed.) *Production of Aluminium and Alumina.* Chichester: John Wiley and Sons.

Ibach, H. & Lüth, H. (2010) *Solid-State Physics: An Introduction to Principles of Materials Science,* London, Springer.

Jeannot, C., Malaman, B., Gérardin, R. & Oulladiaf, B. (2002) Synthesis, Crystal and Magnetic Structures of the Sodium Ferrate (IV) Na4FeO4 Studied by Neutron Diffraction and Mössbauer Techniques. *Journal of Solid State Chemistry,* 165**,** 266-277.

Kaur, N., Grafe, M., Singh, B. & Kennedy, B. (2009) Simultaneous Incorporation of Cr, Zn, Cd, and Pb in the Goethite Structure. *Clays and Clay Minerals,* 57**,** 234-350.

King, W. R. (Year) The iron minerals in Jamaican bauxites. *In:* EDGEWORTH, T. C., ed. The Metallurgical Society of AIME, 1971 New York. Light metals, 18-20.

Kirwan, L. J., Deeney, F. A., Croke, G. M. & Hodnett, K. (2009) Characterisation of various Jamaican bauxite ores by quantitative Rietveld X-ray powder diffraction and 57Fe Mössbauer spectroscopy. *International Journal of Mineral Processing,* 91**,** 14-18.

Klug, H. P. & Alexander, L. E. (1974) *X-ray Diffraction Precedures for Polycrystalline and Amorphous Materials,* New York, Wiley.

Li, D., O'Connor, B. H., Low, I. M. & Riessen, A. (2006a) Mineralogy of Al-substituted goethites. *Powder Diffraction,* 21**,** 289-299.

Li, D., O'Connor, B. H., Low, I. M. & Riessen, A. (2006b) Mineralogy of Al-substituted goethites. *Powder Diffraction,* 21**,** 289-299.

Li, L. Y. & Rutherford, G. K. (1996) Effect of bauxite properties on the settling of red mud. *International Journal of Mineral Processing,* 48**,** 169-182.

Li, L. Y. (1998) Properties of red mud tailings produced under varying Bayer process conditions. *Journal of Environmental Engineering,* 124**,** 254-264.

Li, L. Y. (2001) A study of iron mineral transformation to reduce red mud tailings. *Waste Management,* 21**,** 525-534.

Majzlan, J. & Navrotsky, A. (2003) Thermodynamics of the goethite-diaspore solid solution. *Eur. J. Mineral,* 15**,** 495-501.

Malts, N. S., Poddymov, V. P., Rudashevski, L. S. & Kiselev, V. E. (1985) The intensifying action of lime upon the kinetics of bauxite leaching. *Non-ferrous Metals***,** 38-40.

Malts, N. S. (1991) Efficiency of lime use in Bayer alumina production. *Light Metals***,** 257-262.

McArthur, L. & Greensill, C. (2006) Mineralogical analysis of Weipa bauxite using NIR spectroscopy. *Australian Institute of Physics 17th National Congress 2006*, Brisban.

Mendelovici, E. & Yariv, S. (1981) Interactions between the iron and the aluminum minerals during the heating of Venezuelan lateritic bauxites. I. Infrared spectroscopy investigation. *Thermochimica Acta,* 45**,** 327-337.

Murad, E. & Bowen, L. H. (1987) Magnetic ordering in Al-rich goethites: Influence of crystallinity. *American Mineralogy,* 72**,** 194-200.

Murray, J., Kirwan, L., Loan, M. & Hodnett, B. K. (2009) In-situ synchrotron diffraction study of the hydrothermal transformation of goethite to hematite in sodium aluminate solutions. *Hydrometallurgy,* 95**,** 239-246.

Mylona, E., Kalamboki, T. & Xenidis, A. (2008) Processing of bauxite ores. *In:* MEGGYES, T., ROEHL, K.-E. & DIXON-HARDY, D. (eds.) *Tailings Management Facilities.* EPP Publications.

Newton, R. C. & Smith, J. V. (1967) Investigations concerning the breakdown of albite at depth in the Earth. *Journal of Geology,* 75**,** 268-286.

Ockerman, L. T. & Schreyer, J. M. (1951) Preparation of Sodium Ferrate (VI). *Journal of American Chemistry Society,* 73**,** 5478.

Okinaka, K. & Maekawa, M. 2001. *Spindle-shaped goethite particles, sindle-shaped hematite particles and magnetic sindle-shaped metal particles containing iron as main component*. US patent application.

Orban, F., Pinter, T., Sigmond, G., Siklosi, P., Solymar, K., Toth, P. & Zambo, J. (1973) Processing of bauxites containing goethite. *Hung Teljes,* 6**,** 758.

Ostap, S. (Year) Effect of bauxite mineralogy on its processing characteristics. *In:* JR., L. J., ed., 1984 Los Angeles. 651-671.

Parekh, B. K. & Goldberger, W. M. (1976) An assessment of technology for possible of Bayer process muds. *Environmental Protection Technology Series*.

Perchuk, L. L. & Aranovich, L. Y. (1979) Thermodynamics of minerals of variable composition: Andradite-grossularite and pistacite-clinozoisite solid solutions. *Physical Chemistry of Minerals,* 5**,** 1-14.

Perotta, A. J. & Williams, F. (1995) Hydrocalumite formation in Bayer liquor and its promotional effect on oxalate precipitation. *Light Metals***,** 77-87.

Piszora, P. & Wolska, E. (1998) X-Ray Powder Diffraction Study on the Solubility Limits in the Goethite-diaspore Solid Solutions. *Materials Science Forum,* 278**,** 584-588.

Pomiès, M. P., Menu, M. & Vignaud, C. (1999) TEM observations of goethite dehydration: application to archaeological samples. *Journal of the European Ceramic Society,* 19**,** 1605-1614.

Prasad, P. S. R., Shiva Prasad, K., Krishna Chaitanya, V., Babu, E. V. S. S. K., Sreedhar, B. & Ramana Murthy, S. (2006) In situ FTIR study on the dehydration of natural goethite. *Journal of Asian Earth Sciences,* 27**,** 503-511.

Ruan, H. D., Frost, R. L. & Kloprogge, J. T. (2001) The behavior of hydroxyl units of synthetic goethite and its dehydroxylated product hematite. *Spectrochimica Acta Part A: Molecular and Biomolecular Spectroscopy,* 57**,** 2575-2586.

Ruan, H. D., Frost, R. L., Kloprogge, J. T. & Duong, L. (2002a) Infrared spectroscopy of goethite dehydroxylation: III. FT-IR microscopy of in situ study of the thermal transformation of goethite to hematite. *Spectrochimica Acta Part A: Molecular and Biomolecular Spectroscopy,* 58**,** 967-981.

Ruan, H. D., Frost, R. L., Kloprogge, J. T. & Duong, L. (2002b) Infrared spectroscopy of goethite dehydroxylation. II. Effect of aluminium substitution on the behaviour of hydroxyl units. *Spectrochimica Acta Part A: Molecular and Biomolecular Spectroscopy,* 58**,** 479-491.

Scheinost, A. C., Schulze, D. G. & Schwertmann, U. (1999) Diffuse reflectance spectra of Al substituted goethite; a ligand field approach. *Clays and Clay Minerals,* 47**,** 156-164.

Schultze-Rhonof, E. & Winkhaus, G. (1972) On the chemistry of bauxite extraction I. Studies in the system Na_2O-CaO-Al_2O_3-TiO_2-H_2O at 100^oC and atmospheric pressure. *Z. Anorg. Allg. Chem.,* 390**,** 97-103.

Schultze-Rhonof, E. (1973) On the chemistry of bauxite extraction II. Studies in the system Na_2O-CaO-Al_2O_3-TiO_2-H_2O between 100^oC and 275^oC. *Z. Anorg. Allg. Chem.,* 396**,** 303-307.

Schulze, D. G. (1984) The influence of aluminum on iron oxides. VIII. Unit cell dimensions of Al-substituted goethites and estimation of Al from them. *Clays and Clay Minerals,* 32**,** 36-44.

Schulze, D. G. & Schwertmann, U. (1984) The influence of aluminium on iron oxides. X. Properties of Al-substituted goethites. *Clay Minerals,* 19**,** 521-539.

Schwertmann, U. & Fischer, W. R. (1966) Zur Bildung von a-FeOOH und c~-Fe_2O_3 aus amorphem Eisen(III)-hydroxid.III. *Z. Anorg. Allg. Chem.,* 346**,** 137-142.

Schwertmann, U., Fitzpatrick, R. W., Taylor, R. M. & Lewis, D. G. (1979) The influence of aluminum on iron oxides: Part II. Preparation and properties of Al-substituted hematites. *Clays and Clay Minerals,* 27**,** 105-112.

Schwertmann, U. & Kampf, N. (1985) Properties of goethite and hematite in kaolinitic soils of Southern and Central Brazil. *Soil Science,* 139**,** 344-350.

Schwertmann, U. (1987) Goethite and hematite formation in the presence of clay minerals and gibbsite at 25^{o}C. *Soil Science Society American Journal,* 52**,** 288-291.

Schwertmann, U. (1988) Some properties of soil and synthetic iron oxides. . *In:* STUCKI, J. W., GOODMAN, B. A. & SCHWERTMANN, U. (eds.) *Iron in soils and clay minerals.* Dordrecht: D. Peidel Publishing Company.

Schwertmann, U. & Carlson, L. (1994) Aluminum influence on iron oxides: XVII. Unit-cell parameters and aluminum substitution of natural goethites. *Soil Science Society of American Journal,* 58**,** 256-261.

Schwertmann, U. & Cornell, R. M. (2000) *Iron Oxides in the Laboratory: Preparation and Characterization,* Weinheim, Wiley-VCH.

Schwertmann, U., Friedl, J., Stanjek, H. & Schulze, D. G. (2000) The effect of clay minerals on the formation of goethite and hematite from ferrihydrite after 16 years' ageing at 25 ^{o}C and pH 4-7. *Clay Minerals,* 35**,** 613-623.

Smith, P. (2009) The processing of high silica bauxites -- Review of existing and potential processes. *Hydrometallurgy,* 98**,** 162-176.

Solymar, K., Sajo, I., Steiner, J. & Zoldi, J. (1992) Characteristics and separability of red mud. *Light Metals***,** 209-223.

Stanjek, H. & Schwertmann, U. (1992) The influence of aluminum on iron oxides. Part XVI: hydroxyl and aluminum substitution in synthetic hematite. *Clays and Clay Minerals,* 40**,** 347-354.

Stoffregen, R. E., Alpers, C. N. & Jambor, J. L. (2000) Alunite-jarosite crystallography, thermodynamics, and geochronology. *In:* ALPERS, C. N., JAMBOR, J. L. & NORDSTROM, D. K. (eds.) *Review of Mineral Geochemistry.* Mineralogical Society of America.

Strauss, R., Brummer, G. W. & Barrow, N. J. (1997) Effects of crystallinity of goethite: I. Preparation and properties of goethites of differing crystallinity. *European Journal of Soil Science,* 48**,** 87-99.

Suarez, C. E., Sulpizi, E., Peleato, F. & Saraullo, A. (1990) Application of the philosophy of expert systems to red mud thickeners overflow quality monitoring. *Ligh Metals***,** 79-84.

Sudakar, C., Subbanna, G. N. & Kutty, T. R. N. (2004a) Effect of cationic substituetes on particle morphology of goethite and the magnetic properties of maghemite derived from substituted goethite. *Journal of Materials Science,* 39**,** 4271-4286.

Sudakar, C., Subbanna, G. N. & Kutty, T. R. N. (2004b) Effect of cationic substituents on particle morphology of goethite and the magnetic properties of maghemite derived from substituted goethite. *Journal of Materials Science,* 39**,** 4271-4286.

Suss, A., Fedyaev, A., Kuznetzova, N., Damaskin, A., kuvyrkina, A., Panov, A., paromova, I. & Lukyanov, I. (2010) Technology solutions to increase alumina recovery from aluminogoethitic bauxites. *Light Metals*.

Suss, A. G. & Maltz, N. S. (1992) Aluminium and chromium containing goethite: composition, properties, behaviour in soda aluminate liquors in presence of silicon, titanium and calcium conpounds. *Light Metals***,** 1343-1347.

Szytuta, A., Burewicz, A., Dimitrijevic, Z., Krasnicki, S., Rzany, H., Todorovic, J., Wanic, A. & Wolski, W. (1968) Neutron diffraction studies of α-FeOOH. *Physica Status Solidi,* 26**,** 429-434.

Thiel, R. (1963) Zum system FeOOH-AlOOH. *Z.Anorg. Allg. Chem,* 326.

Vaughan, D. J. & Craig, J. R. (1978) *Mineral Chemistry of Metal Sulfides,* Cambridge, Cambridge University Press.

Vyazovkin, S. (2000) Computational aspects of kinetic analysis.: Part C. The ICTAC Kinetics Project — the light at the end of the tunnel? *Thermochimica Acta,* 355**,** 155-163.

Walter, D., Buxhaum, G. & Laqua, W. (2001) The mechanism of the transformation from goethite to hematite. *Journal of Thermal Analysis and Calorimetry,* 63**,** 733-748.

Wang, H., Pring, A., Ngothai, Y. & O'Neill, B. (2005) A low-temperature kinetic study of the exsolution of pentlandite from the monosulfide solid solution using a refined Avrami method. *Geochimica et Cosmochimica Acta,* 69**,** 415-425.

Watari, F., Delavignette, P., Van Landuty, J. & Amelinckx, S. (1983) Electron microscopic study of dehydration transformations. Part III: High resolution observation of the reaction process FeOOH → Fe2O3. *Journal of Solid State Chemistry,* 48**,** 49-64.

Whittington, B. I. (1996) The chemistry of CaO and Ca(OH)2 relating to the Bayer process. *Hydrometallurgy,* 43**,** 13-35.

Whittington, B. I. & Cardile, C. M. (1996) The chemistry of tricalcium aluminate hexahydrate relating to the Bayer industry. *International Journal of Mineral Processing,* 48**,** 21-38.

Whittington, B. I., Fletcher, B. L. & Talbot, C. (1998) The effect of reaction conditions on the composition of desilication product (DSP) formed under simulated Bayer conditions. *Hydrometallurgy,* 49**,** 1-22.

Wohlfarth, E. P. & Buschow, K. H. J. (1980) *Ferromagnetic materials: a handbook on the properties of magnetically ordered substances,* North Holland, Elsevier.

Wolska, E. (1988) Relations between the existence of hydroxyl ions in the anionic sublattice of hematite and its infrared and X-ray characteristics. *Solid State Ionics,* 28-30**,** 1349-1351.

Wolska, E., Szajda, W. & Piszora, P. (1992a) Synthetic solid solutions formed between goethite and diaspore. *Z. Pflanzenernahr. Bodenk.,* 155**,** 479-482.

Wolska, E., Szajda, W. & Piszora, P. (1992b) Determination of solid solution limits based on the thermal behaviour of aluminium substituted iron hydroxides and oxides. *Journal of Thermal Analysis,* 38**,** 2115-2122.

Wolska, E. & Schwertmann, U. (1993) The mechanism of solid solution formation between goethite and diaspore. 213-223.

Wolska, E., Szajda, W. & Piszora, P. (1994) Mechanism of Al- for Fe-substitution during the α-(Fe, Al) OOH to γ-(Fe, Al)$_2O_3$ transformation. *Solid State Ionics,* 70/71**,** 537-541.

Xu, B. (1991) *Lime chemistry in the Bayer process*. Ph.D., Murdoch University.

Xu, B., Smith, P., Wingate, C. & Silva, L. D. (2010) The effect of anatase and lime on the transformation of sodalite to cancrite in Bayer digestion at 250C. *Light Metals***,** 81-86.

Yamada, K., Harato, T. & Furumi, Y. (1974) Removal of iron compounds from the Bayer liquor. *The Mettallurgical Society of AIME,* New York. 713-723.

Yund, R. A. & Hall, H. T. (1970) Kinetics and mechanism of pyrite exsolution from pyrrhotite. *Journal of Petrol,* 11**,** 381-404.

Yund, R. A. & McCallister, R. H. (1970) Kinetics and mechanism of exsolution. *Chemical Geology,* 6**,** 5-30.

Zwingmann, N., Gilkes, R. J. & Swash, P. M. 2008. Iron oxyhydroxide characterisation and modification in bauxite: tools for predicting and improving Bayer performance. Perth: Minerals and Energy Research Institute of Western Australia.

Appendices

Appendix A

Common iron oxides, hydroxides and oxide-hydroxides in nature*

Oxide-hydroxides and hydroxides		Oxides	
General name	Formula	General name	Formula
Goethite	$\alpha - FeOOH$	Hematite	$\alpha - Fe_2O_3$
Lepidocrocite	$\gamma - FeOOH$	Magnetite	$Fe_3O_4 (Fe^{II} Fe_2^{III} O_4)$
Akaganeite	$\beta - FeOOH$	Maghemite	$\gamma - Fe_2O_3$
Schwertmannite	$Fe_{16}O_{16}(OH)_y(SO_4)_z \cdot nH_2O$		$\beta - Fe_2O_3$
	$\delta - FeOOH$		$\varepsilon - Fe_2O_3$
Feroxyhyte	$\delta' - FeOOH$	Wustite	FeO
Ferrihydrite	$Fe_5HO_8 \cdot 4H_2O$		
	$Fe(OH)_2$		
Green Rusts	$Fe_x^{III} Fe_y^{II} (OH)_{3x+2y-z}(A^-)_z$; $A^- = Cl^-; \frac{1}{2} SO_4^{2-}$		

*(Cornell and Schwertmann, 2003)

Reference:

Cornell, R. M. & Schwertmann, U. (2003) *The Iron Oxides: Structure, Properties, Reactions, Occurrences and Uses*, Weinheim:Wiley-VCH.

Appendix B

Definitions and Terms in Bayer Liquor Chemistry (Courtesy of Peter Smith)

1. Alumina (A)

Alumina in solution (**A**) is expressed as equivalent g/L Al_2O_3. If a solution contains 50 g/L of aluminium (50/27 = 1.85 M) then the **A** value is 50*102/(27*2) = 94.4 (102 is the formula weight of Al_2O_3 and there are 2 atoms of aluminium in Al_2O_3).

2. Caustic or Total caustic (C or TC).

The caustic concentration of a solution (**C**) is the combination of the aluminate and excess hydroxide expressed as equivalent g/L of Na_2CO_3. Consider the two dissolution reactions -

(i) Gibbsite $Al(OH)_3 + 2NaOH = 2Na^+ + Al(OH)_4^- + OH^-$

(ii) Aluminium $Al + 3NaOH + 3H_2O = 3Na^+ + Al(OH)_4^- + 2OH^- + 3/2H_2g$

These are written such that there is excess hydroxide present. In both cases the concentration of the aluminate plus the free hydroxide is the caustic concentration (**C**). Note that the number of moles of reacting hydroxide and the resulting caustic concentration is always the same. In other words the caustic concentration is independent of the alumina loading in the liquor. To convert hydroxide levels to **C**, the hydroxide concentration in g/L is multiplied by 106/(2*40). 106 is the formula weight of Na_2CO_3 and 40 is the formula weight of NaOH. The factor of 2 arises since 2 moles of hydroxide are needed to form one mole of carbonate.

e.g. if into 130g/L NaOH solution 32 g of Al metal is dissolved then **A**=32*102/(27*2) = 60.4 and **C** =130*106/(2*40) = 172

Unfortunately caustic is sometimes called <u>free soda.</u> This is not to be confused with <u>free caustic</u> which is the excess hydroxide expressed as carbonate, i.e.

Free Caustic = **C - [A***106/102**]**.

3. Soda or Total Soda or total alkali (S or TA).

Soda is defined as the caustic concentration + the concentration of carbonate in the solution, again expressed as equivalent g/L (Na_2CO_3). In Bayer plants sodium carbonate levels are usually fairly constant at ~40 g/L. **S** values are then usually (**C** + ~40) g/L. If **C** = 170 (typical for an Alcoa green liquor) then **S** = ~210. The liquor is said to be 170/210 = 81% causticised.

4. A/C.

A/C is a straight ratio of **A** in g/L Al_2O_3 and **C** in g/L Na_2CO_3. It is (almost) a measure of supersaturation of the liquor. Pregnant (green) liquors are usually ~0.7 whereas spent liquors are ~0.35.

Appendix C

Mineral compositions of Jamaican bauxites involved in the thesis

Table XRF analysis of Jamaican bauxites used in the thesis.

Sample	Al_2O_3	av Al_2O_3	Fe_2O_3	SiO_2	CaO	TiO_2	Na_2O	P_2O_5	Minerals
JCB-BLM	48.2	45.9	18.9	1.90	0.04	2.42	0.06	0.253	Gi,Bo(t),He,Go,An
JCB-GPM	47.5	43.8	19.3	2.32	0.06	2.56	0.06	0.311	Gi,Bo,He,Go,An
JCB-PAT	49.7	46.3	17.5	0.80	0.31	2.11	0.06	0.358	Gi,Bo(t),He,Go,An
JCB-ASI	49.5	44.1	18.2	1.12	0.04	2.27	0.05	0.144	Gi,Go,He,An
JCB-218	48.2	41.8	17.5	0.99	0.54	2.31	0.07	2.810	Gi,Bo,Go,An
JCB-090	48.0	39.9	17.6	0.87	0.65	2.35	0.07	3.230	Gi.Bo.Go.An
JCB-270	49.8	41.3	17.4	0.12	0.07	2.48	0.06	0.826	Gi,Bo,Go,An
JCB-BST	46.6	39.8	18.2	4.57	0.15	2.34	0.07	1.000	Gi,Bo,Go,He,An
JCB-WRP	47.9	42.4	18.9	0.56	0.24	2.65	0.07	1.420	Gi,Bo,Go,He,An
JCB-BTM	50.9	49.1	17.3	0.28	0.03	2.25	0.06	0.173	Gi,Go,He,An
JCB-RBM	48.6	46.6	18.8	2.42	0.06	2.33	0.06	0.172	Gi,Bo,He,Go,An
JCB-HAM	48.9	42.9	16.8	3.95	0.06	2.33	0.06	0.166	Gi,Bo,He,Go,An

Note:

*Minerals are determined by XRD patterns. Gi: gibbsite, Bo: boehmite, He: Hematite, Go: goethite, An: anatase and Ka: kaolinite.

**The analysis of available Al_2O_3: 1g of sample was digested in 20g of 80g/L caustic soda at 80~90℃ for 2hours. The digested solution was titrated to calculate the available Al_2O_3.

Appendix D

Diagram of enthalpy of mixing (ΔH_{mix}) vs temperature (K)

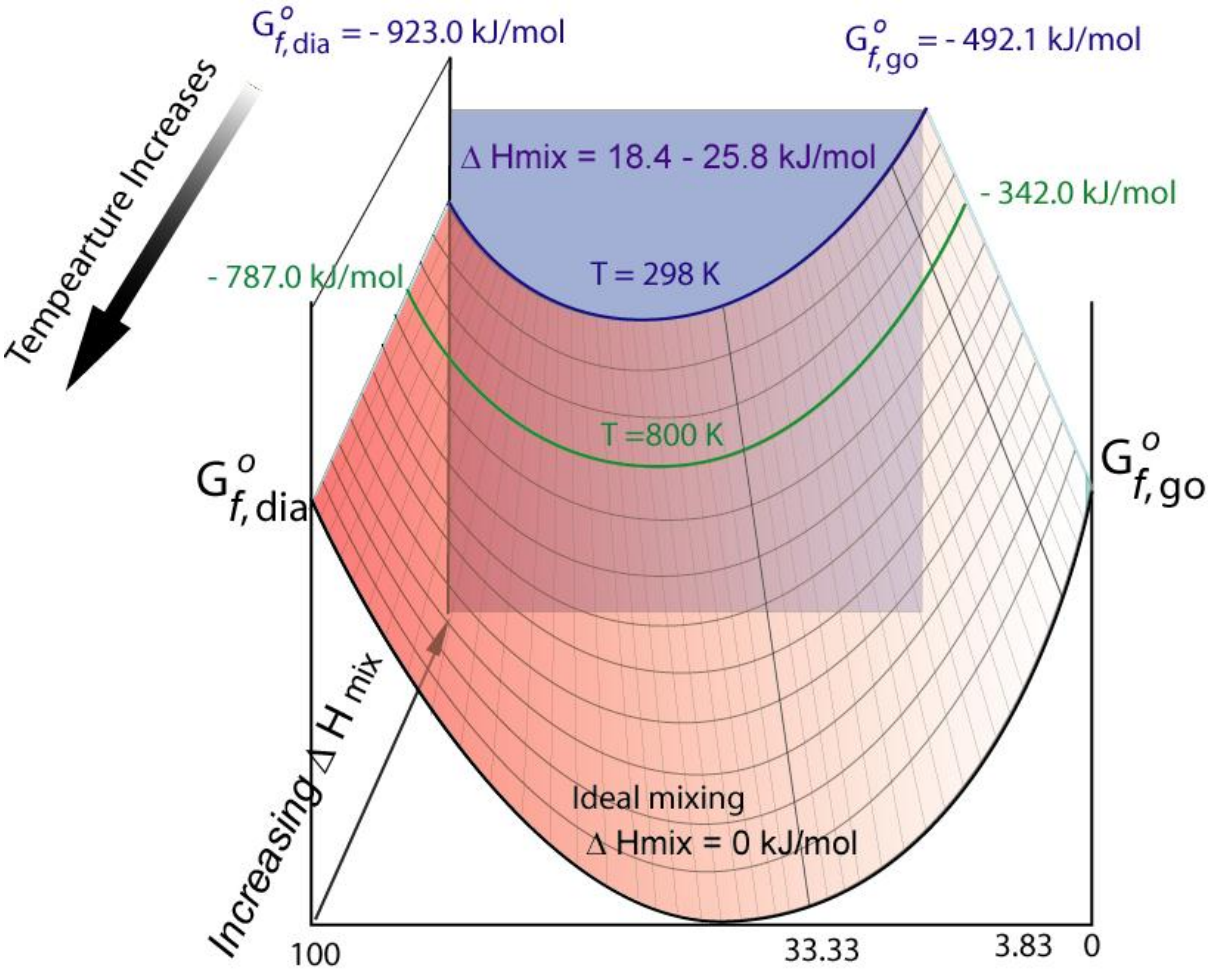

Note: the thermodynamic data after Diakonov *et al.* (1994) and Haas (1972).

Reference

Diakonov, I., Khodakovsky, I., Schott, J. & Sergeeva, E. (1994) Thermodynamic properties of iron oxides and hydroxides. I. Surface and bulk thermodynamic properties of goethite up to 500 K. *European Journal of Mineralogy*, 6**,** 967-983.

Hass, H. (1972) Diaspore-corrundum equilibrium determined by epitaxis of diaspore on corundum. *American Mineralogist*, 157**,** 1375-1385.

Appendix E

The abstract and the poster presented on The 10th Conference of the Asian Crystallographic Association (AsCA2010) held in Busan, South Korea from October 31 to November 3, 2011.

Abstract:

Crystal morphological study on the solubility limits of synthetic Al-substituted goethite

Fei Wu[1, 2], Peter Smith[2], Bill Richmond[1], Franca Jones[1], Kate Wright[1],
[1] *Department of Chemistry, Curtin University, GPO Box U1987, Perth 6845, Australia*
[2] *CSIRO Light Metals Flagship, Parker Centre, CSIRO Minerals, Perth, Australia*
E-mail: Fei.Wu2@postgrad.curtin.edu.au

This study has examined the crystal structure of synthetic Al-substituted goethites and the relationship between the Al substitution and unit cell parameters. We have also attempted to establish the limit of Al for Fe substitution in the formation of Al-goethites based on XRD and TEM analysis.

Aluminium substituted goethites were synthesised by ageing of co-precipitated $Fe(NO_3)_3$ and $Al(NO_3)_3$ in KOH solution at 70℃ [1]. The effects of aluminium substitution on the crystal morphology of the solid solution were studied by XRD and TEM (Fig. 1&2). The particle size decreases with the increase of aluminium substitution (Fig. 2). Elemental analysis suggests that Al for Fe substitution is limited since only a portion of the available aluminium was incorporated in the goethite structure. The strain in the goethite structure, caused by the smaller Al^{3+} ion incorporation could contribute to the substitution limit for aluminous goethite [2]. A more complicated mechanism is expected for the formation of the diaspore-goethite solid solution. Thermal analysis results show two endothermic peaks at ~75℃ and ~290℃ for synthetic Al-goethite, which are attributed to the loss of surface-absorbed water and the dehydroxylation of Al-goethite respectively. The temperature for the latter peak increased with increasing Al substitution.

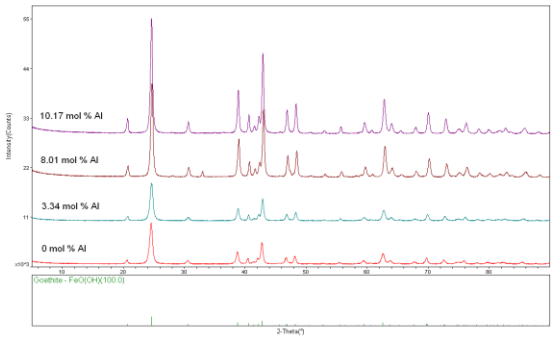

Figure 1. XRD patterns of Al-goethite samples

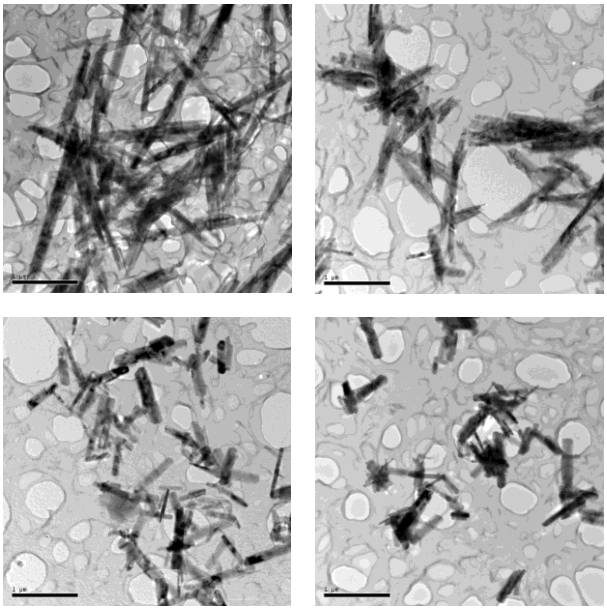

Figure 2. TEM of Al substituted goethite (Al substitution: top left: 0 %; top right: 3.34 %; bottom left: 8.01%; bottom right: 10.0%. Bar=1μm

References:

[1] Schwertmann, U. and Cornell, R. M., "*Iron Oxides in the Laboratory: Preparation and Characterization*", 2nd edition, Weinheim, Wiley-VCH, (2000).

[2] Sudaka, C., Subbanna, G. N. et al., "Effect of cationic substitutents on particle morphology of goethite and the magnetic properties of maghemite derived from substituted goethite", *Journal of Material Science*, Vol. 39, No. 13, (2004), pp 4271-4286.

Poster:

Crystal morphological study on the solubility limits of synthetic Al-substituted goethite

Fei Wu[1, 2], Peter Smith[2], Bill Richmond[1], Franca Jones[1], Kate Wright[1]

Curtin University

[1] Department of Chemistry, Curtin University, GPO Box U1987, Perth 6845, Australia
[2] CSIRO Light Metals Flagship, Parker Centre, CSIRO Minerals, Perth, Australia

Background

- Both natural and synthetic Al-substituted goethite have been widely reported.
- Up to 33% of Fe in goethite can be replaced by Al.
- Aluminous goethite is an important mineral which negatively impacts the settling process and Al recovery in the alumina industry.

Aim to:

- determine the crystal structure and morphology of Al-goethite
- investigate the formation of Al-goethite and the controls on Al substitution limits.

Synthesis of Al-substituted goethite

- **Methods:** Synthesis method described by Schwertmann and Cornell (2000)
- **Materials:** 5M KOH, 1 M $Fe(NO_3)_3$, 0.5 M $Al(NO_3)_3$
- **Conditions:** 70ºC for 14 days, swirled thoroughly once a day
- **Post-treatment:** samples removed by vacuum filtration, washed with KOH and DI water; dried at room temperature for two days; collected and finely ground
- **Characterisation:** XRD and TEM
- **Chemical analysis:** ICP
- **Thermal analysis:** DTA and TG

Sample ID	Initial	Results		
		XRD		ICP
	Al/(Al+Fe)%	Minerals	Al/(Al+Fe)% *	Al/(Al+Fe)%
ALGOE-1	0.0	Goethite	0.89	0.00
ALGOE-2	13.5	Goethite	3.48	3.34
ALGOE-3	10.6	Goethite	3.81	3.83
ALGOE-4	15.1	Goethite	5.93	5.75
ALGOE-5	19.5	Goethite	7.07	7.30
ALGOE-6	20.5	Goethite	6.10	8.01
ALGOE-7	27.0	Goethite	9.35	10.17

* Calculated by regression equation from Schulze (1984) and Li et al. (2006):
Al mol% = -562.6c+1701.0

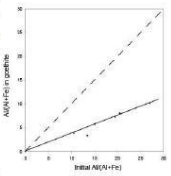

Effects of Al substitution on crystal size and morphology

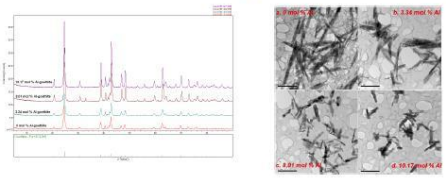

- The crystal size gets smaller with increasing of substitution of Al for Fe in the goethite lattice.

Thermal analysis

- Two endothermic peaks were observed.
- The first peak appears at 75~150ºC, which could be attributed to the loss of water from the surface due to absorption into the crystal structure.
- The main endothermic peak starts at 290ºC for alumina free goethite and the peaks shift to higher temperature up to 318ºC with the increase of Al substitution. It is clearly attributed to the dehydroxylation of Al-goethite to hematite.

$$2Fe_{1-x}Al_xOOH \rightarrow Fe_{2(1-x)}Al_{2x}O_3 + H_2O$$

- The shift of the dehydroxylation peaks is due to the amount of Al substitution, quality of crystalline of Al-goethite and the difference of the particle sizes caused by Al substitution.

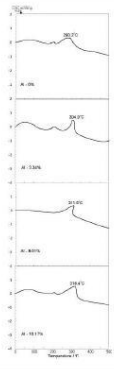

Solubility limits

- The substitution of Al for Fe modifies the crystal size due to the smaller ionic radii of Al^{3+} despite the isomorphous structure of goethite with diaspore.
- The crystal structure is increasingly strained as more Al is introduced into goethite.
- The substitution of Al for Fe is limited due to limited contractibility of anions as well as the strain caused by the size mismatches between Al^{3+} and Fe^{3+}.
- The contribution of anion substitution O^{2-} for OH^- in the goethite structure is yet to be established.

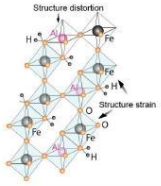

Conclusions

Synthesis of Al-goethite:

- Well-crystallised aluminous goethite was obtained by hydrothermally ageing of Fe-Al nitrate solution in alkaline media.
- Partial Al introduced in the system was incorporated into the goethite structure.

Crystal structure and morphology:

- Crystal size becomes smaller with the increase of Al substitution due to the smaller size of Al^{3+} to Fe^{3+}.

Solubility limit:

- The structure strain of mismatched particle sizes partly causes the solubility limits in the diaspore-goethite solid solution.

Thermal analysis:

- Two endothermic peaks were observed at ~75ºC and ~290ºC, which were attributed to the loss of surface-absorbed water and the dehydroxylation of Al-goethite respectively.

References:

Li, D., O'Connor, B.H., et al. (2006) Mineralogy of Al-substituted goethites, *Powder Diffraction* 21(4): 289-299

Schulze, D. G. (1984) The influence of aluminium on iron oxides. VIII. Unit cell dimensions of Al-substituted goethites and estimation of Al from them, *Clays and Clay Minerals* 32(1): 36-44.

Schwertmann, U and Cornell, R. M. (2000) *Iron Oxides in the Laboratory: Preparation and Characterization*, Weinheim, Wiley-VCH.

National Research FLAGSHIPS Light Metals

CSIRO

We gratefully acknowledge the research funding received from Australian Commonwealth Scientific and Industrial Research Organisation and ALCOA Australia. We acknowledge travel funding provided from Curtin University and CSIRO Flagship Scholarship.

Further information
Email: Fei.Wu2@postgrad.curtin.edu.au
Fei.Wu@csiro.au
www.csiro.au